

World Journal of *Gastroenterology*

World J Gastroenterol 2019 March 14; 25(10): 1171-1288



REVIEW

- 1171 Nutritional and vitamin status in patients with neuroendocrine neoplasms
Clement DS, Tesselaar ME, van Leerdam ME, Srirajakanthan R, Ramage JK

MINIREVIEWS

- 1185 Personalized medicine in functional gastrointestinal disorders: Understanding pathogenesis to increase diagnostic and treatment efficacy
Wang XJ, Camilleri M

ORIGINAL ARTICLE**Basic Study**

- 1197 Quest for the best endoscopic imaging modality for computer-assisted colonic polyp staging
Wimmer G, Gadermayr M, Wolkersdörfer G, Kwitt R, Tamaki T, Tischendorf J, Häfner M, Yoshida S, Tanaka S, Merhof D, Uhl A
- 1210 Short hairpin RNA-mediated knockdown of nuclear factor erythroid 2-like 3 exhibits tumor-suppressing effects in hepatocellular carcinoma cells
Yu MM, Feng YH, Zheng L, Zhang J, Luo GH
- 1224 MicroRNA-596 acts as a tumor suppressor in gastric cancer and is upregulated by promotor demethylation
Zhang Z, Dai DQ

Retrospective Cohort Study

- 1238 Performance of risk stratification systems for gastrointestinal stromal tumors: A multicenter study
Chen T, Ye LY, Feng XY, Qiu HB, Zhang P, Luo YX, Yuan LY, Chen XH, Hu YF, Liu H, Li Y, Tao KX, Yu J, Li GX

Retrospective Study

- 1248 Utility of linked color imaging for endoscopic diagnosis of early gastric cancer
Fujiyoshi T, Miyahara R, Funasaka K, Furukawa K, Sawada T, Maeda K, Yamamura T, Ishikawa T, Ohno E, Nakamura M, Kawashima H, Nakaguro M, Nakatochi M, Hirooka Y
- 1259 Endoloop ligation after endoscopic mucosal resection using a transparent cap: A novel method to treat small rectal carcinoid tumors
Zhang DG, Luo S, Xiong F, Xu ZL, Li YX, Yao J, Wang LS

Observational Study

- 1266 Consecutive fecal calprotectin measurements for predicting relapse in pediatric Crohn's disease patients
Foster AJ, Smyth M, Lakhani A, Jung B, Brant RF, Jacobson K

Prospective Study

- 1278** Non-guided self-learning program for high-proficiency optical diagnosis of diminutive and small colorectal lesions: A single-endoscopist pilot study
Bustamante-Balén M, Satorres C, Puchades L, Navarro B, García-Morales N, Alonso N, Ponce M, Argüello L, Pons-Beltrán V

ABOUT COVER

Editorial board member of *World Journal of Gastroenterology*, Goran Hauser, FEBG, MD, PhD, Associate Professor, Department of Internal Medicine, Division of Gastroenterology, Clinical Hospital Centre, Medical Faculty, Faculty of Health Studies, University of Rijeka, Rijeka 51000, Croatia

AIMS AND SCOPE

World Journal of Gastroenterology (*World J Gastroenterol*, *WJG*, print ISSN 1007-9327, online ISSN 2219-2840, DOI: 10.3748) is a peer-reviewed open access journal. The *WJG* Editorial Board consists of 642 experts in gastroenterology and hepatology from 59 countries.

The primary task of *WJG* is to rapidly publish high-quality original articles, reviews, and commentaries in the fields of gastroenterology, hepatology, gastrointestinal endoscopy, gastrointestinal surgery, hepatobiliary surgery, gastrointestinal oncology, gastrointestinal radiation oncology, etc. *WJG* is dedicated to become an influential and prestigious journal in gastroenterology and hepatology, to promote the development of above disciplines, and to improve the diagnostic and therapeutic skill and expertise of clinicians.

INDEXING/ABSTRACTING

The *WJG* is now indexed in Current Contents®/Clinical Medicine, Science Citation Index Expanded (also known as SciSearch®), Journal Citation Reports®, Index Medicus, MEDLINE, PubMed, PubMed Central, Scopus and Directory of Open Access Journals. The 2018 edition of Journal Citation Report® cites the 2017 impact factor for *WJG* as 3.300 (5-year impact factor: 3.387), ranking *WJG* as 35th among 80 journals in gastroenterology and hepatology (quartile in category Q2).

RESPONSIBLE EDITORS FOR THIS ISSUE

Responsible Electronic Editor: *Shu-Yu Yin* Proofing Editorial Office Director: *Ze-Mao Gong*

NAME OF JOURNAL

World Journal of Gastroenterology

ISSN

ISSN 1007-9327 (print) ISSN 2219-2840 (online)

LAUNCH DATE

October 1, 1995

FREQUENCY

Weekly

EDITORS-IN-CHIEF

Subrata Ghosh, Andrzej S Tarnawski

EDITORIAL BOARD MEMBERS

<http://www.wjgnet.com/1007-9327/editorialboard.htm>

EDITORIAL OFFICE

Ze-Mao Gong, Director

PUBLICATION DATE

March 14, 2019

COPYRIGHT

© 2019 Baishideng Publishing Group Inc

INSTRUCTIONS TO AUTHORS

<https://www.wjgnet.com/bpg/gerinfo/204>

GUIDELINES FOR ETHICS DOCUMENTS

<https://www.wjgnet.com/bpg/GerInfo/287>

GUIDELINES FOR NON-NATIVE SPEAKERS OF ENGLISH

<https://www.wjgnet.com/bpg/gerinfo/240>

PUBLICATION MISCONDUCT

<https://www.wjgnet.com/bpg/gerinfo/208>

ARTICLE PROCESSING CHARGE

<https://www.wjgnet.com/bpg/gerinfo/242>

STEPS FOR SUBMITTING MANUSCRIPTS

<https://www.wjgnet.com/bpg/GerInfo/239>

ONLINE SUBMISSION

<https://www.f6publishing.com>

Nutritional and vitamin status in patients with neuroendocrine neoplasms

Dominique SVM Clement, Margot ET Tesselaar, Monique E van Leerdam, Rajaventhana Srirajaskanthan, John K Ramage

ORCID number: Dominique SVM Clement (0000-0002-8116-962X); Margot ET Tesselaar (0000-0002-8885-4638); Monique E van Leerdam (0000-0002-5719-3208); Rajaventhana Srirajaskanthan (0000-0001-9835-8681); John K Ramage (0000-0003-4824-6600).

Author contributions: Clement DSVM, Tesselaar MET, Srirajaskanthan R, and Ramage JK wrote the manuscript; Clement DSVM generated the figures; van Leerdam ME reviewed the manuscript; Srirajaskanthan R designed the aim; Ramage JK designed the editorial.

Conflict-of-interest statement: No conflict of interest.

Open-Access: This article is an open-access article which was selected by an in-house editor and fully peer-reviewed by external reviewers. It is distributed in accordance with the Creative Commons Attribution Non Commercial (CC BY-NC 4.0) license, which permits others to distribute, remix, adapt, build upon this work non-commercially, and license their derivative works on different terms, provided the original work is properly cited and the use is non-commercial. See: <http://creativecommons.org/licenses/by-nc/4.0/>

Manuscript source: Invited manuscript

Received: December 5, 2018

Peer-review started: December 6, 2018

Dominique SVM Clement, Rajaventhana Srirajaskanthan, John K Ramage, Neuroendocrine Tumour Unit, King's College Hospital ENETS Centre of Excellence, London SE5 9RS, United Kingdom

Margot ET Tesselaar, Department of Medical Oncology, Netherlands Cancer Institute ENETS Centre of Excellence, Amsterdam 1066 CX, Netherlands

Monique E van Leerdam, Department of Gastrointestinal Oncology, Netherlands Cancer Institute, Amsterdam 1066 CX, Netherlands

Rajaventhana Srirajaskanthan, Department of Gastroenterology, King's College Hospital, London SE5 9RS, United Kingdom

Corresponding author: Dominique SVM Clement, MD, Clinical Research Fellow, Neuroendocrine Tumour Unit, King's College Hospital ENETS Centre of Excellence, Denmark Hill, London SE5 9RS, United Kingdom. dominique.clement@nhs.net
Telephone: +44-2032996043
Fax: +44-2032991778

Abstract

Symptoms of gastroenteropancreatic located neuroendocrine neoplasms (GEP-NENs) are often related to food intake and manifest as abdominal pain or diarrhoea which can influence patients nutritional status. Malnutrition is common in cancer patients and influences quality of life, treatment options and survival but is also present in up to 40% of patients with GEP-NENs. As part of malnutrition there are often deficiencies in fat-soluble vitamins, mainly vitamin D. Little knowledge exists on trace elements. Several factors influence the development of malnutrition such as size and localisation of the primary tumour as well as metastases, side effects from treatment but also hormone production of the tumour itself. One of the main influencing factors leading to malnutrition is diarrhoea which leads to dehydration and electrolyte disturbances. Treatment of diarrhoea should be guided by its cause. Screening for malnutrition should be part of routine care in every GEP-NEN patient. Multidisciplinary treatment including dietician support is necessary for all malnourished patients with GEP-NENs.

Key words: Neuroendocrine neoplasm; Nutrition; Malnutrition; Vitamin deficiency; Diarrhoea; Steatorrhoea

First decision: January 18, 2019
Revised: February 13, 2019
Accepted: February 22, 2019
Article in press: February 23, 2019
Published online: March 14, 2019

©The Author(s) 2019. Published by Baishideng Publishing Group Inc. All rights reserved.

Core tip: Patients with gastroenteropancreatic located neuroendocrine neoplasms have a high risk on malnutrition and vitamin deficiency. Multidisciplinary treatment focussing on diarrhoea and nutritional status is warranted.

Citation: Clement DS, Tesselaar ME, van Leerdam ME, Srirajakanthan R, Ramage JK. Nutritional and vitamin status in patients with neuroendocrine neoplasms. *World J Gastroenterol* 2019; 25(10): 1171-1184
URL: <https://www.wjgnet.com/1007-9327/full/v25/i10/1171.htm>
DOI: <https://dx.doi.org/10.3748/wjg.v25.i10.1171>

INTRODUCTION

Neuroendocrine neoplasms (NENs) are rare neoplasms arising from cells of the diffuse neuroendocrine system. NENs commonly arise from the gastroenteropancreatic (GEP) or bronchial tract^[1]. The incidence of NENs is growing worldwide^[2-4]. Based on recent analysis of the United States SEER database this has arisen since 1973 from 1.03 to 6.98 per 100000 in 2012^[2]. In the United Kingdom similar growth in incidence has been demonstrated from 3.9 per 100000 in 2001 to 8.8 per 100000 in 2015^[5]. NENs are classified based on the World Health Organisation (WHO) 2010 classification, based on morphological criteria and proliferative activity (Ki-67 index or mitotic count). The grades are G1 Ki-67: < 2% and mitotic count < 2/10 mm², G2 Ki-67: 3%-20% or mitotic count 2-20/mm² neuroendocrine tumours (NETs) and G3 Ki-67: > 20% neuroendocrine carcinoma (NECs)^[6]. In 2016 the WHO has updated this classification for pancreatic neoplasms and differentiates G3 NETs from small- or large cell NECs^[7]. NENs are difficult to diagnose and have metastasized in around 50% of cases at diagnosis^[8]. GEP-NENs may present a heterogeneous clinical behaviour but many well differentiated tumours (G1-G3) are indolent or slow growing with a 5 year survival which can be up to 50%-70%^[2,9]. Well differentiated NETs can be functional, secreting hormones [the most common is carcinoid syndrome (CS)], or non-functioning^[10].

Surgical removal of the primary tumour is the preferred treatment where it is possible but it can also be considered in metastatic disease and this may have survival benefits for some sites^[11,12]. In the metastasized setting long-acting somatostatin analogues are often the first line of treatment in cases with positive somatostatin receptor imaging^[10]. Due to the position of the tumour within the GEP tract, patients with GEP-NENs can experience gastrointestinal (GI) symptoms like bloating, diarrhoea, abdominal pain and weight loss. Treatments for GEP-NENs can also have side effects such as diarrhoea or steatorrhea. These factors can influence the weight, nutritional and vitamin status of patients with GEP-NENs. Malnutrition influences quality of life but also reduces tolerance to anti-cancer therapy and reduces survival in patients with cancer^[13,14]. Currently the nutritional and vitamin status is a neglected area in patients with GEP-NENs^[15].

This review will discuss the current knowledge regarding nutritional, vitamin and trace element status in patients with GEP-NENs and factors contributing to malnutrition. One of the main influencing factors is diarrhoea and we will discuss ways to analyse the causes of diarrhoea as well as treatment modalities. We will comment on any means of improving nutritional status.

NUTRITIONAL STATUS DEFINITION MALNUTRITION

Nutritional status can be measured based on anthropometric data [weight, height, body mass index (BMI)], biochemical markers like serum proteins (albumin or transferrin) or body composition measures^[16]. There are several definitions for malnutrition from the literature and health care organisations. The WHO, National Health Service and European Society of clinical nutrition and metabolism (ESPEN) nutrition in cancer guideline uses definitions based on intake and metabolic effects^[13,17,18]. The American Society for Parenteral and Enteral Nutrition and ESPEN guidelines on malnutrition include definitions based on BMI, unintentional weight loss and loss of body composition parameters such as fat-free mass or muscle

mass^[19,20].

In patients with cancer as part of their disease and malnutrition a syndrome called cancer cachexia can develop. This is defined as weight loss > 5% in past 6 mo without starvation or weight loss < 2% and BMI < 20 kg/m² or weight loss > 2% and sarcopenia (defined as appendicular skeletal muscle index males < 7.26 kg/m² and females < 5.45 kg/m²)^[14]. Malnutrition can exist even in the absence of weight loss. These broad definitions can be difficult to measure objectively.

MALNUTRITION IN PATIENTS WITH GEP-NENs

Several recent studies show 30%-50% of patients visiting an oncology clinic for the first time are malnourished^[21-23], but not every clinician is aware of this phenomenon. Caccialanza *et al*^[24] performed a survey among all Italian oncologists and only 28% of oncologists reported performing nutritional assessments (based on weight loss, BMI, screening tools or intake) as part of their routine care. About 40% of the oncologists within this survey denied the use of available specialist nutrition teams. A recent abstract from Lim *et al*^[25] reports that less than 50% of patients in NEN clinic had their weight measured, and BMI was available in only 14% of these patients. Forty-three percent of all NEN patients within an outpatient clinic in Denmark were reported to have weight loss at some point during their disease. This is significantly more common in patients with GEP-NENs compared to patients with bronchial NENs or unknown primary^[26].

There are several studies reporting malnutrition in NEN at first or follow up visits which are summarized in Table 1. The range of reported malnutrition is 4.9%-38%^[26,27]. One study reports no malnourished patients^[15] whereas the TELECAST study, a prospective study on diarrhoea, reports 58% of patients with a NET and CS to have metabolic and nutritional disorders^[28]. The studies in Table 1 report on different patient populations. Borre *et al*^[26] included only 70% GEP-NEN patients, Maasberg *et al*^[29] included 77% GEP-NEN patients while Qureshi *et al*^[30] and Robbins *et al*^[27] included only GEP-NEN patients. The patient populations underwent different forms of therapy. The patients in the Qureshi *et al*^[30] and Robbins *et al*^[27] groups had previous surgery in 60% of cases versus 48% in the Borre *et al*^[26] group. Somatostatin analogues were administered in 30% of patients within the Robbins *et al*^[27] group, 41.6% within the Qureshi *et al*^[30] group and 50% in the Maasberg *et al*^[29] and Borre *et al*^[26] groups. Thirty percent of patients within the Maasberg *et al*^[29] group were treated with systemic chemotherapy (this percentage was unknown for the other groups).

The type of tumours differs within the above-mentioned groups. The Borre *et al*^[26], Robbins *et al*^[27] and Qureshi *et al*^[30] groups report 60%-70% G1 tumours versus 32% G1 tumours in the Maasberg *et al*^[29] group. Robbins *et al*^[27] mentions 37.5% of patients to have functional symptoms (diarrhoea and or hot flushes) whereas Maasberg *et al*^[29] mentions 24.1% of patients to have these. The studies reporting on malnutrition used different screening methods. The malnutrition universal screening tool, nutritional risk screening, subjective global assessment are clinical tools based on BMI, weight loss, dietary intake and severity of illness. The international classification of diseases 9 scores were used in 1 study^[31]. Currently a universal screening method for malnutrition in patients with GEP-NENs is lacking. Due to different screening methods, patient selection and different stage of NEN, the published data are too heterogenous to compare.

EFFECTS OF MALNUTRITION ON OUTCOMES

Some studies have reported the correlation of malnutrition to outcomes in terms of response to treatment, length of hospital stay or survival. Maasberg *et al*^[29] reports on the nutritional status of NEN inpatients admitted for staging examinations or therapeutic interventions. Malnourished patients had a longer length of hospital stay compared to well-nourished patients (8 vs 4 d). The survival of malnourished patients was shorter although the malnourished patient group was comprised of a high percentage of NECs.

Glazer *et al*^[31] identified 22096 patients with an abdominal NEN within the national inpatient sample database. In this group malnutrition was associated with a higher inpatient complication rate of 15% compared to 10% in well-nourished patients. Obesity was associated with lower inpatient mortality rates while malnutrition was associated with higher inpatient mortality rates. Ekeblad *et al*^[32] reported being underweight at diagnosis (BMI < 20kg/m²) of a pancreatic NEN was related to a poorer prognosis. Marrache *et al*^[33] studied 67 patients with liver metastasis from a

Table 1 Summary of available studies regarding malnutrition in patients with gastroenteropancreatic neuroendocrine neoplasms

Author	No patients	Patient groups	Score used	Malnutrition definition	Results	BMI \leq 20
Qureshi <i>et al</i> ^[30]	161	All GEP-NEN outpatients	MUST	MUST \geq 1	MUST 1: 9.8% MUST \geq 2: 7.7%	9.9%
Robbins <i>et al</i> ^[27]	183	All GEP-NEN outpatients	MUST	MUST \geq 1	MUST 1: 8.7% MUST \geq 2: 4.9%	4.9%
Borre <i>et al</i> ^[26]	186	All NEN outpatients	NRS	NRS \geq 3	NRS \geq 3: 38%	12%
Maasberg <i>et al</i> ^[29]	203	NEN inpatients (177) NEN outpatients (26)	SGA and NRS	SGA B or C NRS \geq 3	SGA B or C: 21% NRS \geq 3: 25%	N/A
Gallo <i>et al</i> ^[15]	37	All NEN outpatients	BMI		No malnourished patients	0
Glazer <i>et al</i> ^[31]	22096	Abdominal NEN	ICD-9 codes		8% malnourished	N/A

Summary of studies reporting malnutrition, used screening tool, cut-off for malnutrition, results and body mass index scores in patients with gastroenteropancreatic neuroendocrine neoplasms. GEP-NEN: Gastroenteropancreatic neuroendocrine neoplasms; MUST: Malnutrition universal screening tool; NRS: Nutritional risk screening; SGA: Subjective global assessment; BMI: Body mass index; ICD: International classification of diseases.

NEN undergoing transarterial chemoembolization and found that the BMI was a factor predicting tumour response and associated with delayed progression.

FAT SOLUBLE VITAMIN STATUS IN PATIENTS WITH GEP-NENs

Vitamin status can be considered as part of nutritional status. Two studies report on the status of fat-soluble vitamins in patients with NEN. Fiebrich *et al*^[34] analysed the fat soluble vitamin status of 35 patients with metastatic small intestinal NEN on treatment with somatostatin analogues for at least 18 mo. Eighty percent of patients showed abnormally low levels of at least 1 fat soluble vitamin and 32% of patients showed multiple deficiencies. Vitamin deficiencies measured in plasma were reported in 9% of patients for vitamin A, 31% for vitamin D, 14% vitamin E and 69% vitamin K1. In 12% of patients vitamin K1 deficiency resulted in prolonged prothrombin time. Increased stool frequency was not associated with lower vitamin levels. De Hosson *et al*^[35] described 15 patients with a NET that had been on a somatostatin analogue for more than 6 mo. Nine out of fifteen patients had vitamin deficiencies (vitamin A, D, E, K, B12 and B3) and after 10 wk of nutritional intervention and supplementation 7 patients still had deficient vitamin levels.

VITAMIN D STATUS IN PATIENTS WITH GEP-NENs

Vitamin D status has received increasing attention in cancer patients and it is suggested it may play a possible role in the development of different types of tumours^[36]. Vitamin D deficiency (defined as 25 OH vitamin D levels \leq 20 ng/mL) is described in between 46% and 81% of patients with NENs^[27,36-38]. The study populations reporting on the prevalence of vitamin D deficiency could not be compared directly since Motylewska *et al*^[37] included GEP-NENs as well as lung NENs and other NENs, Lind *et al*^[38] included only small intestine NENs while Massironi *et al*^[36] and Robbins *et al*^[27] included all GEP-NENs.

Two studies included the vitamin D status of healthy volunteers. Motylewska *et al*^[37] reported a vitamin D deficiency of 89% in healthy volunteers. Massironi *et al*^[36] found significantly higher vitamin D level (median 23.9 ng/mL) in healthy volunteers compared to GEP-NEN patients (median 12.9 ng/mL). One study describes the overall and progression free survival (OS and PFS) in 138 GEP-NEN patients and found a negative correlation between low vitamin D levels and OS and PFS. Vitamin D supplementation improved the OS in patients with vitamin D deficiency compared to patients with vitamin D deficiency without supplementation.

Vitamin D supplementation with over-the-counter vitamin D preparations improves the vitamin D levels in most GEP-NEN patients. Robbins *et al*^[27] showed a decrease in numbers of patients with vitamin D deficiency from 66.8% at baseline to 44.4% after 1 and 2 years of starting supplementation, although supplementation of vitamin D had not normalised the level in all patients. Lind *et al*^[38] showed only 28% of small intestine NEN patients on oral vitamin D supplementation to be vitamin D

deficient as compared to 46% of patients without supplementation. Vitamin D supplementation does improve the bone mineral density in patients with small intestine NEN. Lind *et al*^[38] describes 2 cohorts of 25 patients with a small intestinal NEN who all had prior surgery. Within the first cohort baseline vitamin D levels and dual-energy x-ray absorptiometry (DEXA) scan were performed. The second cohort was advised to take oral substitution of vitamins and minerals. After 6-15 mo vitamin D levels were measured and a DEXA scan was performed. The DEXA scan results showed low bone density in 76%, osteoporosis in 32% and osteopenia in 44% for the first cohort and respective values of 26%, 24% and 36% in the second cohort.

VITAMIN B3/NIACIN STATUS IN PATIENTS WITH GEP-NENs

Tryptophan is a precursor of serotonin. In healthy individuals only 1% of tryptophan will be used to make serotonin. In patients with NETs and CS up to 60% of tryptophan is used for serotonin production leading to tryptophan deficiency. Pellagra as a result of tryptophan deficiency with symptoms of dermatitis, diarrhoea and dementia can develop in about 5% of patients with CS^[39-41].

Shah *et al*^[42] analysed the niacin levels in blood of 36 patients with CS, 32 patients with a carcinoid tumour but without CS and 24 non-carcinoid patients (patients with pancreatic NEN, other cancers, GI diseases and healthy volunteers). With a cut-off level of 130, 28% of patients (10/36) with CS were niacin deficient and 12.5% (4/32) without CS compared to none in the non-carcinoid patients. Serotonin and tryptophan levels were measured: in patients with increased serotonin levels a decreased niacin and tryptophan level was observed.

Bouma *et al*^[43] identified 42 patients with serotonin producing NEN [based on 5-hydroxyindolacetic acid (5-HIAA) > 3.8 mmol/mol creatinine and/or platelet serotonin > 5.4 nmol/10⁹ platelets] and low tryptophan levels (< 40 umol/L) and/or pellagra-like symptoms. Urine N1-NM (N1-Methylnicotinamide) levels were measured prior and after starting niacin supplementation. Forty five percent of patients showed low N1-NM levels and after starting niacin supplementation all urine levels normalised. 5-HIAA levels showed a negative correlation with niacin status, but the 5-HIAA level did not correlate with the plasma tryptophan level. In view of the difficulties measuring niacin, nicotinamide should be prescribed if pellagra is suspected.

TRACE ELEMENTS IN PATIENTS WITH GEP-NENs

Malnutrition can also result in low levels of trace elements, like cobalt, copper, fluorine, iodine, selenium and zinc. In patients with cancer low levels of selenium and zinc were described and could affect wound healing, cause depressive symptoms and compromise the immune response^[13,44]. Little is known about other trace elements. The role of trace elements in patients with NENs is unknown. One study exists evaluating the selenium level of patients with NENs having peptide receptor radionuclide therapy (PRRT) treatment. Four wk prior to PRRT 5 out of 21 included patients showed normal selenium levels. Four wk after PRRT 18 patients showed significant decrease in selenium levels^[45]. There may be significant issues with blood selenium levels which may not represent whole body stores of selenium.

FACTORS INFLUENCING MALNUTRITION

In patients with NENs several factors can contribute to the development of malnutrition as summarized in [Figure 1](#). In cancer patients the protein, carbohydrate and lipid metabolism are altered resulting in increased metabolic resting rate, insulin resistance, lipolysis and proteolysis. This can lead to weight loss as a sign of malnutrition^[13]. If this process continues, cancer cachexia as a result of decreased energy intake and increased total body energy expenditure (TEE), can develop^[14]. Tumour metabolism and inflammation increase the TEE cytokines and factors in animal models involved are for example IL-6, IL-1, TNF- α , IFN- γ , Leukaemia inhibitor γ factor, GDF15, TWEAK, TRAF, oncostatin M, TNFSF12 and PGE2. Patient data regarding these cytokines and factors are lacking^[46]. In patients with pancreatic adenocarcinoma elevated C-reactive protein levels are a marker for cachexia and predict poor prognosis^[47]. Little knowledge regarding the development of cachexia

and prognosis exists in patients with GEP-NENs. Due to the slow growing nature of GEP-NENs the risk of developing cachexia may be reduced^[29]. In patients with NET and CS, diarrhoea as a result of excessive hormone secretion also contributes to malnutrition^[48-51]. Several foods containing high levels of amines such as mature cheese or chocolate may provoke symptoms in these patients. They tend to avoid these foods which can contribute to decreased nutritional intake^[49,52]. Small intestine NENs can cause strictures or retroperitoneal fibrosis in the GI tract resulting in symptoms such as bowel obstruction, influencing patients' food intake and nutritional status^[53,54].

Uncontrolled diarrhoea leads to dehydration, electrolyte abnormalities, vitamin deficiencies and thus influence malnutrition^[55]. Surgical treatment of a GEP-NEN can result in diarrhoea for several reasons. Loss of absorptive surface after small bowel or Whipple's resection can lead to diarrhoea and malabsorption. In cases of small bowel resection when < 200 cm small bowel remains, short bowel syndrome with inability to maintain fluid- and nutritional status can develop^[15,53,56]. Another cause is removal of a part of the terminal ileum which can result in vitamin B12 deficiency and bile acid malabsorption leading to diarrhoea^[48,53,55,57]. A third cause is following small intestine or Whipple's resection, bacterial overgrowth can develop resulting in diarrhoea with malabsorption and maldigestion as well as malabsorption of fat soluble vitamins^[48,53,55,58]. Resection of small or large bowel as well as Whipple's resection can also influence the bowel transit time with diarrhoea and possible malnutrition as a result^[15,49].

Treatment with somatostatin analogues can result in malnutrition for several reasons. Diarrhoea is one of the most commonly reported side effects due to decreased duodenal absorption of carbohydrates and triglycerides^[59,60]. In addition decreased pancreatic enzyme release in response to a meal is seen as an effect from somatostatin analogues resulting in pancreatic exocrine insufficiency with steatorrhea and malnutrition^[15,55,57]. Chemotherapy can lead to malnutrition due to its side effects such as loss of taste, oral problems, diarrhoea, nausea and vomiting^[13,15,49].

ANALYSING CAUSES OF DIARRHOEA

Diarrhoea is an important factor contributing to malnutrition in patients with GEP-NENs as summarized in **Figure 1**. **Figure 2** summarizes diagnostic approaches to diarrhoea. CS is prevalent in 20% of patients with NETs^[61]. CS is a clinical diagnosis with symptoms of diarrhoea (80% of patients), hot flushes (50%-85% of patients) and wheezing (10%-20% of patients) often in the presence of liver metastasis^[48,62,63]. Twenty-four h urine collection for 5-HIAA, a breakdown product of serotonin, has a sensitivity and specificity around 90% for small intestine NENs^[64]. Certain serotonin-rich foods (bananas, avocados, plums, eggplant, tomatoes, plantain, pineapples, kiwis and nuts) and medications (analgesic acetaminophen, cough syrups and warfarin) can increase urinary 5-HIAA levels and should be avoided 24 h before and during specimen collection.

In case of previous surgery on either small intestine or pancreas, diarrhoea could be caused by bile acid malabsorption, short bowel syndrome, bacterial overgrowth or pancreatic exocrine insufficiency. A Selenium homotaurocholic acid conjugated with taurine (SeHCAT) scan is the gold standard for diagnosing bile acid malabsorption with a sensitivity 100% and specificity 89%^[65]. A capsule containing radiolabelled SeHCAT is ingested and after 1-3 h and after 7 d a gamma scan is performed to measure the SeHCAT retention in the body. Levels of 10%-15% retention are mild, < 10% as moderate and < 5% severe bile acid malabsorption^[66,67]. A study in 57 patients with GEP-NENs showed 80% of patients with bile acid malabsorption^[68].

Following small intestine resection, a short bowel syndrome can develop and this is usually the case when < 200 cm small bowel remains^[69,70]. Adaptation in the postoperative period over 1-2 years is possible^[70]. No data exists on the prevalence of short bowel syndrome in patients with GEP-NENs. Small bowel bacterial overgrowth develops in the case of blind small bowel loops or strictures. A gold standard for the diagnosis of small bowel bacterial overgrowth is lacking. Quantitative culture of jejunal aspirate is frequently described but is an invasive procedure with upper endoscopy and lacks a sterile environment to obtain a culture^[71]. Hydrogen breath tests are a widely used alternative for diagnosing small bowel bacterial overgrowth with a sensitivity of 63% and specificity 83% compared to a jejunal culture^[72,73]. In the earlier mentioned study with 57 patients with GEP-NENs 62% of patients were diagnosed with bacterial overgrowth^[68].

Partially or total resection of the pancreas leads to decreased synthetic capacity of pancreatic enzymes resulting in pancreatic exocrine insufficiency^[74,75]. Faecal elastase

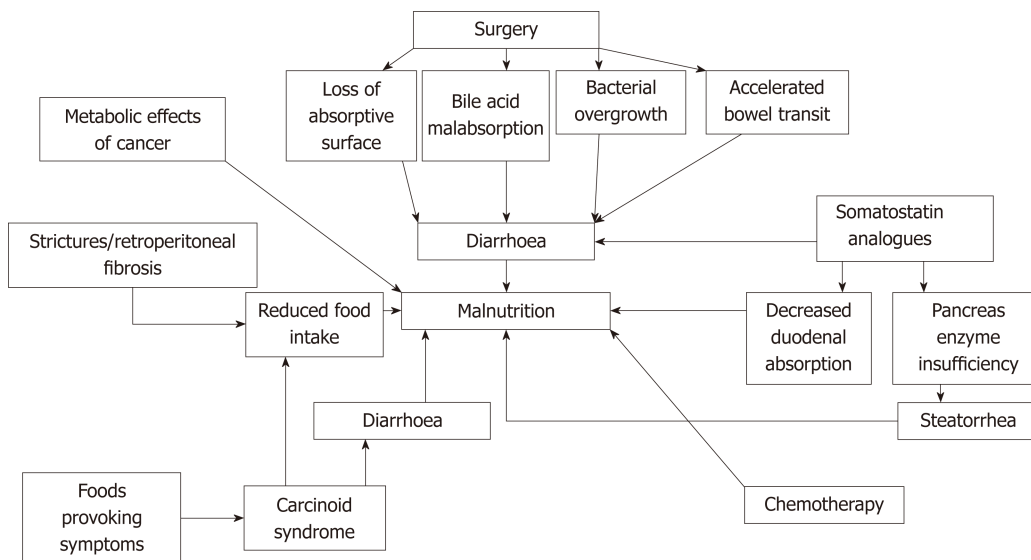


Figure 1 Factors influencing malnutrition in patients with gastroenteropancreatic neuroendocrine neoplasms. Summary of factors influencing the development of malnutrition in patients with gastroenteropancreatic neuroendocrine neoplasms.

can be measured as a marker for pancreatic exocrine insufficiency with a cut-off < 200 µg/g stool. In patients with chronic pancreatitis the sensitivity of faecal elastase diagnosing pancreatic exocrine insufficiency is 63%-100% with a specificity of 83%-93%^[76-78]. In patients with GEP-NENs there is controversy about the role of faecal elastase. In a study of 57 patients with GEP-NENs only 17% of patients had a low faecal elastase despite symptoms of steatorrhea^[68]. Chaudhry *et al*^[79] described 32 patients with GEP-NENs (27 small intestine, 5 pancreas and 7 other) on treatment with a somatostatin analogue and 82% of patients had symptoms of steatorrhea but the faecal elastase was low in only 6 patients. The sensitivity of faecal elastase in this study was only 15.4%. Another study on 50 patients with a metastatic NEN ($n = 30$ small intestine, $n = 11$ pancreas, $n = 6$ lung or $n = 3$ other) on somatostatin analogue treatment the faecal elastase was a good marker for pancreatic exocrine insufficiency although faecal samples were not available from all patients^[80]. Faecal elastase could be a useful marker to diagnose pancreatic exocrine insufficiency although data in small groups of patients with NENs are conflicting.

Steatorrhea could be one of the side effects of treatment with somatostatin analogues due to the inhibition of pancreatic exocrine secretion^[81,82]. A recent study on 50 patients starting with a somatostatin analogue showed that 24% developed pancreatic exocrine insufficiency after a median of 2.9 mo, although the study lacks data about previous surgery and altered anatomy of the GI tract^[80].

TREATMENT OPTIONS

Malnutrition should be treated according to its causes as summarised in **Figure 2**. In patients with diarrhoea due to CS, treatment should be to try to reduce hormone levels^[48]. A first step should be to optimise the dose of long acting somatostatin analogues, and this could be achieved by increasing the dose, shortening the interval or adding a short acting dose^[83-85]. Another step could be palliative debulking surgery or liver directed therapy with chemoembolization of the hepatic artery, radio-frequency ablation/microwave ablation or selective intra-hepatic radio-embolization to lower the tumour burden and reduce hormone production^[86,87]. Clinical (symptomatic) responses after liver directed therapy are reported in up to 75%^[88-91]. Recently telotristat ethyl, an oral inhibitor of tryptophan decarboxylase, has become available for symptomatic patients for whom monotherapy with somatostatin analogues not enough is to control diarrhoea. The TELESTAR trial was a phase III double blind placebo-controlled trial in 135 patients with CS (defined as > 4 bowel movements a day) were randomized to receive 250 mg telotristat ethyl tablet, 500 mg telotristat ethyl tablet or placebo three times daily for 12 wk. There was a statistically significant reduction in bowel movements in 42%-44% of patients (250 mg or 500 mg) compared to 20% reduction in placebo patients after 12 wk. A significant reduction in urine-5 HIAA level and improvement in quality of life scores was seen^[92]. A companion trial (TELECAST) looking at 126 patients with CS and less than 4 bowel

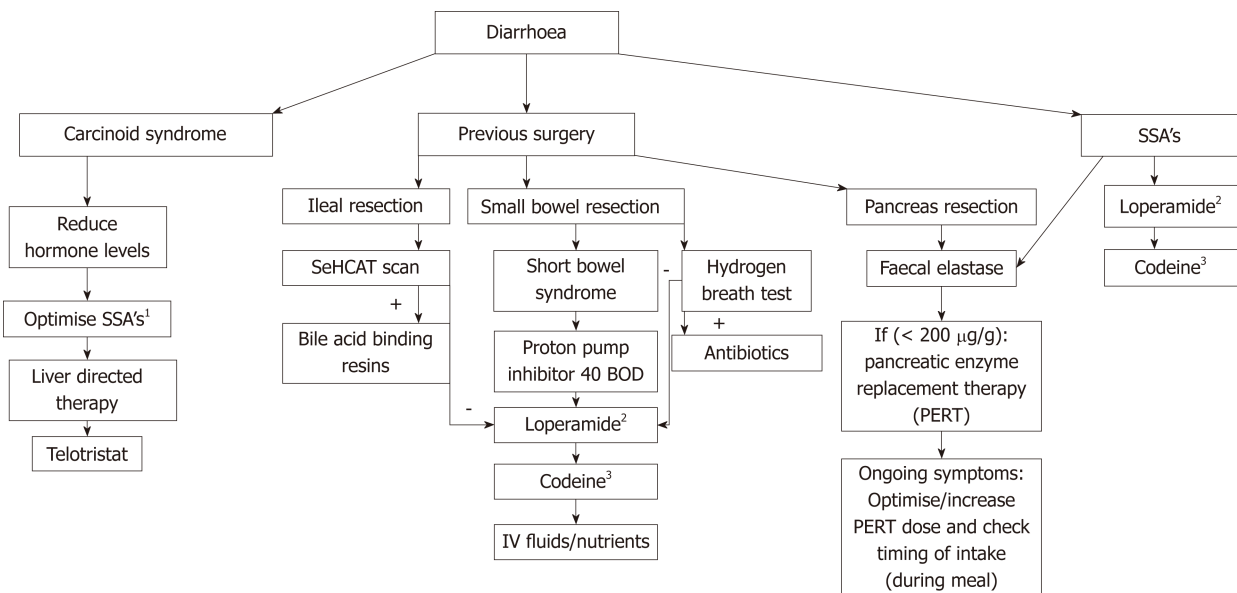


Figure 2 Approach to patients with diarrhoea. Summary of causes of diarrhoea in patients with gastroenteropancreatic neuroendocrine neoplasms, how to analyse and treatment advise. ¹Optimise SSA's: Increase dose, shorten interval or add short acting dose; ²Advise loperamide: Increasing dose 2-4 mg 4 times a day, up to 12-24 mg 4 times a day in short bowel syndrome; ³Advise codeine: 15-60 mg 4 times a day; Advise PERT: 1 × 25000 units of lipase per small meal 2 × 25000 units lipase per large meal, titrate up may need > 80000 units per large meal. SSA's: Somatostatin analogue's; SeHCAT: Selenium homotaurocholic acid conjugated with taurine; BOD: Twice a day; PERT: Pancreatic enzyme replacement therapy.

motions a day and with either loose stools or daily > 2 flushing episodes or abdominal pain or nausea in > 20% of days or 5-HIAA urine levels above normal limits were randomised to telotristat ethyl 250 mg, 500 mg or placebo for 12 wk. This trial showed good safety data and classified 40% of patients on telotristat ethyl as durable responders^[28].

Another study published by Weickert *et al*^[93], investigated the details of 120 patients participating in the TELESTAR trial and telotristat ethyl's effect on nutritional status after 12 wk of treatment. Weight gain and improvement in nutritional markers as albumin, cholesterol levels and triglycerides were seen in patients on telotristat ethyl but not in patients on placebo. In two small studies with 11 and 14 patients with small intestine NENs, liver metastases and CS there were reports of the positive effect of ondansetron reducing diarrhoea^[94,95]. If a SeHCAT shows bile acid malabsorption, treatment with bile acid binding resins is advised. In patients with bile acid malabsorption without NEN a response to colesevelam is reported in 50%-96% of cases^[66,67,96].

Short bowel syndrome should ideally managed by a dedicated multidisciplinary team due its prolonged course and intensive fluid and nutritional management^[69]. Medical treatment includes proton pump inhibitors to reduce gastric acid production in the maximum dose of 40 mg twice daily. Loperamide is the cornerstone of treatment to reduce small bowel mobility. A starting dose of 2 mg 4 times a day (breakfast, lunch, diner, bedtime) is advised. This can be increased to 8 mg 4 times a day but in case of short bowel up to 12-24 mg 4 times a day. Codeine phosphate is less effective than loperamide but can be combined with loperamide to reduce small bowel mobility. Doses starting with 15 mg 4 times a day gradually increasing up to 60 mg 4 times a day are advised. Octreotide 50-200 µg subcutaneously twice daily can be tried for 3-5 d to reduce diarrhoea but many patients with NENs are already receiving treatment with long acting somatostatin analogues. In addition intravenous fluids and total parenteral nutrition (TPN) can be necessary^[70,97].

Small bacterial overgrowth should be treated with antibiotics but there are no guidelines as to which antibiotic is preferable. Broad spectrum antibiotics which affect enteric aerobes and anaerobes are used and rifaximin may be preferable since it is not absorbed (although not licensed for this indication)^[71,98].

Pancreatic exocrine insufficiency as result of pancreatic surgery or a side effect of somatostatin analogue treatment should be treated with pancreatic enzyme replacement. The dose of pancreatic enzymes needs to be individually adjusted based on dietary fat intake^[99]. This would be ideally managed by a specialized dietician. A suggestion for a starting dose could be 25000 units lipase (or equivalent) with a snack and 2 × 25000 units lipase (or equivalent) with a large meal. This could gradually be increased to 1-2 × 400000 units lipase with a small meal and 120000 units lipase with a

large meal. If symptoms persist compliance and timing of ingestion of pancreatic enzymes should be checked. Acid reduction using proton pump inhibitors may also help to increase efficacy of supplements^[99,100].

A more common side effect from somatostatin analogues can be diarrhoea^[101,102]. These side effects often occur for 2-3 d after the injection but can occur daily and decrease 6-12 mo after starting^[103]. A first step in treatment can be loperamide 2-4 mg 4 times a day and can be increased to 8 mg 4 times a day^[104,105]. Codeine can be added 15 mg 4 times a day and gradually increased to 60 mg 4 times a day^[104,105]. In cases of steatorrhoea pancreatic enzyme replacement therapy as described above can be started.

Malnutrition should also be treated with nutritional support to increase body weight. Several authors advise to include a dietician specialised in NENs to be part of the multidisciplinary team^[49,53]. No systematic guidelines for nutritional support exist in patients with NENs. The American carcinoid cancer foundation published a nutritional guideline in 2000 and updated version in 2009^[106]. This guideline, intended for patients, advises all patients to increase protein intake to restrict carbohydrate servings (fruit, vegetables and whole grains) to 5-10 portions/day, moderate to low fat intake (25%-30% of daily calories) and eat a variety of foods. In patients with CS, foods provoking symptoms containing high levels of amines are advised to be avoided. Examples of foods with high levels of amines are: Mature cheeses (cheddar, camembert, stilton), alcohol beverages, smoked/salted or pickled fish or meat, liver, caffeine containing drinks, chocolate, nuts, bananas, avocado, raspberries^[106].

The ESPEN guideline on nutrition^[13] in cancer recommends a total energy intake ranging between 25-30 kcal/kg/day with a protein intake of 1 g/kg/day but ideally 1.5 g/kg/day. If oral nutrition remains inadequate despite interventions, enteral nutrition is the first choice. Only in the case of severe intestinal insufficiency (radiation enteritis, short bowel syndrome, peritoneal carcinomatosis or chylothorax) should parenteral nutrition (TPN) be considered. The role of parenteral nutrition in patients with cancer is controversial. Economics, traditions and ethical issues will differ between countries. In some countries feeding of palliative cases is essential. These countries tend to report survival benefits for TPN and in selected cases TPN improves quality of life^[107-112]. There are risks of life-threatening catheter infections and septicaemia in the use of TPN^[70]. There is one case report on the use of TPN in a patient with a NEN^[113]. The decision to start enteral nutrition should be made by the multidisciplinary team if malnutrition is not improving with maximal oral and medical support for 3-6 mo. The decision on starting TPN should only be made in highly selected cases.

RECOMMENDATIONS

Screen patients with GEP-NENs for malnutrition every clinic visit (weight, BMI and nutrition screening tool). Screen patients with GEP-NENs on treatment with somatostatin analogues for fat soluble vitamin deficiencies once a year and start supplementation. Screen patients with GEP-NENs and previous small bowel surgery, without treatment somatostatin analogues once a year for fat soluble vitamin deficiencies and start supplementation. Data is lacking on screening of trace elements. In patients with diarrhoea try to analyse the cause and base the treatment on its cause. A patient with GEP-NENs and malnutrition (BMI < 18.5 kg/m² or > 5% weight loss in 3 mo) could benefit from dietician input.

CONCLUSION

There are multiple definitions of malnutrition and not all suitable for use in clinical practice. Although the definition of malnutrition is not clearly defined, up to 40% of patients with GEP-NENs are malnourished. Malnutrition is associated with longer hospital stay, higher complication rate and lower response on treatment in a few small studies. As part of the nutritional status fat soluble vitamin deficiencies are often present in patients with GEP-NENs. Supplementation does not normalise vitamin levels in every patient. The influence of vitamin deficiencies on survival is less clear. Several factors may influence the nutritional status and diarrhoea is the main one. Diarrhoea can have multiple causes in patients with GEP-NENs and requires systematic investigation and treatment. Multidisciplinary care with a dietician is necessary for every malnourished patient with GEP-NENs.

REFERENCES

- 1 **Modlin IM**, Sandor A. An analysis of 8305 cases of carcinoid tumors. *Cancer* 1997; **79**: 813-829 [PMID: 9024720]
- 2 **Dasari A**, Shen C, Halperin D, Zhao B, Zhou S, Xu Y, Shih T, Yao JC. Trends in the Incidence, Prevalence, and Survival Outcomes in Patients With Neuroendocrine Tumors in the United States. *JAMA Oncol* 2017; **3**: 1335-1342 [PMID: 28448665 DOI: 10.1001/jamaoncol.2017.0589]
- 3 **Boyar Cetinkaya R**, Aagnes B, Thiis-Evensen E, Tretli S, Bergstuen DS, Hansen S. Trends in Incidence of Neuroendocrine Neoplasms in Norway: A Report of 16,075 Cases from 1993 through 2010. *Neuroendocrinology* 2017; **104**: 1-10 [PMID: 26562558 DOI: 10.1159/000442207]
- 4 **Guo LJ**, Wang CH, Tang CW. Epidemiological features of gastroenteropancreatic neuroendocrine tumors in Chengdu city with a population of 14 million based on data from a single institution. *Asia Pac J Clin Oncol* 2016; **12**: 284-288 [PMID: 27170574 DOI: 10.1111/ajco.12498]
- 5 **Genus T**, Bouvier C, Wong K, Srirajskanthan R, Rous B, Talbot D, Valle J, Khan M S, Pearce N, Elshafie M, Reed N, Ramage J. Incidence and Prevalence of Neuroendocrine Tumors in England. ENETS abstract [Internet]. 15th Annual ENETS conference (2018). Available from: <https://www.enets.org/incidence-and-prevalence-of-neuroendocrine-tumors-in-england.html>.
- 6 **Lloyd RV**, Osamura RY, Klöppel G, Rosai J. World Health Organization Classification of Tumours of Endocrine Organs. IARC [Internet] 2010; Available from: <http://apps.who.int/bookorders/anglais/detart1.jsp?codlan=1codcol=70codcch=4003>.
- 7 **Lloyd RV**, Osamura RY, Klöppel G, Rosai J. World Health Organization Classification of Tumours of Endocrine Organs. IARC [Internet] 2017; Available from: <http://publications.iarc.fr/Book-And-Report-Series/Who-Iarc-Classification-Of-Tumours/Who-Classification-Of-Tumours-Of-Endocrine-Organs-2017>.
- 8 **Partelli S**, Bartsch DK, Capdevila J, Chen J, Knigge U, Niederle B, Nieveen van Dijkum EJM, Pape UF, Pascher A, Ramage J, Reed N, Ruszniewski P, Scoazec JY, Toumpanakis C, Kianmanesh R, Falconi M; Antibes Consensus Conference participants. ENETS Consensus Guidelines for Standard of Care in Neuroendocrine Tumours: Surgery for Small Intestinal and Pancreatic Neuroendocrine Tumours. *Neuroendocrinology* 2017; **105**: 255-265 [PMID: 28237989 DOI: 10.1159/000464292]
- 9 **Strosberg JR**, Halldanarson TR, Bellizzi AM, Chan JA, Dillon JS, Heaney AP, Kunz PL, O'Dorisio TM, Salem R, Segelov E, Howe JR, Pommier RF, Brendtro K, Bashir MA, Singh S, Soulen MC, Tang L, Zacks JS, Yao JC, Bergsland EK. The North American Neuroendocrine Tumor Society Consensus Guidelines for Surveillance and Medical Management of Midgut Neuroendocrine Tumors. *Pancreas* 2017; **46**: 707-714 [PMID: 28609356 DOI: 10.1097/MPA.0000000000000850]
- 10 **Niederle B**, Pape UF, Costa F, Gross D, Kelestimir F, Knigge U, Öberg K, Pavel M, Perren A, Toumpanakis C, O'Connor J, O'Toole D, Krenning E, Reed N, Kianmanesh R; Vienna Consensus Conference participants. ENETS Consensus Guidelines Update for Neuroendocrine Neoplasms of the Jejunum and Ileum. *Neuroendocrinology* 2016; **103**: 125-138 [PMID: 26758972 DOI: 10.1159/000443170]
- 11 **Ahmed A**, Turner G, King B, Jones L, Culliford D, McCance D, Ardill J, Johnston BT, Poston G, Rees M, Buxton-Thomas M, Caplin M, Ramage JK. Midgut neuroendocrine tumours with liver metastases: Results of the UKINETS study. *Endocr Relat Cancer* 2009; **16**: 885-894 [PMID: 19458024 DOI: 10.1677/ERC-09-0042]
- 12 **Ramage JK**, Ahmed A, Ardill J, Bax N, Breen DJ, Caplin ME, Corrie P, Davar J, Davies AH, Lewington V, Meyer T, Newell-Price J, Poston G, Reed N, Rockall A, Steward W, Thakker RV, Toubanakis C, Valle J, Verbeke C, Grossman AB; UK and Ireland Neuroendocrine Tumour Society. Guidelines for the management of gastroenteropancreatic neuroendocrine (including carcinoid) tumours (NETs). *Gut* 2012; **61**: 6-32 [PMID: 22052063 DOI: 10.1136/gutjnl-2011-300831]
- 13 **Arends J**, Bachmann P, Baracos V, Barthelemy N, Bertz H, Bozzetti F, Fearon K, Hütterer E, Isenring E, Kaasa S, Krznaric Z, Laird B, Larsson M, Laviano A, Mühlebach S, Muscaritoli M, Oldervoll L, Ravasco P, Solheim T, Strasser F, de van der Schueren M, Preiser JC. ESPEN guidelines on nutrition in cancer patients. *Clin Nutr* 2017; **36**: 11-48 [PMID: 27637832 DOI: 10.1016/j.clnu.2016.07.015]
- 14 **Fearon K**, Strasser F, Anker SD, Bosaeus I, Bruera E, Fainsinger RL, Jatoi A, Loprinzi C, MacDonald N, Mantovani G, Davis M, Muscaritoli M, Ottery F, Radbruch L, Ravasco P, Walsh D, Wilcock A, Kaasa S, Baracos VE. Definition and classification of cancer cachexia: An international consensus. *Lancet Oncol* 2011; **12**: 489-495 [PMID: 21296615 DOI: 10.1016/S1470-2045(10)70218-7]
- 15 **Gallo M**, Muscogiuri G, Pizza G, Ruggeri RM, Barrea L, Faggiano A, Colao A; NIKE Group. The management of neuroendocrine tumours: A nutritional viewpoint. *Crit Rev Food Sci Nutr* 2017; 1-12 [PMID: 29020456 DOI: 10.1080/10408398.2017.1390729]
- 16 **Teigen LM**, Kuchnia AJ, Nagel EM, Price KL, Hurt RT, Earthman CP. Diagnosing clinical malnutrition: Perspectives from the past and implications for the future. *Clin Nutr ESPEN* 2018; **26**: 13-20 [PMID: 29908677 DOI: 10.1016/j.clnesp.2018.05.006]
- 17 **NHS definition**. Available from: <https://www.nhs.uk/conditions/malnutrition/>
- 18 **WHO definition**. Available from: <http://www.who.int/features/qa/malnutrition/en/>
- 19 **Cederholm T**, Bosaeus I, Barazzoni R, Bauer J, Van Gossum A, Klek S, Muscaritoli M, Nyulasi I, Ockenga J, Schneider SM, de van der Schueren MA, Singer P. Diagnostic criteria for malnutrition - An ESPEN Consensus Statement. *Clin Nutr* 2015; **34**: 335-340 [PMID: 25799486 DOI: 10.1016/j.clnu.2015.03.001]
- 20 **Malone A**, Hamilton C. The Academy of Nutrition and Dietetics/the American Society for Parenteral and Enteral Nutrition consensus malnutrition characteristics: Application in practice. *Nutr Clin Pract* 2013; **28**: 639-650 [PMID: 24177285 DOI: 10.1177/0884533613508435]
- 21 **Muscaritoli M**, Lucia S, Farcomeni A, Lorusso V, Saracino V, Barone C, Plastino F, Gori S, Magarotto R, Carteni G, Chiurazzi B, Pavese I, Marchetti L, Zagonel V, Bergo E, Tonini G, Imperatori M, Iacono C, Maiorana L, Pinto C, Rubino D, Cavanna L, Di Cicilia R, Gamucci T, Quadri S, Palazzo S, Minardi S, Merlano M, Colucci G, Marchetti P; PreMiO Study Group. Prevalence of malnutrition in patients at first medical oncology visit: The PreMiO study. *Oncotarget* 2017; **8**: 79884-79896 [PMID: 29108370 DOI: 10.18632/oncotarget.20168]
- 22 **Du H**, Liu B, Xie Y, Liu J, Wei Y, Hu H, Luo B, Li Z. Comparison of different methods for nutrition assessment in patients with tumors. *Oncol Lett* 2017; **14**: 165-170 [PMID: 28693149 DOI: 10.3892/ol.2017.6154]

Krishnasamy K, Li Yoong T, Mei Chan C, Choong LP, Chinna K. Identifying Malnutrition: Nutritional

- 23 Status in Newly Diagnosed Patients With Cancer. *CJON* 2017; **21**: E23-E29 [DOI: [10.1188/17.CJON.E23-E29](https://doi.org/10.1188/17.CJON.E23-E29)]
- 24 **Caccialanza R**, Cereda E, Pinto C, Cotogni P, Farina G, Gavazzi C, Gandini C, Nardi M, Zagonel V, Pedrazzoli P. Awareness and consideration of malnutrition among oncologists: Insights from an exploratory survey. *Nutrition* 2016; **32**: 1028-1032 [PMID: [27066746](https://pubmed.ncbi.nlm.nih.gov/27066746/) DOI: [10.1016/j.nut.2016.02.005](https://doi.org/10.1016/j.nut.2016.02.005)]
- 25 **Lim S**, Reynolds M, Chaudhry R, Blackhouse J, Rees A, Khan M. Nutritional assessment and vitamin deficiencies in patients with NETs. *Endocrine Abstracts* 2017 [DOI: [10.1530/endoabs.52.P06](https://doi.org/10.1530/endoabs.52.P06)]
- 26 **Borre M**, Dam GA, Knudsen AW, Grønbaek H. Nutritional status and nutritional risk in patients with neuroendocrine tumors. *Scand J Gastroenterol* 2018; **53**: 284-292 [PMID: [29373941](https://pubmed.ncbi.nlm.nih.gov/29373941/) DOI: [10.1080/00365521.2018.1430848](https://doi.org/10.1080/00365521.2018.1430848)]
- 27 **Robbins HL**, Symington M, Mosterman B, Goodby J, Davies L, Dimitriadis GK, Kaltsas G, Randeve HS, Weickert MO. Supplementation of Vitamin D Deficiency in Patients with Neuroendocrine Tumors Using Over-the-Counter Vitamin D3 Preparations. *Nutr Cancer* 2018; **70**: 748-754 [PMID: [29781720](https://pubmed.ncbi.nlm.nih.gov/29781720/) DOI: [10.1080/01635581.2018.1470650](https://doi.org/10.1080/01635581.2018.1470650)]
- 28 **Pavel M**, Gross DJ, Benavent M, Perros P, Srirajakanthan R, Warner RRP, Kulke MH, Anthony LB, Kunz PL, Hörsch D, Weickert MO, Lapuerta P, Jiang W, Kassler-Taub K, Wason S, Fleming R, Fleming D, Garcia-Carbonero R. Telotristat ethyl in carcinoid syndrome: Safety and efficacy in the TELECAST phase 3 trial. *Endocr Relat Cancer* 2018; **25**: 309-322 [PMID: [29330194](https://pubmed.ncbi.nlm.nih.gov/29330194/) DOI: [10.1530/ERC-17-0455](https://doi.org/10.1530/ERC-17-0455)]
- 29 **Maasberg S**, Knappe-Drzikova B, Vonderbeck D, Jann H, Weylandt KH, Grieser C, Pascher A, Scheffold JC, Pavel M, Wiedenmann B, Sturm A, Pape UF. Malnutrition Predicts Clinical Outcome in Patients with Neuroendocrine Neoplasia. *Neuroendocrinology* 2017; **104**: 11-25 [PMID: [26641457](https://pubmed.ncbi.nlm.nih.gov/26641457/) DOI: [10.1159/000442983](https://doi.org/10.1159/000442983)]
- 30 **Qureshi SA**, Burch N, Druce M, Hattersley JG, Khan S, Gopalakrishnan K, Darby C, Wong JL, Davies L, Fletcher S, Shatwell W, Sothi S, Randeve HS, Dimitriadis GK, Weickert MO. Screening for malnutrition in patients with gastro-entero-pancreatic neuroendocrine tumours: A cross-sectional study. *BMJ Open* 2016; **6**: e010765 [PMID: [27147385](https://pubmed.ncbi.nlm.nih.gov/27147385/) DOI: [10.1136/bmjopen-2015-010765](https://doi.org/10.1136/bmjopen-2015-010765)]
- 31 **Glazer E**, Stanko K, Ong E, Guerrero M. Decreased Inpatient Mortality in Obese Patients with Abdominal Nets. *Endocr Pract* 2014; **1**-20 [PMID: [25100391](https://pubmed.ncbi.nlm.nih.gov/25100391/) DOI: [10.4158/EP14203.OR](https://doi.org/10.4158/EP14203.OR)]
- 32 **Ekeblad S**, Skogseid B, Dunder K, Oberg K, Eriksson B. Prognostic factors and survival in 324 patients with pancreatic endocrine tumor treated at a single institution. *Clin Cancer Res* 2008; **14**: 7798-7803 [PMID: [19047107](https://pubmed.ncbi.nlm.nih.gov/19047107/) DOI: [10.1158/1078-0432.CCR-08-0734](https://doi.org/10.1158/1078-0432.CCR-08-0734)]
- 33 **Marrache F**, Vullierme MP, Roy C, El Assoued Y, Couvelard A, O'Toole D, Mity E, Hentic O, Hammel P, Lévy P, Ravaud P, Rougier P, Ruszniewski P. Arterial phase enhancement and body mass index are predictors of response to chemoembolisation for liver metastases of endocrine tumours. *Br J Cancer* 2007; **96**: 49-55 [PMID: [17164755](https://pubmed.ncbi.nlm.nih.gov/17164755/) DOI: [10.1038/sj.bjc.6603526](https://doi.org/10.1038/sj.bjc.6603526)]
- 34 **Fiebrich HB**, Van Den Berg G, Kema IP, Links TP, Kleibeuker JH, Van Beek AP, Walenkamp AM, Sluiter WJ, De Vries EG. Deficiencies in fat-soluble vitamins in long-term users of somatostatin analogue. *Aliment Pharmacol Ther* 2010; **32**: 1398-1404 [PMID: [21050243](https://pubmed.ncbi.nlm.nih.gov/21050243/) DOI: [10.1111/j.1365-2036.2010.04479.x](https://doi.org/10.1111/j.1365-2036.2010.04479.x)]
- 35 **de Hosson LD**, Stelwagen J, Bouma G, Sijtema B, Huitema S, van Faassen HJR, de Bock GH, de Groot DJA, Campmans-Kuijpers MJE, Kema IP, de Vries EGE, Walenkamp AME. Towards optimal personalized diet and vitamin supplementation in NET patients. *Endocr Relat Cancer* 2018; **25**: L23-L26 [PMID: [29431642](https://pubmed.ncbi.nlm.nih.gov/29431642/) DOI: [10.1530/ERC-17-0549](https://doi.org/10.1530/ERC-17-0549)]
- 36 **Massironi S**, Zilli A, Bernasconi S, Fanetti I, Cavalcoli F, Ciafardini C, Felicetta I, Conte D. Impact of Vitamin D on the Clinical Outcome of Gastro-Entero-Pancreatic Neuroendocrine Neoplasms: Report on a Series from a Single Institute. *Neuroendocrinology* 2017; **105**: 403-411 [PMID: [28122374](https://pubmed.ncbi.nlm.nih.gov/28122374/) DOI: [10.1159/000456619](https://doi.org/10.1159/000456619)]
- 37 **Motylewska E**, Gawronska J, Niedziela A, Melen-Mucha G, Lawnicka H, Komorowski J, Swietoslowski J, Stepień H. Somatostatin Analogs and Tumor Localization Do Not Influence Vitamin D Concentration in Patients with Neuroendocrine Tumors. *Nutr Cancer* 2016; **68**: 428-434 [PMID: [27028957](https://pubmed.ncbi.nlm.nih.gov/27028957/) DOI: [10.1080/01635581.2016.1152387](https://doi.org/10.1080/01635581.2016.1152387)]
- 38 **Lind A**, Wängberg B, Ellegård L. Vitamin D and vitamin B12 deficiencies are common in patients with midgut carcinoid (SI-NET). *Eur J Clin Nutr* 2016; **70**: 990-994 [PMID: [27026421](https://pubmed.ncbi.nlm.nih.gov/27026421/) DOI: [10.1038/ejcn.2016.40](https://doi.org/10.1038/ejcn.2016.40)]
- 39 **van der Lely AJ**, de Herder WW. Carcinoid syndrome: Diagnosis and medical management. *Arq Bras Endocrinol Metabol* 2005; **49**: 850-860 [PMID: [16444370](https://pubmed.ncbi.nlm.nih.gov/16444370/) DOI: [10.1590/S0004-27302005000500028](https://doi.org/10.1590/S0004-27302005000500028)]
- 40 **Fukuwatari T**, Shibata K. Nutritional aspect of tryptophan metabolism. *Int J Tryptophan Res* 2013; **6**: 3-8 [PMID: [23922498](https://pubmed.ncbi.nlm.nih.gov/23922498/) DOI: [10.4137/IJTR.S11588](https://doi.org/10.4137/IJTR.S11588)]
- 41 **Bax ND**, Woods HF, Batchelor A, Jennings M. Clinical manifestations of carcinoid disease. *World J Surg* 1996; **20**: 142-146 [PMID: [8661809](https://pubmed.ncbi.nlm.nih.gov/8661809/) DOI: [10.1007/s002689900022](https://doi.org/10.1007/s002689900022)]
- 42 **Shah GM**, Shah RG, Veillette H, Kirkland JB, Pasieka JL, Warner RR. Biochemical assessment of niacin deficiency among carcinoid cancer patients. *Am J Gastroenterol* 2005; **100**: 2307-2314 [PMID: [16181385](https://pubmed.ncbi.nlm.nih.gov/16181385/) DOI: [10.1111/j.1572-0241.2005.00268.x](https://doi.org/10.1111/j.1572-0241.2005.00268.x)]
- 43 **Bouma G**, van Faassen M, Kats-Ugurlu G, de Vries EG, Kema IP, Walenkamp AM. Niacin (Vitamin B3) Supplementation in Patients with Serotonin-Producing Neuroendocrine Tumor. *Neuroendocrinology* 2016; **103**: 489-494 [PMID: [26335390](https://pubmed.ncbi.nlm.nih.gov/26335390/) DOI: [10.1159/000440621](https://doi.org/10.1159/000440621)]
- 44 **Ströhle A**, Zänker K, Hahn A. Nutrition in oncology: The case of micronutrients (review). *Oncol Rep* 2010; **24**: 815-828 [PMID: [20811659](https://pubmed.ncbi.nlm.nih.gov/20811659/) DOI: [10.3892/or.2010.815](https://doi.org/10.3892/or.2010.815)]
- 45 **Moncayo R**, Traeger A. Decreased selenium levels after peptide receptor radionuclide therapy (PRRT) in patients with neuroendocrine tumours: Implications for the antioxidant status. *Eur J Nucl Med Mol Imaging* 2011; **38**: 1580-1581 [PMID: [21604005](https://pubmed.ncbi.nlm.nih.gov/21604005/) DOI: [10.1007/s00259-011-1839-4](https://doi.org/10.1007/s00259-011-1839-4)]
- 46 **Baracos VE**, Martin L, Korc M, Guttridge DC, Fearon KCH. Cancer-associated cachexia. *Nat Rev Dis Primers* 2018; **4**: 17105 [PMID: [29345251](https://pubmed.ncbi.nlm.nih.gov/29345251/) DOI: [10.1038/nrdp.2017.105](https://doi.org/10.1038/nrdp.2017.105)]
- 47 **Vujasinovic M**, Valente R, Del Chiaro M, Permert J, Löhner JM. Pancreatic Exocrine Insufficiency in Pancreatic Cancer. *Nutrients* 2017; **9**: pii: E183 [PMID: [28241470](https://pubmed.ncbi.nlm.nih.gov/28241470/) DOI: [10.3390/nu9030183](https://doi.org/10.3390/nu9030183)]
- 48 **Kaltsas GA**, Besser GM, Grossman AB. The diagnosis and medical management of advanced neuroendocrine tumors. *Endocr Rev* 2004; **25**: 458-511 [PMID: [15180952](https://pubmed.ncbi.nlm.nih.gov/15180952/) DOI: [10.1210/er.2003-0014](https://doi.org/10.1210/er.2003-0014)]
- 49 **Go VL**, Srihari P, Kamerman Burns LA. Nutrition and gastroenteropancreatic neuroendocrine tumors. *Endocrinol Metab Clin North Am* 2010; **39**: 827-837 [PMID: [21095548](https://pubmed.ncbi.nlm.nih.gov/21095548/) DOI: [10.1016/j.ecl.2010.08.003](https://doi.org/10.1016/j.ecl.2010.08.003)]
- 50 **Vinik AI**, Thompson N, Eckhauser F, Moattari AR. Clinical features of carcinoid syndrome and the use of somatostatin analogue in its management. *Acta Oncol* 1989; **28**: 389-402 [PMID: [2663049](https://pubmed.ncbi.nlm.nih.gov/2663049/) DOI: [10.1080/00016348908838949](https://doi.org/10.1080/00016348908838949)]

- 10.3109/02841868909111212]
- 51 **Läuffer JM**, Zhang T, Modlin IM. Review article: Current status of gastrointestinal carcinoids. *Aliment Pharmacol Ther* 1999; **13**: 271-287 [PMID: 10102959 DOI: 10.1046/j.1365-2036.1999.00479.x]
 - 52 **Aggarwal G**, Obideen K, Wehbi M. Carcinoid tumors: What should increase our suspicion? *Cleve Clin J Med* 2008; **75**: 849-855 [PMID: 19088003 DOI: 10.3949/ccjm.75a.08002]
 - 53 **Sagar VM**, Cooper SC, Johnson J, Shetty S, Shah T. Gastrointestinal manifestations of neuroendocrine tumours: Their investigation and management. *Postgrad Med J* 2017; **93**: 494-497 [PMID: 28600342 DOI: 10.1136/postgradmedj-2017-134847]
 - 54 **Daskalakis K**, Karakatsanis A, Ståhlberg P, Norlén O, Hellman P. Clinical signs of fibrosis in small intestinal neuroendocrine tumours. *Br J Surg* 2017; **104**: 69-75 [PMID: 27861745 DOI: 10.1002/bjs.10333]
 - 55 **Dimitriadis GK**, Weickert MO, Randeve HS, Kaltsas G, Grossman A. Medical management of secretory syndromes related to gastroenteropancreatic neuroendocrine tumours. *Endocr Relat Cancer* 2016; **23**: R423-R436 [PMID: 27461388 DOI: 10.1530/ERC-16-0200]
 - 56 **Berghöfer P**, Fragkos KC, Baxter JP, Forbes A, Joly F, Heinze H, Loth S, Pertkiewicz M, Messing B, Jeppesen PB. Development and validation of the disease-specific Short Bowel Syndrome-Quality of Life (SBS-QoL™) scale. *Clin Nutr* 2013; **32**: 789-796 [PMID: 23274148 DOI: 10.1016/j.clnu.2012.12.001]
 - 57 **Arnold R**. Medical treatment of metastasizing carcinoid tumors. *World J Surg* 1996; **20**: 203-207 [PMID: 8661818 DOI: 10.1007/s002689900031]
 - 58 **Zaidel O**, Lin HC. Uninvited Guests: The Impact of Small Intestinal Bacterial Overgrowth on Nutritional Status. *Pract Gastroenterol* 2003; 27-34
 - 59 **Lamrani A**, Vidon N, Sogni P, Nepveux P, Catus F, Blumberg J, Chaussade S. Effects of lanreotide, a somatostatin analogue, on postprandial gastric functions and biliopancreatic secretions in humans. *Br J Clin Pharmacol* 1997; **43**: 65-70 [PMID: 9056054 DOI: 10.1111/j.1365-2125.1997.tb00034.x]
 - 60 **Johansson C**, Kollberg B, Efendic S, Uvnäs-Wallensten K. Effects of graded doses of somatostatin on gallbladder emptying and pancreatic enzyme output after oral glucose in man. *Digestion* 1981; **22**: 24-31 [PMID: 6166507 DOI: 10.1159/000198591]
 - 61 **Halperin DM**, Shen C, Dasari A, Xu Y, Chu Y, Zhou S, Shih YT, Yao JC. Frequency of carcinoid syndrome at neuroendocrine tumour diagnosis: A population-based study. *Lancet Oncol* 2017; **18**: 525-534 [PMID: 28238592 DOI: 10.1016/S1470-2045(17)30110-9]
 - 62 **Fottner C**, Ferrata M, Weber MM. Hormone secreting gastro-entero-pancreatic neuroendocrine neoplasias (GEP-NEN): When to consider, how to diagnose? *Rev Endocr Metab Disord* 2017; **18**: 393-410 [PMID: 29256148 DOI: 10.1007/s11154-017-9438-8]
 - 63 **Cheung VTF**, Khan MS. A guide to midgut neuroendocrine tumours (NETs) and carcinoid syndrome. *Frontline Gastroenterol* 2015; **6**: 264-269 [PMID: 28839822 DOI: 10.1136/flgastro-2014-100483]
 - 64 **Tormey WP**, FitzGerald RJ. The clinical and laboratory correlates of an increased urinary 5-hydroxyindoleacetic acid. *Postgrad Med J* 1995; **71**: 542-545 [PMID: 7479466 DOI: 10.1136/pgmj.71.839.542]
 - 65 **Sciarretta G**, Vicini G, Fagioli G, Verri A, Ginevra A, Malaguti P. Use of 23-selena-25-homocholytaurine to detect bile acid malabsorption in patients with ileal dysfunction or diarrhea. *Gastroenterology* 1986; **91**: 1-9 [PMID: 3710057 DOI: 10.1016/0016-5085(86)90431-2]
 - 66 **Damsgaard B**, Dalby HR, Krogh K, Jørgensen SMD, Arveschou AK, Agnholt J, Dahlerup JF, Jørgensen SP. Long-term effect of medical treatment of diarrhoea in 377 patients with SeHCAT scan diagnosed bile acid malabsorption from 2003 to 2016; a retrospective study. *Aliment Pharmacol Ther* 2018; **47**: 951-957 [PMID: 29368342 DOI: 10.1111/apt.14533]
 - 67 **Wedlake L**, A'Hern R, Russell D, Thomas K, Walters JR, Andreyev HJ. Systematic review: The prevalence of idiopathic bile acid malabsorption as diagnosed by SeHCAT scanning in patients with diarrhoea-predominant irritable bowel syndrome. *Aliment Pharmacol Ther* 2009; **30**: 707-717 [PMID: 19570102 DOI: 10.1111/j.1365-2036.2009.04081.x]
 - 68 **Donnelly L**, Tailor S, Reid K, Williams M, Lewis J, Jones B, Rees A, Khan M. A Prospective Service Evaluation of Systematic Gastroenterological Assessment and Management on Patients with Neuroendocrine Tumours in South East Wales. ENETS abstract [Internet]. 14th Annual ENETS conference (2017). Available from: <https://www.enets.org/a-prospective-service-evaluation-of-systematic-gastroenterological-assessment-and-management-on-patients-with-neuroendocrine-tumours-in-south-east-wales.html>
 - 69 **Pironi L**, Corcos O, Forbes A, Holst M, Joly F, Jonkers C, Klek S, Lal S, Blaser AR, Rollins KE, Sasdelli AS, Shaffer J, Van Gossum A, Wanten G, Zanfi C, Lobo DN; ESPEN Acute and Chronic Intestinal Failure Special Interest Groups. Intestinal failure in adults: Recommendations from the ESPEN expert groups. *Clin Nutr* 2018; **37**: 1798-1809 [PMID: 30172658 DOI: 10.1016/j.clnu.2018.07.036]
 - 70 **Nightingale J**, Woodward JM; Small Bowel and Nutrition Committee of the British Society of Gastroenterology. Guidelines for management of patients with a short bowel. *Gut* 2006; **55** Suppl 4: iv1-ii2 [PMID: 16837533 DOI: 10.1136/gut.2006.091108]
 - 71 **Sachdev AH**, Pimentel M. Gastrointestinal bacterial overgrowth: Pathogenesis and clinical significance. *Ther Adv Chronic Dis* 2013; **4**: 223-231 [PMID: 23997926 DOI: 10.1177/2040622313496126]
 - 72 **Siddiqui I**, Ahmed S, Abid S. Update on diagnostic value of breath test in gastrointestinal and liver diseases. *World J Gastrointest Pathophysiol* 2016; **7**: 256-265 [PMID: 27574563 DOI: 10.4291/wjgp.v7.i3.256]
 - 73 **Corazza GR**, Menozzi MG, Strocchi A, Rasciti L, Vaira D, Lecchini R, Avanzini P, Chezzi C, Gasbarrini G. The diagnosis of small bowel bacterial overgrowth. Reliability of jejunal culture and inadequacy of breath hydrogen testing. *Gastroenterology* 1990; **98**: 302-309 [PMID: 2295385 DOI: 10.1016/0016-5085(90)90818-L]
 - 74 **Gan C**, Chen YH, Liu L, Gao JH, Tong H, Tang CW, Liu R. Efficacy and safety of pancreatic enzyme replacement therapy on exocrine pancreatic insufficiency: A meta-analysis. *Oncotarget* 2017; **8**: 94920-94931 [PMID: 29212278 DOI: 10.18632/oncotarget.21659]
 - 75 **Maignan A**, Ouaïssi M, Turrini O, Regenet N, Loundou A, Louis G, Moutardier V, Dahan L, Pirrò N, Sastre B, Delpero JR, Sielezneff I. Risk factors of exocrine and endocrine pancreatic insufficiency after pancreatic resection: A multi-center prospective study. *J Visc Surg* 2018; **155**: 173-181 [PMID: 29396112 DOI: 10.1016/j.jvisc Surg.2017.10.007]
 - 76 **Löser C**, Möllgaard A, Fölsch UR. Faecal elastase 1: A novel, highly sensitive, and specific tubeless pancreatic function test. *Gut* 1996; **39**: 580-586 [PMID: 8944569 DOI: 10.1136/gut.39.4.580]
 - 77 **Domínguez-Muñoz JE**, Hieronymus C, Sauerbruch T, Malfertheiner P. Fecal elastase test: Evaluation of a

- new noninvasive pancreatic function test. *Am J Gastroenterol* 1995; **90**: 1834-1837 [PMID: 7572904]
- 78 **Gullo L**, Ventrucci M, Tomassetti P, Migliori M, Pezzilli R. Fecal elastase 1 determination in chronic pancreatitis. *Dig Dis Sci* 1999; **44**: 210-213 [PMID: 9952246 DOI: 10.1023/A:1026691209094]
- 79 **Chaudhry R**, Newbould R, Williams M, Reid K, Donnelly L, Lewis J, Khan M. Evaluation of Faecal Elastase 1 in Symptomatic Patients with Neuroendocrine Tumours. *Endocrine Abstracts* 2016 [DOI: 10.1530/endoabs.46.P23]
- 80 **Lamarca A**, McCallum L, Nuttall C, Barriuso J, Backen A, Frizziero M, Leon R, Mansoor W, McNamara MG, Hubner RA, Valle JW. Somatostatin analogue-induced pancreatic exocrine insufficiency in patients with neuroendocrine tumors: Results of a prospective observational study. *Expert Rev Gastroenterol Hepatol* 2018; **12**: 723-731 [PMID: 29923433 DOI: 10.1080/17474124.2018.1489232]
- 81 **Ho PJ**, Boyajy LD, Greenstein E, Barkan AL. Effect of chronic octreotide treatment on intestinal absorption in patients with acromegaly. *Dig Dis Sci* 1993; **38**: 309-315 [PMID: 8425442 DOI: 10.1007/BF01307549]
- 82 **Oberg K**, Kvols L, Caplin M, Delle Fave G, de Herder W, Rindi G, Ruzsiewicz P, Woltering EA, Wiedenmann B. Consensus report on the use of somatostatin analogs for the management of neuroendocrine tumors of the gastroenteropancreatic system. *Ann Oncol* 2004; **15**: 966-973 [PMID: 15151956 DOI: 10.1093/annonc/mdh216]
- 83 **Eriksson B**, Oberg K. Summing up 15 years of somatostatin analog therapy in neuroendocrine tumors: Future outlook. *Ann Oncol* 1999; **10** Suppl 2: S31-S38 [PMID: 10399030 DOI: 10.1093/annonc/10.suppl_2.S31]
- 84 **Strosberg JR**, Benson AB, Huynh L, Duh MS, Goldman J, Sahai V, Rademaker AW, Kulke MH. Clinical benefits of above-standard dose of octreotide LAR in patients with neuroendocrine tumors for control of carcinoid syndrome symptoms: A multicenter retrospective chart review study. *Oncologist* 2014; **19**: 930-936 [PMID: 25096997 DOI: 10.1634/theoncologist.2014-0120]
- 85 **Riechelmann RP**, Pereira AA, Rego JF, Costa FP. Refractory carcinoid syndrome: A review of treatment options. *Ther Adv Med Oncol* 2017; **9**: 127-137 [PMID: 28203303 DOI: 10.1177/1758834016675803]
- 86 **Modlin IM**, Latich I, Kidd M, Zikusoka M, Eick G. Therapeutic options for gastrointestinal carcinoids. *Clin Gastroenterol Hepatol* 2006; **4**: 526-547 [PMID: 16630755 DOI: 10.1016/j.cgh.2005.12.008]
- 87 **Ganetsky A**, Bhatt V. Gastroenteropancreatic neuroendocrine tumors: Update on therapeutics. *Ann Pharmacother* 2012; **46**: 851-862 [PMID: 22589450 DOI: 10.1345/aph.1Q729]
- 88 **Toumpanakis C**, Meyer T, Caplin ME. Cytotoxic treatment including embolization/chemoembolization for neuroendocrine tumours. *Best Pract Res Clin Endocrinol Metab* 2007; **21**: 131-144 [PMID: 17382269 DOI: 10.1016/j.beem.2007.01.005]
- 89 **Kennedy A**, Bester L, Salem R, Sharma RA, Parks RW, Ruzsiewicz P; NET-Liver-Metastases Consensus Conference. Role of hepatic intra-arterial therapies in metastatic neuroendocrine tumours (NET): Guidelines from the NET-Liver-Metastases Consensus Conference. *HPB (Oxford)* 2015; **17**: 29-37 [PMID: 25186181 DOI: 10.1111/hpb.12326]
- 90 **Jia Z**, Wang W. Yttrium-90 radioembolization for unresectable metastatic neuroendocrine liver tumor: A systematic review. *Eur J Radiol* 2018; **100**: 23-29 [PMID: 29496075 DOI: 10.1016/j.ejrad.2018.01.012]
- 91 **Kennedy AS**, Dezam WA, McNeillie P, Coldwell D, Nutting C, Carter D, Murthy R, Rose S, Warner RR, Liu D, Palmedo H, Overton C, Jones B, Salem R. Radioembolization for unresectable neuroendocrine hepatic metastases using resin 90Y-microspheres: Early results in 148 patients. *Am J Clin Oncol* 2008; **31**: 271-279 [PMID: 18525307 DOI: 10.1097/COC.0b013e31815e4557]
- 92 **Kulke MH**, Hörsch D, Caplin ME, Anthony LB, Bergsland E, Öberg K, Welin S, Warner RR, Lombard-Bohas C, Kunz PL, Grande E, Valle JW, Fleming D, Lapuerta P, Banks P, Jackson S, Zambrowicz B, Sands AT, Pavel M. Telotristat Ethyl, a Tryptophan Hydroxylase Inhibitor for the Treatment of Carcinoid Syndrome. *J Clin Oncol* 2017; **35**: 14-23 [PMID: 27918724 DOI: 10.1200/JCO.2016.69.2780]
- 93 **Weickert MO**, Kaltsas G, Hörsch D, Lapuerta P, Pavel M, Valle JW, Caplin ME, Bergsland E, Kunz PL, Anthony LB, Grande E, Öberg K, Welin S, Lombard-Bohas C, Ramage JK, Kittur A, Yang QM, Kulke MH. Changes in Weight Associated With Telotristat Ethyl in the Treatment of Carcinoid Syndrome. *Clin Ther* 2018; **40**: 952-962.e2 [PMID: 29724499 DOI: 10.1016/j.clinthera.2018.04.006]
- 94 **Wymenga AN**, de Vries EG, Leijma MK, Kema IP, Kleibeuker JH. Effects of ondansetron on gastrointestinal symptoms in carcinoid syndrome. *Eur J Cancer* 1998; **34**: 1293-1294 [PMID: 9849494 DOI: 10.1016/S0959-8049(98)00009-4]
- 95 **Kiesewetter B**, Duan H, Lamm W, Haug A, Riss P, Selberherr A, Scheuba C, Raderer M. Oral Ondansetron Offers Effective Antidiarrheal Activity for Carcinoid Syndrome Refractory to Somatostatin Analogs. *Oncologist* 2019; **24**: 255-258 [PMID: 30171068 DOI: 10.1634/theoncologist.2018-0191]
- 96 **Borghede MK**, Schlüter JM, Agnholt JS, Christensen LA, Gormsen LC, Dahlerup JF. Bile acid malabsorption investigated by selenium-75-homocholic acid taurine ((75)SeHCAT) scans: Causes and treatment responses to cholestyramine in 298 patients with chronic watery diarrhoea. *Eur J Intern Med* 2011; **22**: e137-e140 [PMID: 22075299 DOI: 10.1016/j.ejim.2011.08.013]
- 97 **Baker ML**, Williams RN, Nightingale JM. Causes and management of a high-output stoma. *Colorectal Dis* 2011; **13**: 191-197 [PMID: 19888956 DOI: 10.1111/j.1463-1318.2009.02107.x]
- 98 **Gatta L**, Scarpignato C. Systematic review with meta-analysis: Rifaximin is effective and safe for the treatment of small intestine bacterial overgrowth. *Aliment Pharmacol Ther* 2017; **45**: 604-616 [PMID: 28078798 DOI: 10.1111/apt.13928]
- 99 **Sikkens EC**, Cahen DL, van Eijck C, Kuipers EJ, Bruno MJ. The daily practice of pancreatic enzyme replacement therapy after pancreatic surgery: A northern European survey: Enzyme replacement after surgery. *J Gastrointest Surg* 2012; **16**: 1487-1492 [PMID: 22711213 DOI: 10.1007/s11605-012-1927-1]
- 100 **Keller J**, Loyer P. Pancreatic Enzyme Supplementation Therapy. *Curr Treat Options Gastroenterol* 2003; **6**: 369-374 [PMID: 12954143 DOI: 10.1007/s11938-003-0039-0]
- 101 **Rinke A**, Müller HH, Schade-Brittinger C, Klose KJ, Barth P, Wied M, Mayer C, Aminossadati B, Pape UF, Bläker M, Harder J, Arnold C, Gress T, Arnold R; PROMID Study Group. Placebo-controlled, double-blind, prospective, randomized study on the effect of octreotide LAR in the control of tumor growth in patients with metastatic neuroendocrine midgut tumors: A report from the PROMID Study Group. *J Clin Oncol* 2009; **27**: 4656-4663 [PMID: 19704057 DOI: 10.1200/JCO.2009.22.8510]
- 102 **Newman CB**, Melmed S, Snyder PJ, Young WF, Boyajy LD, Levy R, Stewart WN, Klibanski A, Molitch ME, Gagel RF. Safety and efficacy of long-term octreotide therapy of acromegaly: Results of a multicenter trial in 103 patients--a clinical research center study. *J Clin Endocrinol Metab* 1995; **80**: 2768-2775 [PMID: 7673422 DOI: 10.1210/jcem.80.9.7673422]
- 103 **Flogstad AK**, Halse J, Bakke S, Lanrcanjan I, Marbach P, Bruns C, Jervell J. Sandostatin LAR in

- acromegalic patients: Long-term treatment. *J Clin Endocrinol Metab* 1997; **82**: 23-28 [PMID: 8989226 DOI: 10.1210/jcem.82.1.3572]
- 104 **Arnold R**, Simon B, Wied M. Treatment of neuroendocrine GEP tumours with somatostatin analogues: A review. *Digestion* 2000; **62** Suppl 1: 84-91 [PMID: 10940693 DOI: 10.1159/000051861]
- 105 **Arnold R**, Trautmann ME, Creutzfeldt W, Benning R, Benning M, Neuhaus C, Jürgensen R, Stein K, Schäfer H, Bruns C, Dennler HJ. Somatostatin analogue octreotide and inhibition of tumour growth in metastatic endocrine gastroenteropancreatic tumours. *Gut* 1996; **38**: 430-438 [PMID: 8675099 DOI: 10.1136/gut.38.3.430]
- 106 **Warner ME**. Nutritional concerns for the carcinoid patient: Developing nutrition guidelines for persons with carcinoid disease. Carcinoid Cancer Foundation, Inc., New York, 2009. Available from: <https://www.carcinoid.org/for-patients/general-information/nutrition/nutritional-concerns-for-the-carcinoid-patient-developing-nutrition-guidelines-for-persons-with-carcinoid-disease/>
- 107 **Obling SR**, Wilson BV, Pfeiffer P, Kjeldsen J. Home parenteral nutrition increases fat free mass in patients with incurable gastrointestinal cancer. Results of a randomized controlled trial. *Clin Nutr* 2019; **38**: 182-190 [PMID: 29305245 DOI: 10.1016/j.clnu.2017.12.011]
- 108 **Cotogni P**. Enteral versus parenteral nutrition in cancer patients: Evidences and controversies. *Ann Palliat Med* 2016; **5**: 42-49 [PMID: 26841814 DOI: 10.3978/j.issn.2224-5820.2016.01.05]
- 109 **Vashi PG**, Dahlk S, Popiel B, Lammersfeld CA, Ireton-Jones C, Gupta D. A longitudinal study investigating quality of life and nutritional outcomes in advanced cancer patients receiving home parenteral nutrition. *BMC Cancer* 2014; **14**: 593 [PMID: 25128023 DOI: 10.1186/1471-2407-14-593]
- 110 **Senesse P**, Tadmouri A, Culine S, Dufour PR, Seys P, Radji A, Rotarski M, Balian A, Chambrier C. A prospective observational study assessing home parenteral nutrition in patients with gastrointestinal cancer: Benefits for quality of life. *J Pain Symptom Manage* 2015; **49**: 183-191.e2 [PMID: 24945492 DOI: 10.1016/j.jpainsymman.2014.05.016]
- 111 **Bozzetti F**, Cozzaglio L, Biganzoli E, Chiavenna G, De Cicco M, Donati D, Gilli G, Percolla S, Pironi L. Quality of life and length of survival in advanced cancer patients on home parenteral nutrition. *Clin Nutr* 2002; **21**: 281-288 [PMID: 12135587 DOI: 10.1054/clnu.2002.0560]
- 112 **Hoda D**, Jatoi A, Burnes J, Loprinzi C, Kelly D. Should patients with advanced, incurable cancers ever be sent home with total parenteral nutrition? A single institution's 20-year experience. *Cancer* 2005; **103**: 863-868 [PMID: 15641035 DOI: 10.1002/ncr.20824]
- 113 **Giovanis P**, Garna A, Marcante M, Mascanzoni A, Giusto M. Exacerbation of paraneoplastic syndrome of inappropriate antidiuretic hormone by parenteral nutrition in a patient affected by a large-cell neuroendocrine pancreatic cancer. *J Pain Symptom Manage* 2006; **32**: 395-396 [PMID: 17085261 DOI: 10.1016/j.jpainsymman.2006.07.008]

P- Reviewer: Cavalcoli F, Raghov R

S- Editor: Yan JP **L- Editor:** A **E- Editor:** Yin SY



Personalized medicine in functional gastrointestinal disorders: Understanding pathogenesis to increase diagnostic and treatment efficacy

Xiao Jing Wang, Michael Camilleri

ORCID number: Xiao Jing Wang (0000-0001-7842-1161); Michael Camilleri (0000-0001-6472-7514).

Author contributions: The authors contributed equally to writing and revising the manuscript. Wang XJ and Camilleri M drafted and finalized the manuscript.

Conflict-of-interest statement: The authors have declared no conflicts of interest.

Open-Access: This article is an open-access article which was selected by an in-house editor and fully peer-reviewed by external reviewers. It is distributed in accordance with the Creative Commons Attribution Non Commercial (CC BY-NC 4.0) license, which permits others to distribute, remix, adapt, build upon this work non-commercially, and license their derivative works on different terms, provided the original work is properly cited and the use is non-commercial. See: <http://creativecommons.org/licenses/by-nc/4.0/>

Manuscript source: Invited manuscript

Received: January 17, 2019

Peer-review started: January 18, 2019

First decision: January 30, 2019

Revised: February 4, 2019

Accepted: February 22, 2019

Article in press: February 23, 2019

Published online: March 14, 2019

Xiao Jing Wang, Michael Camilleri, Division of Gastroenterology and Hepatology, Clinical Enteric Neuroscience Translational and Epidemiological Research, Mayo Clinic, Rochester, MN 55905, United States

Corresponding author: Michael Camilleri, MD, Doctor, Professor, Division of Gastroenterology and Hepatology, Clinical Enteric Neuroscience Translational and Epidemiological Research, Mayo Clinic, 200 First St. S.W., Rochester, MN 55905, United States. camilleri.michael@mayo.edu

Telephone: +1-507-2662305

Abstract

There is overwhelming evidence that functional gastrointestinal disorders (FGIDs) are associated with specific mechanisms that constitute important targets for personalized treatment. There are specific mechanisms in patients presenting with functional upper gastrointestinal symptoms (UGI Sx). Among patients with UGI Sx, approximately equal proportions (25%) of patients have delayed gastric emptying (GE), reduced gastric accommodation (GA), both impaired GE and GA, or neither, presumably due to increased gastric or duodenal sensitivity. Treatments targeted to the underlying pathophysiology utilize prokinetics, gastric relaxants, or central neuromodulators. Similarly, specific mechanisms in patients presenting with functional lower gastrointestinal symptoms, especially with diarrhea or constipation, are recognized, including at least 30% of patients with functional constipation pelvic floor dyssynergia and 5% has colonic inertia (with neural or interstitial cells of Cajal loss in myenteric plexus); 25% of patients with diarrhea-predominant irritable bowel syndrome (IBSD) has evidence of bile acid diarrhea; and, depending on ethnicity, a varying proportion of patients has disaccharidase deficiency, and less often sucrose-isomaltase deficiency. Among patients with predominant pain or bloating, the role of fermentable oligosaccharides, disaccharides, monosaccharides and polyols should be considered. Personalization is applied through pharmacogenomics related to drug pharmacokinetics, specifically the role of CYP2D6, 2C19 and 3A4 in the use of drugs for treatment of patients with FGIDs. Single mutations or multiple genetic variants are relatively rare, with limited impact to date on the understanding or treatment of FGIDs. The role of mucosal gene expression in FGIDs, particularly in IBS-D, is the subject of ongoing research. In summary, the time for personalization of FGIDs, based on deep phenotyping, is here; pharmacogenomics is relevant in the use of central neuromodulators. There is

still unclear impact of the role of genetics in the management of FGIDs.

Key words: Gastrointestinal symptoms; Gastric emptying; Gastric accommodation; Diarrhea; Constipation; Irritable bowel syndrome; Bile acid diarrhea; Phenotypes; Pharmacogenomics; Prokinetics; Neuromodulators

©The Author(s) 2019. Published by Baishideng Publishing Group Inc. All rights reserved.

Core tip: Functional gastrointestinal disorders (FGIDs) are associated with mechanisms that constitute important targets for personalized treatment. Patients with upper gastrointestinal (GI) symptoms may have delayed gastric emptying (GE), reduced gastric accommodation (GA), both impaired GE and GA, or neither. Treatments targeted to the underlying pathophysiology utilize prokinetics, gastric relaxants, or central neuromodulators. Patients with functional lower GI symptoms may have constipation-predominant irritable bowel syndrome, pelvic floor dyssynergia, colonic inertia, diarrhea-predominant irritable bowel syndrome, bile acid diarrhea, or disaccharidase or sucrose-isomaltase deficiency. Personalization is applied through pharmacogenomics related to drug pharmacokinetics, specifically the role of CYP2D6, 2C19 and 3A4. The time for personalized treatments of FGIDs is here.

Citation: Wang XJ, Camilleri M. Personalized medicine in functional gastrointestinal disorders: Understanding pathogenesis to increase diagnostic and treatment efficacy. *World J Gastroenterol* 2019; 25(10): 1185-1196

URL: <https://www.wjgnet.com/1007-9327/full/v25/i10/1185.htm>

DOI: <https://dx.doi.org/10.3748/wjg.v25.i10.1185>

INTRODUCTION

Functional gastrointestinal disorders (FGIDs) encompass a group of gastrointestinal (GI) conditions characterized by chronic or recurrent GI symptoms without biochemical or structural abnormalities^[1]. The most widely known of the FGIDs include functional dyspepsia and irritable bowel syndrome (IBS), with other conditions such as functional constipation, abdominal bloating, and functional abdominal pain syndrome being increasingly recognized. FGIDs are highly prevalent, with IBS reported in about 10%-15% of the North America population, and with some studies showing up to 20% prevalence^[2]. Similar prevalence rates (7.0%-20.4%) are reported for functional dyspepsia^[3]. While the diseases are generally grouped based on focal primary digestive symptoms (*i.e.*, functional dyspepsia based on upper GI symptoms), it is important to note that the intestinal tract functions as a unit, and disorders in a specific segment can produce symptoms in a separate area, for example, constipation leading to delayed gastric emptying^[4]. **Table 1** provides a summary of the disease phenotypes, characterized by the symptoms and pathophysiology, as well as their diagnosis and treatment. **Table 2** summarizes pharmacological treatments (current or in development) for indications based on accurate phenotyping of GI disorders.

While these conditions generally do not contribute to mortality, they cause significant morbidity and often lead to extensive, often repetitive, diagnostic work-ups, incurring significant cost, as well as frustration for both patient and provider. Evaluation of a teaching hospital gastroenterology clinic showed that 34.9% of new patient referrals in a two-year period had a diagnosis of a FGID^[5]. Preliminary data from our group show that patients undergo an average of three endoscopic procedures and 1.2 cross-sectional imaging tests [computed tomography (CT), magnetic resonance imaging (MRI) of abdomen and pelvis] prior to receiving a diagnosis of bile acid diarrhea. A large systematic review reported that up to 70%-80% of patients undergoing endoscopy for dyspepsia would be diagnosed with functional dyspepsia^[6]. Similarly, in patients who met Rome I criteria for IBS, structural disease was found in only 2% by colonoscopy^[7], suggesting that testing for FGIDs is over utilized.

Despite the prevalence of these conditions, diagnosis and management remain challenging due to their heterogenous nature. However, with improved diagnostic tools and increased understanding of the specific pathophysiological mechanisms

Table 1 Commonly encountered gastrointestinal diseases and their phenotypic presentations (symptoms and pathophysiology) and management principles

Disease phenotype	Symptoms	Pathophysiology	Diagnosis	Treatment options or selections
Functional dyspepsia	Postprandial fullness, early satiety; Epigastric pain, epigastric burning	Alterations in gastric emptying and/or gastric accommodation	Gastric emptying study; Gastric accommodation studies (SPECT, MR imaging)	Reduced GE and/or GA → prokinetic or gastric relaxants; Normal GE and GA → central pain modulator
Outlet dysfunction constipation	Constipation, abdominal pain	Pelvic floor dyssynergia	Anorectal manometry with balloon expulsion test; MR defecography	Pelvic floor rehabilitation with biofeedback training
Slow transit constipation	Constipation, abdominal pain	Decreased colonic motility	Colon transit studies with radiopaque markers or scintigraphy or wireless motility capsule	Prokinetic agents; Secretory + stimulant laxatives; Total colectomy with ileo-rectal anastomosis
Bile acid diarrhea	Diarrhea; Abdominal pain	Increased bile acid synthesis/ decreased bile acid absorption	Total fecal bile acids; Fecal bile acid composition; Serum 7- α -hydroxy-4-cholesten-3-one	Bile acid binders

GE: Gastric emptying; GA: Gastric accommodation; SPECT: Single-photon emission computed tomography; MR: Magnetic resonance.

underlying these conditions, it is possible to identify specific mechanisms among patients presenting with the same symptom complexes in the different categories of FGIDs, allowing for tailored therapy with increased chances of success.

This review proposes an individualized approach to the management of FGIDs: understanding mechanisms that result in patients' symptoms, utilizing appropriate diagnostic testing, and choosing targeted therapies to provide personalized care in the management of the FGID. Four decades ago, there was a plea to move towards positive symptom-based diagnosis of IBS; this led to profuse criteria for diverse symptom complexes, and the criteria have been revised and refined almost every decade since then^[8]. As more specific diagnoses are identified, these disorders could be identified as specific diagnoses instead of being bundled under the "umbrella" diagnosis of FGIDs. For this review, we will follow the current convention of grouping these disorders as "functional" GI disorders, but we will also document specific phenotypes that call for specific, targeted treatments.

Understanding the pathophysiological mechanisms causing FGIDs and developing valid clinical diagnostic tests are the first steps in the process of positive disease diagnosis, moving these disorders from diagnoses of exclusion after extensive or limited evaluations to rule out organic diseases^[9]. With increased recognition of the importance of peripheral mechanisms in the etiopathogenesis of IBS, there is a renaissance^[10,11] in the field of FGIDs, which should lead from a hit-or-miss approach for symptom relief to the targeted, personalized treatment based on specific diagnosis and pharmacogenomics.

GASTRIC DYSFUNCTIONS AS A BASIS FOR TREATMENT IN FUNCTIONAL DYSPEPSIA

Functional dyspepsia is defined by Rome IV criteria as any combination of postprandial fullness, early satiety, epigastric pain, and epigastric burning occurring at least three days per week over the last three months, with an onset of at least six months prior to evaluation^[12]. In the absence of alarm symptoms and signs, treatment can be initiated empirically without endoscopic evaluation. Functional dyspepsia is further subdivided into postprandial distress syndrome and epigastric pain syndrome, depending on whether the symptoms are associated with meal ingestion. Most patients have been treated with or tried anti-acid secretory medications by the time they see a gastroenterologist. The empiric choice follows a "hunch", a perception by the clinician of the underlying cause of the patient's symptoms. Indeed, it may be feasible to select a prokinetic for postprandial distress or a central neuromodulator for epigastric pain syndrome.

While there are many proposed mechanisms for the pathophysiology of functional dyspepsia, alterations in gastric function, as measured by gastric emptying (GE) and gastric accommodation (GA), have been correlated with symptoms and are potential targets for treatment. Among 1287 patients who underwent GE and GA studies,

Table 2 Pharmacological treatments (current or in-development) for indications based on accurate phenotyping of gastrointestinal disorders

Drug	Mechanism of action	Indication	Typical doses	Phases of trials completed	Study design	Important results
Relamorelin	Synthetic ghrelin analog	Diabetic gastroparesis	10 µg <i>b.i.d.</i> SQ	Phase 2 (Phase 3 ongoing); Multicenter, randomized, double-blind, placebo-controlled, parallel-group study; 2 wk single-blind, placebo run-in ^[18]	Diabetic gastroparesis patients (<i>n</i> = 393); Placebo (<i>n</i> = 104) <i>vs</i> relamorelin [10 µg (<i>n</i> = 98), 30 µg (<i>n</i> = 109), 100 µg (<i>n</i> = 82)] twice daily × 12 wk	Symptoms of diabetic gastroparesis (but not vomiting frequency) significantly reduced <i>vs</i> placebo in all relamorelin groups; Significant acceleration of GE from baseline <i>vs</i> placebo; Dose-related worsening of glycemic control in relamorelin arm ^[18]
Acotiamide	Acetylcholinesterase inhibitor	Functional dyspepsia	100 mg <i>t.i.d.</i>	Phase 3 Multicenter, single arm, open label safety trial ^[66]	Functional Dyspepsia patients (<i>n</i> = 207); Acotiamide three times daily × 1 yr	Improved postprandial fullness, early satiation, quality of life, work productivity; No significant adverse effects ^[66]
Colesevelam	Bile acid sequestrants	BAD	625-1875mg <i>b.i.d.</i>	FDA approved for DM2 and hyperlipidemia; Single center, unblinded single-dose trial in IBS with BAD ^[67]	IBS-D with prior evidence of increased bile acid synthesis/excretion (<i>n</i> = 12): colesevelam 1875 mg twice daily × 10 d	Increased fecal total bile acid, and deoxycholic acid excretion by sequestration by BA binder; Increased serum C4; More solid stool consistency ^[67]
Colestipol		BAD	5 g daily initially, + 5 g/ mo increase up to 30 g daily	FDA approved for primary hypercholesterolemia	No large trials for primary therapy in treatment of bile acid diarrhea ^[68]	Can consider in those who do not tolerate colesevelam or cholestyramine ^[68]
Prucalopride	5-HT ₄ receptor agonist	CC	1 mg (> 65 yr); 2 mg (< 65 yr) <i>q.d.</i>	FDA approved; Multiple Phase 3: multicenter, randomized, placebo-controlled, parallel group trials ^[69]	Chronic constipation patients (<i>n</i> = 620); Placebo <i>vs</i> prucalopride 2 mg <i>vs</i> prucalopride 4 mg	Significant increase in patients with three or more spontaneous, complete bowel movements/week with 2 mg prucalopride <i>vs</i> placebo NNT = 5 ^[69]
Tegaserod		IBS-C and CC	2 or 6mg bid	FDA approved for patients with low cardiovascular risk; Multiple phase 3 and 4 trials with several; Systematic reviews and Meta-analyses showing consistent efficacy ^[70]	9242 patients in 11 trials (3 only females, 8 studies with constipation predominant patients); Tegaserod 0.5-12 mg twice daily for 4 to 20 wk	Relative risk of symptoms persisting = 0.85% (95% CI: 0.80-0.90, <i>I</i> ² = 57%); NNT = 10 ^[70]
Alosetron	5-HT ₃ receptor antagonist	IBS-D	0.5-1.0 mg <i>b.i.d.</i>	FDA approved; Multiple phase 3 and 4 trials with several; Systematic reviews and Meta-analyses showing consistent efficacy ^[70]	4987 IBS patients in 8 trials (5 with only female participants); Alosetron (dose range studied 0.1 to 8 mg) twice daily compared to placebo	Relative risk of symptoms persisting = 0.79; (95% CI: 0.69-0.90, <i>I</i> ² = 85%) NNT = 8 ^[70]

BAD: Bile acid diarrhea; CC: Chronic constipation; IBS: Irritable bowel syndrome; IBS-C: IBS-constipation; IBS-D: IBS-diarrhea; FDA: Food and Drug Administration; DM2: Type 2 diabetes mellitus; GE: Gastric emptying; NNT: Number needed to treat; CI: Confidence interval.

patients with delayed GE had more frequent nausea, vomiting, and weight loss, and less frequent bloating. Nausea, vomiting, and belching symptoms were significantly different among patients with normal, increased, or decreased GA. Vomiting was

more prevalent in patients with both abnormal GA and GE^[13]. A meta-analysis of 25 studies showed significant associations between altered GE and nausea, vomiting, abdominal pain, and early satiety in patients presenting with upper GI symptoms^[14]. Importantly, a review of the current literature showed significant heterogeneity in GE and GA testing, with significant differences observed in the relationship of delayed GE with upper GI symptoms between studies that used optimal versus suboptimal methods. GE and GA testing should be conducted with appropriate meal and testing length in order to ensure accurate results^[15].

In patients with functional dyspepsia with altered GE and/or GA, treatments such as prokinetic medications or gastric relaxants, respectively, may be beneficial in symptom management. Conversely, in patients with upper GI symptoms, but no alteration in gastric functions, central pain modulators such as tricyclic antidepressants (nortriptyline, amitriptyline), a combination antidepressant that acts by antagonizing adrenergic α_2 -autoreceptors and α_2 -heteroreceptors as well as by blocking 5-HT₂ and 5-HT₃ receptors (mirtazapine), or an $\alpha 2\delta$ ligand (Pregabalin) may be more beneficial as initial therapy to treat duodenal hypersensitivity. It is important to note that these medications, particularly mirtazapine, also impact gastric function^[16] and may provide relief by addressing underlying dysfunction as well as pain modulation.

However, there is a dearth of evidence from large phase 3 trials in the literature assessing this pathophysiology-centered approach in functional dyspepsia and a lack of effective treatments. The best proof-of-principle comes from phase 2 studies of relamorelin, albeit in patients with diabetes with gastroparesis, whose GE and symptoms improved^[17,18], and from studies with acotiamide in less than 40 patients which showed concordant results between GA and symptoms^[19].

MECHANISMS AND TREATMENTS OF FUNCTIONAL LOWER GI DISORDERS

Functional lower GI disorders include diarrhea-IBS (IBS-D), IBS-constipation (IBS-C), or IBS-mixed, as well as the overlapping disorders of functional diarrhea and functional constipation. The important distinguishing factor between IBS and the functional bowel alterations according to Rome IV criteria is the presence of pain associated with alteration of bowel habits with IBS diagnosis, that is, the presence of pain with alteration of bowel movements and relief of pain with defecation^[20]. These “umbrella diagnoses” can be further characterized by mechanism or pathophysiology, leading to targeted treatment.

Outlet dysfunction constipation, colonic inertia and overlap with lower FGIDs with constipation

It is recognized that, among patients with lower FGIDs and constipation, at least 30% suffer from pelvic floor dyssynergia, causing outlet dysfunction constipation, and 5% from colonic inertia (with neural or ICC loss in myenteric plexus), causing slow transit constipation. Importantly, up to 50% of patients with outlet dysfunction constipation have slow transit constipation as a result of the evacuation disorder^[21]. Therefore, the diagnostic assessment should begin with anorectal testing, including digital rectal exam, anorectal manometry and balloon expulsion testing. A digital rectal exam, performed by an experienced clinician, can correctly identify features such as high anal sphincter tone and paradoxical contraction of the pelvic floor that is associated with abnormal anal relaxation or abnormal rectoanal pressure differential. The balloon expulsion time of 60 seconds has a low sensitivity for identifying rectal evacuation disorder^[22]. If, on digital rectal exam, there is concern about mucosal intussusception, pelvic organ prolapse, or descending perineum syndrome^[23] which is increasingly recognized in Ehlers-Danlos syndrome^[24], magnetic resonance defecography can be pursued to evaluate the rectal region during active evacuation^[25]. If anorectal evaluation is normal, evaluation for slow transit constipation can be considered, utilizing radiopaque markers, colonic transit scintigraphy, or wireless motility capsules^[26].

In patients who show abnormal parameters on anorectal manometry or with failure to pass a rectal balloon in 60 s, treatment of pelvic dyssynergia should be undertaken with pelvic floor rehabilitation. The benefit of pelvic floor rehabilitation largely lies in biofeedback training, in which patients are taught to control their pelvic floor muscles and anal sphincters to reverse maladaptive learning including paradoxical movements or relax high pressures, depending on the manometric abnormality. Biofeedback training has been reported to improve more than 60% of patients with constipation due to pelvic floor dyssynergia; patients who used digital maneuvers

and those with lower baseline levels of bowel satisfaction were more likely to have treatment success^[27]. Home-based biofeedback retraining has been as effective as office-based retraining^[28], which was previously shown to be superior to diet, exercise, and laxatives as standard therapy for constipation^[29].

In patients with slow colonic motility alone who are refractory to treatment with laxatives, further testing can be undertaken with colonic manometry and barostat studies to evaluate colonic motor activity, including meal-induced gastrocolonic response and response to stimulant laxatives and cholinesterase inhibitors (neostigmine)^[30,31]. If there is evidence of colonic motor activity in response to physiological and pharmacological stimuli, treatment with the oral cholinesterase inhibitor, pyridostigmine, can be considered^[32]. Recently, the selective serotonin-4 (5-HT₄) receptor agonist, prucalopride, which stimulates colonic peristalsis and enhances bowel motility, received FDA approval and can be considered in patients with evidence of reduced colonic motility. If there is no evidence of normal motor activity and no response to stimulation with neostigmine or supervised therapeutic trial, laparoscopic colectomy with ileorectal anastomosis can be considered.

Bile acid diarrhea

While bile acid diarrhea is usually recognized in patients with ileal disease or ileal resection, recent studies have documented that between 25% and 50% of patients with functional diarrhea or IBS-D have bile acid diarrhea, and have symptom improvement on bile acid sequestrants^[33]. In primary or idiopathic bile acid malabsorption, also known as type 2 bile acid malabsorption, there is an increased fecal load of bile acids in the absence of ileal or other structural gastrointestinal diseases. While the etiology of the increase is unclear, the prevailing theories include a deficiency in feedback inhibition of bile acid synthesis by fibroblast growth factor (FGF)-19 causing excess hepatic production due to reduced ileal enterocyte mRNA expression^[34], or genetic variants in the hepatocyte receptor or associated protein (KLB and FGFR4)^[35] that are activated by FGF-19 to reduce CYP7A1, the rate-limiting enzyme in the synthesis of bile acids. These bile acids act in the colon to increase colonic mucosal permeability, water secretion, mucus production, and to accelerate colonic motility^[36].

To assess patients for bile acid diarrhea, fecal bile acid load can be evaluated directly by measurement of total and individual fecal bile acids, with excretion of > 2337 μmol per 48 h or > 10% primary bile acids (chenodeoxycholic acid, deoxycholic acid) as an indication of bile acid malabsorption. Mild elevations in total bile acids should be interpreted with caution, as increased colonic transit may lead to reduced passive absorption of bile acids in the colon and an increase in the fecal levels^[37]. If available, serum C4 (7- α -hydroxy-4-cholesten-3-one) is a simple blood test measuring bile acid synthesis, with a sensitivity of 90% and specificity of 79% for the diagnosis of bile acid malabsorption^[38]. This test should be performed on a fasting serum sample collected in the morning before 10:00 a.m., due to diurnal variability.

If diagnosed, bile acid diarrhea can be treated with intraluminal bile acid binders, cholestyramine and colestipol, though evidence of efficacy comes mainly from open-label studies. These intraluminal bile acid binders have shown benefit in bowel symptoms and global symptoms in the treatment of patients with IBS-D with evidence of bile acid malabsorption, but are limited by their poor palatability. Colesevelam is better tolerated and has shown efficacy in improvement in stool consistency, but its use may be limited by cost^[36].

Disaccharidase malabsorption

Worldwide, about 65% of adults lose the ability to digest lactose, with ethnically determined prevalence ranging from less than 10% in Northern Europeans to over 90% in East Asians^[39]. In the absence of adequate lactase at the intestinal brush-border, lactose is unable to be cleaved to monosaccharides (glucose and galactose) and, thus, it reaches the colon unabsorbed. In the colon, lactose is broken down by commensal bacteria, producing hydrogen gas and symptoms of abdominal pain, distension, borborygmi, flatus, and diarrhea^[40]. Lactase deficiency can be evaluated with a simple hydrogen breath test following lactose load. While this diagnosis is commonly known, studies have found that symptoms in up to 25.8% of patients diagnosed with IBS-D were related to lactose deficiency, and 52% of patients were unaware of symptoms association with lactose ingestion^[41]. Once diagnosed, most patients are able to tolerate lactose intake equivalent to 240 mL of milk without symptoms, particularly, if ingested in divided amounts rather than a single dose^[42]. Otherwise, dietary avoidance or the use of digestive aids can provide adequate symptom control.

While sucrose-isomaltase deficiency is an uncommon congenital condition, the diagnosis is often not recognized, and children can present with unexplained signs and symptoms which persist into adulthood. Similar to undigested lactose, arrival of these non-absorbed disaccharides in the colon can lead to gas fermentation by

bacteria, as well as osmotic diarrhea. Malabsorbed sugars, such as fructose and lactose, lead to clusters of gastrointestinal symptoms, rather than symptoms typically associated with brain dysfunction^[43]. Other uncommon genetic carbohydrate intolerances include glucose-galactose malabsorption. These conditions can be severe enough to cause failure to thrive and malnutrition in children, but tolerance can improve as the children age. In patients with prolonged history of symptoms, particularly if related to meals, diagnostic evaluation can be pursued with disaccharidase activity assays on proximal small bowel biopsies^[44].

Abdominal pain, bloating and the low fermentable oligosaccharides, disaccharides, monosaccharides and polyol diet

Among patients with predominant pain or bloating, the role of fermentable oligosaccharides, disaccharides, monosaccharides and polyols (FODMAPs) may be considered. As above, lactase insufficiency should first be evaluated prior to implementing the nutritionally-restrictive full low-FODMAP diet. Biologically, humans are unable to enzymatically cleave the fructose-fructose bonds needed to break down the oligosaccharides which compose fructans and galactans. Polyols, or sugar alcohols, are also incompletely absorbed and can reach the colon intact. These components can be fermented similar to undigested lactose and cause osmotic diarrhea, leading to symptoms of IBS-D. Monosaccharides and disaccharides are generally absorbed by brush border transporters and enzymes, and, in the absence of congenital deficiencies above, should not cause significant GI distress.

Once a low FODMAP diet is implemented, if symptoms are controlled, dietary components should be slowly reintroduced as tolerated in order to allow patients a larger variety of nutritional sources and improved quality of life. If symptoms continue to be uncontrolled or if patients manifest other features, concern for chronic pain syndrome and central neuromodulators would be indicated. Dietary fiber supplementation may be beneficial for patients with IBS-C or chronic constipation. In addition, prebiotics, ingredients unable to be digested by the human intestinal tract but that support the growth of intestinal microbiota, may play a role in improvement of the gut microbiome^[45,46]. Conversely, ultra-processed foods may be associated with a higher risk of IBS^[47]. Dietary fibers, as well as prebiotics, are often empirically utilized, and it is unclear whether phenotyping can identify the best candidates for these therapies.

Brain-gut permeability-microbiome interactions

An authoritative review in 2014 opined that it was unclear whether IBS symptoms are caused by alterations in brain signaling from the intestine to the microbiota or primary disruption of the microbiota, and whether they are involved in altered interactions between the brain and intestine during development^[48]. Recent data support these interactions in part through increased intestinal permeability. This interaction likely underlies the strong association between FGIDs and psychological disorders, with up to 50%-94% of IBS patients carrying diagnoses of general anxiety disorder or major depression^[49]. De Palma *et al.* showed that engraftment of fecal microbiota from IBS patients into germ-free mice led to development of not only increased GI transit and gut barrier dysfunction, but also anxiety-like behavior compared to those receiving fecal microbiota from control patients^[50]. In addition to central neuromodulators, patients with concomitant psychological disorders may benefit from cognitive behavior therapy or hypnotherapy^[51].

Studies *in vitro* of permeability of colonic mucosa^[52] from patients with IBS suggested that there is increased paracellular permeability to ⁵¹Cr-EDTA; these data confirm a significant literature documenting increased intestinal or colonic permeability in IBS using orally administered probe molecules, principally saccharides^[53]. Bednarska *et al.*^[52] also showed increased transcellular permeability to live bacteria. Gaps among terminal ileal epithelial cells in IBS or among duodenal cells have also been documented in response to food allergens^[54,55]. These data may provide the rationale for bacteria or their toxins impacting brain function, as demonstrated through correlations of permeability and brain structure and function^[56]. A probiotic^[57], *B. infantis* M-63, has seemed to be effective in improving mental health in patients who developed IBS after floods, and this may be due to restoration of microbial balance and the gut-brain axis.

Fecal microbiota transplantation has also been explored as a potential treatment of FGIDs, particularly IBS, with the intent of restoring the microbiome to a healthy state^[58]. Further studies are needed to help determine the appropriate goal of the microbiota change and the composition of "healthy gut" microbiota. Rigorous trials need to be conducted to evaluate the safety of these transplants for use in FGIDs, which generally carry low mortality risk, as well as to evaluate the long-term durability of results.

For this field to advance, we require further validated measurements of permeability that are applicable noninvasively in clinical practice as an essential first step, followed by provision of evidence that interventions (dietary, probiotic, microbial transplant, or pharmacological) can restore barrier function to normal. At present, none of the three dimensions (intestinal permeability, microbiome or brain imaging) is applicable in the personalized medicine arena.

THE “-OMICS” AND PRECISION MEDICINE

Pharmacogenomics and drug pharmacokinetics

Pharmacogenomics evaluates the impact of changes in an individual patient’s genetic code on drug metabolism or on a therapeutic target. Genetic differences in drug metabolism can lead to increased or decreased response to a standard dose of medication in different patients and may lead to unintended toxicity or poor response, respectively. The cytochrome p (CYP) 450 enzymes are responsible for phase I metabolism of numerous drugs, and genetic variations in several of these enzymes have been implicated in response to treatment in FGIDs.

Central pain modulators, including the tricyclic antidepressants and the selective serotonin reuptake inhibitors (SSRIs), are frequently used to treat pain in patients with FGIDs. These drugs are metabolized by the CYP2D6 enzyme, which has more than 100 genetic variations that determine functionality of the enzymes. The number of functional *CYP2D6* genes was shown to correlate with nortriptyline metabolism^[59], but the clinical implications of this observation are still unproven in clinical trials or practice, except in individual patients.

CYP2C19 is responsible for inactivation of proton pump inhibitors, as well as the H₂ receptor antagonist, cimetidine. Increased activity variants of CYP2C19 can lead to poor response to proton pump inhibitors (PPIs) in patients with functional dyspepsia. In these cases, rabeprazole should be considered, as it is metabolized through the CYP3A4 system. The CYP3A4 system is also responsible for the metabolism of alosetron, a 5HT₃ receptor antagonist used in treatment of IBS-D. Decreased activity variants of CYP3A4 or concomitant use of benzodiazepines, which are also metabolized by the same enzyme, may lead to increased drug effects and higher risk of toxicity^[60].

Mutations and genetic variants in FGIDs

While specific genetic variants have not been identified as therapeutic targets, there are several polymorphisms which alter GI transit and may influence the development of FGIDs. The serotonin-transporter protein (SERT) is located on a presynaptic neuron and clears 5-HT from the synaptic cleft, limiting downstream activation of receptors that stimulate colonic transit. Allelic variants of the gene *5-HTTLPR*, which determines SERT synthesis, can cause decreased SERT protein and increased serotonergic activation and accelerated colonic transit^[61]. The presence of variations causing decreased SERT has also been seen to decrease the response to the 5HT₃ receptor antagonist, alosetron, and to increase the response to the 5HT₄ receptor agonist, tegaserod, both used in the treatment of IBS-C^[62].

Mucosal gene expression and FGIDs

Several studies have now evaluated mucosal gene expression in FGIDs, particularly in patients with IBS. In the IBS-D cohort, prior studies have shown altered transcription of proteins involved in ion transport, barrier function, immune regulation, and mast cell activation in jejunal and colorectal mucosa^[63,64]. Further study of these changes may allow improved understanding of the pathophysiology of IBS and potentially influence development of future therapeutic targets.

LIMITATIONS

Recommendations suggested in our review are limited by the lack of availability of “deep phenotyping”, even in specialty or academic centers. For example, nuclear medicine SPECT imaging and MRI for measurement of gastric accommodation are only available or offered in limited facilities. In addition, there is currently significant heterogeneity in testing protocols and interpretation of results which leads to lack of standardization, both in clinical data and in research. This is often observed in gastric emptying studies where different protocol meals are utilized, leading to different expected parameters. Similarly, balloon expulsion times in anorectal manometry have “normal” cut offs ranging from 60 s to up to 3 min in different centers. Lastly, there is

currently a lack of robust evidence that understanding or deeply characterizing patient phenotype will lead to improved patient outcomes, partly due to lack of effective treatments available, particularly for gastroparesis and gastric dysaccommodation. However, we perceive that the future clinical practice will be enhanced by standardization of measurements in research and clinical practice and will facilitate development of new targeted therapies, and ultimately improve patient care.

CONCLUSION

In summary, the time for personalization of treatments for FGIDs, based on “deep phenotyping”, is here. FGIDs should no longer be considered diagnoses of exclusion following extensive structural work-up. Instead, after a thorough history, patients should receive targeted assessment and testing, depending on their symptom profile, to evaluate the likely subtypes of FGIDs, with subsequent targeted treatment. This shift in approach will improve patient compliance, decrease costs for work-ups^[65], and potentially decrease both patient and provider frustration. Pharmacogenetics is currently clinically relevant in the use of central neuromodulators and PPIs, and evaluation for genetic variants should be considered in patients who are not responding as expected to treatment. The role of genetics in the management of FGIDs is still a maturing field. With greater understanding of the pathophysiology of these disorders and validation of clinically-applicable diagnostic tests, patient-based research will provide more personalization of diagnosis and management for patients with FGIDs. As the etiologies and pathophysiologies of these disorders are identified and symptoms are able to become classified under specific diagnoses, we anticipate that the umbrella category of “functional” GI disorders will ultimately be replaced by separate and specific diseases. The examples of slow transit constipation, rectal evacuation disorders and bile acid diarrhea already demonstrate the clinical relevance of these phenotypes to personalize medicine.

REFERENCES

- 1 **Drossman DA.** The functional gastrointestinal disorders and the Rome III process. *Gastroenterology* 2006; **130**: 1377-1390 [PMID: 16678553 DOI: 10.1053/j.gastro.2006.03.008]
- 2 **Saito YA, Schoenfeld P, Locke GR.** The epidemiology of irritable bowel syndrome in North America: a systematic review. *Am J Gastroenterol* 2002; **97**: 1910-1915 [PMID: 12190153 DOI: 10.1111/j.1572-0241.2002.05913.x]
- 3 **Oshima T, Miwa H.** Epidemiology of Functional Gastrointestinal Disorders in Japan and in the World. *J Neurogastroenterol Motil* 2015; **21**: 320-329 [PMID: 26095436 DOI: 10.5056/jnm14165]
- 4 **Tjeerdma HC, Smout AJ, Akkermans LM.** Voluntary suppression of defecation delays gastric emptying. *Dig Dis Sci* 1993; **38**: 832-836 [PMID: 8482181]
- 5 **Shivaji UN, Ford AC.** Prevalence of functional gastrointestinal disorders among consecutive new patient referrals to a gastroenterology clinic. *Frontline Gastroenterol* 2014; **5**: 266-271 [PMID: 28839783 DOI: 10.1136/flgastro-2013-100426]
- 6 **Ford AC, Marwaha A, Lim A, Moayyedi P.** What is the prevalence of clinically significant endoscopic findings in subjects with dyspepsia? Systematic review and meta-analysis. *Clin Gastroenterol Hepatol* 2010; **8**: 830-837, 837.e1-837.e2 [PMID: 20541625 DOI: 10.1016/j.cgh.2010.05.031]
- 7 **Hamm LR, Sorrells SC, Harding JP, Northcutt AR, Heath AT, Kapke GF, Hunt CM, Mangel AW.** Additional investigations fail to alter the diagnosis of irritable bowel syndrome in subjects fulfilling the Rome criteria. *Am J Gastroenterol* 1999; **94**: 1279-1282 [PMID: 10235207 DOI: 10.1111/j.1572-0241.1999.01077.x]
- 8 **Manning AP, Thompson WG, Heaton KW, Morris AF.** Towards positive diagnosis of the irritable bowel. *Br Med J* 1978; **2**: 653-654 [PMID: 698649]
- 9 **Moayyedi P, Mearin F, Azpiroz F, Andresen V, Barbara G, Corsetti M, Emmanuel A, Hungin APS, Leyer P, Stanghellini V, Whorwell P, Zerbib F, Tack J.** Irritable bowel syndrome diagnosis and management: A simplified algorithm for clinical practice. *United European Gastroenterol J* 2017; **5**: 773-788 [PMID: 29026591 DOI: 10.1177/2050640617731968]
- 10 **Camilleri M.** Peripheral mechanisms in irritable bowel syndrome. *N Engl J Med* 2012; **367**: 1626-1635 [PMID: 23094724 DOI: 10.1056/NEJMra1207068]
- 11 **Chang L, Heitkemper MM, Wiley JW, Camilleri M.** 2015 James W. Freston Single Topic Conference: A Renaissance in the Understanding and Management of Irritable Bowel Syndrome. *Gastroenterology* 2016; **151**: e1-e8 [PMID: 27215658 DOI: 10.1053/j.gastro.2016.05.010]
- 12 **Stanghellini V, Chan FK, Hasler WL, Malagelada JR, Suzuki H, Tack J, Talley NJ.** Gastrointestinal Disorders. *Gastroenterology* 2016; **150**: 1380-1392 [PMID: 27147122 DOI: 10.1053/j.gastro.2016.02.011]
- 13 **Park SY, Acosta A, Camilleri M, Burton D, Harmsen WS, Fox J, Szarka LA.** Gastric Motor Dysfunction in Patients With Functional Gastrointestinal Symptoms. *Am J Gastroenterol* 2017; **112**: 1689-1699 [PMID: 28895582 DOI: 10.1038/ajg.2017.264]
- 14 **Vijayvargiya P, Jameie-Oskooei S, Camilleri M, Chedid V, Erwin PJ, Murad MH.** Association between delayed gastric emptying and upper gastrointestinal symptoms: a systematic review and meta-analysis. *Gut* 2018 [PMID: 29860241 DOI: 10.1136/gutjnl-2018-316405]
- 15 **Pathikonda M, Sachdeva P, Malhotra N, Fisher RS, Maurer AH, Parkman HP.** Gastric emptying scintigraphy: is four hours necessary? *J Clin Gastroenterol* 2012; **46**: 209-215 [PMID: 21959322 DOI: 10.1007/s12664-012-0209-2]

- 10.1097/MCG.0b013e31822f3ad2]
- 16 **Carbone F**, Vanuytsel T, Tack J. The effect of mirtazapine on gastric accommodation, gastric sensitivity to distention, and nutrient tolerance in healthy subjects. *Neurogastroenterol Motil* 2017; **29** [PMID: 28695632 DOI: 10.1111/nmo.13146]
 - 17 **Lembo A**, Camilleri M, McCallum R, Sastre R, Breton C, Spence S, White J, Currie M, Gottesdiener K, Stoner E; RM-131-004 Trial Group. Relamorelin Reduces Vomiting Frequency and Severity and Accelerates Gastric Emptying in Adults With Diabetic Gastroparesis. *Gastroenterology* 2016; **151**: 87-96.e6 [PMID: 27055601 DOI: 10.1053/j.gastro.2016.03.038]
 - 18 **Camilleri M**, McCallum RW, Tack J, Spence SC, Gottesdiener K, Fiedorek FT. Efficacy and Safety of Relamorelin in Diabetics With Symptoms of Gastroparesis: A Randomized, Placebo-Controlled Study. *Gastroenterology* 2017; **153**: 1240-1250.e2 [PMID: 28760384 DOI: 10.1053/j.gastro.2017.07.035]
 - 19 **Kusunoki H**, Haruma K, Manabe N, Imamura H, Kamada T, Shiotani A, Hata J, Sugioka H, Saito Y, Kato H, Tack J. Therapeutic efficacy of acotiamide in patients with functional dyspepsia based on enhanced postprandial gastric accommodation and emptying: randomized controlled study evaluation by real-time ultrasonography. *Neurogastroenterol Motil* 2012; **24**: 540-545, e250-e251 [PMID: 22385472 DOI: 10.1111/j.1365-2982.2012.01897.x]
 - 20 **Mearin F**, Lacy BE, Chang L, Chey WD, Lembo AJ, Simren M, Spiller R. Bowel Disorders. *Gastroenterology* 2016 [PMID: 27144627 DOI: 10.1053/j.gastro.2016.02.031]
 - 21 **American Gastroenterological Association**; Bharucha AE, Dorn SD, Lembo A, Pressman A. American Gastroenterological Association medical position statement on constipation. *Gastroenterology* 2013; **144**: 211-217 [PMID: 23261064 DOI: 10.1053/j.gastro.2012.10.029]
 - 22 **Chedid V**, Vijayvargiya P, Halawi H, Park SY, Camilleri M. Audit of the diagnosis of rectal evacuation disorders in chronic constipation. *Neurogastroenterol Motil* 2019; **31**: e13510 [PMID: 30426597 DOI: 10.1111/nmo.13510]
 - 23 **Harewood GC**, Coulie B, Camilleri M, Rath-Harvey D, Pemberton JH. Descending perineum syndrome: audit of clinical and laboratory features and outcome of pelvic floor retraining. *Am J Gastroenterol* 1999; **94**: 126-130 [PMID: 9934742 DOI: 10.1111/j.1572-0241.1999.00782.x]
 - 24 **Vijayvargiya P**, Camilleri M, Cima RR. COL1A1 Mutations Presenting as Descending Perineum Syndrome in a Young Patient With Hypermobility Syndrome. *Mayo Clin Proc* 2018; **93**: 386-391 [PMID: 29502568 DOI: 10.1016/j.mayocp.2018.01.007]
 - 25 **Flusberg M**, Sahni VA, Erturk SM, Morte KJ. Dynamic MR defecography: assessment of the usefulness of the defecation phase. *AJR Am J Roentgenol* 2011; **196**: W394-W399 [PMID: 21427302 DOI: 10.2214/AJR.10.4445]
 - 26 **Kim ER**, Rhee PL. How to interpret a functional or motility test - colon transit study. *J Neurogastroenterol Motil* 2012; **18**: 94-99 [PMID: 22323993 DOI: 10.5056/jnm.2012.18.1.94]
 - 27 **Patcharatrakul T**, Valestin J, Schmeltz A, Schulze K, Rao SSC. Factors Associated With Response to Biofeedback Therapy for Dyssynergic Defecation. *Clin Gastroenterol Hepatol* 2018; **16**: 715-721 [PMID: 29111136 DOI: 10.1016/j.cgh.2017.10.027]
 - 28 **Rao SSC**, Valestin JA, Xiang X, Hamdy S, Bradley CS, Zimmerman MB. Home-based versus office-based biofeedback therapy for constipation with dyssynergic defecation: a randomised controlled trial. *Lancet Gastroenterol Hepatol* 2018; **3**: 768-777 [PMID: 30236904 DOI: 10.1016/S2468-1253(18)30266-8]
 - 29 **Rao SS**, Valestin J, Brown CK, Zimmerman B, Schulze K. Long-term efficacy of biofeedback therapy for dyssynergic defecation: randomized controlled trial. *Am J Gastroenterol* 2010; **105**: 890-896 [PMID: 20179692 DOI: 10.1038/ajg.2010.53]
 - 30 **Lee YY**, Erdogan A, Rao SS. How to perform and assess colonic manometry and barostat study in chronic constipation. *J Neurogastroenterol Motil* 2014; **20**: 547-552 [PMID: 25230902 DOI: 10.5056/jnm14056]
 - 31 **Parthasarathy G**, Ravi K, Camilleri M, Andrews C, Szarka LA, Low PA, Zinsmeister AR, Bharucha AE. Effect of neostigmine on gastroduodenal motility in patients with suspected gastrointestinal motility disorders. *Neurogastroenterol Motil* 2015; **27**: 1736-1746 [PMID: 26387781 DOI: 10.1111/nmo.12669]
 - 32 **Bharucha AE**, Low PA, Camilleri M, Burton D, Gehrking TL, Zinsmeister AR. Pilot study of pyridostigmine in constipated patients with autonomic neuropathy. *Clin Auton Res* 2008; **18**: 194-202 [PMID: 18622640 DOI: 10.1007/s10286-008-0476-x]
 - 33 **Wedlake L**, A'Hern R, Russell D, Thomas K, Walters JR, Andreyev HJ. Systematic review: the prevalence of idiopathic bile acid malabsorption as diagnosed by SeHCAT scanning in patients with diarrhoea-predominant irritable bowel syndrome. *Aliment Pharmacol Ther* 2009; **30**: 707-717 [PMID: 19570102 DOI: 10.1111/j.1365-2036.2009.04081.x]
 - 34 **Johnston IM**, Nolan JD, Pattni SS, Appleby RN, Zhang JH, Kennie SL, Madhan GK, Jameie-Oskooei S, Pathmasriringam S, Lin J, Hong A, Dixon PH, Williamson C, Walters JR. Characterizing Factors Associated With Differences in FGF19 Blood Levels and Synthesis in Patients With Primary Bile Acid Diarrhea. *Am J Gastroenterol* 2016; **111**: 423-432 [PMID: 26856750 DOI: 10.1038/ajg.2015.424]
 - 35 **Wong BS**, Camilleri M, Carlson PJ, Guicciardi ME, Burton D, McKinzie S, Rao AS, Zinsmeister AR, Gores GJ. A Klotho β variant mediates protein stability and associates with colon transit in irritable bowel syndrome with diarrhea. *Gastroenterology* 2011; **140**: 1934-1942 [PMID: 21396369 DOI: 10.1053/j.gastro.2011.02.063]
 - 36 **Camilleri M**. Bile Acid diarrhea: prevalence, pathogenesis, and therapy. *Gut Liver* 2015; **9**: 332-339 [PMID: 25918262 DOI: 10.5009/gnl14397]
 - 37 **Peleman C**, Camilleri M, Busciglio I, Burton D, Donato L, Zinsmeister AR. Colonic Transit and Bile Acid Synthesis or Excretion in Patients With Irritable Bowel Syndrome-Diarrhea Without Bile Acid Malabsorption. *Clin Gastroenterol Hepatol* 2017; **15**: 720-727.e1 [PMID: 27856362 DOI: 10.1016/j.cgh.2016.11.012]
 - 38 **Sauter GH**, Münzing W, von Ritter C, Paumgartner G. Bile acid malabsorption as a cause of chronic diarrhea: diagnostic value of 7 α -hydroxy-4-cholesten-3-one in serum. *Dig Dis Sci* 1999; **44**: 14-19 [PMID: 9952217]
 - 39 **Lomer MC**, Parkes GC, Sanderson JD. Review article: lactose intolerance in clinical practice--myths and realities. *Aliment Pharmacol Ther* 2008; **27**: 93-103 [PMID: 17956597 DOI: 10.1111/j.1365-2036.2007.03557.x]
 - 40 **Deng Y**, Misselwitz B, Dai N, Fox M. Lactose Intolerance in Adults: Biological Mechanism and Dietary Management. *Nutrients* 2015; **7**: 8020-8035 [PMID: 26393648 DOI: 10.3390/nu7095380]
 - 41 **Tolliver BA**, Herrera JL, DiPalma JA. Evaluation of patients who meet clinical criteria for irritable bowel syndrome. *Am J Gastroenterol* 1994; **89**: 176-178 [PMID: 8304298]

- 42 **Suarez FL**, Savaiano DA, Levitt MD. A comparison of symptoms after the consumption of milk or lactose-hydrolyzed milk by people with self-reported severe lactose intolerance. *N Engl J Med* 1995; **333**: 1-4 [PMID: 7776987 DOI: 10.1056/NEJM199507063330101]
- 43 **Wilder-Smith CH**, Olesen SS, Materna A, Drewes AM. Fermentable Sugar Ingestion, Gas Production, and Gastrointestinal and Central Nervous System Symptoms in Patients With Functional Disorders. *Gastroenterology* 2018; **155**: 1034-1044.e6 [PMID: 30009815 DOI: 10.1053/j.gastro.2018.07.013]
- 44 **Townley RR**, Khaw KT, Shwachman H. Quantitative assay of disaccharidase activities of small intestinal mucosal biopsy specimens in infancy and childhood. *Pediatrics* 1965; **36**: 911-921 [PMID: 5846834]
- 45 **Saulnier DM**, Ringel Y, Heyman MB, Foster JA, Bercik P, Shulman RJ, Versalovic J, Verdu EF, Dinan TG, Hecht G, Guarner F. The intestinal microbiome, probiotics and prebiotics in neurogastroenterology. *Gut Microbes* 2013; **4**: 17-27 [PMID: 23202796 DOI: 10.4161/gmic.22973]
- 46 **Quigley EMM**. Prebiotics and Probiotics in Digestive Health. *Clin Gastroenterol Hepatol* 2019; **17**: 333-344 [PMID: 30267869 DOI: 10.1016/j.cgh.2018.09.028]
- 47 **Schnabel L**, Buscail C, Sabate JM, Bouchoucha M, Kesse-Guyot E, Allès B, Touvier M, Monteiro CA, Herberg S, Benamouzig R, Julia C. Association Between Ultra-Processed Food Consumption and Functional Gastrointestinal Disorders: Results From the French NutriNet-Santé Cohort. *Am J Gastroenterol* 2018; **113**: 1217-1228 [PMID: 29904158 DOI: 10.1038/s41395-018-0137-1]
- 48 **Mayer EA**, Savidge T, Shulman RJ. Brain-gut microbiome interactions and functional bowel disorders. *Gastroenterology* 2014; **146**: 1500-1512 [PMID: 24583088 DOI: 10.1053/j.gastro.2014.02.037]
- 49 **Levy RL**, Olden KW, Naliboff BD, Bradley LA, Francisconi C, Drossman DA, Creed F. Psychosocial aspects of the functional gastrointestinal disorders. *Gastroenterology* 2006; **130**: 1447-1458 [PMID: 16678558 DOI: 10.1053/j.gastro.2005.11.057]
- 50 **De Palma G**, Lynch MD, Lu J, Dang VT, Deng Y, Jury J, Umeh G, Miranda PM, Pigrau Pastor M, Sidani S, Pinto-Sanchez MI, Philip V, McLean PG, Hagelsieb MG, Surette MG, Bergonzelli GE, Verdu EF, Britz-McKibbin P, Neufeld JD, Collins SM, Bercik P. Transplantation of fecal microbiota from patients with irritable bowel syndrome alters gut function and behavior in recipient mice. *Sci Transl Med* 2017; **9** [PMID: 28251905 DOI: 10.1126/scitranslmed.aaf6397]
- 51 **Palsson OS**, Whitehead WE. Psychological treatments in functional gastrointestinal disorders: a primer for the gastroenterologist. *Clin Gastroenterol Hepatol* 2013; **11**: 208-16; quiz e22-3 [PMID: 23103907 DOI: 10.1016/j.cgh.2012.10.031]
- 52 **Bednarska O**, Walter SA, Casado-Bedmar M, Ström M, Salvo-Romero E, Vicario M, Mayer EA, Keita ÁV. Vasoactive Intestinal Polypeptide and Mast Cells Regulate Increased Passage of Colonic Bacteria in Patients With Irritable Bowel Syndrome. *Gastroenterology* 2017; **153**: 948-960.e3 [PMID: 28711627 DOI: 10.1053/j.gastro.2017.06.051]
- 53 **Camilleri M**, Lasch K, Zhou W. Irritable bowel syndrome: methods, mechanisms, and pathophysiology. The confluence of increased permeability, inflammation, and pain in irritable bowel syndrome. *Am J Physiol Gastrointest Liver Physiol* 2012; **303**: G775-G785 [PMID: 22837345 DOI: 10.1152/ajpgi.00155.2012]
- 54 **Turcotte JF**, Kao D, Mah SJ, Claggett B, Saltzman JR, Fedorak RN, Liu JJ. Breaks in the wall: increased gaps in the intestinal epithelium of irritable bowel syndrome patients identified by confocal laser endomicroscopy (with videos). *Gastrointest Endosc* 2013; **77**: 624-630 [PMID: 23357497 DOI: 10.1016/j.gie.2012.11.006]
- 55 **Fritscher-Ravens A**, Schuppan D, Ellrichmann M, Schoch S, Röcken C, Brasch J, Bethge J, Böttner M, Klose J, Milla PJ. Confocal endomicroscopy shows food-associated changes in the intestinal mucosa of patients with irritable bowel syndrome. *Gastroenterology* 2014; **147**: 1012-20.e4 [PMID: 25083606 DOI: 10.1053/j.gastro.2014.07.046]
- 56 **Witt ST**, Bednarska O, Keita ÁV, Icenhour A, Jones MP, Elsenbruch S, Söderholm JD, Engström M, Mayer EA, Walter S. Interactions between gut permeability and brain structure and function in health and irritable bowel syndrome. *Neuroimage Clin* 2018 [PMID: 30472166 DOI: 10.1016/j.nicl.2018.11.012]
- 57 **Ma ZF**, Yusof N, Hamid N, Lawenko RM, Mohammad WMZW, Liang MT, Sugahara H, Odamaki T, Xiao J, Lee YY. Bifidobacterium infantis M-63 improves mental health in victims with irritable bowel syndrome developed after a major flood disaster. *Benef Microbes* 2018; 1-10 [PMID: 30525951 DOI: 10.3920/BM2018.0008]
- 58 **Vaughn BP**, Rank KM, Khoruts A. Fecal Microbiota Transplantation: Current Status in Treatment of GI and Liver Disease. *Clin Gastroenterol Hepatol* 2019; **17**: 353-361 [PMID: 30055267 DOI: 10.1016/j.cgh.2018.07.026]
- 59 **Drossman DA**, Tack J, Ford AC, Szigethy E, Törnblom H, Van Oudenhove L. Neuromodulators for Functional Gastrointestinal Disorders (Disorders of Gut-Brain Interaction): A Rome Foundation Working Team Report. *Gastroenterology* 2018; **154**: 1140-1171.e1 [PMID: 29274869 DOI: 10.1053/j.gastro.2017.11.279]
- 60 **D'Souza DL**, Levasseur LM, Nezamis J, Robbins DK, Simms L, Koch KM. Effect of alosetron on the pharmacokinetics of alprazolam. *J Clin Pharmacol* 2001; **41**: 452-454 [PMID: 11304902]
- 61 **Camilleri M**. The role of pharmacogenetics in nonmalignant gastrointestinal diseases. *Nat Rev Gastroenterol Hepatol* 2012; **9**: 173-184 [PMID: 22310916 DOI: 10.1038/nrgastro.2012.2]
- 62 **Li Y**, Nie Y, Xie J, Tang W, Liang P, Sha W, Yang H, Zhou Y. The association of serotonin transporter genetic polymorphisms and irritable bowel syndrome and its influence on tegaserod treatment in Chinese patients. *Dig Dis Sci* 2007; **52**: 2942-2949 [PMID: 17394071 DOI: 10.1007/s10620-006-9679-y]
- 63 **Camilleri M**, Carlson P, Acosta A, Busciglio I, Nair AA, Gibbons SJ, Farrugia G, Klee EW. RNA sequencing shows transcriptomic changes in rectosigmoid mucosa in patients with irritable bowel syndrome-diarrhea: a pilot case-control study. *Am J Physiol Gastrointest Liver Physiol* 2014; **306**: G1089-G1098 [PMID: 24763552 DOI: 10.1152/ajpgi.00068.2014]
- 64 **Camilleri M**, Carlson P, Valentin N, Acosta A, O'Neill J, Eckert D, Dyer R, Na J, Klee EW, Murray JA. Pilot study of small bowel mucosal gene expression in patients with irritable bowel syndrome with diarrhea. *Am J Physiol Gastrointest Liver Physiol* 2016; **311**: G365-G376 [PMID: 27445342 DOI: 10.1152/ajpgi.00037.2016]
- 65 **Gikas A**, Triantafyllidis JK. The role of primary care physicians in early diagnosis and treatment of chronic gastrointestinal diseases. *Int J Gen Med* 2014; **7**: 159-173 [PMID: 24648750 DOI: 10.2147/IJGM.S58888]
- 66 **Tack J**, Pokrotnieks J, Urbonas G, Banciu C, Yakusevich V, Bunganic I, Törnblom H, Kleban Y, Eavis P, Tsuchikawa M, Miyagawa T. Long-term safety and efficacy of acotiamide in functional dyspepsia (postprandial distress syndrome)-results from the European phase 3 open-label safety trial. *Neurogastroenterol Motil* 2018; **30**: e13284 [PMID: 29315999 DOI: 10.1111/nmo.13284]

- 67 **Camilleri M**, Acosta A, Busciglio I, Bolding A, Dyer RB, Zinsmeister AR, Lueke A, Gray A, Donato LJ. Effect of colesvelam on faecal bile acids and bowel functions in diarrhoea-predominant irritable bowel syndrome. *Aliment Pharmacol Ther* 2015; **41**: 438-448 [PMID: 25594801 DOI: 10.1111/apt.13065]
- 68 **Wilcox C**, Turner J, Green J. Systematic review: the management of chronic diarrhoea due to bile acid malabsorption. *Aliment Pharmacol Ther* 2014; **39**: 923-939 [PMID: 24602022 DOI: 10.1111/apt.12684]
- 69 **Camilleri M**, Kerstens R, Rykx A, Vandeplassche L. A placebo-controlled trial of prucalopride for severe chronic constipation. *N Engl J Med* 2008; **358**: 2344-2354 [PMID: 18509121 DOI: 10.1056/NEJ-Moa0800670]
- 70 **Ford AC**, Brandt LJ, Young C, Chey WD, Foxx-Orenstein AE, Moayyedi P. Efficacy of 5-HT3 antagonists and 5-HT4 agonists in irritable bowel syndrome: systematic review and meta-analysis. *Am J Gastroenterol* 2009; **104**: 1831-1843; quiz 1844 [PMID: 19471254 DOI: 10.1038/ajg.2009.223]

P- Reviewer: Bouchoucha M, Cao HL, Chiba T, Kakisaka Y, Wang YP

S- Editor: Ma RY **L- Editor:** A **E- Editor:** Yin SY



Basic Study

Quest for the best endoscopic imaging modality for computer-assisted colonic polyp staging

Georg Wimmer, Michael Gadermayr, Gernot Wolkersdörfer, Roland Kwitt, Toru Tamaki, Jens Tischendorf, Michael Häfner, Shigeto Yoshida, Shinji Tanaka, Dorit Merhof, Andreas Uhl

ORCID number: Georg Wimmer (0000-0001-5529-0154); Michael Gadermayr (0000-0003-3145-9896); Gernot Wolkersdörfer (0000-0001-9425-2345); Roland Kwitt (0000-0001-9947-4465); Toru Tamaki (0000-0001-9712-7777); Jens Tischendorf (0000-0001-7052-4537); Michael Häfner (0000-0003-0686-4638); Shigeto Yoshida (0000-0003-2698-1030); Shinji Tanaka (0000-0001-5423-9074); Dorit Merhof (0000-0002-1672-2185); Andreas Uhl (0000-0002-5921-8755).

Author contributions: Wimmer G and Gadermayr M performed the experiments; Wimmer G, Gadermayr M, Merhof D and Uhl A coordinated the research; Tamaki T, Tischendorf J, Häfner M, Yoshida S and Tanaka S provided the endoscopic image databases; Wimmer G, Gadermayr M, Wolkersdörfer G and Uhl A wrote the paper.

Supported by the Austrian Science Fund (FWF), KLI project 429, No. TRP206.

Conflict-of-interest statement: There are no conflicts of interest.

Data sharing statement: No additional data are available.

ARRIVE guidelines statement: The authors have read the ARRIVE guidelines, and the manuscript was prepared and revised according to the ARRIVE guidelines.

Open-Access: This article is an

Georg Wimmer, Roland Kwitt, Andreas Uhl, Department of Computer Sciences, University of Salzburg, Salzburg 5020, Austria

Michael Gadermayr, Dorit Merhof, Interdisciplinary Imaging and Vision Institute Aachen, RWTH Aachen, Aachen 52074, Germany

Gernot Wolkersdörfer, Department of Internal Medicine I, Paracelsus Medical University/Salzburger Landeskliniken (SALK), Salzburg 5020, Austria

Toru Tamaki, Department of Information Engineering, Graduate School of Engineering, Hiroshima University, Hiroshima 7398527, Japan

Jens Tischendorf, Internal Medicine and Gastroenterology, University Hospital Aachen, Würselen 52146, Germany

Michael Häfner, Department of Gastroenterologie and Hepatologie, Krankenhaus St. Elisabeth, Wien 1080, Austria

Shigeto Yoshida, Department of Endoscopy and Medicine, Graduate School of Biomedical and Health Science, Hiroshima University, Hiroshima 7348551, Japan

Shinji Tanaka, Department of Endoscopy, Hiroshima University Hospital, Hiroshima 7348551, Japan

Corresponding author: Georg Wimmer, PhD, Postdoc, Department of Computer Sciences, University of Salzburg, Jakob Haringer Strasse 2, Salzburg 5020, Austria.

gwimmer@cosy.sbg.ac.at

Telephone: +43-662-80446035

Abstract

BACKGROUND

It was shown in previous studies that high definition endoscopy, high magnification endoscopy and image enhancement technologies, such as chromoendoscopy and digital chromoendoscopy [narrow-band imaging (NBI), i-Scan] facilitate the detection and classification of colonic polyps during endoscopic sessions. However, there are no comprehensive studies so far that analyze which endoscopic imaging modalities facilitate the automated classification of colonic polyps. In this work, we investigate the impact of endoscopic imaging modalities on the results of computer-assisted diagnosis systems for colonic polyp staging.

open-access article which was selected by an in-house editor and fully peer-reviewed by external reviewers. It is distributed in accordance with the Creative Commons Attribution Non Commercial (CC BY-NC 4.0) license, which permits others to distribute, remix, adapt, build upon this work non-commercially, and license their derivative works on different terms, provided the original work is properly cited and the use is non-commercial. See: <http://creativecommons.org/licenses/by-nc/4.0/>

Manuscript source: Invited manuscript

Received: December 14, 2018

Peer-review started: December 14, 2018

First decision: January 18, 2019

Revised: February 13, 2019

Accepted: February 15, 2019

Article in press: February 16, 2019

Published online: March 14, 2019

AIM

To assess which endoscopic imaging modalities are best suited for the computer-assisted staging of colonic polyps.

METHODS

In our experiments, we apply twelve state-of-the-art feature extraction methods for the classification of colonic polyps to five endoscopic image databases of colonic lesions. For this purpose, we employ a specifically designed experimental setup to avoid biases in the outcomes caused by differing numbers of images per image database. The image databases were obtained using different imaging modalities. Two databases were obtained by high-definition endoscopy in combination with i-Scan technology (one with chromoendoscopy and one without chromoendoscopy). Three databases were obtained by high-magnification endoscopy (two databases using narrow band imaging and one using chromoendoscopy). The lesions are categorized into non-neoplastic and neoplastic according to the histological diagnosis.

RESULTS

Generally, it is feature-dependent which imaging modalities achieve high results and which do not. For the high-definition image databases, we achieved overall classification rates of up to 79.2% with chromoendoscopy and 88.9% without chromoendoscopy. In the case of the database obtained by high-magnification chromoendoscopy, the classification rates were up to 81.4%. For the combination of high-magnification endoscopy with NBI, results of up to 97.4% for one database and up to 84% for the other were achieved. Non-neoplastic lesions were classified more accurately in general than non-neoplastic lesions. It was shown that the image recording conditions highly affect the performance of automated diagnosis systems and partly contribute to a stronger effect on the staging results than the used imaging modality.

CONCLUSION

Chromoendoscopy has a negative impact on the results of the methods. NBI is better suited than chromoendoscopy. High-definition and high-magnification endoscopy are equally suited.

Key words: Endoscopy; Colonic polyps; Automated diagnosis system; Narrow-band imaging; Chromoendoscopy; Imaging modalities; Image enhancement technologies

©The Author(s) 2019. Published by Baishideng Publishing Group Inc. All rights reserved.

Core tip: To determine which endoscopic imaging modalities are most suited for the automated diagnosis of colonic polyps, we apply a high number of state-of-the-art diagnosis systems to 5 endoscopic image databases obtained by different imaging modalities. We show that narrow-band imaging is well suited, whereas chromoendoscopy clearly decreases the results. High-definition and high-magnification endoscopy perform equally well. The image recording conditions have a great impact on the performance of the automated diagnosis systems.

Citation: Wimmer G, Gadermayr M, Wolkersdörfer G, Kwitt R, Tamaki T, Tischendorf J, Häfner M, Yoshida S, Tanaka S, Merhof D, Uhl A. Quest for the best endoscopic imaging modality for computer-assisted colonic polyp staging. *World J Gastroenterol* 2019; 25(10): 1197-1209

URL: <https://www.wjgnet.com/1007-9327/full/v25/i10/1197.htm>

DOI: <https://dx.doi.org/10.3748/wjg.v25.i10.1197>

INTRODUCTION

The demand for cost saving strategies with respect to discovery, treatment and surveillance of precursor lesions of colorectal cancer is high.

To date, the discovery of areas or lesions of interest depends on the endoscopist's

awareness, skills, experience and knowledge. Subsequent evaluation relies mainly on a variety of established classification systems^[1] that utilize different image enhancement technologies.

Detection, surveillance and treatment all require high diagnostic accuracy. Threshold criteria have been suggested by professional societies like the American Society for Gastrointestinal Endoscopy (ASGE)^[2].

Although image enhancement technologies such as chromoendoscopy and digital chromoendoscopy [*e.g.*, narrow-band imaging (NBI), Pentax's i-Scan or Fujinon's FICE] improve the detection, characterization and classification of colonic precursor lesions, it has been argued that this improvement applies for specialist centers only. Technical features of modern endoscopes and the body of information, which have to be applied during endoscopy, are rising steadily and, therefore, pose a challenge to the endoscopist. In fact, even after educational programs to train endoscopists, not all ASGE goals could be met by the majority of doctors, leading to misdiagnoses and inadequate surveillance strategies^[3].

Chromoendoscopy can be subdivided into conventional chromoendoscopy (CC) and digital chromoendoscopy: (1) CC came into clinical use 40 years ago. Staining the mucosa using (indigo-carmin) dye spray enables an easier detection and staging of colonic polyps; and (2) digital chromoendoscopy is a technique to facilitate 'chromoendoscopy without dyes'^[4] and can be subdivided into optical (NBI, blue laser imaging) and virtual chromoendoscopy (FICE, i-Scan).

In this work, we evaluate which of the image enhancement technologies (except for the FICE and the BLI system) and endoscopic modalities [high-definition (HD) or high-magnification (HM)] are most suited for computer-assisted colonic polyp staging. For this purpose, we utilize endoscopic imagery obtained from HD as well as HM endoscopes.

Clinical scenarios for the application of automated polyp staging systems are that the endoscopist either receives a staging suggestion after triggering the classification procedure to be applied to some captured area or that a continuous automated mucosa analysis is performed raising alarm in case of the identification of potentially malignant and precursor lesions.

In this work, we aim to answer the following two questions which were only partly or not at all answered in the previous literature: (1) which imaging modalities are best suited for automated colonic polyp staging systems? And (2) how strong is the influence of the image recording conditions on the results of automated diagnosis systems?

To answer these questions, we apply experiments with twelve different feature extraction methods on five colonic polyp image data sets from different imaging modalities.

To determine which imaging modality is best suited to stage colonic polyps, we use a specifically designed experimental setup to avoid biases in the outcome caused by differing numbers of images per modality. Only one prior work systematically analyzed the influence of imaging modalities on the results of automated diagnosis systems. However, only HD endoscopic imagery in combination with i-Scan technology, chromoendoscopy and traditional white light (WL) endoscopy was used. In this work, we additionally employ HM and NBI endoscopic imagery and a more systematic approach is taken.

To answer the second question, we analyze the influence of the image recording conditions, such as the viewpoint or the quality of the recorded images on the results of automated diagnosis systems. To the best of our knowledge, this has not been done before for automated polyp diagnosis systems.

Background

In the following, we (1) briefly summarize findings from different clinical studies, comparing the effectiveness of endoscopic imaging modalities for the detection and/or staging of colonic polyps for human endoscopists; and (2) review related algorithms for the automated staging of colonic polyps.

Modality comparison - human endoscopist: Clinical studies have shown that i-Scan technology, NBI and chromoendoscopy can be considered equivalent and typically achieve better prediction results compared to traditional WL endoscopy in case of HD endoscopes^[5,6].

It has been shown that HM NBI and HM chromoendoscopy achieve similar results for the diagnosis of colorectal polyps (non-neoplastic *vs* neoplastic)^[7,8]. Additionally, HM NBI and HM chromoendoscopy achieve higher diagnosis accuracies than standard WL endoscopy^[8].

In a survey on HD and HM endoscopes^[9], it was shown that HM endoscopes as well as HD endoscopes, with or without mucosal enhancement techniques, improve the detection and diagnosis of mucosal lesions compared to low definition

endoscopes. In a survey about digital chromoendoscopy techniques in colonoscopy^[10], it was found that NBI, i-Scan and FICE show encouraging results in predicting the histopathology of colonic polyps.

In summary, HM and HD- endoscopy both improve the detection and diagnosis of colonic polyps compared to low-definition endoscopy. Furthermore, image enhancement technologies such as i-Scan, NBI and chromoendoscopy generally improve the diagnosis of colonic polyps compared to standard WL endoscopy.

Computer-assisted polyp staging: The topic of this work is the computer-assisted staging of colonic polyps using endoscopic image data gathered from flexible endoscopes with different imaging enhancement technologies. We do not deal with automated detection of colonic polyps based on geometric properties (which is more often conducted for capsule endoscopic data due to the high effort required for human annotation of these data).

Previous works on computer-assisted staging of colonic polyps in combination with different image enhancement technologies can be divided in three categories depending on the used imaging modality: (1) HD endoscopes combined with or without staining the mucosa and the i-Scan technology: Previous works employed shape and contrast features extracted from blobs^[11], fractal analysis-based features^[12] and convolutional neural networks^[13]. (2) HM chromoendoscopy: Former studies estimated the pit density using Delaunay triangulation^[14], applied local binary patterns (LBP)^[15] and extracted features from wavelet transform subbands^[16-18]. And (3) HM endoscopy with NBI: Dense SIFT features were applied^[19,20], and features based on the vessel structure were extracted^[21].

MATERIALS AND METHODS

In this work, we use the two-class classification scheme differentiating between non-neoplastic (normal mucosa and hyperplastic polyps) and neoplastic lesions (adenomatous and malignant polyps). A sub-classification between adenomatous and malignant lesions cannot be performed because of missing label information for the two NBI databases and the very limited amount of malignant polyps for the remaining three databases (Table 1).

HD endoscopy combined the i-Scan technology and chromoendoscopy

HD-endoscopy has the advantage of a higher resolution compared to standard definition endoscopes. Our HD-endoscopic images are gathered by traditional WL and three i-Scan modes, both with and without CC. The i-Scan (Pentax) image processing technology^[21,22] is a digital contrast enhancement method that consists of combinations of surface enhancement, contrast enhancement and tone enhancement. Figure 1 shows images of an adenomatous polyp using WL endoscopy (Figure 1A), i-Scan (Figure 1B-D), CC (Figure 1E) and combinations of CC and i-Scan (Figure 1F-H). Figure 2A and B shows exemplar images of the two classes using CC and i-Scan mode 2.

The images were acquired at St. Elisabeth Hospital in Vienna by extracting patches 256×256 in size from frames of HD-endoscopic (Pentax HiLINE HD+90i Colonoscope) videos. Most of the videos contain sequences from eight imaging modalities [with or without i-Scan (modes 1,2,3) and with or without staining], but in some of the videos, only a subset of the eight imaging modalities occurs.

A previous work^[23] showed that it is generally favorable to combine images of different i-Scan modes and WL endoscopy for classifier training, but the chromoendoscopy mode (chromoendoscopy or no chromoendoscopy) should be identical for training and evaluation images. This outcome motivated us to group the HD images into two separate image databases, one consisting of images without using chromoendoscopy (no matter which i-Scan mode or WL) and the other one consisting of images using chromoendoscopy. The two HD databases are further denoted as 'HD-no-chromo' (HDNC) and 'HD-chromo' (HDC). Table 1 lists the number of images and patients per class. The two HD databases consist of between 102 and 154 images per i-Scan mode and WL endoscopy, respectively.

HM endoscopy in combination with chromoendoscopy

HM endoscopes are defined by the capacity to perform optical zoom/magnification by using a moveable lens in the tip of the endoscope. In that way, magnified images are obtained without losing display quality. HM endoscopy enables the visualization of mucosal details that cannot be seen with standard endoscopy. The CCHM database was acquired using zoom-endoscopy with 150-fold magnification in combination with chromoendoscopy. The CCHM image data set was acquired at the Medical University of Vienna using a zoom-colonoscope (Olympus Evis Exera CF-Q160ZI/L) with a

Table 1 Ground truth information of the investigated image data sets

		Non-neoplastic	Neoplastic	Total
HDNC	Images	144	334 (301 A, 33 M)	478
	Patients	39	77	81
HDC	Images	213	307 (276 A, 31 M)	520
	Patients	50	78	84
CCHM	Images	198	518 (420 A, 98 M)	716
	Patients	14	32	40
NBI-A	Images	173	214	387
	Patients	98	135	211
NBI-H	Images	112	186	298
	Patients	84	120	182

Ground truth information of the investigated image datasets. The ground truth is based on histology [all data sets except the high-magnification narrow-band imaging Hiroshima (NBI-H) dataset] or the optical appearance of the polyps (NBI-H). The number of adenomatous and malignant lesions is provided for those databases with available information (the two high-definition databases and the high-magnification chromoendoscopy database). A: Adenomatous; M: Malignant; CCHM: High-magnification chromoendoscopy; NBI-A: High magnification narrow-band imaging, Aachen; NBI-H: High magnification narrow-band imaging, Hiroshima; HDC: High-definition chromoendoscopy; HDNC: High-definition, no chromoendoscopy.

magnification factor of 150 and indigocarmine dye-spraying. The database is acquired by extracting patches 256×256 in size from 327 endoscopic color images (either 624×533 pixels or 586×502 pixels in size) of 40 patients (Table 1). Example images of the two classes can be seen in Figure 2C and D.

HM endoscopy in combination with NBI

NBI is a videoendoscopic system using RGB rotary filters placed in front of a WL source to narrow the bandwidth of the spectral transmittance. NBI enhances the visibility of microvessels and their fine structure on the colorectal surface. The pits are also indirectly observable since the microvessels between the pits are enhanced in black, while the pits remain white.

In this work, we employ two different data sets gathered by HM endoscopy using NBI. The images of the NBI-HM database Aachen (NBI-A) were acquired at the University Hospital Aachen using an NBI zoom endoscope, which can magnify the image to a maximum of 150-fold (CF-Q160ZI, Olympus Medical Systems Europe). The database was acquired by extracting patches 256×256 in size from 387 endoscopic color images 502×586 in size from 211 patients (Table 1). Exemplar images of the two classes are shown in Figure 2E and F.

The NBI-HM database Hiroshima (NBI-H) was acquired at the Hiroshima University Hospital using an NBI zoom endoscope, which can magnify the image to a maximum of 75-fold (CF-H260AZ/I, Olympus Optical Co.). Care was taken that the lighting conditions, zooming and optical magnification were kept as similar as possible across different images. The database (Table 1) is acquired by extracting patches 256×256 in size from captured images 1440×1080 pixels in size. Exemplar images of the two can be seen in Figure 2G and H.

In contrast to the other databases, whose image labels were provided according to their histological diagnosis, the image labels of the NBI-H database were provided according to the optical appearance of the polyps (by at least two experts).

Feature extraction methods

In this section, we briefly describe the twelve feature extraction methods. All methods have proven to be well suited for the diagnosis of colonic polyps in the literature for certain imaging settings.

Non-adapted CNN and adapted CNN: Two convolutional neural networks. One is learned on the ImageNet database [non-adapted CNN (NA-CNN)] and the other one is adapted to colonic polyp classification (A-CNN) by training it on our polyp databases^[24].

Delaunay^[14]: This approach analyzes the pit-pattern structure and was developed for HM-endoscopic imagery using chromoendoscopy.

BlobShape^[11], BALFD^[25] and BSAGLFD^[12]: Three methods that are analyzing the pit-pattern structure and were designed for HD-endoscopic image data.

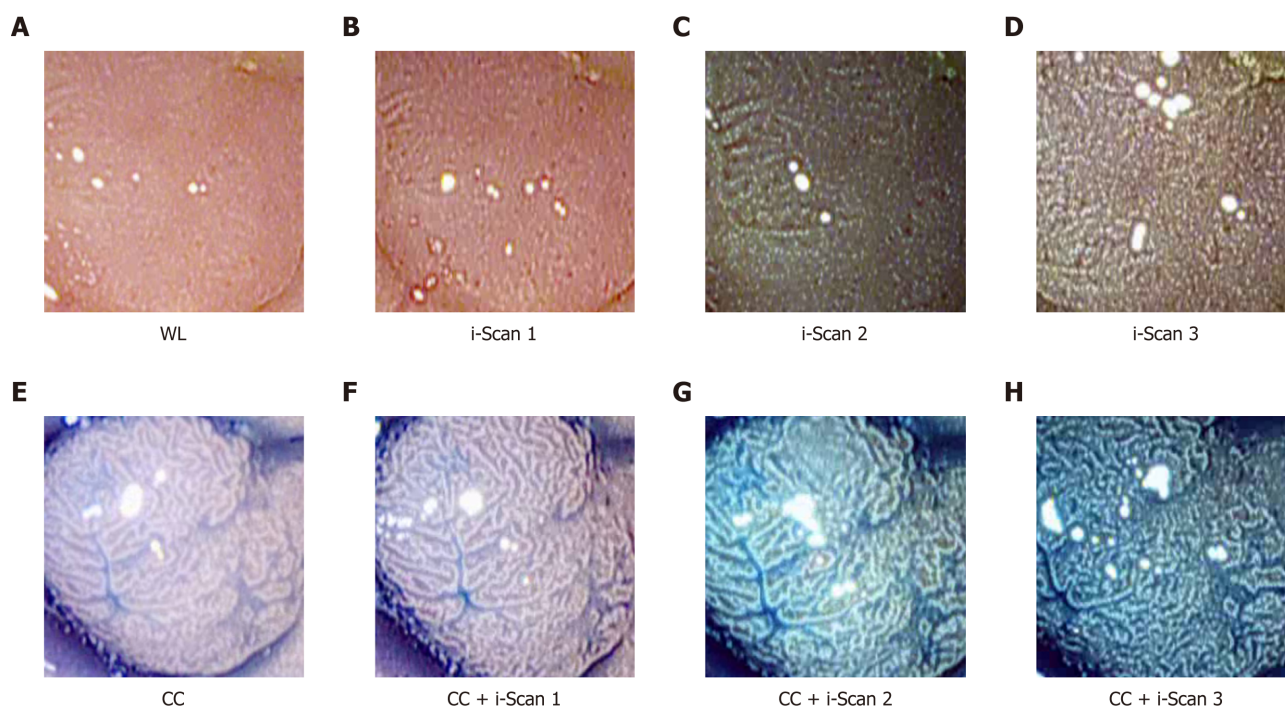


Figure 1 Images of a polyp using digital (i-Scan) and/or conventional chromoendoscopy. WL: White light endoscopy; CC: Conventional chromoendoscopy.

Dual-tree complex wavelet transform, Gabor wavelet transform-Weibull and Shearlet-Weibull: Three wavelet based transforms [dual-tree complex wavelet transform (DT-CWT), Gabor wavelet transform (GWT) and shearlet transform] whose subbands are fitted by the two-parameter Weibull distribution^[18].

Local color vector patterns and multiscale block binary patterns: Two methods based on LBP. Multiscale local color vector patterns (LCVP)^[15] were developed for HM-endoscopic imagery using chromoendoscopy, and the multiscale block binary patterns (MB-LBP) operator^[26] is a general purpose image descriptor.

VesselFeature: This approach^[21] analyzes the blood vessel structure and is designed for NBI images.

Experimental setup

For our experiments classifying the five endoscopic image databases, we rely on a protocol based on the selection of repeated random splits, as is common practice in machine learning. In one iteration, the classification model is trained and evaluated with randomly selected samples from the overall data set. This selection is performed in a way to ensure that the images of one patient are either all in the training or in the evaluation data set (similar to the leave-one-patient-out protocol^[15]). To facilitate a fair comparison between image data sets, the amount of training samples is fixed and balanced over the two classes. Specifically, we randomly select 80 samples per class for training and 20 samples per class for evaluation.

Statistical analysis

To obtain stable outcomes, we apply 32 random splits and report the mean accuracies as well as the standard deviations. Additionally, we report the sensitivity, specificity, positive predictive value (PPV) and negative predictive value (NPV).

Classification is performed using linear support vector machines (SVMs)^[27]. The optimal SVM's *c*-value is assessed during inner cross-validation using the training data only.

RESULTS

In **Figure 3**, we show the SVM classification results of our 12 feature extraction methods on each of our 5 colonic polyp image data sets. In each subplot, we see the classification accuracies on the 5 image data sets using one certain image representation. **Figure 4** shows a boxplot that summarizes the results in **Figure 3**. This figure gives an overview of the results of the different feature extraction techniques per data set.

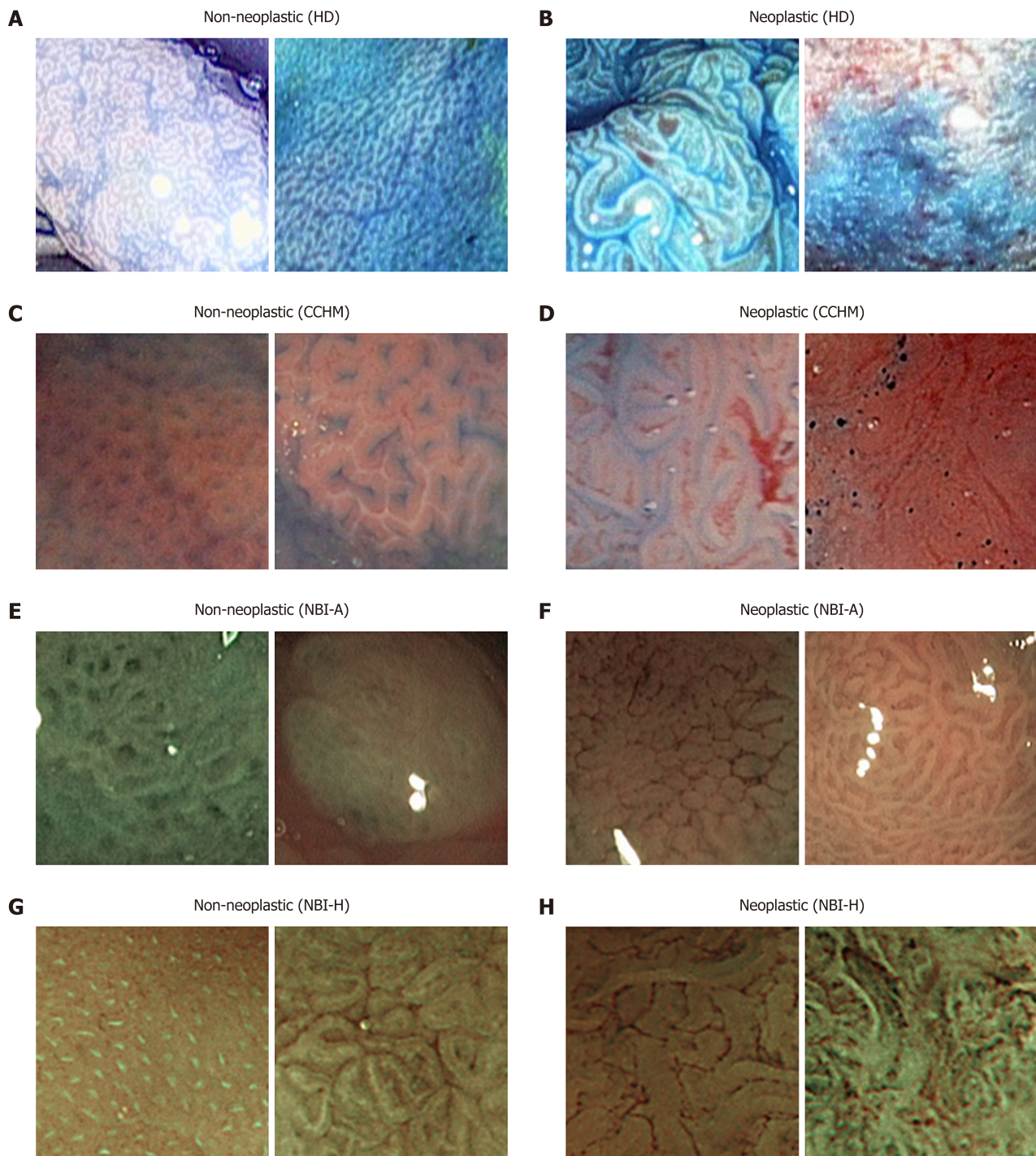


Figure 2 Example images of the two classes from the employed image databases. HD: High-definition endoscopy; CCHM: High-magnification chromoendoscopy; NBI-A: High-magnification narrow-band imaging, Aachen; NBI-H: High-magnification narrow-band imaging, Hiroshima.

Generally, it is feature dependent which imaging modalities achieve high results and which do not. This outcome was to be expected since many of the employed feature extraction methods were specifically developed for certain imaging modalities.

For the two HD image databases, overall classification rates were achieved of up to 79.2% (HDC) and up to 88.9% (HDNC). The classification rates for the database obtained by CCHM reached up to 81.4%. For the two databases combining HM endoscopy with NBI, results of up to 97.4% (NBI-H) and 84% (NBI-A) were achieved.

In **Figure 3**, we can observe that the NBI-H set achieves the highest overall classification rates for 11 out of 12 feature extraction methods (all except the Delaunay feature).

Comparing the results of the two NBI-based data sets, we notice that the NBI-A image data shows distinctly lower classification rates compared to the NBI-H data set.

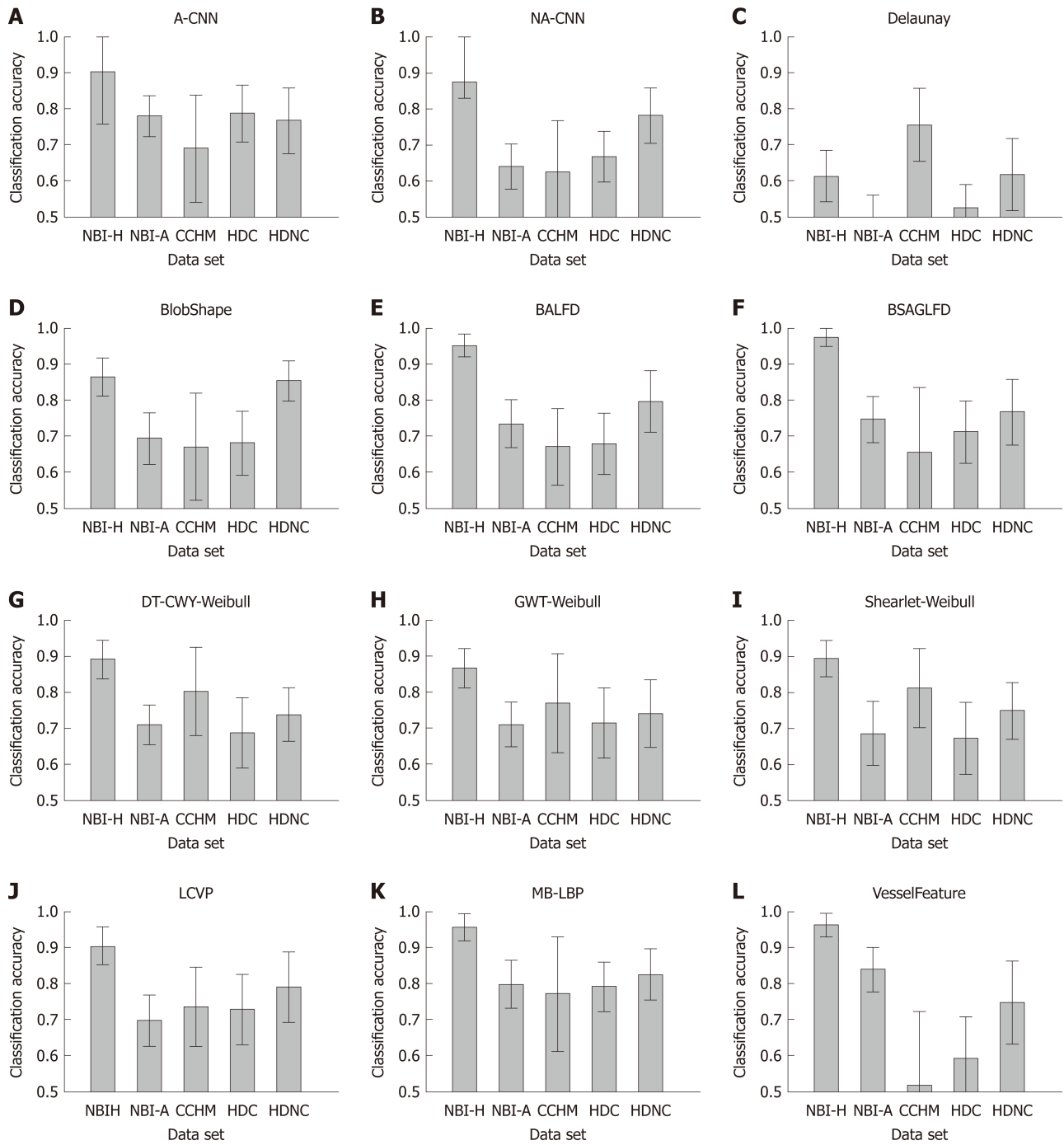


Figure 3 Mean classification accuracies and standard deviations of the methods per data set. HDC: High-definition chromoendoscopy; HDNC: High-definition, no chromoendoscopy; CCHM: High-magnification chromoendoscopy; NBI-A: High-magnification narrow-band imaging, Aachen; NBI-H: High-magnification narrow-band imaging, Hiroshima; A-CNN: Adapted CNN; NA-CNN: Non-adapted CNN; DT-CWT: Dual-tree complex wavelet transform; GWT: Gabor wavelet transform.

Considering the results of the two HD-endoscopic data sets HDC and HDNC, it can be observed that the obtained rates using chromoendoscopy are inferior in 11 out of 12 cases (all except the A-CNN approach).

Figure 5 gives an overview of the results of the methods for the statistical performance measures specificity, sensitivity, PPV and NPV per data set. The specificity rates are in general clearly higher than the sensitivity rates (in four of five databases) which means that non-neoplastic lesions are classified more correctly than neoplastic lesions.

DISCUSSION

Influence of the image recording conditions on the results

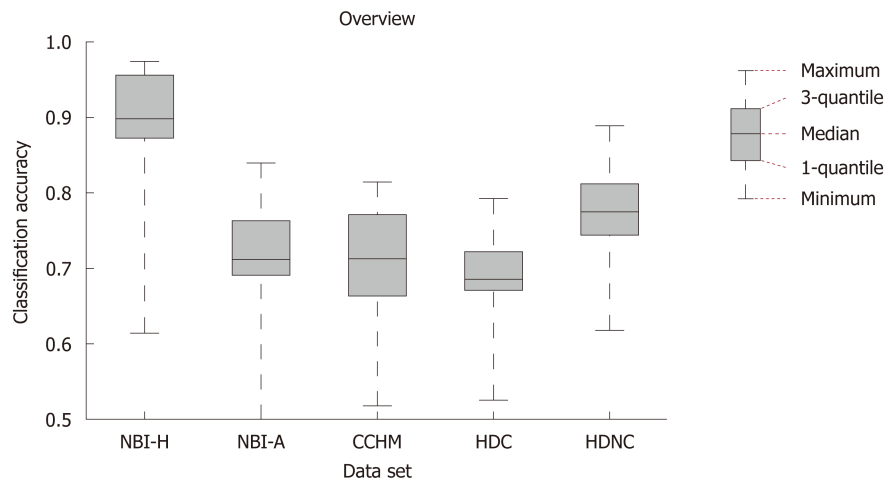


Figure 4 Box plot showing the median, the quantiles and the minimum and maximum accuracies obtained by the different feature extraction techniques per imaging modality. NBI-H: High-magnification narrow-band imaging, Hiroshima; NBI-A: High-magnification narrow-band imaging, Aachen; CCHM: High-magnification chromoendoscopy; HDC: High-definition chromoendoscopy; HDNC: High-definition, no chromoendoscopy.

The classification results of the considered computer-assisted staging systems depend on not only the used feature extraction methods and image modalities, but also to a considerable extent on the quality of the gathered images (blur, lighting conditions, in focus *vs* out of focus, visibility of the mucosal structures, visibility of markers for the respective classes, and other factors) and the uniformity of the image recording conditions such as the viewpoint (distance and angle of view of the endoscope towards the mucosa wall) and the lighting conditions across the images of a database.

When we compare our two NBI databases, there are clear advantages with respect to the visibility of markers for the respective classes and the consistency of the image recording conditions for the NBI-H database. For the NBI-H database, special care was taken to keep lighting conditions, zoom and optical magnification as similar as possible across different images. The NBI-H database is the only database whose labeling is based on the optical appearance of the polyps^[19] (especially the microvessels); thus, special care was taken to ensure that class-specific characteristics were well visible on each image. In **Figure 6**, we can see some example images from the NBI-A database that were acquired with poor illumination, poor visibility of mucosal structures or reflections.

To quantify the differences in the image quality between the two NBI databases we conduct two experiments that will show us differences in the visibility of mucosal structures and the amount of reflections in the images. To show the amount of reflections in an image we simply add up the number of overexposed pixels (gray value bigger than 240) per image. Our approach to show the visibility of mucosal structures per image is based on difference of Gaussians (DoG). We apply DoG by subtracting a Gaussian blurred image from the original image. By using a Gaussian filter kernel with $\sigma = 3$ and size 8×8 , the resulting DoG image of a grayscale endoscopic image highlights mucosal structures, such as the pit-pattern structure. The mean over the absolute values of the DoG image gives an indication about the visibility of mucosal structures in an image. The higher the mean value, the better the visibility of mucosal structures. In **Figure 7**, we present two histograms showing differences in image quality between the two NBI databases.

We can clearly see in **Figure 7** that the NBI-A database clearly contains more reflections in the images as the NBI-H database. The average DoG values are clearly higher in the NBI-H database, which indicates a better visibility of mucosal structures in the NBI-H database.

A third experiment comparing the number of underexposed pixels per image showed that the NBI-A database has a higher percentage of images where large areas of the image are underexposed, but the differences between the two NBI databases are rather small, which is why we only show figures for reflections and the visibility of mucosal structures, where clear differences occur.

Thus, it is not surprising that the NBI-H database achieved distinctly better results than the NBI-A database in our experiments. Therefore, the image recording conditions do have a high impact on automated diagnosis systems.

The fact that the image recording conditions have significant impact on the classification results and that it is difficult to quantify the quality of the images and

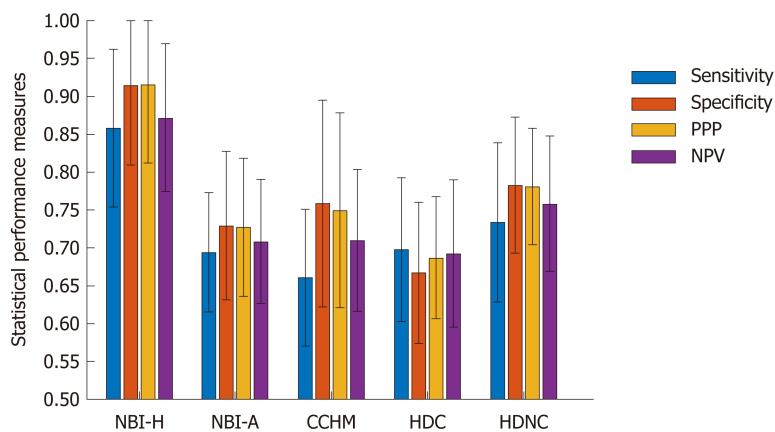


Figure 5 Bar plot showing the means and standard deviations of four statistical performance measures (sensitivity, specificity, positive predictive value and negative predictive value) over the different feature extraction techniques per data set. NPV: Negative predictive value; PPV: Positive predictive value; NBI-H: High-magnification narrow-band imaging, Hiroshima; NBI-A: High-magnification narrow-band imaging, Aachen; CCHM: High-magnification chromoendoscopy; HDC: High-definition chromoendoscopy; HDNC: High-definition, no chromoendoscopy.

the uniformity of the image recording conditions in the different databases makes it difficult to assess which imaging modality is best suitable for the staging of colonic polyps.

However, for example the two HD databases are gathered from the same endoscopic videos (taken by the same endoscopist); thus, their quality and the uniformity of the image recording conditions are quite similar. The images from the CCHM database are taken from the same endoscopist as the videos of the HD database; therefore, their quality could also be assumed to be at least similar. The images of the CCHM database as well as the two HD databases are acquired under varying viewpoint and lighting conditions, but the mucosal structure (the pit-pattern structure) is always visible for these three databases. Only the NBI-A database contains images without visible mucosal structures.

Chromoendoscopy vs NBI

When we compare the results on the two NBI-HM databases (NBI-H and NBI-A) with the results on the CCHM, we see that the results for the NBI-H database are clearly better than those for the CCHM database and that the results for the NBI-A database are quite similar to those for the CCHM database. Therefore, we cannot clearly answer the question which of the two imaging modalities, chromoendoscopy or NBI, is better suited for the automated staging of colonic polyps. However, because of the similar results of the NBI-A and CCHM databases, despite the higher image quality of the CCHM database, and the distinctly higher results on the NBI-H database it seems safe to assume that NBI is better suited than chromoendoscopy.

Chromoendoscopy vs no chromoendoscopy

When we compare the results of the two HD-endoscopic data sets, then we can observe that chromoendoscopy decreases the classification rates for all feature extraction methods except for one. Therefore, chromoendoscopy should not be used for automated diagnosis systems.

HM vs HD

Based on the overall similar results of the two chromoendoscopic databases (CCHM and HDC) shown in Figures 3 and 4, HD endoscopy and HM endoscopy are approximately equally well suited for automated diagnosis systems. However, the results are not strictly conclusive since most of the HD-endoscopic images are gathered using different i-Scan modes, in contrast to the HM images which are gathered without digital chromoendoscopy.

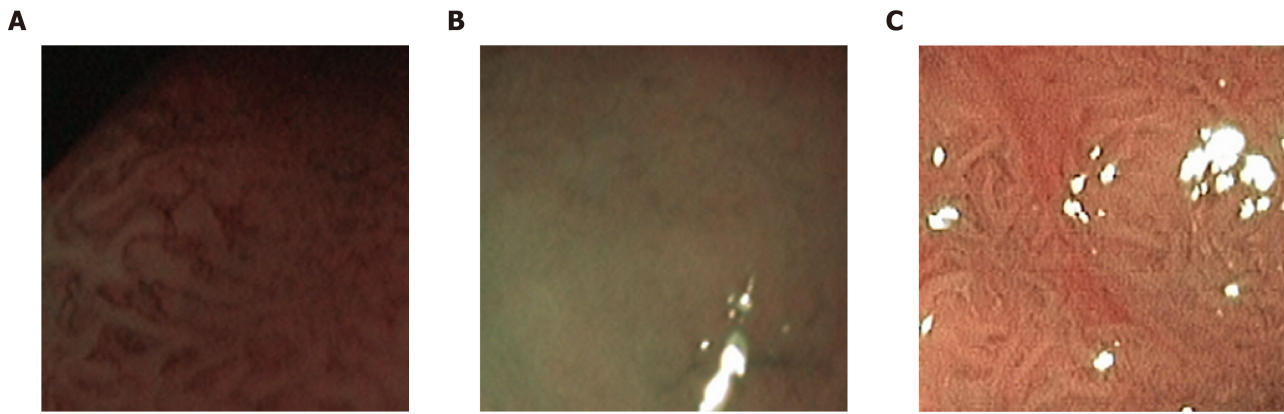


Figure 6 Example images of the high magnification narrow-band imaging Aachen database showing poor illumination (A) poor visibility of mucosal structures (B) and reflections (C).

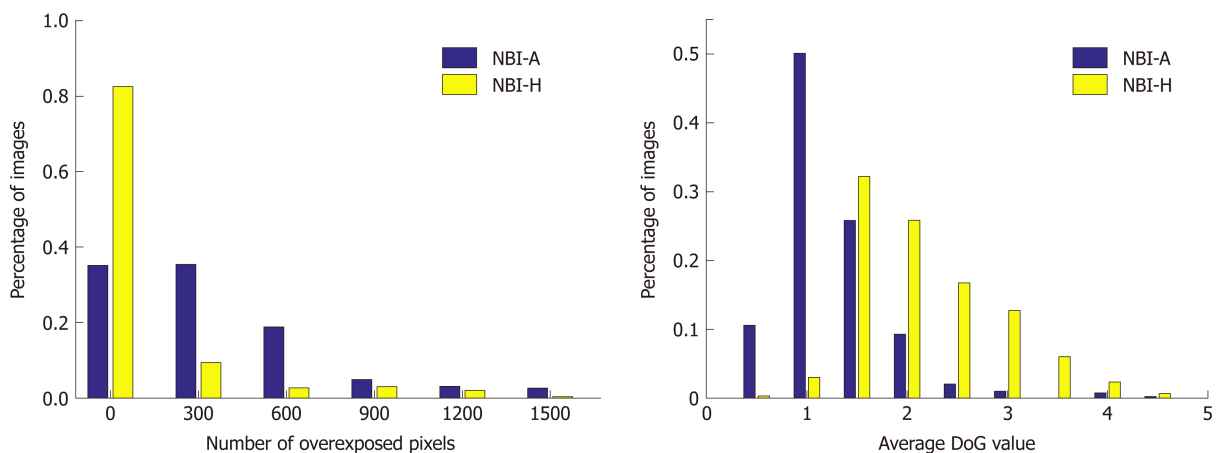


Figure 7 Histograms showing the number of overexposed pixels (A) respectively the average difference of Gaussians values (B) per image of the two narrow-band imaging databases. NBI-A: High-magnification narrow-band imaging, Aachen; NBI-H: High-magnification narrow-band imaging, Hiroshima; DoG: Difference of Gaussians.

ARTICLE HIGHLIGHTS

Research background

Colorectal cancer is the second most common cause of cancer death worldwide. Computer-aided decision support systems (CADSSs) aim at helping physicians to detect and classify colonic polyps more accurately. Since about two decades, there is a rising interest in CADSSs and a rising number on publications on CADSSs for colonic polyp staging.

Research motivation

Clinical studies showed that high definition endoscopy, high magnification endoscopy and image enhancement technologies, such as chromoendoscopy and digital chromoendoscopy [narrow-band imaging (NBI), i-Scan] facilitate the detection and classification of colonic polyps during endoscopic sessions. However, there are no comprehensive studies so far that analyze which endoscopic imaging modalities facilitate CADSSs for colonic polyp staging.

Research objectives

In this work, we assess which endoscopic imaging modalities are best suited for the computer-assisted classification of colonic polyps.

Research methods

In our experiments, we apply twelve automated polyp staging systems to five endoscopic image databases of colonic lesions. The image databases were obtained using different endoscopic imaging modalities. By comparing the classification results of the different image databases, we aim to find out which imaging modalities are most suited for the automated classification of colonic polyps.

Research results

The high-definition (HD) image databases obtained with chromoendoscopy achieved overall classification rates of up to 79.2% whereas the HD image databases without chromoendoscopy achieved results up to 88.9%. The classification rates of the image database obtained by high-magnification (HM) chromoendoscopy were up to 81.4%. For the two image databases obtained by HM endoscopy in combination with NBI, one database achieved classification rates up to 97.4%, whereas the other one only achieved classification rates up to 84%.

Research conclusions

The results strongly indicate that chromoendoscopy has a negative impact on the automated diagnosis. The results also indicate that HD and HM endoscopy perform equally well, although the results are not strictly conclusive. Given the higher costs of HM systems and the difficulty in acquiring high quality imagery due to the HM (which definitely requires a well-trained endoscopist), HD systems should be the better option in clinical computer-assisted staging practice. In case of the comparison of chromoendoscopy *vs* NBI, there are strong indications that NBI is favorable. However, it turned out that the image recording conditions partly contribute to a stronger effect on the staging results than the used imaging modality.

Research perspectives

We showed that CADSSs for colonic polyp staging should not be applied to endoscopic image data obtained by chromoendoscopy, whereas image data obtained by NBI is suited for automated diagnosis systems. Important factors for the success of CADSSs are the image quality of the endoscopic image data and the uniformity of the image recording conditions.

REFERENCES

- 1 Berr F, Oyama T, Ponchon T, Yahagi N. *Early Neoplasias of the Gastrointestinal Tract: Endoscopic Diagnosis and Therapeutic Decisions*. Boston: Springer 2014; [DOI: [10.1007/978-1-4614-8292-5](https://doi.org/10.1007/978-1-4614-8292-5)]
- 2 Rex DK, Kahi C, O'Brien M, Levin TR, Pohl H, Rastogi A, Burgart L, Imperiale T, Ladabaum U, Cohen J, Lieberman DA. The American Society for Gastrointestinal Endoscopy PIVI (Preservation and Incorporation of Valuable Endoscopic Innovations) on real-time endoscopic assessment of the histology of diminutive colorectal polyps. *Gastrointest Endosc* 2011; **73**: 419-422 [PMID: [21353837](https://pubmed.ncbi.nlm.nih.gov/21353837/) DOI: [10.1016/j.gie.2011.01.023](https://doi.org/10.1016/j.gie.2011.01.023)]
- 3 Patel SG, Schoenfeld P, Kim HM, Ward EK, Bansal A, Kim Y, Hosford L, Myers A, Foster S, Craft J, Shopinski S, Wilson RH, Ahnen DJ, Rastogi A, Wani S. Real-Time Characterization of Diminutive Colorectal Polyp Histology Using Narrow-Band Imaging: Implications for the Resect and Discard Strategy. *Gastroenterology* 2016; **150**: 406-418 [PMID: [26522260](https://pubmed.ncbi.nlm.nih.gov/26522260/) DOI: [10.1053/j.gastro.2015.10.042](https://doi.org/10.1053/j.gastro.2015.10.042)]
- 4 ASGE Technology Committee; Manfredi MA, Abu Dayyeh BK, Bhat YM, Chauhan SS, Gottlieb KT, Hwang JH, Komanduri S, Konda V, Lo SK, Maple JT, Murad FM, Siddiqui UD, Wallace MB, Banerjee S. Electronic chromoendoscopy. *Gastrointest Endosc* 2015; **81**: 249-261 [PMID: [25484330](https://pubmed.ncbi.nlm.nih.gov/25484330/) DOI: [10.1016/j.gie.2014.06.020](https://doi.org/10.1016/j.gie.2014.06.020)]
- 5 Hoffman A, Kagel C, Goetz M, Tresch A, Mudter J, Biesterfeld S, Galle PR, Neurath MF, Kiesslich R. Recognition and characterization of small colonic neoplasia with high-definition colonoscopy using i-Scan is as precise as chromoendoscopy. *Dig Liver Dis* 2010; **42**: 45-50 [PMID: [19473893](https://pubmed.ncbi.nlm.nih.gov/19473893/) DOI: [10.1016/j.dld.2009.04.005](https://doi.org/10.1016/j.dld.2009.04.005)]
- 6 Bouwens MW, de Ridder R, Masclee AA, Driessen A, Riedl RG, Winkens B, Sanduleanu S. Optical diagnosis of colorectal polyps using high-definition i-scan: an educational experience. *World J Gastroenterol* 2013; **19**: 4334-4343 [PMID: [23885144](https://pubmed.ncbi.nlm.nih.gov/23885144/) DOI: [10.3748/wjg.v19.i27.4334](https://doi.org/10.3748/wjg.v19.i27.4334)]
- 7 Tischendorf JJ, Wasmuth HE, Koch A, Hecker H, Trautwein C, Winograd R. Value of magnifying chromoendoscopy and narrow band imaging (NBI) in classifying colorectal polyps: a prospective controlled study. *Endoscopy* 2007; **39**: 1092-1096 [PMID: [18072061](https://pubmed.ncbi.nlm.nih.gov/18072061/) DOI: [10.1055/s-2007-966781](https://doi.org/10.1055/s-2007-966781)]
- 8 Chang CC, Hsieh CR, Lou HY, Fang CL, Tiong C, Wang JJ, Wei IV, Wu SC, Chen JN, Wang YH. Comparative study of conventional colonoscopy, magnifying chromoendoscopy, and magnifying narrow-band imaging systems in the differential diagnosis of small colonic polyps between trainee and experienced endoscopist. *Int J Colorectal Dis* 2009; **24**: 1413-1419 [PMID: [19603174](https://pubmed.ncbi.nlm.nih.gov/19603174/) DOI: [10.1007/s00384-009-0760-9](https://doi.org/10.1007/s00384-009-0760-9)]
- 9 ASGE Technology Committee. High-definition and high-magnification endoscopes. *Gastrointest Endosc* 2014; **80**: 919-927 [PMID: [25442091](https://pubmed.ncbi.nlm.nih.gov/25442091/) DOI: [10.1016/j.gie.2014.06.019](https://doi.org/10.1016/j.gie.2014.06.019)]
- 10 Rameshshanker R, Wilson A. Electronic Imaging in Colonoscopy: Clinical Applications and Future Prospects. *Curr Treat Options Gastroenterol* 2016; **14**: 140-151 [PMID: [26923476](https://pubmed.ncbi.nlm.nih.gov/26923476/) DOI: [10.1007/s11938-016-0075-1](https://doi.org/10.1007/s11938-016-0075-1)]
- 11 Häfner M, Uhl A, Wimmer G. Medical Computer Vision. A novel shape feature descriptor for the classification of polyps in HD colonoscopy. *Medical Computer Vision. Large Data in Medical Imaging*. Cham: Springer 2014; 205-213 [DOI: [10.1007/978-3-319-05530-5_20](https://doi.org/10.1007/978-3-319-05530-5_20)]
- 12 Häfner M, Tamaki T, Tanaka S, Uhl A, Wimmer G, Yoshida S. Local fractal dimension based approaches for colonic polyp classification. *Med Image Anal* 2015; **26**: 92-107 [PMID: [26385078](https://pubmed.ncbi.nlm.nih.gov/26385078/) DOI: [10.1016/j.media.2015.08.007](https://doi.org/10.1016/j.media.2015.08.007)]
- 13 Ribeiro E, Uhl A, Wimmer G, Häfner M. Exploring Deep Learning and Transfer Learning for Colonic Polyp Classification. *Comput Math Methods Med* 2016; **2016**: 6584725 [PMID: [27847543](https://pubmed.ncbi.nlm.nih.gov/27847543/) DOI: [10.1155/2016/6584725](https://doi.org/10.1155/2016/6584725)]
- 14 Häfner M, Liedlgruber M, Uhl A, Vécsei A, Wrba F. Delaunay triangulation-based pit density estimation for the classification of polyps in high-magnification chromo-colonoscopy. *Comput Methods Programs Biomed* 2012; **107**: 565-581 [PMID: [22325257](https://pubmed.ncbi.nlm.nih.gov/22325257/) DOI: [10.1016/j.cmpb.2011.12.012](https://doi.org/10.1016/j.cmpb.2011.12.012)]
- 15 Häfner M, Liedlgruber M, Uhl A, Vécsei A, Wrba F. Color treatment in endoscopic image classification using multi-scale local color vector patterns. *Med Image Anal* 2012; **16**: 75-86 [PMID: [21624846](https://pubmed.ncbi.nlm.nih.gov/21624846/) DOI: [10.1016/j.media.2011.05.006](https://doi.org/10.1016/j.media.2011.05.006)]
- 16 Häfner M, Kwitt R, Uhl A, Gangl A, Wrba F, Vécsei A. Computer-assisted pit-pattern classification in different wavelet domains for supporting dignity assessment of colonic polyps. *Pattern Recognition* 2008;

- 42: 1180-1191 [DOI: [10.1016/j.patcog.2008.07.012](https://doi.org/10.1016/j.patcog.2008.07.012)]
- 17 **Häfner M**, Liedlgruber M, Uhl A. Colonic polyp classification in high-definition video using complex wavelet-packets. *Bildverarbeitung für die Medizin* 2015; 365-370 [DOI: [10.1007/978-3-662-46224-9_63](https://doi.org/10.1007/978-3-662-46224-9_63)]
- 18 **Wimmer G**, Tamaki T, Tischendorf JJ, Häfner M, Yoshida S, Tanaka S, Uhl A. Directional wavelet based features for colonic polyp classification. *Med Image Anal* 2016; **31**: 16-36 [PMID: [26948110](https://pubmed.ncbi.nlm.nih.gov/26948110/) DOI: [10.1016/j.media.2016.02.001](https://doi.org/10.1016/j.media.2016.02.001)]
- 19 **Tamaki T**, Yoshimuta J, Kawakami M, Raytchev B, Kaneda K, Yoshida S, Takemura Y, Onji K, Miyaki R, Tanaka S. Computer-aided colorectal tumor classification in NBI endoscopy using local features. *Med Image Anal* 2013; **17**: 78-100 [PMID: [23085199](https://pubmed.ncbi.nlm.nih.gov/23085199/) DOI: [10.1016/j.media.2012.08.003](https://doi.org/10.1016/j.media.2012.08.003)]
- 20 **Kominami Y**, Yoshida S, Tanaka S, Sanomura Y, Hirakawa T, Raytchev B, Tamaki T, Koide T, Kaneda K, Chayama K. Computer-aided diagnosis of colorectal polyp histology by using a real-time image recognition system and narrow-band imaging magnifying colonoscopy. *Gastrointest Endosc* 2016; **83**: 643-649 [PMID: [26264431](https://pubmed.ncbi.nlm.nih.gov/26264431/) DOI: [10.1016/j.gie.2015.08.004](https://doi.org/10.1016/j.gie.2015.08.004)]
- 21 **Gross S**, Palm S, Tischendorf JJW, Behrens A, Trautwein C, Aach T. Automated classification of colon polyps in endoscopic image data. *SPIE Proceedings Medical Imaging 2012: Computer-Aided Diagnosis*, 83150W. [DOI: [10.1117/12.911177](https://doi.org/10.1117/12.911177)]
- 22 **Kodashima S**, Fujishiro M. Novel image-enhanced endoscopy with i-scan technology. *World J Gastroenterol* 2010; **16**: 1043-1049 [PMID: [20205272](https://pubmed.ncbi.nlm.nih.gov/20205272/) DOI: [10.3748/wjg.v16.i9.1043](https://doi.org/10.3748/wjg.v16.i9.1043)]
- 23 **Wimmer G**, Gadermayr M, Kwitt R, Häfner M, Merhof D, Uhl A. Evaluation of i-scan virtual chromoendoscopy and traditional chromoendoscopy for the automated diagnosis of colonic polyp. *Proceedings of the 3rd International Workshop on Computer-Assisted and Robotic Endoscopy (CARE)*. Cham: Springer 2016; 59-71 [DOI: [10.1007/978-3-319-54057-3_6](https://doi.org/10.1007/978-3-319-54057-3_6)]
- 24 **Wimmer G**, Ve'csei A, Uhl A. Cnn transfer learning for the automated diagnosis of celiac disease. *Proceedings of the Sixth International Conference on Image Processing Theory, Tools and Applications (IPTA)* 2016; 1-6 [DOI: [10.1109/IPTA.2016.7821020](https://doi.org/10.1109/IPTA.2016.7821020)]
- 25 **Häfner M**, Uhl A, Wimmer G. *Shape and size adapted local fractal dimension for the classification of polyps in HD colonoscopy* 2014; Oct 27-30; Paris, France. IEEE, 2014 [DOI: [10.1109/ICIP.2014.7025466](https://doi.org/10.1109/ICIP.2014.7025466)]
- 26 **Liao S**, Zhu X, Lei Z, Zhang L, Li SZ. *Learning multi-scale block local binary patterns for face recognition*. In: Proceedings of the 2007; Springer, 2007: 828-837 [DOI: [10.1007/978-3-540-74549-5_87](https://doi.org/10.1007/978-3-540-74549-5_87)]
- 27 **Fan RE**, Chang KW, Hsieh CJ, Wang XR, Lin CJ. LIBLINEAR: A library for large linear classification. *J Mach Learn Res* 2008; **9**: 1871-1874

P- Reviewer: De Silva AP, Kwon KA

S- Editor: Ma RY **L- Editor:** A **E- Editor:** Yin SY



Basic Study

Short hairpin RNA-mediated knockdown of nuclear factor erythroid 2-like 3 exhibits tumor-suppressing effects in hepatocellular carcinoma cells

Miao-Mei Yu, Yue-Hua Feng, Lu Zheng, Jun Zhang, Guang-Hua Luo

ORCID number: Miao-Mei Yu (0000-0002-8287-0725); Yue-Hua Feng (0000-0002-1767-0946); Lu Zheng (0000-0002-5563-4348); Jun Zhang (0000-0002-1826-6099); Guang-Hua Luo (0000-0001-8339-2828).

Author contributions: Yu MM and Luo GH designed this study; Feng YH and Zhang J performed the experiments; Yu MM, Feng YH, and Zheng L wrote the manuscript; Yu MM and Luo GH performed the bioinformatic prediction; Yu MM and Luo GH conducted statistical analysis; all authors read and approved the final manuscript.

Supported by the Changzhou High-Level Medical Talents Training Project, No. 2016ZCLJ002.

Institutional review board

statement: The clinicopathological features involved in this study are all from the TCGA database, thus, no institutional review board document is provided.

Conflict-of-interest statement: None declared.

Data sharing statement: No additional data are available.

ARRIVE guidelines statement: The authors have read the ARRIVE guidelines and prepared the manuscript accordingly.

Open-Access: This article is an open-access article which was selected by an in-house editor and fully peer-reviewed by external

Miao-Mei Yu, Yue-Hua Feng, Lu Zheng, Jun Zhang, Guang-Hua Luo, Comprehensive Laboratory, the Third Affiliated Hospital of Soochow University, Changzhou 213003, Jiangsu Province, China

Corresponding author: Guang-Hua Luo, MD, PhD, Professor, Senior Researcher, Comprehensive Laboratory, the Third Affiliated Hospital of Soochow University, No. 185, Juqian Street, Tianning District, Changzhou 213003, Jiangsu Province, China. shineroar@163.com

Telephone: +86-519-68870619

Fax: +86-519-86621235

Abstract

BACKGROUND

Hepatocellular carcinoma (HCC) is one of the most common malignant tumors with high mortality-to-incidence ratios. Nuclear factor erythroid 2-like 3 (NFE2L3), also known as NRF3, is a member of the cap 'n' collar basic-region leucine zipper family of transcription factors. NFE2L3 is involved in the regulation of various biological processes, whereas its role in HCC has not been elucidated.

AIM

To explore the expression and biological function of NFE2L3 in HCC.

METHODS

We analyzed the expression of NFE2L3 in HCC tissues and its correlation with clinicopathological parameters based on The Cancer Genome Atlas (TCGA) data portal. Short hairpin RNA (shRNA) interference technology was utilized to knock down NFE2L3 *in vitro*. Cell apoptosis, clone formation, proliferation, migration, and invasion assays were used to identify the biological effects of NFE2L3 in BEL-7404 and SMMC-7721 cells. The expression of epithelial-mesenchymal transition (EMT) markers was examined by Western blot analysis.

RESULTS

TCGA analysis showed that NFE2L3 expression was significantly positively correlated with tumor grade, T stage, and pathologic stage. The qPCR and Western blot results showed that both the mRNA and protein levels of NFE2L3 were significantly decreased after shRNA-mediated knockdown in BEL-7404 and SMMC-7721 cells. The shRNA-mediated knockdown of NFE2L3 could induce

reviewers. It is distributed in accordance with the Creative Commons Attribution Non Commercial (CC BY-NC 4.0) license, which permits others to distribute, remix, adapt, build upon this work non-commercially, and license their derivative works on different terms, provided the original work is properly cited and the use is non-commercial. See: <http://creativecommons.org/licenses/by-nc/4.0/>

Manuscript source: Unsolicited manuscript

Received: January 4, 2019

Peer-review started: January 4, 2019

First decision: January 23, 2019

Revised: February 13, 2019

Accepted: February 15, 2019

Article in press: February 16, 2019

Published online: March 14, 2019

apoptosis and inhibit the clone formation and cell proliferation of SMMC-7721 and BEL-7404 cells. NFE2L3 knockdown also significantly suppressed the migration, invasion, and EMT of the two cell lines.

CONCLUSION

Our study showed that shRNA-mediated knockdown of NFE2L3 exhibited tumor-suppressing effects in HCC cells.

Key words: Nuclear factor erythroid 2-like 3; Hepatocellular carcinoma; The Cancer Genome Atlas; Short hairpin RNA; Epithelial-mesenchymal transition

©The Author(s) 2019. Published by Baishideng Publishing Group Inc. All rights reserved.

Core tip: Nuclear factor erythroid 2-like 3 (NFE2L3), as a key regulator of the cellular stress response, is involved in the regulation of various tumors, whereas its role in hepatocellular carcinoma (HCC) has not been elucidated. Our present study identified that NFE2L3 was closely associated with the grade and stage of HCC patients based on The Cancer Genome Atlas database. Furthermore, our study showed that short hairpin RNA-mediated knockdown of NFE2L3 exhibited tumor-suppressing effects in HCC cells.

Citation: Yu MM, Feng YH, Zheng L, Zhang J, Luo GH. Short hairpin RNA-mediated knockdown of nuclear factor erythroid 2-like 3 exhibits tumor-suppressing effects in hepatocellular carcinoma cells. *World J Gastroenterol* 2019; 25(10): 1210-1223

URL: <https://www.wjgnet.com/1007-9327/full/v25/i10/1210.htm>

DOI: <https://dx.doi.org/10.3748/wjg.v25.i10.1210>

INTRODUCTION

Hepatocellular carcinoma (HCC), one of the most common malignant tumors, ranks as the third leading cause of cancer-related death worldwide, resulting in at least 700000 deaths each year^[1,2]. Microvascular invasion, occult metastasis, recurrence, and resistance to chemotherapy contribute to the poor prognosis and low survival rate of HCC patients. Hepatitis B virus (HBV) and hepatitis C virus (HCV) infection, alcoholic cirrhosis, non-alcoholic steatohepatitis, and the ingestion of aflatoxin B1 are the main risk factors for HCC development^[3]. Current therapeutic strategies for HCC include chemotherapy, surgical resection, liver transplantation, radiofrequency ablation, and drug therapy^[4,5]. The mechanism of HCC is very complex, and more research is needed to provide more detailed clues.

Nuclear factor erythroid 2-like 3 (NFE2L3), also known as NRF3, was first identified and reported in 1999 and is a member of the cap 'n' collar basic-region leucine zipper family of transcription factors^[6]. The human NFE2L3 transcript encodes a 694-amino acid protein that can bind to antioxidant response elements by heterodimerizing with small musculoaponeurotic fibrosarcoma factors^[6,7]. NFE2L3, as a key regulator of the cellular stress response, is expressed in a wide variety of tissues such as the heart, brain, lung, liver, kidney, and pancreas, particularly abundant in the placenta^[8,9]. Accumulating evidence suggests that NFE2L3 is involved in the regulation of various biological processes, such as transcription, signal transduction, cell cycle, growth, development, differentiation, and inflammation. In addition to these functions, Chevillard *et al*^[10] showed that the absence of NFE2L3 predisposes mice to lymphoma development, suggesting a protective role for this transcription factor in hematopoietic malignancies. Wang *et al*^[11] reported that NFE2L3 is necessary for RCAN1-4-mediated enhanced growth and invasion, and its overexpression independently enhances these effects in thyroid cancer cells. Chowdhury *et al*^[12] demonstrated that NFE2L3 promotes colon cancer cell proliferation by activating UHMK1 gene expression. These findings suggest that NFE2L3 may be a crucial regulator of cancer progression. However, the roles of NFE2L3 in HCC and their underlying molecular mechanisms have yet to be elucidated.

In the present study, we analyzed the expression of NFE2L3 in HCC and its correlation with clinicopathological parameters based on the Cancer Genome Atlas (TCGA) data portal. In addition, we utilized short hairpin RNA (shRNA) interference

technology to knock down NFE2L3 *in vitro* and systematically evaluated the biological function of NFE2L3 in HCC cells.

MATERIALS AND METHODS

HCC patient data in the Cancer Genome Atlas

A total of 344 HCC patients with clinicopathological information and RNA-Seq expression data were obtained from TCGA database (<https://cancer-genome.nih.gov/>). The gene expression data were normalized using the RNA normalization method described in TCGA National Cancer Institute (NCI) Wiki.

Cell lines and cell culture

Human HCC cell lines (SMMC-7721 and BEL-7404) were purchased from the Type Culture Collection of the Chinese Academy of Sciences (Shanghai, China) and identified by short tandem repeat analysis. SMMC-7721 and BEL-7404 cells were cultured in RPMI 1640 medium (Gibco, NY, United States) supplemented with 10% fetal bovine serum (FBS) (Gibco, Sydney, Australia), 100 U/mL penicillin, and 100 µg/mL streptomycin (Gibco, NY, United States) and incubated at 37 °C in a humidified atmosphere with 5% CO₂.

Short hairpin RNA lentivirus infection

An NFE2L3 shRNA interference lentiviral vector was constructed and synthesized by GeneChem Co., Ltd (Shanghai, China). The NFE2L3 shRNA interference target sequence was 5'-AGTCAATCCCAACCACTAT-3' (shNFE2L3), and a scramble sequence 5'-TTCTCCGAACGTGTCACGT-3' was used as a negative control (shCtrl). The lentiviral vectors were transfected into SMMC-7721 and BEL-7404 cells according to the manufacturer's instructions. The cells were seeded (2×10^5 cells/mL) onto 6-well plates and incubated for 24 h to reach 50% confluence, and then replaced with infection medium containing lentiviral vectors at a multiplicity of infection of 10 plaque-forming units/cell. Successfully infected cells were green fluorescent protein positive and observed under a fluorescence microscope after 72 h, and the interference efficiency of NFE2L3 shRNA was determined using quantitative real-time PCR (qPCR) and Western blot.

RNA extraction and real-time PCR

Total RNA was extracted with TRIzol reagent (Pufei Biotechnology, Shanghai, China). The RNA concentration and purity were assessed using the OD260 and OD260/OD280 ratio, respectively, and cDNA was synthesized with M-MLV RT (Promega, United States) according to the manufacturers' instructions. qPCR was performed using a SYBR Green master mix (Takara Biotechnology, Dalian, China) on the Stratagene Mx3000P (Agilent Technologies, United States). The sequences of the primers are as follows: NFE2L3, forward: 5'-ACACTTACCACTTACAGCCAACT-3', reverse: 5'-CTTCGTCTGATGTCACGGAT-3'; GAPDH, forward: 5'-TGACTTCAACAGCGACACCCA-3', reverse: 5'-CACCCGTGTTGCTGTAGCCAAA-3'. Relative mRNA levels were calculated by the comparative threshold cycle method ($2^{-\Delta Ct}$)^[33] using GAPDH as the internal control.

Flow cytometry assay

The cells were seeded (2×10^5 cells/mL) onto 6-well plates at 72 h posttransfection and incubated to reach approximately 85% confluence. Both supernatant and adherent cells were harvested, centrifuged, washed with D-Hanks solution, and re-suspended at a density of 1×10^6 cells/mL in $1 \times$ binding buffer solution. The cells were stained with Annexin V-APC for 15 min at room temperature using the Annexin V Apoptosis Detection Kit APC (eBioscience, San Diego, CA, United States) following the manufacturer's instructions. Flow cytometry was performed on a Guava easyCyt HT system (Millipore, Billerica, MA, United States) and analyzed using Guava InCyt software (Millipore).

Clone-forming assay

The cells were seeded (8×10^2 cells/well) onto 6-well plates at 72 h posttransfection and cultured for 9 d with a medium change every 3 d. The cell clones were photographed using a fluorescence microscope (Olympus, Tokyo, Japan) before the termination of the culture. The cells were fixed with 4% paraformaldehyde for 30 min and washed once with phosphate-buffered saline (PBS), followed by staining with Giemsa (Sigma-Aldrich, United States). After washing with distilled deionized water and drying completely, the cell clones were photographed with a digital camera and

then counted. Each experimental group was performed in triplicate.

Cell proliferation assay

The cells were seeded onto 96-well plates at a density of 2×10^3 cells/well and cultured at 37 °C in 5% CO₂ for 24 h. Direct counting of cells in the 96-well plates was scanned and analyzed using a Celigo cytometer (Nexcelom, Manchester, United Kingdom) from the next day of plating for a continuous 5 d. By adjusting the input parameters of the analysis settings, the number of cells with green fluorescence was accurately calculated and statistically analyzed. Cell count-fold represents the cell count at each time point relative to the average on day 1, indicating changes in cell proliferation. Cell growth curves were plotted based on the cell count-fold value at different time points.

The cells were seeded onto a 96-well plate at a density of 5×10^3 cells/well and incubated for 24 h. Then, 20 µL of 3-(4,5-dimethylthiazol-2-yl)-2,5-diphenyl-tetrazolium bromide (MTT; Genview, Houston, TX, United States; 5 mg/mL) in PBS was added to each well, and the cells were incubated for an additional 4 h. After termination of incubation, the supernatants were discarded and replaced with 100 µL dimethyl sulfoxide to dissolve the formazan crystals. The optical density values were measured at 490 nm to estimate viable cells. OD490-fold represents the OD values at each time point relative to the average of day 1, indicating changes in cell proliferation.

Cell migration assay

The cell density was adjusted to 9×10^4 cells/well with basic medium. The apical chamber was loaded with 100 µL of cell suspension, and the basolateral chamber was supplied with 600 µL of the culture medium containing 30% FBS. After incubation for 48 h, the medium was removed from the upper chamber, and the cells were scraped off with a cotton swab. The cells that invaded to the other side of the membrane were fixed with 4% paraformaldehyde for 30 min, followed by staining with Giemsa (Sigma-Aldrich, United States). Migratory cells were counted under an inverted microscope (200 ×) in at least three randomly selected fields.

Cell invasion assay

The cell density was adjusted to 5×10^4 cells/well with basic medium. Before seeding, 24-well transwell chambers with 8 µm pores (Corning, United States) were coated with Matrigel (BD Biosciences, San Jose, CA, United States), followed by the hydration of the Matrigel matrix layer. The apical chamber was loaded with 500 µL of cell suspension, and the basolateral chamber was supplied with 750 µL of the culture medium containing 30% FBS. After incubation for 60 h, the medium was removed from the upper chamber, and the cells were scraped off with a cotton swab. The cells that invaded to the other side of the membrane were stained with Giemsa. The invaded cells were counted under an inverted microscope in at least three randomly selected fields.

Western blot analysis

The cells were harvested and washed twice with ice-cold PBS and then lysed using protein RIPA lysis buffer (Beyotime, Shanghai, China). The protein concentration was determined using a BCA protein assay kit (Beyotime, Shanghai, China). The protein samples were mixed with 5× SDS-PAGE loading buffer (Beyotime, Shanghai, China) and boiled for 5 min. A total of 30 µg of protein was separated using 10% SDS-PAGE and then transferred onto polyvinylidene fluoride membranes (Merck Millipore, Billerica, MA, United States). Subsequently, the membranes were blocked in Tris-buffered saline/Tween 20 (TBST) solution containing 5% skim milk at room temperature for 1 h and then incubated separately overnight at 4 °C with the following primary antibodies: Anti-NFE2L3 (NBP2-30870, 1:200, Novus), anti-N-Cadherin (13116, 1:1000, Cell Signaling Technology), anti-Vimentin (ab92547, 1:2500, Abcam), anti-Snai1 (3879, 1:1000, Cell Signaling Technology), anti-Snai2 (9585, 1:1000, Cell Signaling Technology), and anti-GAPDH (sc-32233, 1:2000, Santa Cruz). GAPDH was used as the internal control to normalize protein loading. After washing four times with TBST, the membranes were incubated for 1.5 h at room temperature with horseradish peroxidase-conjugated AffiniPure goat anti-mouse IgG (sc-2005, Santa Cruz) or anti-rabbit IgG (sc-2004, Santa Cruz). The protein bands were visualized with the Pierce ECL Western Blotting Substrate kit (Thermo Scientific, Rockford, IL, United States) after washing with TBST.

Statistical analysis

Statistical analyses were performed using GraphPad Prism 6.0 software (GraphPad Prism 6.0 Software Inc., San Diego, CA, United States). We used a chi-square test to

analyze the differences between groups and the Spearman rank correlation test to examine the correlations. Student's *t* test (two-tailed) was used to determine significant differences between two groups. One-way analysis of variance (ANOVA), followed by Dunn's multiple comparison test, was used for multiple comparisons. The data are presented as the mean \pm SD. Differences with *P*-values $<$ 0.05 were considered statistically significant.

RESULTS

Correlation between NFE2L3 expression and clinicopathological features

To evaluate NFE2L3 expression in HCC, we analyzed 344 HCC patients with detailed clinicopathological information, and RNA-Seq expression data were obtained from the TCGA database. For the statistical analysis, the patients were divided into two groups based on the median expression level of NFE2L3: A low expression group ($n = 172$) and a high expression group ($n = 172$). The association between NFE2L3 expression and clinicopathological features are listed in [Table 1](#), which revealed that NFE2L3 expression was related to tumor grade ($P = 0.0006$), T stage ($P = 0.007$), and pathologic stage ($P = 0.0138$). As shown in [Figure 1A](#), the expression level of NFE2L3 in G3/4 HCC patients was significantly higher than that in G1/2 grade patients. [Figure 1B](#) and [C](#) shows that NFE2L3 expression gradually increased with the advancement of T stage and pathologic stage, and the difference was significant in T3/4 patients compared to T1 patients ($P < 0.01$) and was also significant in stage III/IV patients compared to stage I patients ($P < 0.01$). In addition, the Spearman rank correlation analysis demonstrated that there was a significant correlation between NFE2L3 expression and tumor grade ($P < 0.0001$), T stage ($P = 0.0004$), and pathologic stage ($P = 0.0007$), but there was no significant correlation between different clinicopathological features ([Table 2](#)).

Expression of NFE2L3 mRNA and protein in HCC cell lines

To investigate the potential role of NFE2L3, we performed shRNA interference to knock down NFE2L3 in BEL-7404 and SMMC-7721 cells. The interference efficiency of NFE2L3 shRNA was measured by qPCR and Western blot. As shown in [Figure 2A](#) and [B](#), NFE2L3 mRNA levels were significantly reduced by more than 50% ($P < 0.05$) in the two cell lines infected with NFE2L3 shRNA (shNFE2L3) compared with the negative control cells (shCtrl). Additionally, the Western blot results indicated that the protein level of NFE2L3 was markedly decreased after shRNA-mediated knockdown in BEL-7404 and SMMC-7721 cells.

Role of NFE2L3 in the apoptosis, clone formation, and proliferation of HCC cells

Flow cytometry results demonstrated that the apoptosis rate of the shNFE2L3 group was significantly higher than that of the shCtrl group in BEL-7404 and SMMC-7721 cells ($P < 0.05$, [Figure 3A](#) and [B](#)). The clone formation assay of BEL-7404 and SMMC-7721 cells showed that NFE2L3 shRNA reduced the number of clones by approximately 50% compared with those in the shCtrl group ([Figure 3C](#) and [D](#)). After 5 d of continuous detection by Celigo cytometry, the number of cells with green fluorescence was accurately calculated and statistically analyzed. The cell count-fold values of the shNFE2L3 group were significantly lower than those of the shCtrl group in BEL-7404 and SMMC-7721 cells, especially on day 4 and day 5 ([Figure 3E](#) and [F](#)). Subsequently, the MTT results revealed that the OD 490-fold values of the shNFE2L3 group in BEL-7404 and SMMC-7721 cells were significantly lower than those of the shCtrl group on days 4 and 5 ([Figure 3G](#) and [H](#)), which are consistent with the results detected by the Celigo cytometer.

ShRNA-mediated knockdown of NFE2L3 suppresses the migration, invasion, and epithelial-mesenchymal transition (EMT) of HCC cells

We further explored the effect of NFE2L3 knockdown on the migration, invasion, and EMT of HCC cells. The cell migration assay showed that compared with the shCtrl group, shRNA-mediated knockdown of NFE2L3 in BEL-7404 and SMMC-7721 cells resulted in markedly decreased migration ability, as indicated by a significant reduction in the average number of migrated cells ([Figure 4A](#) and [B](#)). Furthermore, the transwell invasion assay showed that NFE2L3 knockdown significantly weakened the invasion capacity of BEL-7404 and SMMC-7721 cells *in vitro*, as evidenced by a significant decrease in the mean number of cells that invaded through the Matrigel-coated membrane ([Figure 4C](#) and [D](#)). As shown in [Figure 4E](#) and [F](#), shRNA-mediated knockdown of NFE2L3 dramatically decreased the levels of mesenchymal markers (N-cadherin and Vimentin) and EMT transcription regulators (Snail1 and Snail2) in

Table 1 Association of nuclear factor erythroid 2-like 3 expression with clinicopathological features of hepatocellular carcinoma patients in The Cancer Genome Atlas dataset *n* (%)

Variable	NFE2L3 expression		Total cases	P-value
	Low (<i>n</i> = 172)	High (<i>n</i> = 172)		
Tumor grade				0.0006
G1/2	122 (70.9)	91 (52.9)	213	
G3/4	50 (29.1)	81 (47.1)	131	
T stage				0.0070
T1	100 (58.1)	71 (41.2)	171	
T2	35 (20.3)	52 (30.2)	87	
T3/4	37 (21.5)	49 (28.5)	86	
Pathologic stage				0.0138
I	98 (57.0)	71 (41.2)	169	
II	35 (20.3)	50 (29.1)	85	
III/IV	39 (22.7)	51 (29.7)	90	

NFE2L3: Nuclear factor erythroid 2-like 3.

BEL-7404 and SMMC-7721 cells.

DISCUSSION

HCC is the result of many variable etiological factors, such as HBV, HCV, alcohol, aflatoxin, congenital and acquired metabolic diseases^[14,15]. Thus, HCC caused by different risk factors may have a different molecular basis involving the loss of cell cycle control and senescence control, the dysregulation of apoptosis, liver inflammation, and hepatocarcinogenesis^[16]. As a potent transcriptional regulator, NFE2L3 can regulate carcinogenesis, inflammation, and stem cell differentiation by activating or inhibiting the transcription of its target genes depending on the cellular context^[12,17]. Additionally, DNA methylation is associated with metabolic diseases^[18], which are the main risk factors of HCC. Thus, the methylation level of NFE2L3 gene may be involved in hepatocarcinogenesis. However, the role of NFE2L3 in HCC and its underlying molecular mechanisms have not been investigated.

In the present study, we first reported the expression and biological function of NFE2L3 in HCC. TCGA analysis showed that NFE2L3 expression was significantly positively correlated with tumor grade, T stage, and pathologic stage. Subsequently, we selected SMMC-7721 and BEL-7404 for shRNA interference and functional studies. Knockdown of NFE2L3 could induce apoptosis and inhibit the clone formation and cell proliferation of HCC cells. NFE2L3 knockdown also significantly suppressed the migration and invasion of HCC cells. Additionally, our results showed that shRNA-mediated knockdown of NFE2L3 dramatically decreased the levels of mesenchymal markers (N-cadherin and Vimentin) and EMT transcription regulators (Snail1 and Snail2) in BEL-7404 and SMMC-7721 cells. EMT is essential for tumor metastasis and involves a cellular reprogramming process in which polarized, immotile epithelial cells lose adherent and tight junctions, exhibit increased motility, and acquire a mesenchymal phenotype^[19,20]. N-cadherin, a mesenchymal cadherin associated with EMT, has been widely studied in various tumor types. Vimentin, as a type 3 intermediate filament protein, is also a critical EMT mesenchymal cell marker. Several transcription factors, including the Snail/Slug family, Twist, and ZEB1, function as molecular switches of the EMT program^[21]. As a critical regulator of multiple signaling pathways leading to EMT, the expression of Snail is closely associated with cancer metastasis. Slug, another member of the Snail family of transcription factors, has been characterized as a strong E-cadherin repressor and a major EMT inducer and is correlated with distant metastasis^[22]. Thus, the decrease in the levels of N-cadherin, Vimentin, Snail1, and Snail2 represents a block in the EMT process. These observations will help us to further investigate the molecular mechanisms of NFE2L3 in HCC, which will be reported in the near future.

Based on the published literature, we speculated on the possible mechanism underlying the role of NFE2L3 in HCC. Chenais *et al*^[7] found that NRF3 (NFE2L3) mRNA and protein expression is upregulated by the proinflammatory cytokine tumor

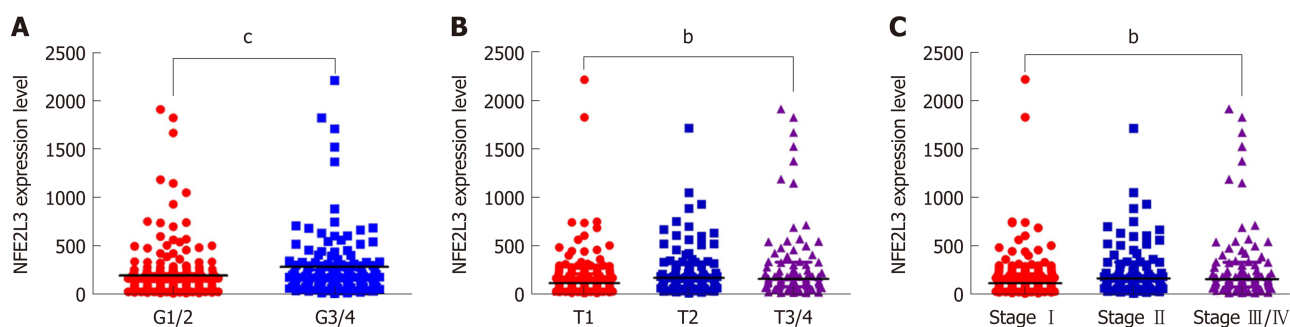


Figure 1 Association of nuclear factor erythroid 2-like 3 expression with clinicopathological features of hepatocellular carcinoma patients in The Cancer Genome Atlas dataset. A: Nuclear factor erythroid 2-like 3 (NFE2L3) expression in G1/2 ($n = 213$) and G3/4 ($n = 131$) hepatocellular carcinoma (HCC) patients; B: NFE2L3 expression in T1 ($n = 171$), T2 ($n = 87$) and T3/4 ($n = 86$) HCC patients; C: NFE2L3 expression in stage I ($n = 169$), stage II ($n = 85$), and stage III/IV ($n = 90$) HCC patients. ^b $P < 0.01$, ^c $P < 0.001$. NFE2L3: Nuclear factor erythroid 2-like 3; HCC: Hepatocellular carcinoma.

necrosis factor- α (TNF- α). Huang *et al*^[23] reported that TNF- α could enhance migration and inhibit the apoptosis of the HCC cell line HepG2 by upregulating heat shock protein 70 (HSP70). Jing *et al*^[24] indicated that TNF- α promoted HCC carcinogenesis through the activation of hepatic progenitor cells. Therefore, we hypothesized that the cancer-promoting role of NFE2L3 in HCC might be regulated by TNF- α . Moreover, Xiao *et al*^[25] indicated that NFE2L3 could directly activate the phospholipase A2, group 7 (Pla2g7) gene at the transcriptional level. Pla2g7 was upregulated in more than half of the tumors in hepatitis C virus-associated HCC^[26]. Pla2g7, associated with aggressive prostate cancer, promoted prostate cancer cell migration and invasion and was inhibited by statins^[27]. Low *et al*^[28] found that Pla2g7 is important in regulating tumor cell migration and acts as a novel tumor-promoting factor in nasopharyngeal carcinoma. It could be speculated that NFE2L3 might promote HCC cell migration and invasion *via* directly activating Pla2g7 transcription. Additionally, NFE2L3 was identified as a negative regulator of the peroxiredoxin 6 (PRDX6) promoter in human pulmonary A549 cells by reporter gene assay^[9,29]. PRDX6, as a bifunctional enzyme with both peroxidase and calcium-independent phospholipase A2 (iPLA2) activity, induces S phase arrest and promotes apoptosis in HCC cells, and inhibits HCC tumorigenicity in mice injected with cancer cells^[30]. From these data, we hypothesized that shRNA-mediated knockdown of NFE2L3 might induce apoptosis and inhibit hepatocarcinogenesis through negative regulation of PRDX6. The discovery and identification of NFE2L3 target genes are essential for understanding the molecular mechanisms underlying their roles. Although several potential target genes of NFE2L3 have been reported, further experiments are required to confirm whether the genes mentioned above are genuine targets of NFE2L3 in HCC.

While our current research provides important and instructive findings, some limitations do exist. Due to partial loss of follow-up, it was not possible to perform survival analyses for some clinical cases. In future studies, we will expand the sample size, strengthen follow-up, and conduct detailed analyses. In addition, we have investigated the function of NFE2L3 at the cellular level *in vitro*, but no animal experiments have been performed *in vivo*. We need to further validate the role of NFE2L3 through *in vivo* experiments and explore the molecular mechanisms underlying its roles in HCC.

In conclusion, we identified that NFE2L3 was closely associated with the grade and stage of HCC patients based on the TCGA database. Furthermore, our study showed that shRNA-mediated knockdown of NFE2L3 exhibited tumor-suppressing effects in HCC cells.

Table 2 Pearson correlation coefficients for the relationship of nuclear factor erythroid 2-like 3 expression and clinicopathological features

	NFE2L3 expression		Tumor grade		T stage		Pathologic stage	
	<i>r</i>	<i>P</i> -value	<i>r</i>	<i>P</i> -value	<i>r</i>	<i>P</i> -value	<i>r</i>	<i>P</i> -value
NFE2L3 expression	1.000		0.2354	< 0.0001	0.1913	0.0004	0.1811	0.0007
Tumor grade	0.2354	< 0.0001	1.000		-0.0032	0.9522	-0.0069	0.8985
T stage	0.1913	0.0004	-0.0032	0.9522	1.000		0.9814	< 0.0001
Pathologic stage	0.1811	0.0007	-0.0069	0.8985	0.9814	< 0.0001	1.000	

NFE2L3: Nuclear factor erythroid 2-like 3.

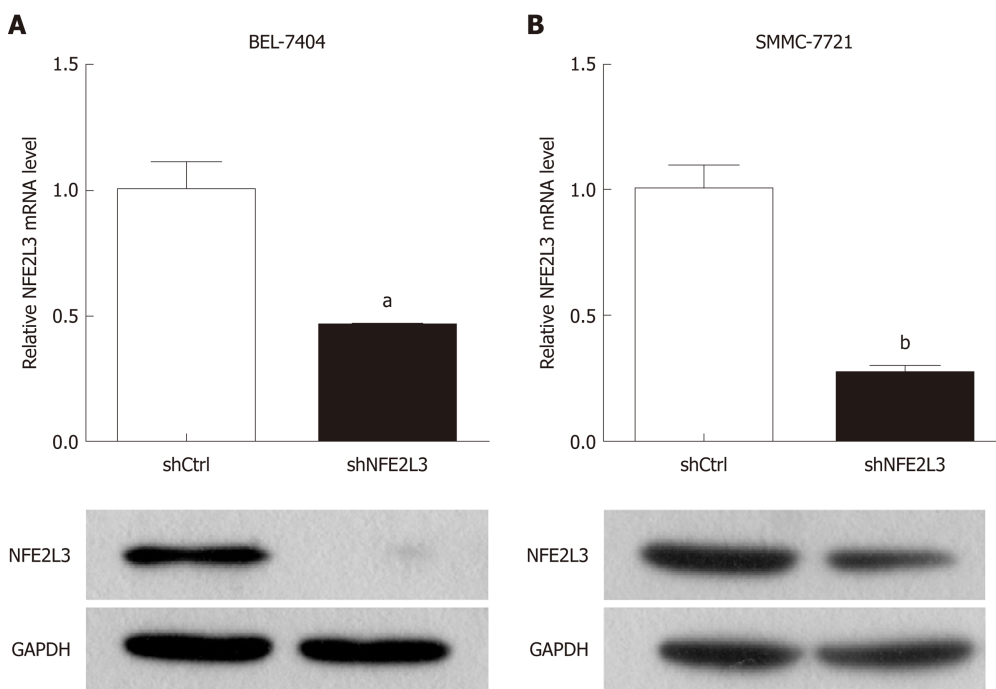
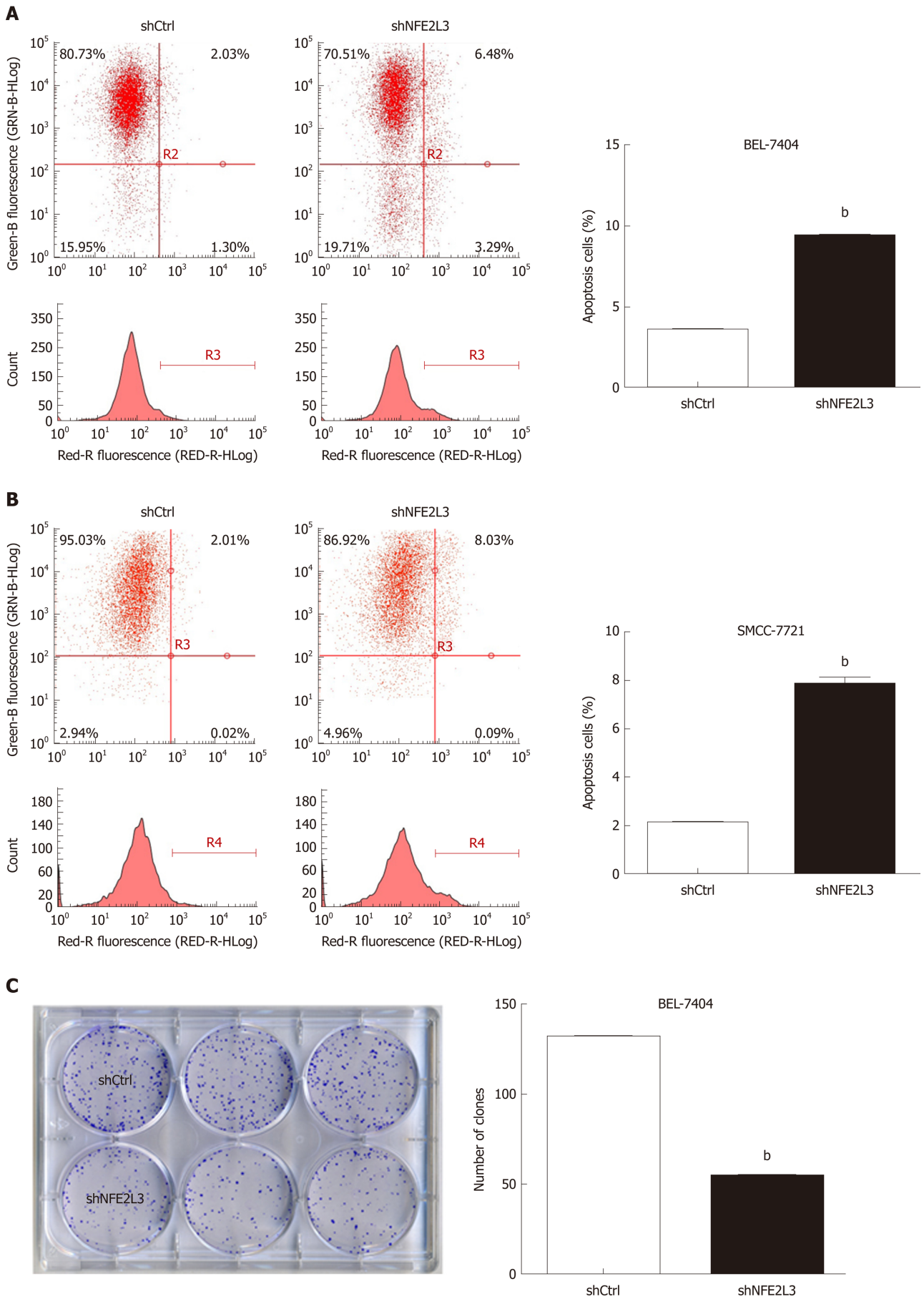


Figure 2 Expression of nuclear factor erythroid 2-like 3 mRNA and protein in hepatocellular carcinoma cell lines. A: Nuclear factor erythroid 2-like 3 (NFE2L3) mRNA levels in BEL-7404 and SMMC-7721 cells infected with shNFE2L3 (NFE2L3 short hairpin RNA) were measured by qPCR; B: NFE2L3 protein levels in BEL-7404 and SMMC-7721 cells infected with shNFE2L3 were measured by Western blot. Data shown are the mean \pm SEM, ^a*P* < 0.05, ^b*P* < 0.01 vs shCtrl. NFE2L3: Nuclear factor erythroid 2-like 3; shCtrl: Negative control cells; shNFE2L3: Nuclear factor erythroid 2-like 3 short hairpin RNA.



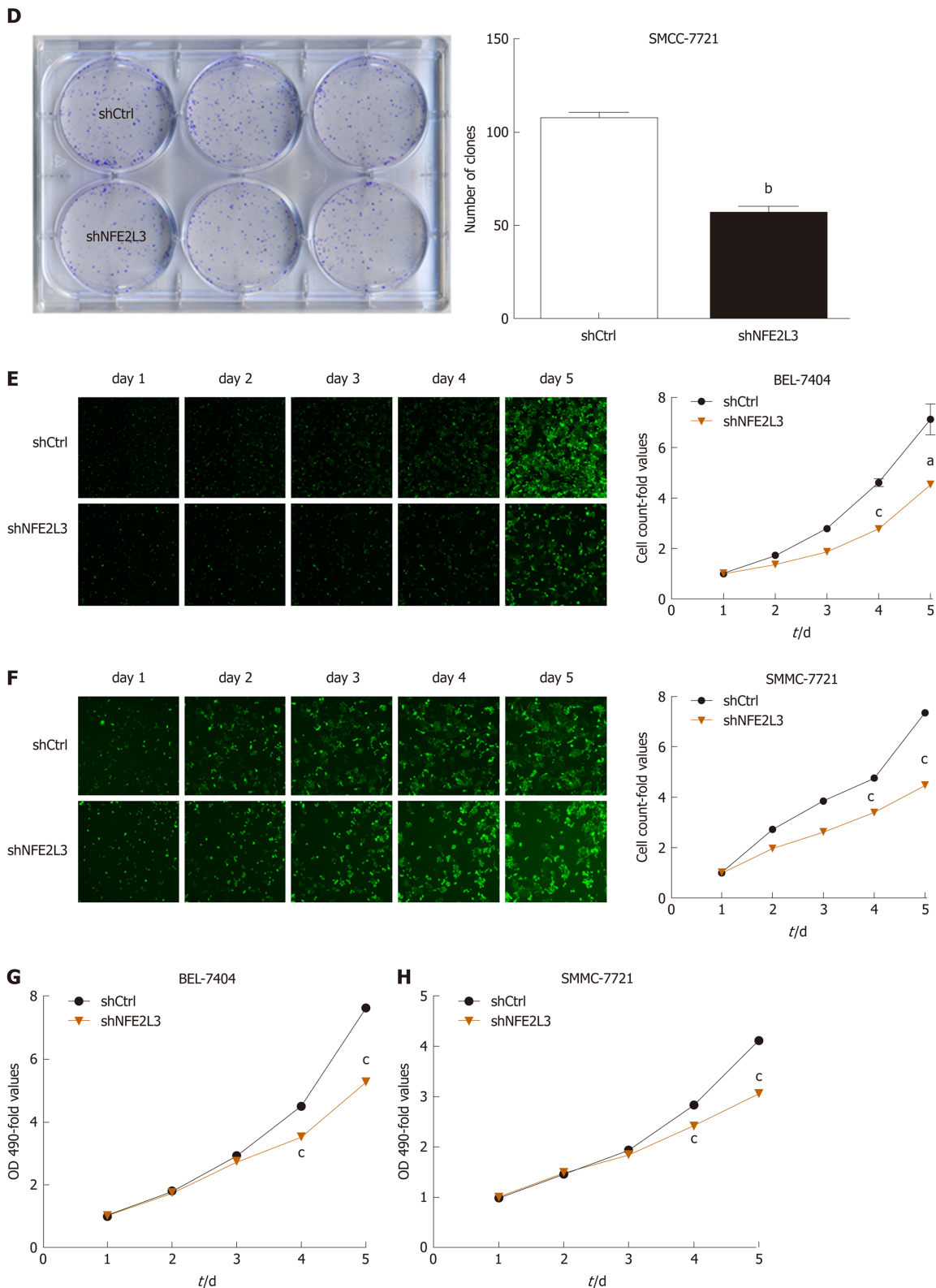


Figure 3 Role of nuclear factor erythroid 2-like 3 in apoptosis, clone formation, and proliferation of hepatocellular carcinoma cells. A and B: Apoptotic cells were stained with Annexin V-APC and measured using flow cytometry. The abscissa represents red fluorescence (RED-R-HLog), and the ordinate represents green fluorescence (GRN-B-HLog) and cell count; C and D: Cell clones were stained with Giemsa and photographed with a digital camera. The number of clones was accurately calculated and statistically analyzed; E and F: Successfully infected cells were green fluorescent protein positive and cell images were taken with a Celigo cytometer for a continuous 5 d. Cell count-fold represents cell count at each time point relative to the average of day 1; G and H: OD values were measured at 490 nm after the treatment of MTT. Cell growth curves were plotted based on OD 490-fold at different time point. Data shown are the mean \pm SEM. Student's *t* test was used to analyze significant differences, ^a*P* < 0.05, ^b*P* < 0.01, ^c*P* < 0.001 vs shCtrl. shCtrl: Negative control cells; shNFE2L3: Nuclear factor erythroid 2-like 3 short hairpin RNA.

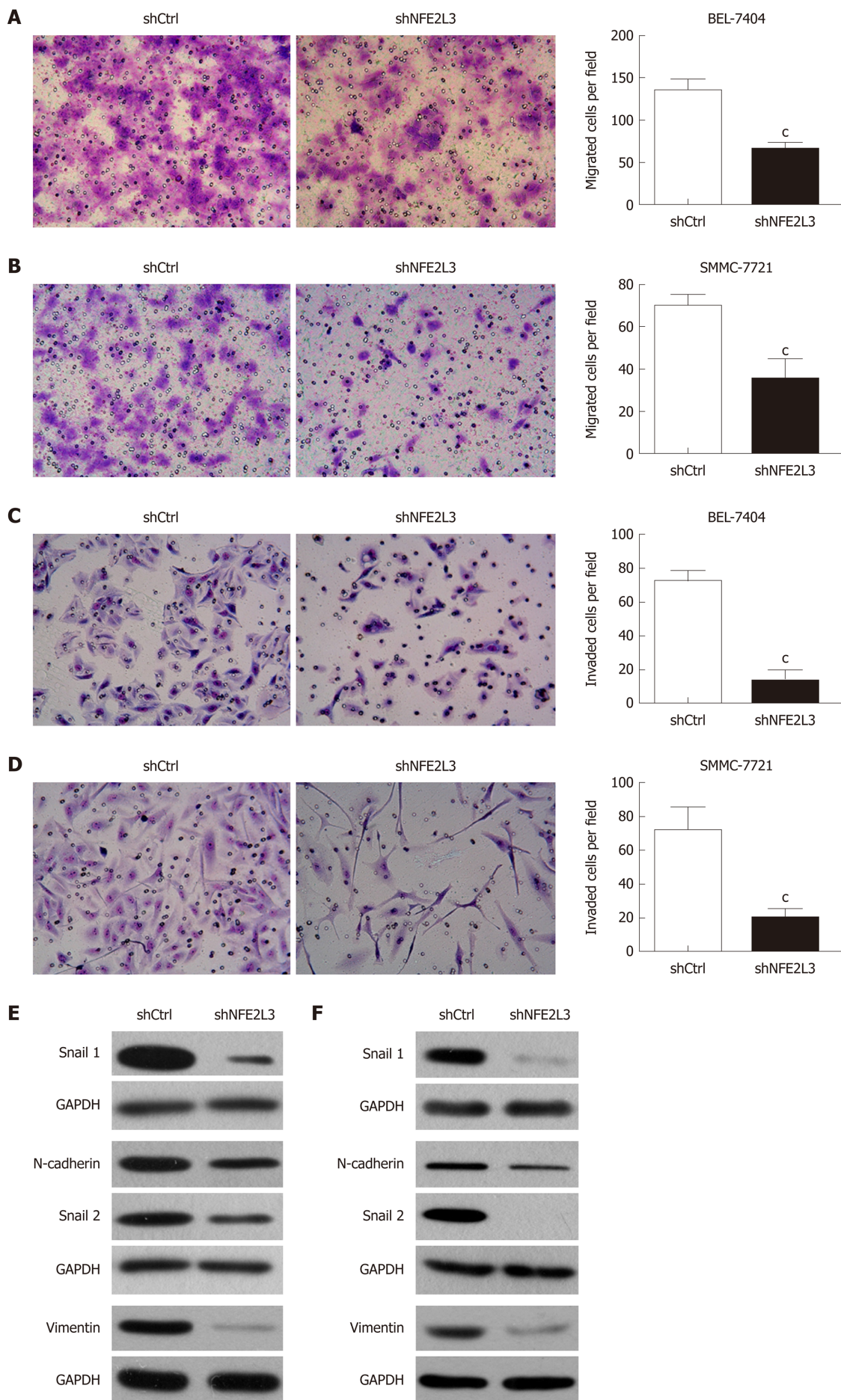


Figure 4 Short hairpin RNA-mediated knockdown of nuclear factor erythroid 2-like 3 suppresses migration, invasion, and epithelial-mesenchymal

transition of hepatocellular carcinoma cells. A and B: Cell migration assay showed that migrated cells of the shNFE2L3 group were less than that of the shCtrl group in BEL-7404 and SMMC-7721 cells; C and D: Cell invasion assay showed that invaded cells of the shNFE2L3 group were less than that of the shCtrl group in BEL-7404 and SMMC-7721 cells. Both cell migration and invasion were measured with transwell assays. Migrated and invaded cells were stained with Giemsa and imaged and counted under a microscope. Scale bar = 150 μ m; E and F: Snail 1, N-cadherin, Snail 2, and Vimentin protein levels were analyzed using Western blot. GAPDH was a loading control. Data shown are the mean \pm SEM. Student's *t* test was used to analyze significant differences, **P* < 0.001 vs shCtrl. shCtrl: Negative control cells; shNFE2L3: Nuclear factor erythroid 2-like 3 short hairpin RNA.

ARTICLE HIGHLIGHTS

Research background

Hepatocellular carcinoma (HCC) is one of the most common malignant tumors. Many factors can induce HCC, such as viral infection, alcoholic cirrhosis, and aflatoxin, while the underlying mechanism remains unclear. Nuclear factor erythroid 2-like 3 (NFE2L3) is a member of the cap 'n' collar basic-region leucine zipper family of transcription factors. Studies have shown that NFE2L3 acts as a crucial regulator in a variety of cancer progression involving proliferation, migration, and invasion of tumor cells.

Research motivation

The roles of NFE2L3 in HCC and their underlying molecular mechanisms have yet to be elucidated.

Research objectives

Our study aimed to examine NFE2L3 expression in HCC and to analyze its association with clinicopathological features, and to systematically investigate the biological effects of NFE2L3 in HCC cell lines.

Research methods

Based on The Cancer Genome Atlas data portal, we analyzed NFE2L3 expression in 344 HCC patients and its correlation with clinicopathological features. Short hairpin RNA (shRNA) interference technology was utilized to knock down NFE2L3 in SMMC-7721 and BEL-7404 cells. NFE2L3 mRNA levels were quantified using qPCR. Flow cytometry, clone-forming, 3-(4,5-dimethylthiazol-2-yl)-2,5-diphenyltetrazolium bromide, and transwell assays were performed to evaluate the apoptosis, clone formation, proliferation, migration, and invasion of HCC cells. The protein levels of NFE2L3 and epithelial-mesenchymal transition (EMT) markers were examined by Western blot.

Research results

Our results revealed that NFE2L3 expression in G3/4 HCC patients was significantly higher than that in G1/2 grade patients, and its expression gradually increased with the advancement of T stage and pathologic stage. The Spearman rank correlation analysis showed that NFE2L3 expression was significantly correlated with tumor grade, T stage, and pathologic stage. The qPCR and Western blot results indicated that both mRNA and protein levels of NFE2L3 were markedly decreased after shRNA-mediated knockdown in BEL-7404 and SMMC-7721 cells. Flow cytometry results demonstrated that shRNA-mediated knockdown of NFE2L3 could promote the apoptosis of HCC cells. Meanwhile, NFE2L3 knockdown significantly suppressed the clone formation, cell proliferation, migration, and invasion of HCC cells. Additionally, our results showed that NFE2L3 knockdown dramatically decreased the levels of mesenchymal markers (N-cadherin and Vimentin) and EMT transcription regulators (Snail1 and Snail2) in HCC cells.

Research conclusions

The present study identified that NFE2L3 was closely associated with the grade and stage of HCC patients, and shRNA-mediated knockdown of NFE2L3 exhibited tumor-suppressing effects in HCC cells.

Research perspectives

Our study preliminarily explored the possible role of NFE2L3 in HCC. Future studies should focus on the following aspects. First, we will expand the sample size, strengthen follow-up, and conduct survival analyses. Second, animal experiments will be performed to further validate the role of NFE2L3 *in vivo*. Finally, we need to further explore the molecular mechanisms underlying its roles in HCC.

REFERENCES

- 1 Torre LA, Bray F, Siegel RL, Ferlay J, Lortet-Tieulent J, Jemal A. Global cancer statistics, 2012. *CA Cancer J Clin* 2015; **65**: 87-108 [PMID: 25651787 DOI: 10.3322/caac.21262]
- 2 Waller LP, Deshpande V, Pylsopoulos N. Hepatocellular carcinoma: A comprehensive review. *World J Hepatol* 2015; **7**: 2648-2663 [PMID: 26609342 DOI: 10.4254/wjh.v7.i26.2648]
- 3 Llovet JM, Zucman-Rossi J, Pikarsky E, Sangro B, Schwartz M, Sherman M, Gores G. Hepatocellular carcinoma. *Nat Rev Dis Primers* 2016; **2**: 16018 [PMID: 27158749 DOI: 10.1038/nrdp.2016.18]

- 4 **Tunissiolli NM**, Castanhole-Nunes MMU, Biselli-Chicote PM, Pavarino EC, da Silva RF, da Silva RC, Goloni-Bertollo EM. Hepatocellular Carcinoma: A Comprehensive Review of Biomarkers, Clinical Aspects, and Therapy. *Asian Pac J Cancer Prev* 2017; **18**: 863-872 [PMID: 28545181 DOI: 10.22034/APJCP.2017.18.4.863]
- 5 **Medavaram S**, Zhang Y. Emerging therapies in advanced hepatocellular carcinoma. *Exp Hematol Oncol* 2018; **7**: 17 [PMID: 30087805 DOI: 10.1186/s40164-018-0109-6]
- 6 **Kobayashi A**, Ito E, Toki T, Kogame K, Takahashi S, Igarashi K, Hayashi N, Yamamoto M. Molecular cloning and functional characterization of a new Cap'n' collar family transcription factor Nrf3. *J Biol Chem* 1999; **274**: 6443-6452 [PMID: 10037736 DOI: 10.1074/jbc.274.10.6443]
- 7 **Chénais B**, Derjuga A, Massrieh W, Red-Horse K, Bellingard V, Fisher SJ, Blank V. Functional and placental expression analysis of the human NRF3 transcription factor. *Mol Endocrinol* 2005; **19**: 125-137 [PMID: 15388789 DOI: 10.1210/me.2003-0379]
- 8 **Zhang Y**, Kobayashi A, Yamamoto M, Hayes JD. The Nrf3 transcription factor is a membrane-bound glycoprotein targeted to the endoplasmic reticulum through its N-terminal homology box 1 sequence. *J Biol Chem* 2009; **284**: 3195-3210 [PMID: 19047052 DOI: 10.1074/jbc.M805337200]
- 9 **Chevillard G**, Blank V. NFE2L3 (NRF3): The Cinderella of the Cap'n'Collar transcription factors. *Cell Mol Life Sci* 2011; **68**: 3337-3348 [PMID: 21687990 DOI: 10.1007/s00018-011-0747-x]
- 10 **Chevillard G**, Paquet M, Blank V. Nfe2l3 (Nrf3) deficiency predisposes mice to T-cell lymphoblastic lymphoma. *Blood* 2011; **117**: 2005-2008 [PMID: 21148084 DOI: 10.1182/blood-2010-02-271460]
- 11 **Wang C**, Saji M, Justiniano SE, Yusof AM, Zhang X, Yu L, Fernández S, Wakely P, La Perle K, Nakanishi H, Pohlman N, Ringel MD. RCAN1-4 is a thyroid cancer growth and metastasis suppressor. *JCI Insight* 2017; **2**: e90651 [PMID: 28289712 DOI: 10.1172/jci.insight.90651]
- 12 **Chowdhury AMMA**, Katoh H, Hatanaka A, Iwanari H, Nakamura N, Hamakubo T, Natsume T, Waku T, Kobayashi A. Multiple regulatory mechanisms of the biological function of NRF3 (NFE2L3) control cancer cell proliferation. *Sci Rep* 2017; **7**: 12494 [PMID: 28970512 DOI: 10.1038/s41598-017-12675-y]
- 13 **Schmittgen TD**, Livak KJ. Analyzing real-time PCR data by the comparative C (T) method. *Nat Protoc* 2008; **3**: 1101-1108 [PMID: 18546601 DOI: 10.1038/nprot.2008.73]
- 14 **Sengupta S**, Parikh ND. Biomarker development for hepatocellular carcinoma early detection: Current and future perspectives. *Hepat Oncol* 2017; **4**: 111-122 [PMID: 30191058 DOI: 10.2217/hep-2017-0019]
- 15 **Scalera A**, Tarantino G. Could metabolic syndrome lead to hepatocarcinoma via non-alcoholic fatty liver disease? *World J Gastroenterol* 2014; **20**: 9217-9228 [PMID: 25071314 DOI: 10.3748/wjg.v20.i28.9217]
- 16 **De Stefano F**, Chacon E, Turcios L, Marti F, Gedaly R. Novel biomarkers in hepatocellular carcinoma. *Dig Liver Dis* 2018; **50**: 1115-1123 [PMID: 30217732 DOI: 10.1016/j.dld.2018.08.019]
- 17 **Siegenthaler B**, Defila C, Muzumdar S, Beer HD, Meyer M, Tanner S, Bloch W, Blank V, Schäfer M, Werner S. Nrf3 promotes UV-induced keratinocyte apoptosis through suppression of cell adhesion. *Cell Death Differ* 2018; **25**: 1749-1765 [PMID: 29487353 DOI: 10.1038/s41418-018-0074-y]
- 18 **Schwenk RW**, Vogel H, Schürmann A. Genetic and epigenetic control of metabolic health. *Mol Metab* 2013; **2**: 337-347 [PMID: 24327950 DOI: 10.1016/j.molmet.2013.09.002]
- 19 **Dongre A**, Weinberg RA. New insights into the mechanisms of epithelial-mesenchymal transition and implications for cancer. *Nat Rev Mol Cell Biol* 2019; **20**: 69-84 [PMID: 30459476 DOI: 10.1038/s41580-018-0080-4]
- 20 **Prieto-García E**, Díaz-García CV, García-Ruiz I, Agulló-Ortuño MT. Epithelial-to-mesenchymal transition in tumor progression. *Med Oncol* 2017; **34**: 122 [PMID: 28560682 DOI: 10.1007/s12032-017-0980-8]
- 21 **Gheldof A**, Berx G. Cadherins and epithelial-to-mesenchymal transition. *Prog Mol Biol Transl Sci* 2013; **116**: 317-336 [PMID: 23481201 DOI: 10.1016/B978-0-12-394311-8.00014-5]
- 22 **Wang Y**, Shi J, Chai K, Ying X, Zhou BP. The Role of Snail in EMT and Tumorigenesis. *Curr Cancer Drug Targets* 2013; **13**: 963-972 [PMID: 24168186 DOI: 10.2174/15680096113136660102]
- 23 **Huang BP**, Lin CS, Wang CJ, Kao SH. Upregulation of heat shock protein 70 and the differential protein expression induced by tumor necrosis factor- α enhances migration and inhibits apoptosis of hepatocellular carcinoma cell HepG2. *Int J Med Sci* 2017; **14**: 284-293 [PMID: 28367089 DOI: 10.7150/ijms.17861]
- 24 **Jing Y**, Sun K, Liu W, Sheng D, Zhao S, Gao L, Wei L. Tumor necrosis factor- α promotes hepatocellular carcinogenesis through the activation of hepatic progenitor cells. *Cancer Lett* 2018; **434**: 22-32 [PMID: 29981431 DOI: 10.1016/j.canlet.2018.07.001]
- 25 **Xiao Q**, Pepe AE, Wang G, Luo Z, Zhang L, Zeng L, Zhang Z, Hu Y, Ye S, Xu Q. Nrf3-Pla2g7 interaction plays an essential role in smooth muscle differentiation from stem cells. *Arterioscler Thromb Vasc Biol* 2012; **32**: 730-744 [PMID: 22247257 DOI: 10.1161/ATVBAHA.111.243188]
- 26 **Smith MW**, Yue ZN, Geiss GK, Sadovnikova NY, Carter VS, Boix L, Lazaro CA, Rosenberg GB, Bumgarner RE, Fausto N, Bruix J, Katze MG. Identification of novel tumor markers in hepatitis C virus-associated hepatocellular carcinoma. *Cancer Res* 2003; **63**: 859-864 [PMID: 12591738 DOI: 10.1002/cncr.11257]
- 27 **Vainio P**, Lehtinen L, Mirtti T, Hilvo M, Seppänen-Laakso T, Virtanen J, Sankila A, Nordling S, Lundin J, Rannikko A, Orešič M, Kallioniemi O, Iljin K. Phospholipase PLA2G7, associated with aggressive prostate cancer, promotes prostate cancer cell migration and invasion and is inhibited by statins. *Oncotarget* 2011; **2**: 1176-1190 [PMID: 22202492 DOI: 10.18632/oncotarget.397]
- 28 **Low HB**, Png CW, Li C, Wang Y, Wong SB, Zhang Y. Monocyte-derived factors including PLA2G7 induced by macrophage-nasopharyngeal carcinoma cell interaction promote tumor cell invasiveness. *Oncotarget* 2016; **7**: 55473-55490 [PMID: 27487154 DOI: 10.18632/oncotarget.10980]
- 29 **Chowdhury I**, Mo Y, Gao L, Kazi A, Fisher AB, Feinstein SI. Oxidant stress stimulates expression of the human peroxiredoxin 6 gene by a transcriptional mechanism involving an antioxidant response element. *Free Radic Biol Med* 2009; **46**: 146-153 [PMID: 18973804 DOI: 10.1016/j.freeradbiomed.2008.09.027]
- 30 **Xu X**, Lu D, Zhuang R, Wei X, Xie H, Wang C, Zhu Y, Wang J, Zhong C, Zhang X, Wei Q, He Z, Zhou L, Zheng S. The phospholipase A2 activity of peroxiredoxin 6 promotes cancer cell death induced by tumor necrosis factor alpha in hepatocellular carcinoma. *Mol Carcinog* 2016; **55**: 1299-1308 [PMID: 26293541 DOI: 10.1002/mc.22371]

P- Reviewer: Gazouli M, Tarantino G

S- Editor: Yan JP L- Editor: Wang TQ E- Editor: Yin SY



Basic Study

MicroRNA-596 acts as a tumor suppressor in gastric cancer and is upregulated by promotor demethylation

Zhen Zhang, Dong-Qiu Dai

ORCID number: Zhen Zhang (0000-0001-6586-4625); Dong-Qiu Dai (0000-0002-1154-3276).

Author contributions: Dai DQ designed this study; Zhang Z performed the experiments and analyzed the data; Dai DQ and Zhang Z drafted the article, made critical revisions related to the intellectual content of the manuscript, and approved the final version of the article to be published.

Supported by National Natural Science Foundation of China, No. 30572162; and Natural Science Foundation of Liaoning Province, No. 201602817.

Institutional review board

statement: All gastric cancer specimens from the patients were taken after informed consent and ethical permission were obtained for participation in the study.

Conflict-of-interest statement: The authors declare that there is no conflict of interest related to this study.

Data sharing statement: No additional data are available.

Open-Access: This article is an open-access article which was selected by an in-house editor and fully peer-reviewed by external reviewers. It is distributed in accordance with the Creative Commons Attribution Non Commercial (CC BY-NC 4.0) license, which permits others to distribute, remix, adapt, build upon this work non-commercially, and license their derivative works

Zhen Zhang, Dong-Qiu Dai, Department of Gastroenterological Surgery, the Fourth Affiliated Hospital of China Medical University, Shenyang 110032, Liaoning Province, China

Corresponding author: Dong-Qiu Dai, PhD, Chief Doctor, Professor, Surgical Oncologist, Department of Gastroenterological Surgery, the Fourth Affiliated Hospital of China Medical University, 4 Chongshan Road, Shenyang 110032, Liaoning Province, China.

daidq63@163.com

Telephone: +86-24-62043110

Fax: +86-24-62043110

Abstract**BACKGROUND**

In the present study, we investigated a suppressive role of microRNA-596 (miR-596) in gastric cancer (GC). Moreover, the downregulation of miR-596 in GC cell lines was associated with an increase of miR-596 promoter methylation. We also established that miR-596 controls the expression of peroxiredoxin 1 (PRDX1), which has never been reported before, suggesting that this interaction could play an important role in GC progression.

AIM

To study the potential role and possible regulatory mechanism of miR-596 in GC.

METHODS

The expression levels of miR-596 and PRDX1 in gastric cancer tissues and cell lines were detected by quantitative real-time PCR (qRT-PCR). Western blot and luciferase reporter assay were used to detect the effect of miR-596 on PRDX1 expression. Then, the proliferation, metastasis, and invasion of GC cell lines transfected with miR-596 mimics were analyzed, respectively, by Cell Counting Kit-8 proliferation assay, wound healing assay, and transwell invasion assay. Meanwhile, the methylation status of the promoter CpG islands of miR-596 in GC cell lines was detected by methylation-specific PCR (MSP).

RESULTS

Expression of miR-596 was decreased and PRDX1 was upregulated in GC tissues and cell lines. Overexpression of miR-596 decreased the expression of PRDX1 and luciferase reporter assays detected the direct binding of miR-596 to the 3'-untranslated region (UTR) of PRDX1 transcripts. Furthermore, we found that overexpression of miR-596 remarkably suppressed cell proliferation, migration, and invasion in GC cells. We further analyzed miR-596 promoter methylation by MSP and qRT-PCR, and found the downregulation of miR-596 was associated

on different terms, provided the original work is properly cited and the use is non-commercial. See: <http://creativecommons.org/licenses/by-nc/4.0/>

Manuscript source: Unsolicited manuscript

Received: December 11, 2018

Peer-review started: December 11, 2018

First decision: December 28, 2018

Revised: January 27, 2019

Accepted: January 28, 2019

Article in press: January 28, 2019

Published online: March 14, 2019

with promoter methylation status in GC cell lines. Moreover, DNA demethylation and reactivation of miR-596 after treatment with 5-Aza-2'-deoxycytidine inhibited the proliferative ability of GC cells.

CONCLUSION

MiR-596 has a tumor suppressive role in GC and is downregulated partly due to promoter hypermethylation. Furthermore, PRDX1 is one of the putative target genes of miR-596.

Key words: Gastric cancer; MicroRNA-596; Methylation; Peroxiredoxin 1

©The Author(s) 2019. Published by Baishideng Publishing Group Inc. All rights reserved.

Core tip: In the present study, we investigated a suppressive role of microRNA-596 (miR-596) in gastric cancer (GC). MiR-596 was downregulated in human specimens of GC and GC cell lines, and overexpression of miR-596 significantly reduced GC cell proliferation. Downregulation of miR-596 in GC cell lines was associated with an increase of miR-596 promoter methylation. We also established that miR-596 controls the expression of peroxiredoxin 1, which has never been reported before, suggesting that this interaction could play an important role in GC progression. Overall, this study has an impact in understanding the role of miRNAs in cancer progression.

Citation: Zhang Z, Dai DQ. MicroRNA-596 acts as a tumor suppressor in gastric cancer and is upregulated by promoter demethylation. *World J Gastroenterol* 2019; 25(10): 1224-1237

URL: <https://www.wjgnet.com/1007-9327/full/v25/i10/1224.htm>

DOI: <https://dx.doi.org/10.3748/wjg.v25.i10.1224>

INTRODUCTION

Gastric cancer (GC) is one of the most common digestive malignancies and remains the second most common cause of cancer-related mortality worldwide^[1]. Currently, most patients are diagnosed at an advanced stage, leading to a low cure rate and a low 5-year survival rate. Therefore, it is necessary to further study the molecular mechanism of GC and identify more effective biomarkers for the diagnosis and treatment of GC. A greater understanding of these factors will play an important role in early diagnosis and treatment of GC and improvement of prognosis.

MicroRNAs (miRNAs) are a class of endogenous non-coding RNA with a length of approximately 23 nucleotides, which can bind to complementary sequences in the 3'-untranslated regions (UTRs) of specific mRNAs, resulting in degradation of target mRNAs or inhibition of their translation into functional proteins^[2]. Accumulating studies have indicated that miRNAs have been associated with almost all known physiological and pathological processes, including cancer^[3,4]. In addition, it is suggested in recent studies that epigenetic modification, especially DNA methylation, is one of many mechanisms of miRNA suppression in human cancer^[5,6]. MicroRNA-596 (miR-596) is located on human chromosome 8p23.3 and is an intergenic miRNA gene. In recent years, studies have found that miR-596 is downregulated in a variety of cancers, such as oral cancer^[7], endometrial cancer^[8], melanoma^[9], and bladder cancer^[10,11]. Additionally, miR-596 was previously found to be silenced by promoter CpG island hypermethylation in hepatocellular carcinoma^[12,13], endometrial cancer^[14], and oral cancer^[7]. In GC, Song *et al*^[15] reported that miR-596 had low expression and could target CLDN4 to inhibit the invasion of GC cells. However, whether the expression of miR-596 is associated with promoter methylation alteration in GC remains unclear and whether other targets of miR-596 exist in GC remains to be studied.

In this study, we confirmed that the expression of miR-596 was markedly downregulated in GC tissues and cell lines. Upregulation of miR-596 suppressed the proliferation, migration, and invasion of GC cells. The decreased expression of miR-596 was associated with promoter DNA methylation in GC. Moreover, it was indicated that peroxiredoxin 1 (PRDX1) is one of the putative targets of miR-596 in GC. All these results suggest that there is a critical role for miR-596 in the pathogenesis of GC and it may serve as a potential therapeutic target for patients with

this disease.

MATERIALS AND METHODS

Human tissue samples

A total of 55 paired surgically resected GC tissues and adjacent normal gastric tissues, which were diagnosed by an independent pathologist, were collected from the Fourth Affiliated Hospital of China Medical University, between 2014 and 2015. The specimens were promptly collected following surgery and all were pathologically confirmed. None of the patients enrolled in this study had previously received preoperative chemotherapy or radiotherapy. Informed consent was obtained from all patients. The Medical Association Ethics Committee of the Fourth Affiliated Hospital of China Medical University approved all aspects of the present study in accordance with the Helsinki Declaration.

Gastric cells and culture

One immortalized normal gastric cell line (GES-1) and four human GC cell lines (AGS, SGC-7901, MKN-45, and MGC-803) were obtained from the Institute of Biochemistry and Cell Biology, Chinese Academy of Sciences (Shanghai, China). These cells were cultured in RPMI 1640 medium (Invitrogen, Carlsbad, CA, United States) containing 10% fetal bovine serum (Invitrogen) in a humidified atmosphere of 5% CO₂ at 37 °C.

RNA isolation and quantitative real-time PCR (qRT-PCR)

Total RNA was extracted from tissues or cultured cells using Trizol reagent (Invitrogen). According to the protocol of the Poly(A) Tailing Kit (Tiangen, Beijing, China), poly(A) tails were added to the miRNA. The PrimeScript™ RT reagent Kit with gDNA Eraser (Takara, Dalian, China) and gene-specific primers or random primers were used to generate cDNA. Real-time PCR was performed in a Light Cycler 480 II Real-Time PCR system (Roche Diagnostics, Basel, Switzerland) using SYBR® Green (Takara). Glyceraldehyde phosphate dehydrogenase (GAPDH) and U6 snRNA were employed as endogenous controls for mRNA and miRNA, respectively. The comparative Ct method was used to calculate the relative expression of RNA. Primer sequences are displayed in [Table 1](#).

Western blot analysis

Transfected cells were lysed with lysis buffer (Beyotime, Shanghai, China) containing 1 mmol/L PMSF. The protein concentrations were measured using the bicinchoninic acid (BCA) protein assay kit (Beyotime). Equal amounts (30 µg) of protein were separated by 15% SDS-PAGE and electro-transferred to PVDF membranes (Millipore), which were then incubated with primary antibodies against PRDX1 (1:500 dilution; Proteintech, Wuhan, China) and β-actin (1:1000 dilution; Proteintech) overnight at 4 °C. After incubation with peroxidase-conjugated affinity-purified goat anti-rabbit IgG or peroxidase-conjugated affinity-purified goat anti-mouse IgG (Beyotime), the bands were visualized using an electrochemiluminescence (ECL) detection kit (ThermoFisher Inc, Rockford, IL, United States). Protein bands were scanned and quantified using densitometric software (Bio-Rad, California, United States).

Transfection

Transfections were performed using the Lipofectamine3000 Reagent (Invitrogen) according to the manufacturer's protocol. Final concentrations of 50 nmol/L of miR-596 mimics (5'-AAGCCUGCCCGGCUCUCGGG-3')/ miR-NC (5'-UUGUACUACACAAAAGUACUG-3') and 0.75 µg/mL plasmids were used for each transfection in a six-well plate with 2 mL culture medium. Total RNA and protein were collected 48 h after transfection.

Luciferase reporter assay

MiR-596 mimics or miR-NC, reporter construct, or control vector was cotransfected into MGC-803 cells for 48 h. Dual luciferase Reporter Gene Assay Kit (Tiangen, Beijing, China) was used to detect luciferase activity. Each test was repeated three times.

Cell Counting Kit-8 proliferation assay

Cell proliferation was determined with the Cell Counting Kit-8 (CCK-8) kit (Dojindo, Japan); 3000 cells were seeded into 96-well plates for 24 h and then treated with NC, miR-NC, or miR-596 mimics. After 0, 24, 48, and 72 h of treatment, 100 µL cultural supernatant was collected to another 96-well plate and then 10 µL CCK-8 solution was added for incubation at 37 °C for 4 h. The absorbance was measured at 450 nm

Table 1 Sequences of primers for quantitative real-time PCR

Name	Sequence (5'-3')
Primers used for mRNA detection	
miR-596 (forward)	AAGCCTGCCCGGCTCCT
miR-596 (reverse)	GCTGTCAACGATACGCTACGT
miR-596 (RT)	(GCTGTCAACGATACGCTACGTAACGGCATGACA; GGTGTTTTTTTTTTTTTTTTTTTTTTTTC)
U6 (forward)	CGCTTCGGCAGCACATATAC
U6 (reverse)	TTACAGAAATTTGCGTG TCAT
U6 (RT)	(GCTGTCAACGATACGCTACGTAACGGCATGACAG; TGTTTTTTTTTTTTTTTTTTTTTTTG)
PRDX1 (forward)	AAGAAACTCAACTGCCAAGTG
PRDX1 (reverse)	CAGCCTTTAAGACCCATAAT
GAPDH (forward)	CGGATTGGTTCGTATTGGG
GAPDH (reverse)	CTGGAAGATGGTATGGGATT

PRDX1: Peroxiredoxin 1; MiR-596: MicroRNA-596; GAPDH: Glyceraldehyde phosphate dehydrogenase.

wavelength using spectrophotometry (BioTek, United States).

Wound healing assay

Cells were seeded in six-well plates and treated with NC, miR-NC, or miR-596 mimics. Linear scratch wounds were created on cell monolayers with a sterile 200 μ L pipette tip, and the scratched areas were photographed at $\times 100$ magnification using a Leica DMI3000B computer-assisted microscope (Leica, Buffalo Grove, United States). Images were captured at 0, 24, 48, and 72 h after the scratch was made. Images were analyzed using Image-Pro Plus v6.0 image analysis software (Media Cybernetics, Rockville, MD, United States).

In vitro invasion assay

Transwell plates (BD, Biosciences, United States) were used for GC cell invasion assay. The bottom chamber contained complete medium and the upper chamber has serum-free medium. Matrigel (BD) was added to the RPMI 1640 medium for detecting invading cells. After transfection with NC, miR-NC, or miR-596 mimics, GC cells were appropriately seeded into the cell culture. After incubation at 37 °C for 24 h, the invaded cells were fixed and stained using Giemsa. The images of cells were photographed with a microscope (Leica) at $\times 100$ magnification and the cell number counted in three random fields of view. The results are presented as a column graph with statistics.

DNA extraction and methylation-specific PCR (MSP)

Genomic DNA was extracted from the cultured cells by SDS/proteinase K treatment, followed by phenol-chloroform extraction and ethanol precipitation. The bisulfite treatment was performed using the kit EZ DNA Methylation-Gold Kit (Zymo Research, CA, United States) according to the manufacturer's protocol. The methylated primers were 5'-GAG GTT CGG GAT GTA TCG TT-3' (forward) and 5'-TAA CTT CCG CAA TAA CCG TAT-3' (reverse), which result in a 193 bp band; the unmethylated primers were 5'-GTG GAG GTT TGG GAT GTA TTG-3' (forward) and 5'-CTC TTA ACT TCC ACA ATA ACC ATA-3' (reverse), which result in a 200 bp band. The PCR reaction conditions were as follows: 94 °C for 5 min, 40 cycles of 94 °C for 30 s, 56 °C for 30 s, and 72 °C for 45 s, and 72 °C for 10 min. Agarose gel electrophoresis and ethidium bromide staining were then performed. Data from the gels were collected with a laser density scanner (Pharmacia LKB Ultrascan) and subsequently analyzed. All experiments were repeated three times, and the mean value was used for statistical analysis.

5-Aza-2'-deoxycytidine (5-Aza-dC) treatment

GC cells were seeded at 5×10^5 cells per well in six-well culture plates and cultured in RPMI 1640 medium (Invitrogen) containing 10% fetal bovine serum in a humidified atmosphere of 5% CO₂ at 37 °C for 24 h. The cells were incubated in culture medium with 0, 2.5, 5, or 10 μ mol/L of 5-Aza-dC (Sigma, Shanghai, China) for 3 d, with daily medium replacement. After that, total RNA and DNA were isolated from these treated cells for qRT-PCR and MSP analysis, respectively.

Cell viability assay

GC cells were seeded on 96-well plates and treated with different concentrations of 5-Aza-dC in triplicate. After 24, 48, 72, or 144 h of incubation, cells were washed using PBS and cultured in 100 mL RPMI 1640, including 10 mL CCK-8 solution for another 4 h. The absorbance at 450 nm was measured using spectrophotometry (BioTek).

Statistical analysis

All statistical analyses were performed with SPSS 17.0 software package (SPSS, Chicago, IL, United States). Data are expressed as the mean \pm SD. χ^2 test, Student's *t* test, and one-way ANOVA analysis were used for comparisons. *P*-values < 0.05 were considered statistically significant.

RESULTS

MiR-596 is downregulated and PRDX1 upregulated in GC tissues and cell lines

In the present study, the levels of miR-596 expression in 55 pairs of GC and normal control tissues and cell lines were initially assessed using qRT-PCR. The results demonstrated that miR-596 was significantly downregulated in GC tissues compared with paired control tissues (Figure 1A). Furthermore, endogenous expression of miR-596 was investigated in different gastric cell lines, including AGS, SGC-7901, MKN-45, MGC-803, and GES-1. It was shown that the GC cell lines (AGS, SGC-7901, MKN-45, and MGC-803) exhibited relatively low miR-596 expression levels compared to the normal gastric cell line GES-1 (Figure 1B). In addition, PRDX1 expression was analyzed in 55 paired GC and control tissues and cell lines by qRT-PCR. The results indicated that PRDX1 expression was significantly upregulated in GC tissues and cell lines when compared to corresponding non-tumorous tissue and the normal gastric cell line GES-1 (Figure 1C and D). Moreover, Pearson's correlation analysis revealed that the expression of miR-596 was inversely correlated with PRDX1 in GC tissues (Figure 1E). Then, we further examined the relationship between miR-596 expression and clinicopathological factors in 55 GC tissues by Pearson's χ^2 test. MiR-596 expression was significantly related to tumor differentiation grade and TNM stage, but not with age, sex, tumor size, tumor site, Borrmann type, or lymph node metastasis (Table 2).

PRDX1 as a putative target of miR-596

Using three bioinformatic databases (TargetScan, miRWalk, and miRanda), PRDX1 was selected as a predicted target gene of miR-596 (Figure 2A). PRDX1 expression was analyzed in GC cell lines and the GES-1 cell line by Western blot. The results indicated that PRDX1 expression was significantly upregulated in GC cell lines when compared to the normal gastric cell lines GES-1 (Figure 2B). To further validate this prediction, miR-NC or miR-596 mimics was co-transfected into MKN-45 and MGC-803 cell lines and cultured for 48 h. qRT-PCR and Western blot analysis approved that overexpression of miR-596 (Figure 2C) significantly inhibited PRDX1 expression at the mRNA and protein levels in MKN-45 and MGC-803 cell lines (Figure 2D). Furthermore, the luciferase activity of the PRDX1_WT vector was significantly suppressed by the miR-596 mimics, but miR-596 mimics could not affect the luciferase activity of PRDX1_MUT vector or the miR-NC (Figure 2E). These results suggested that miR-596 may bind directly to PRDX1 and inhibit its expression.

MiR-596 suppresses GC cell proliferation

To investigate the role of miR-596 in GC cell proliferation, we utilized ectopic expression of miR-596 and measured cell growth of two GC cell lines MKN-45 and MGC-803 using the CCK-8 method. The results revealed that cell proliferation was clearly suppressed in MKN-45 (Figure 3A) and MGC-803 (Figure 3B) cells after manipulation of miR-596 mimics at 48 and 72 h, but no significant difference was observed at 24 h.

MiR-596 inhibits GC cell migration and invasion

To further evaluate the role of miR-596 in the progression and metastasis of GC, we performed wound healing and Transwell invasion assays in MKN-45 and MGC-803 cells transfected with miR-NC or miR-596 mimics. Transfection with miR-596 mimics significantly suppressed cell migration (Figure 4A and B) and invasion (Figure 4C) in the MKN-45 and MGC-803 cells compared to the NC and miR-NC groups.

MiR-596 is regulated by epigenetic mechanisms in GC

First, to detect whether low expression of miR-596 is related to DNA methylation, we detected the DNA methylation status of miR-596 promoter region in GC cell lines. Data from our MSP analysis displayed that there was a significant negative

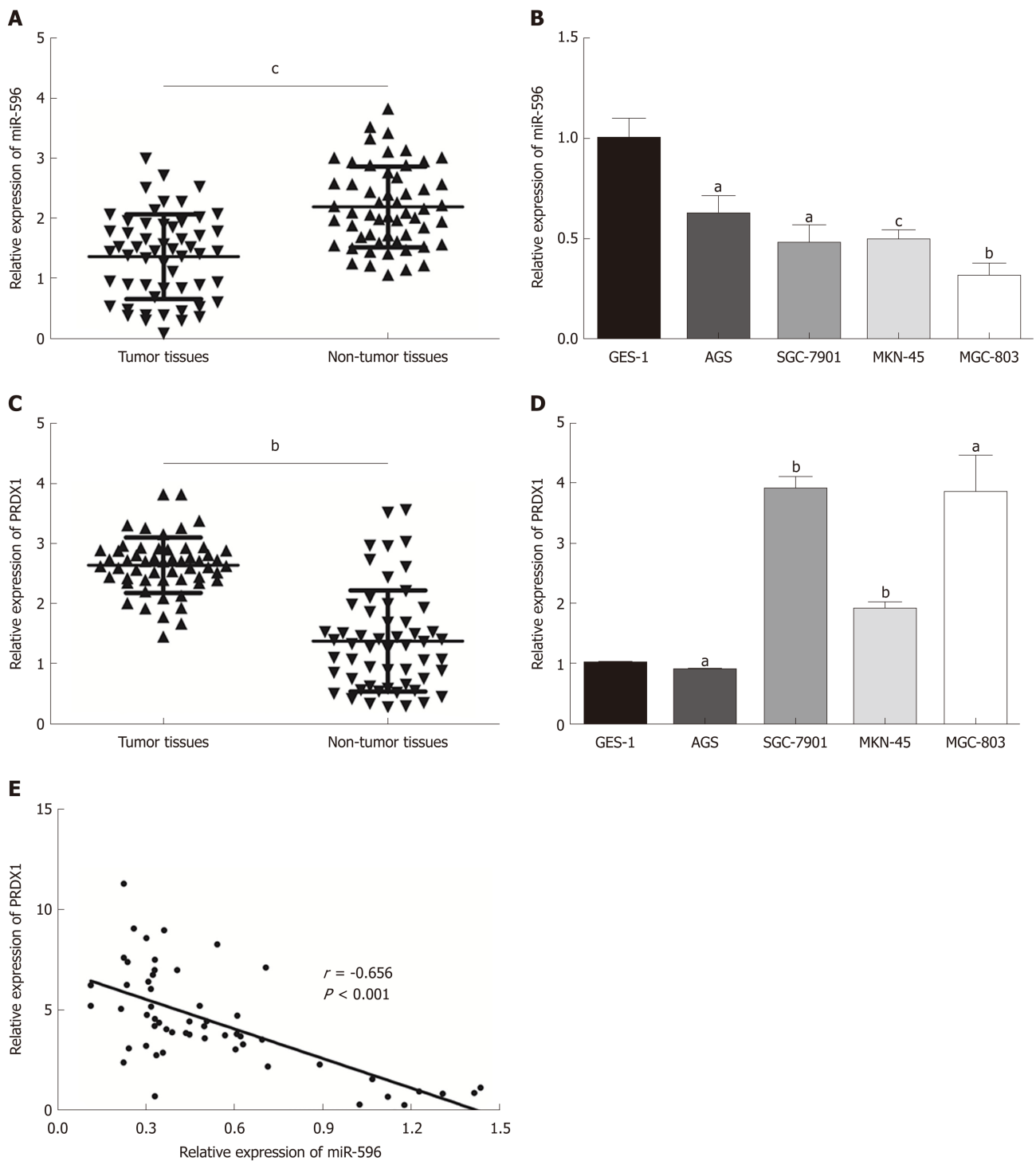


Figure 1 MicroRNA-596 is downregulated and peroxiredoxin 1 upregulated in gastric cancer tissues and cell lines. A and B: Expression of miR-596 in 55 pairs of gastric cancer (GC) and non-tumor tissues (A) and human GC cells (B). C and D: Expression of peroxiredoxin 1 (PRDX1) mRNA in 55 GC samples and corresponding non-tumor tissues (C) and human GC cells (D). E: Pearson's correlation analysis of the relative expression levels of miR-596 and the relative PRDX1 mRNA expression levels in the same set of patients. β -actin was used as an internal control. ^a $P < 0.05$, ^b $P < 0.01$, ^c $P < 0.001$ vs non-tumor tissues or GES-1. PRDX1: Peroxiredoxin 1; MiR-596: MicroRNA-596.

correlation between miR-596 promoter methylation and expression levels in GC cell lines (Figure 5A). Meanwhile, we treated the miR-596-silenced cell lines, MKN-45 and MGC-803, with the demethylating agent 5-Aza-dC, to confirm whether miR-596 expression could be restarted. We observed that the methylation status of miR-596 promoter region was significantly decreased in MKN-45 and MGC-803 cells after treatment with 5-Aza-dC, the expression of miR-596 was obviously increased, and the highest expression occurred at a concentration of 5 $\mu\text{mol/L}$ (Figure 5B). Moreover, it was found that the expression of PRDX1 mRNA was slightly upregulated in MKN-45 and MGC-803 cells after treatment with 5-Aza-dC, but the expression of PRDX1

Table 2 Correlation between microRNA-596 expression and clinicopathological variables of gastric cancer

Variable	No. of Patients	Low expression	High expression	P-value
Age (yr)				0.667
< 60	18	14	4	
≥ 60	37	32	5	
Gender				1.000
Male	36	30	6	
Female	19	16	3	
Size (cm)				0.227
< 5	18	13	5	
≥ 5	37	33	4	
Tumor differentiation				0.043 ^a
Well/moderate	23	16	7	
Poor	32	30	2	
Tumor location				0.827
Upper	5	4	1	
Middle	12	11	1	
Lower	38	31	7	
Borrmann type				0.545
I + II	6	4	2	
III + V	49	42	7	
TNM stage				0.031 ^a
I + II	22	15	7	
III + IV	33	31	2	
Lymph node metastasis				0.239
No	13	9	4	
Yes	42	37	5	

^a*P* < 0.05.

protein was significantly downregulated (Figure 5C). MSP products were sequenced, which confirmed that sodium bisulfite modification was sufficient for DNA (Figure 5D).

5-Aza-dC treatment decreases proliferation in GC cell lines

To evaluate whether 5-Aza-dC treatment affects GC cell growth, we analyzed the proliferation of MKN-45 (Figure 6A) and MGC-803 (Figure 6B) cells treated with 5-Aza-dC. The results of the CCK-8 assay showed that the cell inhibition rate was significantly increased as the 5-Aza-dC concentration or the culture time was increased as compared with the untreated control group.

DISCUSSION

Accumulating evidence has demonstrated that miRNAs may play an important role in GC initiation and development^[16,17]. In the present study, we found that miR-596 expression was significantly decreased in GC tissue and cell lines. Moreover, artificial ectopic expression of miR-596 potentially suppressed GC cell proliferation, migration, and invasion. This indicates that miR-596 may function as a tumor suppressor in GC and that miR-596 expression may contribute to the development of GC.

MiRNAs are dysregulated in nearly all human tumours and can function as either tumour suppressors or oncogenes, depending on their target transcripts^[18,19]. They work by binding to complementary sequences in the 3'-UTRs of specific mRNAs, leading to translation inhibition^[20]. Moreover, due to a non-strict hybridization of the seed match region, one miRNA can bind to multiple mRNA targets, allowing simultaneous downregulation of multiple target mRNAs. Similarly, multiple miRNAs can bind to the same mRNA target and enhance translational repression^[21,22]. In our research, bioinformatic analysis show that PRDX1 is a potential target of miR-596.

A

	Predicted consequential pairing of target region (top) and miRNA (bottom)		Site type
Position 201-208 of PRDX1 3' UTR	5' . . .	GAGUUGGCGUUGUGG SCAGGCUA . . .	8mer
hsa-miR-596	3'	GGGCUCCUCGGCCCGUCCGAA	

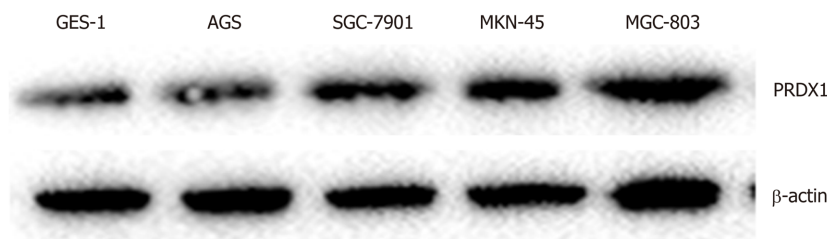
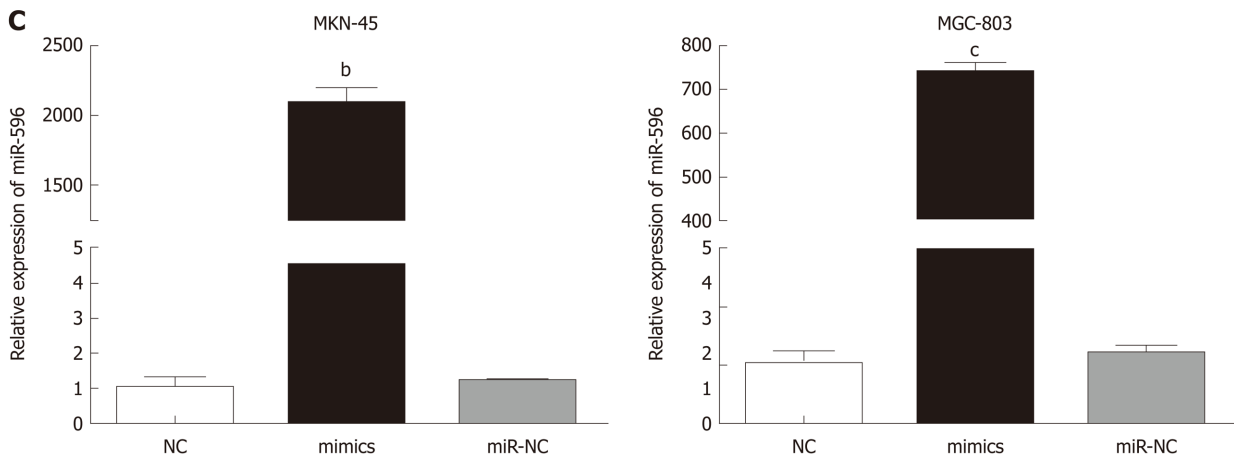
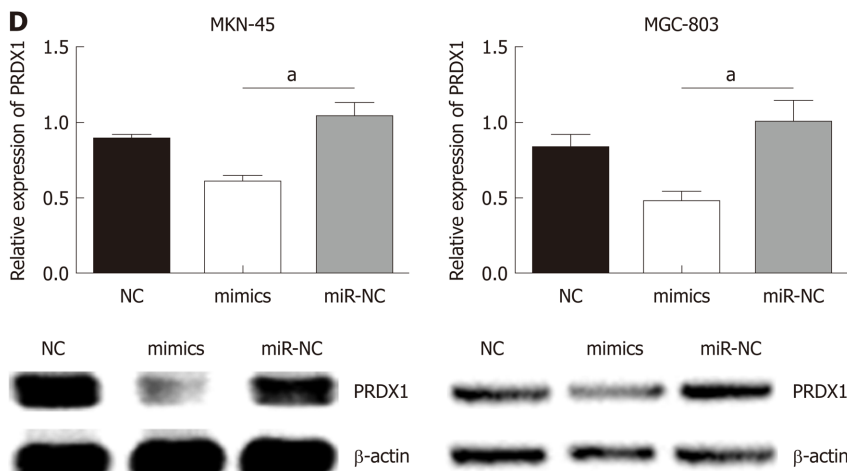
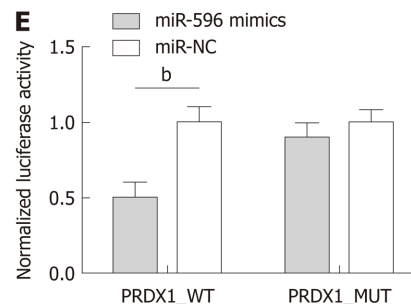
B**C****D****E**

Figure 2 Peroxiredoxin 1 as a putative target of microRNA-596 in gastric cancer cells. A: The predicted binding sites for microRNA-596 (miR-596) in the 3'-UTR of peroxiredoxin 1 (PRDX1). B: Expression of PRDX1 protein in human gastric cancer (GC) cells. C: Quantitative real-time PCR (qRT-PCR) for determining miR-596 expression in MKN-45 and MGC-803 cells transfected with miR-NC or miR-596 mimics. D: PRDX1 mRNA and protein expression in MKN-45 and MGC-803 cells transfected with miR-NC or miR-596 mimics. β -actin was used as an internal control. E: Relative luciferase activity of PRDX1 in wild-type (WT-UTR) or mutant (MUT-UTR). ^a $P < 0.05$, ^b $P < 0.01$, ^c $P < 0.001$ vs miR-NC. PRDX1: Peroxiredoxin 1; MiR-596: MicroRNA-596.

PRDX1 belongs to the peroxiredoxin family and is composed of thiol-specific antioxidant enzymes, which can reduce H_2O_2 and alkyl hydroperoxide^[23], and is related to the reduction of oxidative damage^[24]. PRDX1 overexpression was associated with tumor growth and poor prognosis in numerous cancers including breast cancer^[25], lung cancer^[26], and esophageal squamous cell cancer^[27]. However, the expression profile and potential role of PRDX1 in GC remain to be investigated. In this study, we found that the expression of PRDX1 was substantially upregulated in cancer tissues and cell lines by qRT-PCR and was inversely correlated with miR-596 in GC tissues. Additionally, the results showed that overexpression of miR-596 decreased the expression of PRDX1 and luciferase reporter assays detected the direct

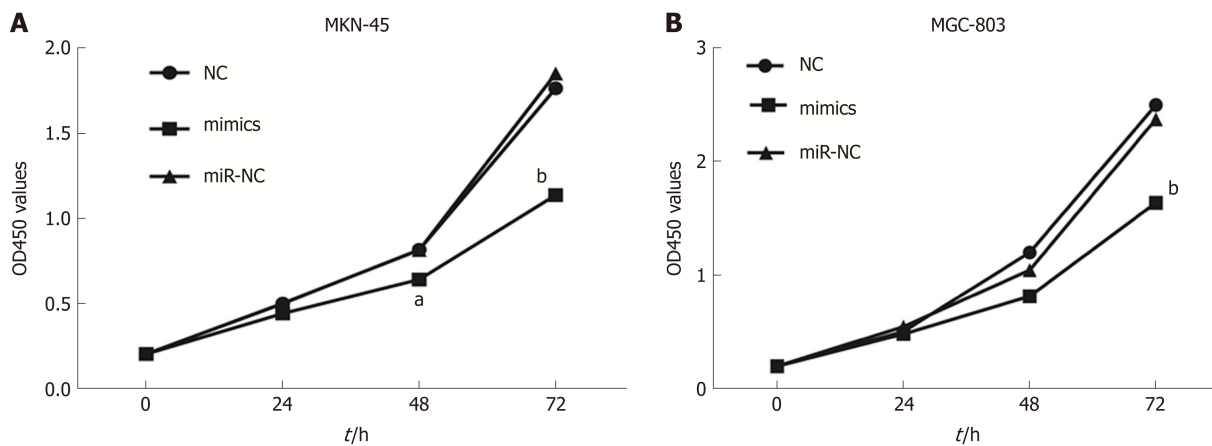


Figure 3 MicroRNA-596 suppresses gastric cancer cell proliferation. NC, miR-NC, or miR-596 mimics was transfected into MKN-45 (A) and MGC-803 (B) cells. The cell growth rate was determined by measuring Cell Counting Kit-8 absorbance at 450 nm every 24 h (^a $P < 0.05$, ^b $P < 0.01$ vs miR-NC).

binding of miR-596 to the 3'-UTR of PRDX1 transcripts. Our results provided a theoretical basis for further study of the mechanism of miR-596 and PRDX1 in GC.

Previous studies showed that transcription of miRNAs can also be epigenetically regulated by methylation in CpG islands^[28,29]. In addition, DNA methylation is a reversible signal, similar to other physiological biochemical modifications^[30]. The silencing of tumor suppressor genes is closely related to DNA hypermethylation and can be effectively reversed by DNA methyltransferase inhibitors, thereby inhibiting tumor growth^[31]. In the present research, DNA methylation analysis by MSP indicated that there was a markedly negative correlation between miR-596 promoter methylation and expression levels in GC cell lines. Furthermore, treatment with the demethylating agent 5-Aza-dC raised the expression of miR-596 in GC cell lines. In addition, the expression of its target gene PRDX1 protein was significantly downregulated. These results showed that the downregulation of miR-596 in GC is attributed, at least in part, to the hypermethylation of CpG sequences in its promoter.

5-Aza-dC as a demethylating agent has been recently used for treatment of myelodysplastic syndromes and acute myelomonocytic leukemia^[32]. The main mechanism of 5-Aza-dC is to reduce its activity by binding to DNA methyltransferase I (DNMT1), selectively induce DNMT degradation, and inhibit tumor growth by inducing apoptosis, affecting cell cycle and cytotoxicity^[33]. Moreover, 5-Aza-dC is cytotoxic at high concentrations and demethylated at low concentrations^[34]. Therefore, our study suggested that the inhibitory effect of 5-Aza-dC on the proliferative ability of GC cells may be due in part to the demethylation and reactivation of miR-596.

In conclusion, our current study demonstrated that the expression of miR-596 was downregulated in GC cells and GC tissues. The *in vitro* data further suggested that miR-596 expression was able to inhibit GC cell growth, migration, and invasion. Furthermore, miR-596 expression was regulated by epigenetic mechanisms. The downregulation of miR-596 was associated with promoter methylation status in GC cell lines. DNA demethylation and reactivation of miR-596 after treatment with 5-Aza-dC inhibited the proliferative ability of GC cells. Moreover, we identified that PRDX1 is one of the putative target genes of miR-596. Our results further emphasize that miR-596 functions as a crucial tumor suppressor that is regulated by epigenetic mechanisms in GC and may offer a promising novel therapeutic approach for GC. Nonetheless, more studies are required to determine the precise mechanism of miR-596 in the progression of GC.

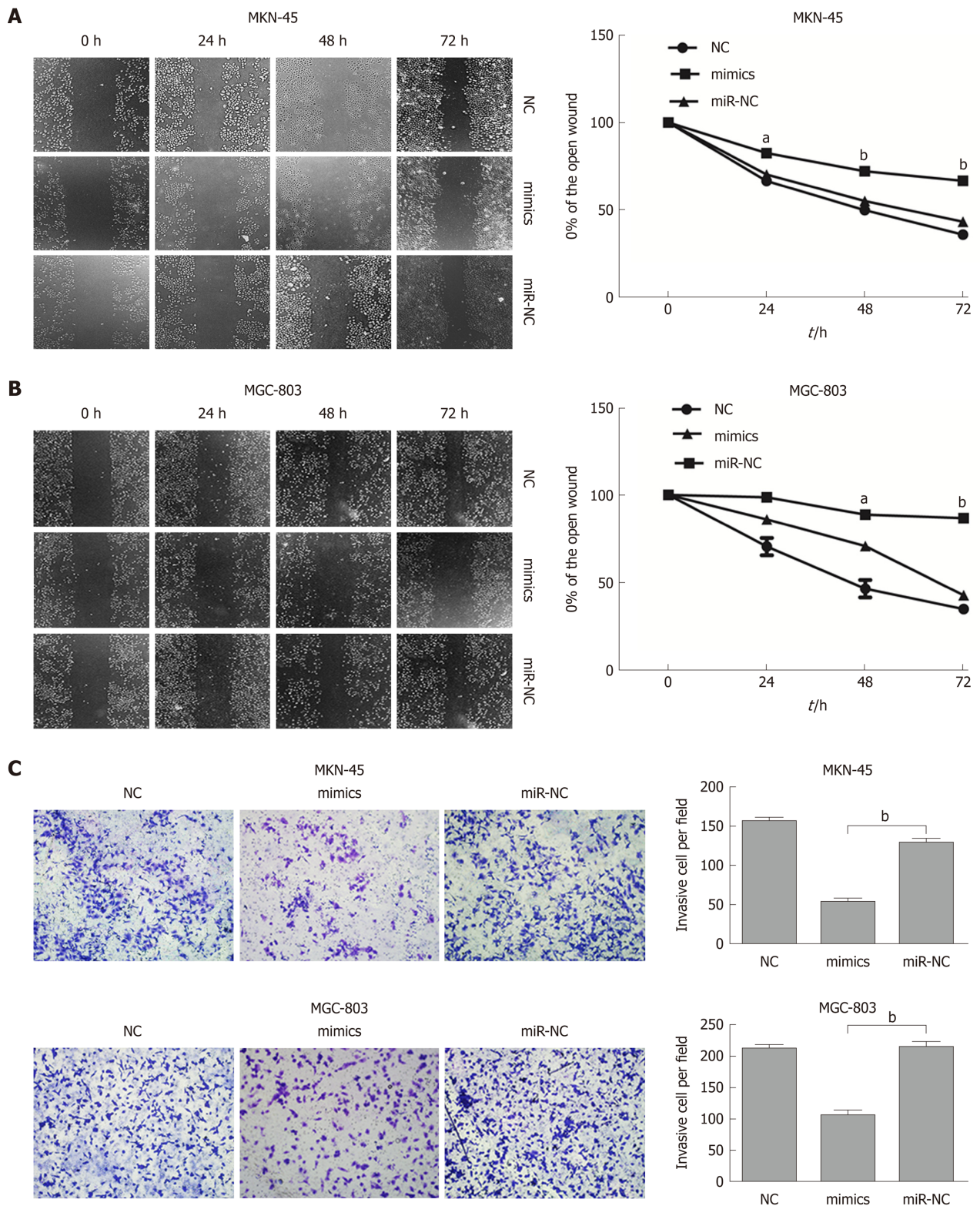


Figure 4 MicroRNA-596 inhibits gastric cancer cell migration and invasion. A and B: The wound healing assay for detecting cell migration in MKN-45 (A) and MGC-803 (B) cells transfected with miR-NC or microRNA-596 (miR-596) mimics. C: The Transwell invasion assay for detecting cell invasion in MKN-45 and MGC-803 cells transfected with miR-NC or miR-596 mimics. ^a $P < 0.05$, ^b $P < 0.01$ vs miR-NC.

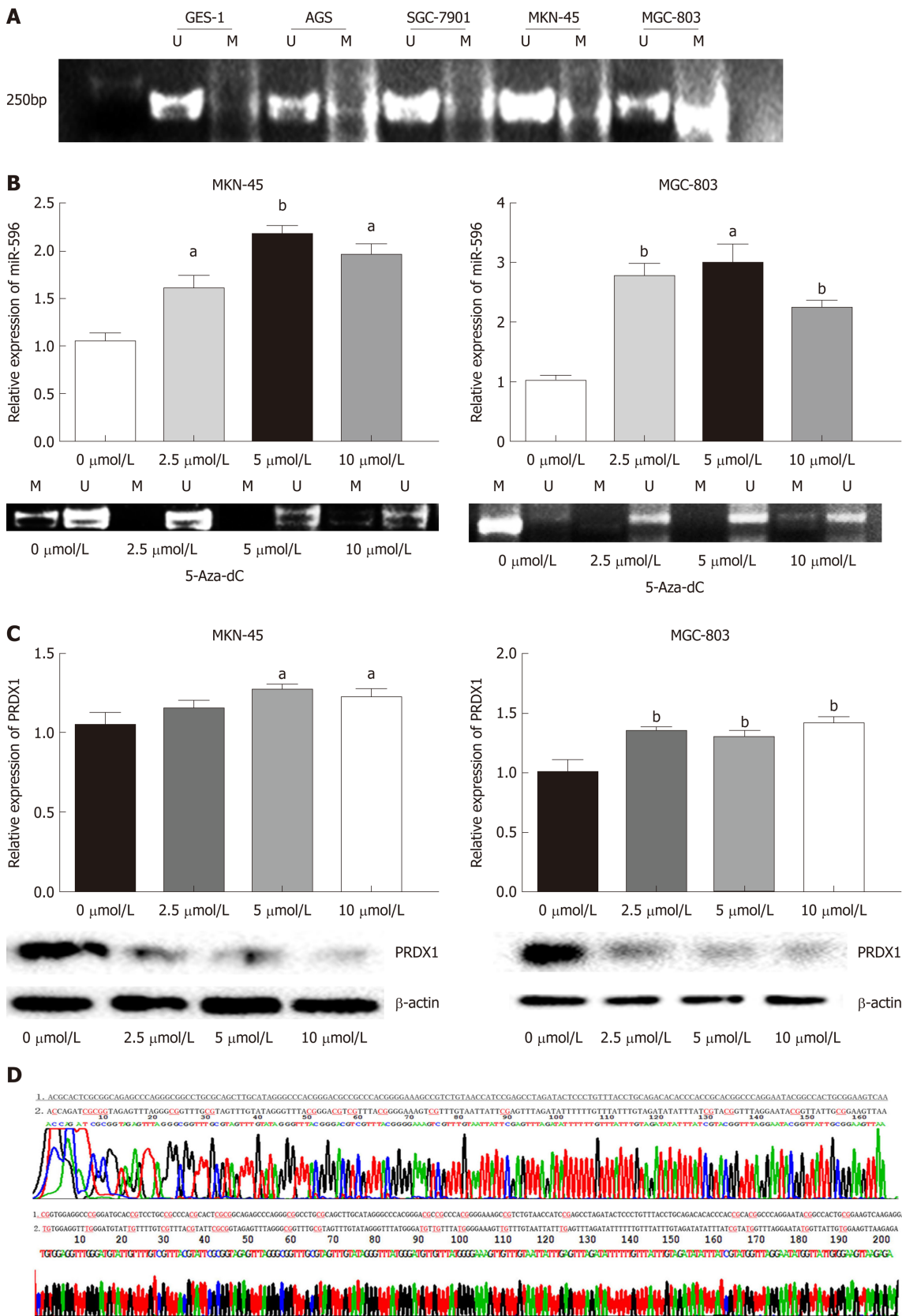


Figure 5 MicroRNA-596 is regulated by epigenetic mechanisms in gastric cancer. A: Methylation-specific PCR (MSP) analysis of microRNA-596 (miR-596) promoter region methylation in gastric cancer (GC) cell lines. B: Quantitative real-time PCR (qRT-PCR) and MSP analysis of miR-596 expression after treatment with 5-Aza-2'-deoxycytidine (5-Aza-dC) (2.5, 5, or 10 μmol/L) in MKN-45 and MGC-803 cells, ^a*P* < 0.05, ^b*P* < 0.01 vs control cells. C: qRT-PCR and Western blot analysis of PRDX1 expression after treatment with 5-Aza-dC (2.5, 5 or 10 μmol/L) in MKN-45 and MGC-803 cells, ^a*P* < 0.05, ^b*P* < 0.01 vs control cells. D: The promoter sequence of miR-596 after treatment with sodium bisulfate. Unmethylation of cytosine was transformed to uracil, but methylated cytosine remained unchanged. 1: DNA sequence of miR-596 promoter; 2: Sequence after sodium bisulfate modification; U: Unmethylation lane; M: Methylation lane; PRDX1: Peroxiredoxin 1; MiR-596: MicroRNA-596; 5-Aza-dC: 5-Aza-2'-deoxycytidine.

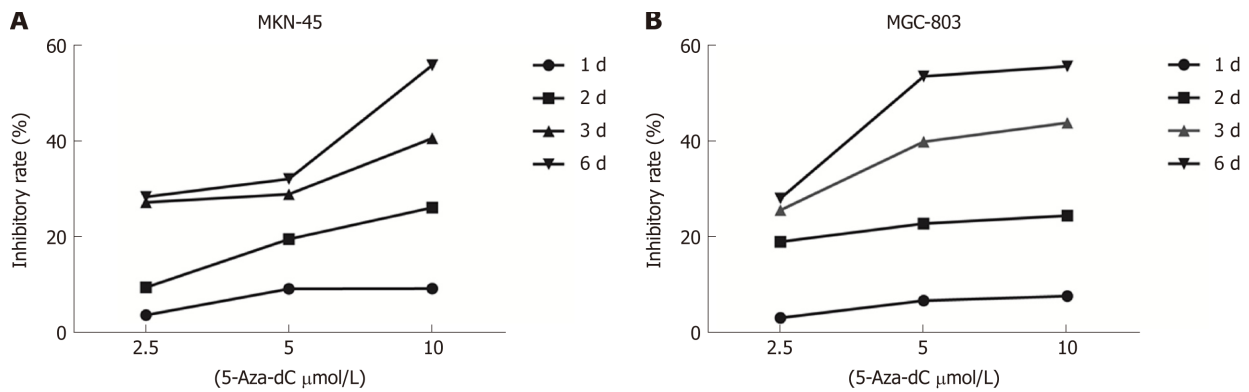


Figure 6 5-Aza-2'-deoxycytidine treatment decreases proliferation in the MKN-45 (A) and MGC-803 (B) cells. Inhibition rate (%) = $(OD_{\text{untreated control}} - OD_{\text{treated}}) / OD_{\text{untreated control}} \times 100\%$. 5-Aza-dC: 5-Aza-2'-deoxycytidine.

ARTICLE HIGHLIGHTS

Research background

Gastric cancer (GC) is one of the most common digestive malignancies and remains the second most common cause of cancer-related mortality worldwide. Currently, most patients are diagnosed at an advanced stage, leading to a low cure rate and a low 5-year survival rate. Therefore, it is necessary to further study the molecular mechanism of GC and identify more effective biomarkers for the diagnosis and treatment of GC.

Research motivation

Accumulating studies have indicated that microRNAs (miRNAs) have been associated with almost all known physiological and pathological processes, including cancer. In addition, it is suggested in recent studies that epigenetic modification, especially DNA methylation, is one of many mechanisms of miRNA suppression in human cancer. A greater understanding of these factors will play an important role in early diagnosis and treatment of GC and improvement of prognosis.

Research objectives

To study the potential role and possible regulatory mechanism of microRNA-596 (miR-596) in GC, and whether other targets of miR-596 exist in GC.

Research methods

In the present study, the levels of miR-596 expression in 55 pairs of GC and normal control tissues and cell lines were initially assessed using quantitative real-time (qRT-PCR). We further examined the relationship between miR-596 expression and clinicopathological factors in 55 GC tissues by Pearson's χ^2 test. In addition, peroxiredoxin 1 (PRDX1) expression was analyzed in 55 paired GC and control tissues and cell lines by qRT-PCR. Western blot and luciferase reporter assay were used to detect the effect of miR-596 on PRDX1 expression. Then, the proliferation, metastasis, and invasion of GC cells transfected with miR-596 mimics were analyzed, respectively, by Cell Counting Kit-8 proliferation assay, wound healing assay, and transwell invasion assay. The methylation status of the promoter CpG islands of miR-596 in GC cell lines was detected by methylation-specific PCR. Meanwhile, we treated GC cells with the demethylating agent 5-Aza-2'-deoxycytidine (5-Aza-dC) to confirm whether miR-596 expression could be restarted. Finally, in order to evaluate whether 5-Aza-dC treatment affects GC cell growth, we analyzed the proliferation of GC cells treated with 5-Aza-dC.

Research results

Our current study demonstrated that the expression of miR-596 was downregulated in GC cells and GC tissues. The *in vitro* data further suggested that miR-596 expression was able to inhibit GC cell growth, migration, and invasion. Furthermore, miR-596 expression was regulated by epigenetic mechanisms. Moreover, we identified that PRDX1 is one of the putative target genes of miR-596.

Research conclusions

In the present study, we have investigated a suppressive role of microRNA-596 in GC. We reported that miR-596 was downregulated in human specimens of GC and GC cell lines, and that overexpression of miR-596 significantly reduced GC cell proliferation. Moreover, the downregulation of miR-596 in GC cell lines was associated with an increase of miR-596 promoter methylation. We also established that miR-596 controls the expression of PRDX1, which has never been reported before, suggesting that this interaction could play an important role in GC progression.

Research perspectives

Our results further emphasize that miR-596 functions as a crucial tumor suppressor that is regulated by epigenetic mechanisms in GC and may offer a promising novel therapeutic approach for GC. Nonetheless, more studies are required to determine the precise mechanism of miR-596 in the progression of GC.

REFERENCES

- Global Burden of Disease Cancer Collaboration;** Fitzmaurice C, Dicker D, Pain A, Hamavid H, Moradi-Lakeh M, MacIntyre MF, Allen C, Hansen G, Woodbrook R, Wolfe C, Hamadeh RR, Moore A, Werdecker A, Te Ao B, Gessner BD, McMahon B, Karimkhani C, Yu C, Cooke GS, Schwebel DC, Carpenter DO, Pereira DM, Nash D, De Leo D, Woodbrook R, Plass D, Ukwaia KN, Thurston GD, Yun Jin K, Simard EP, Mills E, Park EK, Catalá-López F, deVeber G, Gotay C, Khan G, Hosgood HD 3rd, Santos IS, Leasher JL, Singh J, Leigh J, Jonas JB, Sanabria J, Beardesley J, Jacobsen KH, Takahashi K, Franklin RC, Ronfani L, Montico M, Naldi L, Tonelli M, Geleijnse J, Petzold M, Shrimo MG, Younis M, Yonemoto N, Breitborde N, Yip P, Pourmalek F, Lotufo PA, Esteghamati A, Hankey GJ, Ali R, Lunevicius R, Malekzadeh R, Dellavalle R, Weintraub R, Lucas R, Hay R, Rojas-Rueda D, Westerman R, Sepanlou SG, Nolte S, Patten S, Weichenthal S, Abera SF, Fereshhtehnejad SM, Shiue I, Driscoll T, Vasankari T, Alsharif U, Rahimi-Movaghar V, Vlassov VV, Marcesen WS, Mekonnen W, Melaku YA, Yano Y, Artaman A, Campos I, MacLachlan J, Mueller U, Kim D, Trillini M, Eshrati B, Williams HC, Shibuya K, Dandona R, Murthy K, Cowie B, Amare AT, Antonio CA, Castañeda-Orjuela C, van Gool CH, Violante F, Oh IH, Deribe K, Soreide K, Knibbs L, Kereselidze M, Green M, Cardenas R, Roy N, Tillmann T, Li Y, Krueger H, Monasta L, Dey S, Sheikhbahaei S, Hafezi-Nejad N, Kumar GA, Sreeramareddy CT, Dandona L, Wang H, Vollset SE, Mokdad A, Salomon JA, Lozano R, Vos T, Forouzanfar M, Lopez A, Murray C, Naghavi M. The Global Burden of Cancer 2013. *JAMA Oncol* 2015; **1**: 505-527 [PMID: 26181261 DOI: 10.1001/jamaoncol.2015.0735]
- Bartel DP.** MicroRNAs: target recognition and regulatory functions. *Cell* 2009; **136**: 215-233 [PMID: 19167326 DOI: 10.1016/j.cell.2009.01.002]
- Lujambio A, Lowe SW.** The microcosmos of cancer. *Nature* 2012; **482**: 347-355 [PMID: 22337054 DOI: 10.1038/nature10888]
- Mendell JT, Olson EN.** MicroRNAs in stress signaling and human disease. *Cell* 2012; **148**: 1172-1187 [PMID: 22424228 DOI: 10.1016/j.cell.2012.02.005]
- Lopez-Serra P, Esteller M.** DNA methylation-associated silencing of tumor-suppressor microRNAs in cancer. *Oncogene* 2012; **31**: 1609-1622 [PMID: 21860412 DOI: 10.1038/onc.2011.354]
- Lujambio A, Esteller M.** CpG island hypermethylation of tumor suppressor microRNAs in human cancer. *Cell Cycle* 2007; **6**: 1455-1459 [PMID: 17581274]
- Endo H, Muramatsu T, Furuta M, Uzawa N, Pimkhaokham A, Amagasa T, Inazawa J, Kozaki K.** Potential of tumor-suppressive miR-596 targeting LGALS3BP as a therapeutic agent in oral cancer. *Carcinogenesis* 2013; **34**: 560-569 [PMID: 23233740 DOI: 10.1093/carcin/bgs376]
- Ma M, Yang J, Wang B, Zhao Z, Xi JJ.** High-Throughput Identification of miR-596 Inducing p53-Mediated Apoptosis in HeLa and HCT116 Cells Using Cell Microarray. *SLAS Technol* 2017; **22**: 636-645 [PMID: 28732184 DOI: 10.1177/2472630317720870]
- Liu SM, Lin CH, Lu J, Lin IY, Tsai MS, Chen MH, Ma N.** miR-596 Modulates Melanoma Growth by Regulating Cell Survival and Death. *J Invest Dermatol* 2018; **138**: 911-921 [PMID: 29183729 DOI: 10.1016/j.jid.2017.11.016]
- Olivieri M, Ferro M, Terreri S, Durso M, Romanelli A, Avitabile C, De Cobelli O, Messere A, Bruzzese D, Vannini I, Marinelli L, Novellino E, Zhang W, Incoronato M, Ildardi G, Staibano S, Marra L, Franco R, Perdonà S, Terracciano D, Czerniak B, Liguori GL, Colonna V, Fabbri M, Febbraio F, Calin GA, Cimmino A.** Long non-coding RNA containing ultraconserved genomic region 8 promotes bladder cancer tumorigenesis. *Oncotarget* 2016; **7**: 20636-20654 [PMID: 26943042 DOI: 10.18632/oncotarget.7833]
- Terreri S, Durso M, Colonna V, Romanelli A, Terracciano D, Ferro M, Perdonà S, Castaldo L, Febbraio F, de Nigris F, Cimmino A.** New Cross-Talk Layer between Ultraconserved Non-Coding RNAs, MicroRNAs and Polycomb Protein YY1 in Bladder Cancer. *Genes (Basel)* 2016; **7** [PMID: 27983635 DOI: 10.3390/genes7120127]
- Anwar SL, Albat C, Krech T, Hasemeier B, Schipper E, Schweitzer N, Vogel A, Kreipe H, Lehmann U.** Concordant hypermethylation of intergenic microRNA genes in human hepatocellular carcinoma as new diagnostic and prognostic marker. *Int J Cancer* 2013; **133**: 660-670 [PMID: 23364900 DOI: 10.1002/ijc.28068]
- Potapova A, Albat C, Hasemeier B, Haessler K, Lamprecht S, Suerbaum S, Kreipe H, Lehmann U.** Systematic cross-validation of 454 sequencing and pyrosequencing for the exact quantification of DNA methylation patterns with single CpG resolution. *BMC Biotechnol* 2011; **11**: 6 [PMID: 21235780 DOI: 10.1186/1472-6750-11-6]
- Huang YW, Kuo CT, Chen JH, Goodfellow PJ, Huang TH, Rader JS, Uyar DS.** Hypermethylation of miR-203 in endometrial carcinomas. *Gynecol Oncol* 2014; **133**: 340-345 [PMID: 24530564 DOI: 10.1016/j.ygyno.2014.02.009]
- Song YX, Sun JX, Zhao JH, Yang YC, Shi JX, Wu ZH, Chen XW, Gao P, Miao ZF, Wang ZN.** Non-coding RNAs participate in the regulatory network of CLDN4 via ceRNA mediated miRNA evasion. *Nat Commun* 2017; **8**: 289 [PMID: 28819095 DOI: 10.1038/s41467-017-00304-1]
- Ueda T, Volinia S, Okumura H, Shimizu M, Taccioli C, Rossi S, Alder H, Liu CG, Oue N, Yasui W, Yoshida K, Sasaki H, Nomura S, Seto Y, Kaminishi M, Calin GA, Croce CM.** Relation between microRNA expression and progression and prognosis of gastric cancer: a microRNA expression analysis. *Lancet Oncol* 2010; **11**: 136-146 [PMID: 20022810 DOI: 10.1016/S1470-2045(09)70343-2]
- Kiga K, Mimuro H, Suzuki M, Shinozaki-Ushiku A, Kobayashi T, Sanada T, Kim M, Ogawa M, Iwasaki YW, Kayo H, Fukuda-Yuzawa Y, Yashiro M, Fukayama M, Fukao T, Sasakawa C.** Epigenetic silencing of miR-210 increases the proliferation of gastric epithelium during chronic Helicobacter pylori infection. *Nat Commun* 2014; **5**: 4497 [PMID: 25187177 DOI: 10.1038/ncomms5497]
- Di Leva G, Garofalo M, Croce CM.** MicroRNAs in cancer. *Annu Rev Pathol* 2014; **9**: 287-314 [PMID: 24079833 DOI: 10.1146/annurev-pathol-012513-104715]
- Kwan JY, Psarianos P, Bruce JP, Yip KW, Liu FF.** The complexity of microRNAs in human cancer. *J Radiat Res* 2016; **57** Suppl 1: i106-i111 [PMID: 26983984 DOI: 10.1093/jrr/rww009]

- 20 **Gu S**, Jin L, Zhang F, Sarnow P, Kay MA. Biological basis for restriction of microRNA targets to the 3' untranslated region in mammalian mRNAs. *Nat Struct Mol Biol* 2009; **16**: 144-150 [PMID: 19182800 DOI: 10.1038/nsmb.1552]
- 21 **Ameres SL**, Zamore PD. Diversifying microRNA sequence and function. *Nat Rev Mol Cell Biol* 2013; **14**: 475-488 [PMID: 23800994 DOI: 10.1038/nrm3611]
- 22 **Pinweha P**, Rattanapornsompong K, Charoensawan V, Jitrapakdee S. MicroRNAs and oncogenic transcriptional regulatory networks controlling metabolic reprogramming in cancers. *Comput Struct Biotechnol J* 2016; **14**: 223-233 [PMID: 27358718 DOI: 10.1016/j.csbj.2016.05.005]
- 23 **Kim JH**, Lee JM, Lee HN, Kim EK, Ha B, Ahn SM, Jang HH, Lee SY. RNA-binding properties and RNA chaperone activity of human peroxiredoxin 1. *Biochem Biophys Res Commun* 2012; **425**: 730-734 [PMID: 22877757 DOI: 10.1016/j.bbrc.2012.07.142]
- 24 **Aeby E**, Ahmed W, Redon S, Simanis V, Lingner J. Peroxiredoxin 1 Protects Telomeres from Oxidative Damage and Preserves Telomeric DNA for Extension by Telomerase. *Cell Rep* 2016; **17**: 3107-3114 [PMID: 28009281 DOI: 10.1016/j.celrep.2016.11.071]
- 25 **Cha MK**, Suh KH, Kim IH. Overexpression of peroxiredoxin I and thioredoxin1 in human breast carcinoma. *J Exp Clin Cancer Res* 2009; **28**: 93 [PMID: 19566940 DOI: 10.1186/1756-9966-28-93]
- 26 **Jiang H**, Wu L, Mishra M, Chawsheen HA, Wei Q. Expression of peroxiredoxin 1 and 4 promotes human lung cancer malignancy. *Am J Cancer Res* 2014; **4**: 445-460 [PMID: 25232487]
- 27 **Gong F**, Hou G, Liu H, Zhang M. Peroxiredoxin 1 promotes tumorigenesis through regulating the activity of mTOR/p70S6K pathway in esophageal squamous cell carcinoma. *Med Oncol* 2015; **32**: 455 [PMID: 25579166 DOI: 10.1007/s12032-014-0455-0]
- 28 **Poddar S**, Kesharwani D, Datta M. Interplay between the miRNome and the epigenetic machinery: Implications in health and disease. *J Cell Physiol* 2017; **232**: 2938-2945 [PMID: 28112397 DOI: 10.1002/jcp.25819]
- 29 **Suzuki H**, Yamamoto E, Nojima M, Kai M, Yamano HO, Yoshikawa K, Kimura T, Kudo T, Harada E, Sugai T, Takamaru H, Niinuma T, Maruyama R, Yamamoto H, Tokino T, Imai K, Toyota M, Shinomura Y. Methylation-associated silencing of microRNA-34b/c in gastric cancer and its involvement in an epigenetic field defect. *Carcinogenesis* 2010; **31**: 2066-2073 [PMID: 20924086 DOI: 10.1093/carcin/bgq203]
- 30 **Ramchandani S**, Bhattacharya SK, Cervoni N, Szyf M. DNA methylation is a reversible biological signal. *Proc Natl Acad Sci USA* 1999; **96**: 6107-6112 [PMID: 10339549]
- 31 **Lyko F**, Brown R. DNA methyltransferase inhibitors and the development of epigenetic cancer therapies. *J Natl Cancer Inst* 2005; **97**: 1498-1506 [PMID: 16234563 DOI: 10.1093/jnci/dji311]
- 32 **Das PM**, Singal R. DNA methylation and cancer. *J Clin Oncol* 2004; **22**: 4632-4642 [PMID: 15542813 DOI: 10.1200/jco.2004.07.151]
- 33 **Mai A**, Altucci L. Epi-drugs to fight cancer: from chemistry to cancer treatment, the road ahead. *Int J Biochem Cell Biol* 2009; **41**: 199-213 [PMID: 18790076 DOI: 10.1016/j.biocel.2008.08.020]
- 34 **Muraki Y**, Banno K, Yanokura M, Kobayashi Y, Kawaguchi M, Nomura H, Hirasawa A, Susumu N, Aoki D. Epigenetic DNA hypermethylation: clinical applications in endometrial cancer (Review). *Oncol Rep* 2009; **22**: 967-972 [PMID: 19787208]

P- Reviewer: Dalay N, Kopljar M

S- Editor: Ma RY **L- Editor:** Wang TQ **E- Editor:** Yin SY



Retrospective Cohort Study

Performance of risk stratification systems for gastrointestinal stromal tumors: A multicenter study

Tao Chen, Liang-Ying Ye, Xing-Yu Feng, Hai-Bo Qiu, Peng Zhang, Yi-Xin Luo, Li-Yi Yuan, Xin-Hua Chen, Yan-Feng Hu, Hao Liu, Yong Li, Kai-Xiong Tao, Jiang Yu, Guo-Xin Li

ORCID number: Tao Chen (0000-0003-1306-6538); Liang-Ying Ye (0000-0001-9721-2074); Xing-Yu Feng (0000-0002-8525-1559); Hai-Bo Qiu (0000-0002-4221-3309); Peng Zhang (0000-0002-9805-2743); Yi-Xin Luo (0000-0002-5592-162X); Li-Yi Yuan (0000-0002-3453-6289); Xin-Hua Chen (0000-0002-1879-4318); Yan-Feng Hu (0000-0001-7742-8820); Hao Liu (0000-0001-6131-9398); Yong Li (0000-0003-4681-263X); Kai-Xiong Tao (0000-0002-1193-2458); Jiang Yu (0000-0003-0086-1604); Guo-Xin Li (0000-0003-2773-7048).

Author contributions: Chen T, Ye LY, Feng XY, Qiu HB, Zhang P, Li Y, Tao KX, and Li GX designed the research; Chen T, Luo YX, Yuan LY, Chen XH, and Yu J performed the research; Hu YF and Liu H contributed new reagents/analytic tools; all authors wrote the paper.

Supported by the State Key Project of Research and Development Plan, No. 2017YFC0108300 and No. 2017YFC0108303; and 2018 Special Funds for the Cultivation of Guangdong College Students' Scientific and Technological Innovation (Climbing Program Special Funds), No. pdjha0094.

Institutional review board statement: The study was approved for publication by our Institutional Reviewer.

Informed consent statement: All study participants or their legal guardian provided informed written consent about personal and medical data collection prior to

Tao Chen, Yi-Xin Luo, Li-Yi Yuan, Xin-Hua Chen, Yan-Feng Hu, Hao Liu, Jiang Yu, Guo-Xin Li, Department of General Surgery, Nanfang Hospital, Southern Medical University, Guangzhou 510515, Guangdong Province, China

Liang-Ying Ye, Department of Gastroenterology, Nanfang Hospital, Southern Medical University, Guangzhou 510515, Guangdong Province, China

Xing-Yu Feng, Yong Li, Department of General Surgery, Guangdong General Hospital, Guangdong Academy of Medical Sciences, Guangzhou 510080, Guangdong Province, China

Hai-Bo Qiu, Department of Gastric Surgery, Sun Yat-sen University Cancer Center, Sun Yat-sen University, Guangzhou 510060, Guangdong Province, China

Peng Zhang, Kai-Xiong Tao, Department of General Surgery, Wuhan Union Hospital, Huazhong University of Science and Technology, Wuhan 430022, Hubei Province, China

Corresponding author: Guo-Xin Li, FRCS (Gen Surg), MD, PhD, Professor, Department of General Surgery, Nanfang Hospital, Southern Medical University, 1838 North Guangzhou Avenue, Guangzhou 510515, Guangdong Province, China. gzliguoxin@163.com

Telephone: +86-20-61411681

Fax: +86-20-62787626

Abstract

BACKGROUND

Gastrointestinal stromal tumors (GISTs) are the most common mesenchymal tumor type in the gastrointestinal system. Presently, various classification systems to prognosticate GISTs have been proposed.

AIM

To evaluate the application value of four different risk stratification systems for GISTs.

METHODS

Patients who were diagnosed with GISTs and underwent surgical resection at four hospitals from 1998 to 2015 were identified from a database. Risk of recurrence was stratified by the modified National Institute of Health (NIH) criteria, the Armed Forces Institute of Pathology (AFIP) criteria, the Memorial Sloan Kettering Cancer Center (MSKCC) prognostic nomogram, and the contour maps. Receiver operating characteristic (ROC) curves were established to compare the four abovementioned risk stratification systems based on the area

study enrolment.

Conflict-of-interest statement: All authors have no conflict of interest related to the manuscript.

Data sharing statement: The original anonymous dataset is available on request from the corresponding author at gzliguoxin@163.com.

STROBE statement: The authors have read the STROBE Statement-checklist of items, and the manuscript was prepared and revised according to the STROBE Statement-checklist of items.

Open-Access: This article is an open-access article which was selected by an in-house editor and fully peer-reviewed by external reviewers. It is distributed in accordance with the Creative Commons Attribution Non Commercial (CC BY-NC 4.0) license, which permits others to distribute, remix, adapt, build upon this work non-commercially, and license their derivative works on different terms, provided the original work is properly cited and the use is non-commercial. See: <http://creativecommons.org/licenses/by-nc/4.0/>

Manuscript source: Unsolicited manuscript

Received: November 12, 2018

Peer-review started: November 12, 2018

First decision: December 12, 2019

Revised: January 30, 2019

Accepted: February 15, 2019

Article in press: February 16, 2019

Published online: March 14, 2019

under the curve (AUC).

RESULTS

A total of 1303 patients were included in the study. The mean age of the patients was 55.77 ± 13.70 yr; 52.3% of the patients were male. The mean follow-up period was 64.91 ± 35.79 mo. Approximately 67.0% the tumors were located in the stomach, and 59.5% were smaller than 5 cm; 67.3% of the patients had a mitotic count $\leq 5/50$ high-power fields (HPFs). Thirty-four tumors ruptured before and during surgery. Univariate analysis demonstrated that tumor size > 5 cm ($P < 0.05$), mitotic count $> 5/50$ HPFs ($P < 0.05$), non-gastric location ($P < 0.05$), and tumor rupture ($P < 0.05$) were significantly associated with increased recurrence rates. According to the ROC curve, the AFIP criteria showed the largest AUC (0.754).

CONCLUSION

According to our data, the AFIP criteria were associated with a larger AUC than the NIH modified criteria, the MSKCC nomogram, and the contour maps, which might indicate that the AFIP criteria have better accuracy to support therapeutic decision-making for patients with GISTs.

Key words: Gastrointestinal stromal tumors; Risk stratification; Prognosis; Modified National Institute of Health criteria; Armed Forces Institute of Pathology criteria; Memorial Sloan Kettering Cancer Center prognostic nomogram; Contour maps; Gastrointestinal tumors

©The Author(s) 2019. Published by Baishideng Publishing Group Inc. All rights reserved.

Core tip: Our study evaluated the application value of four different risk stratification systems for gastrointestinal stromal tumors (GISTs). Patients who were diagnosed with GISTs and underwent surgical resection at four hospitals from 1998 to 2015 were identified from a database and were stratified by four different stratification systems. According to our data, the Armed Forces Institute of Pathology (AFIP) criteria were associated with a larger area under the curve than the National Institute of Health modified criteria, the Memorial Sloan Kettering Cancer Center nomogram, and the contour maps, which indicated that the AFIP criteria have better accuracy to support therapeutic decision-making for patients with GISTs.

Citation: Chen T, Ye LY, Feng XY, Qiu HB, Zhang P, Luo YX, Yuan LY, Chen XH, Hu YF, Liu H, Li Y, Tao KX, Yu J, Li GX. Performance of risk stratification systems for gastrointestinal stromal tumors: A multicenter study. *World J Gastroenterol* 2019; 25(10): 1238-1247

URL: <https://www.wjgnet.com/1007-9327/full/v25/i10/1238.htm>

DOI: <https://dx.doi.org/10.3748/wjg.v25.i10.1238>

INTRODUCTION

Gastrointestinal stromal tumors (GISTs) are the most common type of mesenchymal tumor in the gastrointestinal (GI) system. They can occur anywhere in the human GI tract, including the stomach (60%-70%), small intestine (20%-30%), duodenum (4%-5%), rectum (4%-5%), colon ($< 2\%$), and esophagus ($< 1\%$)^[1-2]. Their overall incidence has been estimated to be 10 to 20 per million, including incidental minimal tumors. What's more, only 18% of these tumors were considered benign, whereas 35% were considered to have some malignant potential and 47% were of undetermined potential. A 42% recurrence rate with a median time to recurrence of 22 months was found in surgically resected tumors^[3].

GISTs arise from interstitial cells of Cajal, are generally immunohistochemically positive for KIT (CD117), and contain KIT- or PDGFRA-activating mutations^[4-7]. Until 2000, the treatment of GISTs was limited in radical surgery, as GISTs are resistant to chemo- and radiotherapy. In 2000, imatinib was first used in GISTs as a tyrosine kinase inhibitor (TKI). This significantly improved median overall survival from < 1 yr to > 5 yr nowadays^[8]. Adjuvant therapy with imatinib benefits patients with a high

risk of recurrence, with studies suggesting most benefit with at least 3 yr of therapy. TKI treatment was also recommended by the National Comprehensive Cancer Network (NCCN) in 2015, for GIST patients with a moderate or high risk of recurrence. In other words, patients in the low-risk group may not benefit from TKI treatment. Otherwise, overtreatment may bring them adverse effects and financial burden. Another important thing is the frequency of reexamination. For patients with a low risk to recur, computed tomography examination is recommended to be taken every 6 mo, lasting 5 yr. However, for patients with a median or high risk to recur, examination should be taken every 3 mo in the first 3 yr. Therefore, the accuracy of risk stratification is very important in the treatment of GISTs.

Fletcher published a consensus approach to diagnose GISTs based on tumor size, tumor site, and mitosis number. It was approved by the National Institutes of Health (NIH) in 2002 and was the first guide in risk stratification for GISTs^[9]. Subsequently, the Armed Forces Institute of Pathology (AFIP) criteria were put forward by Miettinen and Lasota^[10] in 2006 according to the long-term follow-up results of 1684 patients. In 2008, the NIH system was modified to include both tumor location and rupture; these new criteria have been widely accepted around the world because they are easier to apply than the AFIP criteria^[11]. In 2009, a prognostic nomogram was developed by the Memorial Sloan Kettering Cancer Center (MSKCC) to predict the risk of recurrence^[12]. A novel risk stratification method was developed by Joensuu *et al.*^[13] in 2011, in which tumor size and mitosis count were treated as continuous non-linear variables. Although there are many grading methods available, clinicians are sometimes confused as to which one should be used to determine a patient's risk rating.

The present study aimed to compare the predictive accuracy of the modified HIN criteria, the AFIP criteria, the MSKCC nomogram, and the Joensuu's contour maps. To the best of our knowledge, this study constitutes the first comparison of these four risk criteria based on multicenter data. Our aim was to elucidate which risk stratification system provides the best support for therapeutic decision-making.

MATERIALS AND METHODS

Patients

We searched a database for patients who were diagnosed with GISTs by standard pathologic criteria at the Southern Medical University Nanfang Hospital, Sun Yat-sen University Cancer Center, Guangdong General Hospital, and Wuhan Union Hospital from January 1998 to December 2015. Patients who underwent complete resection with negative margins and no metastasis and did not undergo or did not completely undergo TKI therapy in a neoadjuvant or adjuvant setting were included in the study. Pregnant or breastfeeding women and patients with other serious diseases or with a history of malignancy were excluded. Patients with uncomplete data were also excluded.

Between January 1998 and December 2015, a total of 2661 patients who were diagnosed with GISTs and underwent complete gross resection at Southern Medical University Nanfang Hospital (692), Sun Yat-sen University Cancer Center (667), Guangdong General Hospital (548), and Wuhan Union Hospital (754) were identified. Of these, 122 patients whose tumors were not primary and 86 patients who had a history of malignant tumor were excluded from the analysis. Six patients had positive margins, and 86 patients showed evidence of metastatic disease at diagnosis. Four hundred and thirty-three patients without complete data and 368 patients lost to follow-up were also excluded. Two hundred and fifty-seven patients regularly underwent TKI therapy in a neoadjuvant or adjuvant setting. Thus, a total of 1303 patients were included in the present study (Figure 1).

Data collection and analysis

We collected the demographic and clinicopathologic data of the included patients accurately. Tumor size and mitotic index were measured by the pathologists. Mitotic index was defined as the number of mitoses per 50 randomly selected microscopic high-power fields (HPFs). Tumor rupture included those ruptures before and during the surgery. Continuous variables are presented as the mean (standard deviation) and median (minimum, maximum). Categorical variables are presented as the frequency (percentage). Patients were classified using the modified NIH consensus criteria, the AFIP criteria, the MSKCC nomogram, and the Joensuu's contour maps. The Wilcoxon-Mann-Whitney test and the Chi-squared/Fisher's exact test were used to analyze continuous variables and categorical variables, respectively. Univariate analysis was performed for exploring the relationship between the above

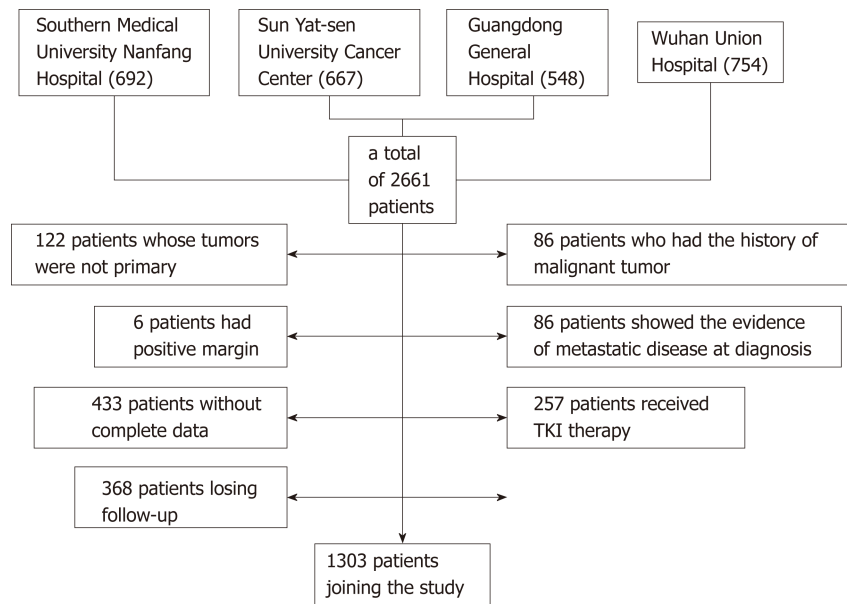


Figure 1 Flow diagram for extracting eligible cases for comparison. TKI: Tyrosine kinase inhibitor.

characteristics and tumor recurrence. A binary logistic regression model was used to calculate odds ratios (ORs).

Recurrence-free survival and overall survival

Recurrence-free survival (RFS) was defined as the time from diagnosis to recurrence of the tumor after complete resection. Patients who were alive without recurrence at the time of data collection and those who died without recurrence were censored. Overall survival was calculated from the date of surgery or diagnosis to the date of death. RFS and overall survival between groups were compared using the Kaplan-Meier life-table method and a non-stratified Cox proportional hazards model or log-rank test. Receiver operating characteristic (ROC) curves were used to compare the accuracy of the risk stratification criteria. Both 2- and 5-year RFS rates were reported in the MSKCC nomogram. The areas under the curve (AUCs) of all the risk stratification systems were calculated. Comparisons between ROC curves were performed. Two-tailed *P*-values were reported and were considered to be statistically significant when *P* < 0.05.

RESULTS

Table 1 shows the demographic and clinicopathologic data of the included population. The average age of the included patients was 55.77 ± 13.70 yr; 52.3% were male. The mean follow-up period was 64.91 ± 35.79 months. Approximately 67.0% of the tumors were located in the stomach, and 59.5% were smaller than 5 cm; 67.3% of patients had a mitotic count $\leq 5/50$ HPFs. There were 34 tumors that ruptured, including those ruptures before and during surgery. According to the modified NIH criteria, 347 (26.6%) patients were in the very-low-risk group, while 400 (30.7%) were in the high-risk group. Recurrent disease was found in 107 (8%) patients; 77.6% of these patients were classified in a moderate- or high-risk group by the modified NIH criteria, while 71.0% were designated such by the AFIP criteria. A total of 159 persons died during our research. According to the contour map criteria, age (*P* = 0.118), gender (*P* = 0.339), or follow-up period (*P* = 0.067) among the different risk groups showed no difference. Neither age (*P* = 0.333) nor gender (*P* = 0.067) showed a difference between the recurrence group and the non-recurrence group. Univariate analysis demonstrated that tumor size > 5 cm [OR 4.694, 95% confidence interval (CI) (3.003, 7.337), *P* < 0.05], mitotic count > 5/50 HPFs [OR 3.286, 95% CI (2.193, 4.923), *P* < 0.05], non-gastric location [OR 4.200, 95% CI (2.774, 6.359), *P* < 0.05], and tumor rupture [OR 57.327, 95% CI (24.220, 135.685), *P* < 0.05] were significantly associated with increased recurrence rates.

Figure 2 shows the overall survival and RFS for the entire cohort of patients. The mean overall survival was 188.28 (2.915) mo, while the RFS was 195.697 (2.234) mo. According to the AFIP criteria, the high-risk group showed the shortest RFS [122.212

Table 1 Demographic and clinicopathologic characteristics *n* (%)

	Overall (<i>n</i> = 1303)	Recurrence (107)	No recurrence (1196)	OR (95%CI)	<i>P</i> -value
Gender					
Male	681 (52.3)	65 (60.7)	616 (51.5)		
Female	622 (47.7)	42 (39.3)	580 (48.5)	0.686 (0.458, 1.028)	0.067
Age (yr)					
Mean (SD)	55.77 (13.696)	55.76 (0.390)	55.83 (1.538)	1.000 (0.986, 1.015)	0.276
Tumor location					
Gastric	873 (67.0)	38 (35.5)	835 (69.8)		
Non-gastric	430 (33.0)	69 (64.5)	361 (30.2)	4.200 (2.774, 6.359)	< 0.05
Follow-up period (mo)					
Mean (SD)	64.91 (35.793)	75.36 (4.608)	63.98 (0.995)	1.008 (1.003, 1.013)	< 0.05
Tumor size					
Mean (SD)	5.14 (4.862)	9.01 (0.663)	4.80 (0.130)	1.128 (1.092, 1.165)	< 0.05
≤ 5 cm	775 (59.5)	28 (26.2)	747 (62.5)		
> 5 cm	528 (40.5)	79 (73.8)	449 (37.5)	4.694 (3.003, 7.337)	< 0.05
Mitotic index					
≤ 5/50 HPFs	877 (67.3)	44 (41.1)	833 (69.6)		
> 5/50 HPFs	426 (32.7)	63 (58.9)	363 (30.4)	3.286 (2.193, 4.923)	< 0.05
Tumor rupture					
Yes	34 (2.6)	27 (25.2)	7 (0.6)	57.327 (24.220, 135.685)	
No	1269 (97.4)	80 (74.8)	1189 (99.4)		< 0.05
Modified NIH					
Very low risk	347 (26.6)	14 (13.10)	333 (27.80)	0.182 (0.101, 0.329)	< 0.05
Low risk	394 (30.2)	10 (9.30)	384 (32.10)	0.113 (0.057, 0.222)	< 0.05
Intermediate risk	162 (12.4)	8 (7.50)	154 (12.90)	0.225 (0.106, 0.478)	< 0.05
High risk	400 (30.7)	75 (70.10)	325 (27.20)		
AFIP criteria					
Very low risk	619 (47.5)	15 (14.00)	604 (50.50)	0.081 (0.045, 0.146)	< 0.05
Low risk	250 (19.2)	16 (15.00)	234 (19.60)	0.224 (0.125, 0.401)	< 0.05
Intermediate risk	173 (13.3)	15 (14.00)	158 (13.20)	0.311 (0.170, 0.568)	< 0.05
High risk	261 (20.0)	61 (57.00)	200 (16.70)		

OR: Odds ratio; CI: Confidence interval; SD: Standard deviation; HPF: High-power field; AFIP: Armed Forces Institute of Pathology; NIH: National Institutes of Health.

(4.364) mo, $P < 0.05$] and overall survival [158.542 (5.193) months, $P < 0.05$] (Figure 3).

We performed ROC analysis to compare the accuracy of the above GIST risk stratification systems (Figure 4). Both the 2- and 5-year predicated probabilities of RFS were calculated in the MSKCC nomogram. The AUCs of modified NIH, AFIP, MSKCC (2-year), MSKCC (5-year), and contour map criteria were 0.726, 0.754, 0.725, 0.737, and 0.739, respectively. Pairwise comparisons of the ROC curves are shown in Table 2.

DISCUSSION

Proper stratification is important to determine whether a patient should undergo TKI therapy or whether frequent review is necessary. Tumor size > 5 cm, mitotic count > 5/50 HPFs, non-gastric location, and tumor rupture were significantly associated with increased recurrence rates in our study. Jumniensuk *et al*^[14] found that metastasis happened in 27.7% of GIST patients, which mostly occurred within 2 yr. They also found that metastasis correlated with tumor size > 10 cm ($P = 0.023$) and mitotic count > 5/5 mm² ($P = 0.000$). In the study of Supsamutchai *et al*^[15], they demonstrated that there were significant differences between mitotic index or tumor size and the risk of recurrence or metastasis ($P = 0.036$). Our data demonstrated that tumor location was also an important factor affecting recurrence. According to common dogma, intestinal GISTs are associated with a worse prognosis compared with gastric GISTs^[16]. Emory *et*

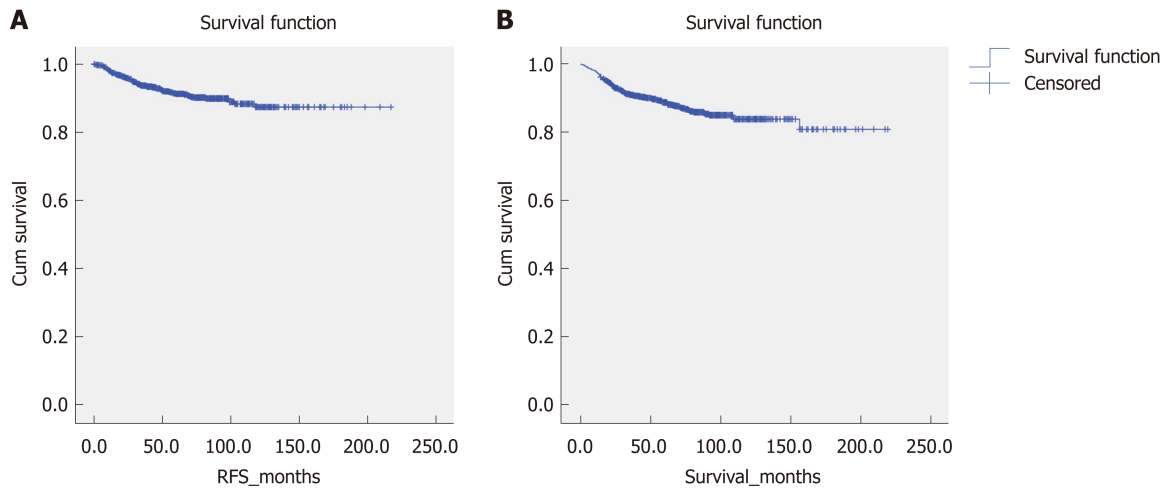


Figure 2 Recurrence-free survival and overall survival for the entire cohort of patients. A: Recurrence-free survival; B: Overall survival. RFS: Recurrence-free survival.

al^[17] showed that overall survival was best for those patients with tumors confined to the esophagus and worst for those whose tumors originating in the small bowel ($P = 0.00109$). Tumors located in the fundus or at the gastroesophageal junction were associated with recurrence ($P < 0.001$)^[18]. However, none of the currently available prognostic criteria take tumor site inside the stomach into account when calculating the risk of recurrence of GISTs. According to our study, tumor rupture is another factor that should be considered, which is consistent with the study of Rutkowski *et al*^[19]. Hohenberger *et al*^[20] showed that 15 patients with a GIST rupturing into the abdominal cavity recurred in 16 (94%) patients without adjuvant treatment. The AFIP criteria, which demonstrated the largest AUC in our study, cover all these prognostic factors.

Upon pairwise comparison of the ROC curves, the AUC of the AFIP criteria was greater than that of the modified NIH criteria ($P < 0.05$), although the other pairwise comparisons were not significantly different. This result is consistent with the recommendation made by the NCCN on GISTs in 2017, which also concluded that the AFIP criteria have advantages over the modified NIH criteria based on a number of studies. The study by Goh *et al* also illustrated that the AFIP risk criteria performed best among the three systems (NIH, modified NIH, and AFIP) for primary localized GISTs^[21]. However, in the study by Belfiori *et al*^[22], the MSKCC nomogram seemed to perform better than the NIH, modified NIH, and AFIP criteria in their sample and was suggested for use in clinical practice to predict the risk of recurrence. However, this study only covered 37 GISTs and observed 9 (24%) recurrences with a median follow-up period of 65 mo, which was shorter than the follow-up period in our study. The study by Chok *et al*^[23] reached the same conclusion. It is hard to explain the exact reasons why the AFIP criteria better predicted recurrence compared to the other risk classification systems in our included patients. However, the AFIP criteria are based on a population of 1684 patients, which is much larger than those corresponding to the other prognostic classification systems, and this difference may support the more objective nature of the AFIP criteria. In addition, the AFIP system draws a wider prognostic divergence between tumors located in the gastric region and the non-gastric region. For example, a tumor smaller than 2 cm with a mitotic count between 5 and 10 per 50 HPFs in a non-gastric location would be classified in the intermediate-risk group by the modified NIH criteria, whereas the AFIP criteria would classify such a tumor in the high-risk group. In contrast, for the nomogram criteria, the risk levels depend on whether the tumor location is colorectal or intestinal. Although intestinal GISTs show a worse prognosis than colorectal tumors, the low proportion of intestinal GISTs in our study limited this predictive impact. Moreover, the nomogram method tends to overestimate the probability of recurrence in low-risk tumors, as a result of the fact that its performance tends to be poorer in study cohorts with a high proportion of low-risk tumors as our data. With regard to the contour maps, these emphasize tumors outside of the GI tract and those which have ruptured. In clinical work, it is rare to encounter tumors outside of the GI tract and those that rupture. Moreover, the reported frequency of rupture in GISTs varies greatly, from 2% to 22%^[19,24]. In our multicenter data, the frequency of rupture was 2.6%. However, contour maps might benefit for the individual prognosis estimation because the

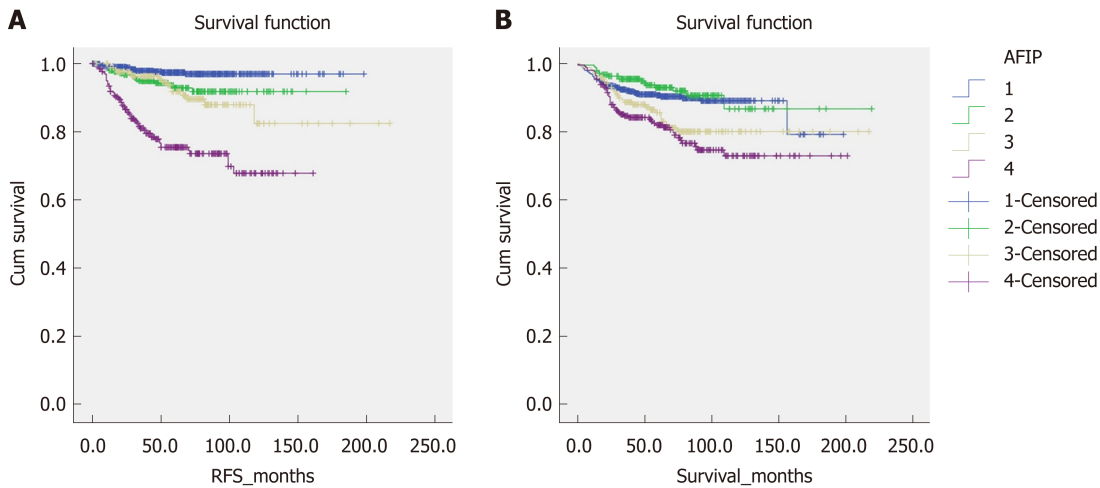


Figure 3 Recurrence-free survival and overall survival between different groups according to the Armed Forces Institute of Pathology criteria. A: Recurrence-free survival; B: Overall survival. RFS: Recurrence-free survival; AFIP: Armed Forces Institute of Pathology.

tumor size and mitotic count are integrated as continuous variables, especially when the tumor size or mitotic count is close to the cutoff values of modified NIH or AFIP criteria based on the categories. Nevertheless, further studies should focus on more rigorous analysis of the accuracy of the nomogram method and contour maps.

A number of other factors have recently been shown to be associated with the prognosis of stromal tumors, from the genetic level to the protein level^[25-29]. In 2016, Feng *et al* found that the parameters in peripheral blood cells such as high neutrophil-to-lymphocyte ratio and monocyte-to-lymphocyte ratio were associated with a poor prognosis among GISTs and thus may constitute a convenient, reproducible, and inexpensive approach to predict the prognosis of these tumors^[30]. These factors may have the opportunity to be added to the prognosis evaluation systems for stromal tumors in the future, which requires further studies.

There is no denying that there are still some deficiencies in our research. First, our study was a retrospective study, and prospective studies are needed to verify our conclusions. Second, the follow-up time was relatively short and a large number of people were lost to follow-up. All of these factors might result in bias during the analysis. We are establishing better follow-up systems and diagnostic methods, hoping to enlarge our sample size. We firmly believe that more accurate data can be obtained in the future.

In summary, our results demonstrate that the AFIP criteria performed better than the NIH modified criteria, the MSKCC nomogram, and the contour maps in Chinese patients and may therefore be preferred to use in clinical practice to predict the risk of recurrence for GISTs in the Chinese population.

Table 2 Pairwise comparisons of receiver operating characteristic curves

	Difference (95%CI)	P-value
AFIP-MAP	0.3485	0.7275
AFIP-MSKCC_2 yr	-0.2933	0.7693
AFIP-MSKCC_5 yr	0.5597	0.5757
AFIP-Modified NIH	4.2594	< 0.05
MAP-MSKCC_2 yr	-0.4296	0.6675
MAP-MSKCC_5 yr	0.3559	0.7219
MAP-Modified NIH	1.7202	0.0854
MSKCC_2 yr-MSKCC_5 yr	0.7895	0.4298
MSKCC_2 yr-Modified NIH	1.2829	0.1995
MSKCC_5 yr-Modified NIH	0.5711	0.5679

MSKCC_2 yr: The 2-yr predicted probability of recurrence-free survival; MSKCC_5 yr: The 5-yr predicted probability of recurrence-free survival; MAP: Contour maps. AFIP: Armed Forces Institute of Pathology; MSKCC: Memorial Sloan Kettering Cancer Center; NIH: National Institutes of Health; CI: Confidence interval.

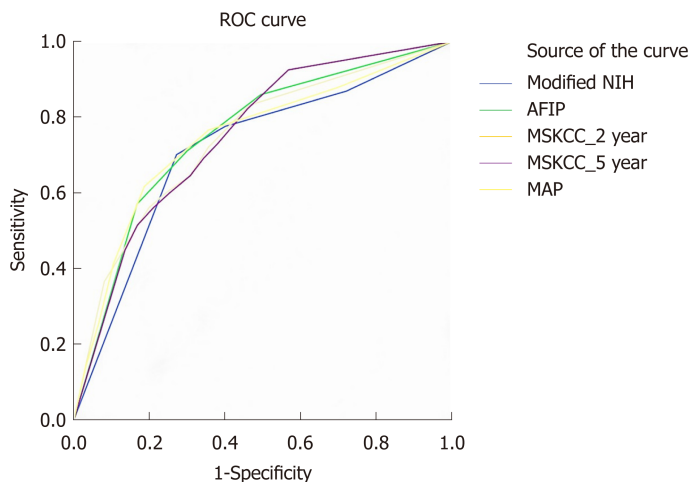


Figure 4 Receiver operating characteristic curve analysis of the risk of gastrointestinal stromal tumor recurrence. MAP: Contour maps; MSKCC_2 year: The 2-year predicted probability of recurrence-free survival; MSKCC_5 year: The 5-year predicted probability of recurrence-free survival; NIH: National Institute of Health; MSKCC: Memorial Sloan Kettering Cancer Center; AFIP: Armed Forces Institute of Pathology; ROC: Receiver operating characteristic.

ARTICLE HIGHLIGHTS

Research background

Gastrointestinal stromal tumors (GISTs) are the most common mesenchymal tumor type in the gastrointestinal (GI) system. Presently, various classification systems to prognosticate GISTs have been proposed.

Research motivation

It is unknown which classification system is more accurate when predicting the prognosis of patient with GISTs. This study will help doctors decide when considering the frequency of reexamination and whether to take a tyrosine kinase inhibitor.

Research objectives

The aim of this study was to evaluate the application value of four different risk stratification systems for GISTs.

Research methods

Patients who were diagnosed with GISTs and underwent surgical resection at four hospitals from 1998 to 2015 were identified from a database. Risk of recurrence was stratified by the modified National Institute of Health (NIH) criteria, the Armed Forces Institute of Pathology (AFIP) criteria, the Memorial Sloan Kettering Cancer Center (MSKCC) prognostic nomogram, and the contour maps. Receiver operating characteristic (ROC) curves were established to compare the four abovementioned risk stratification systems based on the area under the curve (AUC).

Research results

According to the ROC curve, the AFIP criteria showed the largest AUC (0.754).

Research conclusions

According to our data, the AFIP criteria were associated with a larger AUC than the NIH modified criteria, the MSKCC nomogram, and the contour maps, which might indicate that the AFIP criteria have better accuracy to support therapeutic decision-making for patients with GISTs.

Research perspectives

The study evaluated the application value of four different risk stratification systems for GISTs and found that the AFIP criteria have better accuracy in clinical application. Due to the imperfection of China's follow-up system and the particularity of its medical system, there may be some bias in this data. In the future, we will improve the follow-up mechanism to ensure the accuracy of data, and prospective studies may bring more accurate results.

REFERENCES

- 1 **Heinrich MC**, Corless CL, Blanke CD, Demetri GD, Joensuu H, Roberts PJ, Eisenberg BL, von Mehren M, Fletcher CD, Sandau K, McDougall K, Ou WB, Chen CJ, Fletcher JA. Molecular correlates of imatinib resistance in gastrointestinal stromal tumors. *J Clin Oncol* 2006; **24**: 4764-4774 [PMID: 16954519 DOI: 10.1200/JCO.2006.06.2265]
- 2 **Dematteo RP**, Gold JS, Saran L, Gönen M, Liao KH, Maki RG, Singer S, Besmer P, Brennan MF, Antonescu CR. Tumor mitotic rate, size, and location independently predict recurrence after resection of primary gastrointestinal stromal tumor (GIST). *Cancer* 2008; **112**: 608-615 [PMID: 18076015 DOI: 10.1002/cncr.23199]
- 3 **Machado-Aranda D**, Malamet M, Chang YJ, Jacobs MJ, Ferguson L, Silapaswan S, Goriel Y, Kolachalam R, Mittal VK. Prevalence and management of gastrointestinal stromal tumors. *Am Surg* 2009; **75**: 55-60 [PMID: 19213398]
- 4 **Heinrich MC**, Corless CL, Duensing A, McGreevey L, Chen CJ, Joseph N, Singer S, Griffith DJ, Haley A, Town A, Demetri GD, Fletcher CD, Fletcher JA. PDGFRA activating mutations in gastrointestinal stromal tumors. *Science* 2003; **299**: 708-710 [PMID: 12522257 DOI: 10.1126/science.1079666]
- 5 **Hirota S**, Isozaki K, Moriyama Y, Hashimoto K, Nishida T, Ishiguro S, Kawano K, Hanada M, Kurata A, Takeda M, Muhammad Tunio G, Matsuzawa Y, Kanakura Y, Shinomura Y, Kitamura Y. Gain-of-function mutations of c-kit in human gastrointestinal stromal tumors. *Science* 1998; **279**: 577-580 [PMID: 9438854 DOI: 10.1126/science.279.5350.577]
- 6 **Hirota S**, Nishida T, Isozaki K, Taniguchi M, Nakamura J, Okazaki T, Kitamura Y. Gain-of-function mutation at the extracellular domain of KIT in gastrointestinal stromal tumors. *J Pathol* 2001; **193**: 505-510 [PMID: 11276010 DOI: 10.1002/1096-9896(2000)9999:9999<::AID-PATH818>3.0.CO;2-E]
- 7 **Lux ML**, Rubin BP, Biase TL, Chen CJ, Maclure T, Demetri G, Xiao S, Singer S, Fletcher CD, Fletcher JA. KIT extracellular and kinase domain mutations in gastrointestinal stromal tumors. *Am J Pathol* 2000; **156**: 791-795 [PMID: 10702394 DOI: 10.1016/S0002-9440(10)64946-2]
- 8 **Langenberg SMCH**, Reyners AKL, Wymenga ANM, Sieling GCM, Veldhoven CMM, van Herpen CML, Prins JB, van der Graaf WTA. Caregivers of patients receiving long-term treatment with a tyrosine kinase inhibitor (TKI) for gastrointestinal stromal tumour (GIST): A cross-sectional assessment of their distress and burden. *Acta Oncol* 2018; **1-9** [PMID: 30280630 DOI: 10.1080/0284186X.2018.1518592]
- 9 **Fletcher CD**, Berman JJ, Corless C, Gorstein F, Lasota J, Longley BJ, Miettinen M, O'Leary TJ, Remotti H, Rubin BP, Shmookler B, Sobin LH, Weiss SW. Diagnosis of gastrointestinal stromal tumors: A consensus approach. *Hum Pathol* 2002; **33**: 459-465 [PMID: 12094370 DOI: 10.1053/hupa.2002.123545]
- 10 **Miettinen M**, Lasota J. Gastrointestinal stromal tumors: Pathology and prognosis at different sites. *Semin Diagn Pathol* 2006; **23**: 70-83 [PMID: 17193820 DOI: 10.1053/j.semdp.2006.09.001]
- 11 **Joensuu H**. Risk stratification of patients diagnosed with gastrointestinal stromal tumor. *Hum Pathol* 2008; **39**: 1411-1419 [PMID: 18774375 DOI: 10.1016/j.humpath.2008.06.025]
- 12 **Gold JS**, Gönen M, Gutiérrez A, Broto JM, García-del-Muro X, Smyrk TC, Maki RG, Singer S, Brennan MF, Antonescu CR, Donohue JH, DeMatteo RP. Development and validation of a prognostic nomogram for recurrence-free survival after complete surgical resection of localised primary gastrointestinal stromal tumour: A retrospective analysis. *Lancet Oncol* 2009; **10**: 1045-1052 [PMID: 19793678 DOI: 10.1016/S1470-2045(09)70242-6]
- 13 **Joensuu H**, Veltari A, Riihimäki J, Nishida T, Steigen SE, Brabec P, Plank L, Nilsson B, Cirilli C, Braconi C, Bordoni A, Magnusson MK, Linke Z, Sufliarsky J, Federico M, Jonasson JG, Dei Tos AP, Rutkowski P. Risk of recurrence of gastrointestinal stromal tumour after surgery: An analysis of pooled population-based cohorts. *Lancet Oncol* 2012; **13**: 265-274 [PMID: 22153892 DOI: 10.1016/S1470-2045(11)70299-6]
- 14 **Jumniensuk C**, Charoenpitakchai M. Gastrointestinal stromal tumor: Clinicopathological characteristics and pathologic prognostic analysis. *World J Surg Oncol* 2018; **16**: 231 [PMID: 30509310 DOI: 10.1186/s12957-018-1532-1]
- 15 **Supsamutchai C**, Wilasrusmee C, Hiranyathep P, Jirasiritham J, Rakchob T, Choikrua P. A cohort study of prognostic factors associated with recurrence or metastasis of gastrointestinal stromal tumor (GIST) of stomach. *Ann Med Surg (Lond)* 2018; **35**: 1-5 [PMID: 30258625 DOI: 10.1016/j.amsu.2018.08.010]
- 16 **Dematteo RP**, Ballman KV, Antonescu CR, Maki RG, Pisters PW, Demetri GD, Blackstein ME, Blanke CD, von Mehren M, Brennan MF, Patel S, McCarter MD, Polikoff JA, Tan BR, Owzar K; American College of Surgeons Oncology Group (ACOSOG) Intergroup Adjuvant GIST Study Team. Adjuvant imatinib mesylate after resection of localised, primary gastrointestinal stromal tumour: A randomised, double-blind, placebo-controlled trial. *Lancet* 2009; **373**: 1097-1104 [PMID: 19303137 DOI: 10.1016/S0140-6736(09)60500-6]
- 17 **Emory TS**, Sobin LH, Lukes L, Lee DH, O'Leary TJ. Prognosis of gastrointestinal smooth-muscle (stromal) tumors: Dependence on anatomic site. *Am J Surg Pathol* 1999; **23**: 82-87 [PMID: 9888707 DOI:

- 10.1097/00000478-199901000-00009]
- 18 **Miettinen M**, Sobin LH, Lasota J. Gastrointestinal stromal tumors of the stomach: A clinicopathologic, immunohistochemical, and molecular genetic study of 1765 cases with long-term follow-up. *Am J Surg Pathol* 2005; **29**: 52-68 [PMID: 15613856 DOI: 10.1097/01.pas.0000146010.92933.de]
 - 19 **Rutkowski P**, Nowecki ZI, Michej W, Debiec-Rychter M, Woźniak A, Limon J, Siedlecki J, Grzesiakowska U, Kakol M, Osuch C, Polkowski M, Głuszek S, Zurawski Z, Ruka W. Risk criteria and prognostic factors for predicting recurrences after resection of primary gastrointestinal stromal tumor. *Ann Surg Oncol* 2007; **14**: 2018-2027 [PMID: 17473953 DOI: 10.1245/s10434-007-9377-9]
 - 20 **Hohenberger P**, Ronellenfitsch U, Oladeji O, Pink D, Ströbel P, Wardelmann E, Reichardt P. Pattern of recurrence in patients with ruptured primary gastrointestinal stromal tumour. *Br J Surg* 2010; **97**: 1854-1859 [PMID: 20730857 DOI: 10.1002/bjs.7222]
 - 21 **Goh BK**, Chow PK, Yap WM, Kesavan SM, Song IC, Paul PG, Ooi BS, Chung YF, Wong WK. Which is the optimal risk stratification system for surgically treated localized primary GIST? Comparison of three contemporary prognostic criteria in 171 tumors and a proposal for a modified Armed Forces Institute of Pathology risk criteria. *Ann Surg Oncol* 2008; **15**: 2153-2163 [PMID: 18546045 DOI: 10.1245/s10434-008-9969-z]
 - 22 **Belfiori G**, Sartelli M, Cardinali L, Tranà C, Bracci R, Gesuita R, Marmorale C. Risk stratification systems for surgically treated localized primary Gastrointestinal Stromal Tumors (GIST). Review of literature and comparison of the three prognostic criteria: MSKCC Nomogram, NIH-Fletcher and AFIP-Miettinen. *Ann Ital Chir* 2015; **86**: 219-227 [PMID: 26098671]
 - 23 **Chok AY**, Goh BK, Koh YX, Lye WK, Allen JC, Quek R, Teo MC, Chow PK, Ong HS, Chung AY, Wong WK. Validation of the MSKCC Gastrointestinal Stromal Tumor Nomogram and Comparison with Other Prognostication Systems: Single-Institution Experience with 289 Patients. *Ann Surg Oncol* 2015; **22**: 3597-3605 [PMID: 25652053 DOI: 10.1245/s10434-015-4400-z]
 - 24 **Yanagimoto Y**, Takahashi T, Muguruma K, Toyokawa T, Kusanagi H, Omori T, Masuzawa T, Tanaka K, Hirota S, Nishida T. Re-appraisal of risk classifications for primary gastrointestinal stromal tumors (GISTs) after complete resection: Indications for adjuvant therapy. *Gastric Cancer* 2015; **18**: 426-433 [PMID: 24853473 DOI: 10.1007/s10120-014-0386-7]
 - 25 **Miyamoto H**, Kunisaki C, Otsuka Y, Takahashi M, Takagawa R, Misuta K, Kameda K, Makino H, Matsuda G, Yamaguchi N, Kamiya N, Murakami T, Morita S, Akiyama H, Endo I. Macroscopic type is a prognostic factor for recurrence-free survival after resection of gastric GIST. *Anticancer Res* 2014; **34**: 4267-4273 [PMID: 25075057 DOI: 10.1016/j.urolonc.2014.05.010]
 - 26 **Bednarski BK**, Araujo DM, Yi M, Torres KE, Lazar A, Trent JC, Cormier JN, Pisters PW, Lev DC, Pollock RE, Feig BW, Hunt KK. Analysis of prognostic factors impacting oncologic outcomes after neoadjuvant tyrosine kinase inhibitor therapy for gastrointestinal stromal tumors. *Ann Surg Oncol* 2014; **21**: 2499-2505 [PMID: 24639192 DOI: 10.1245/s10434-014-3632-7]
 - 27 **Martin-Broto J**, Gutierrez A, Garcia-del-Muro X, Lopez-Guerrero JA, Martinez-Trufero J, de Sande LM, Lainez N, Maurel J, De Juan A, Losa F, Andres R, Casado A, Tejido PG, Blanco R, Carles J, Bellmunt J, Gomez-España A, Ramos R, Martinez-Serra J, Llombart-Bosch A, Poveda A. Prognostic time dependence of deletions affecting codons 557 and/or 558 of KIT gene for relapse-free survival (RFS) in localized GIST: A Spanish Group for Sarcoma Research (GEIS) Study. *Ann Oncol* 2010; **21**: 1552-1557 [PMID: 20231303 DOI: 10.1093/annonc/mdq047]
 - 28 **Qi Y**, Zhao W, Wang Z, Li T, Meng X. Tumor sites and microscopic indicators are independent prognosis predictors of gastrointestinal stromal tumors. *Tohoku J Exp Med* 2014; **233**: 65-72 [PMID: 24827382 DOI: 10.1620/tjem.233.65]
 - 29 **Li CF**, Liu TT, Chuang IC, Chen YY, Fang FM, Chan TC, Li WS, Huang HY. PLCB4 copy gain and PLCB4 overexpression in primary gastrointestinal stromal tumors: Integrative characterization of a lipid-catabolizing enzyme associated with worse disease-free survival. *Oncotarget* 2017; **8**: 19997-20010 [PMID: 28212550 DOI: 10.18632/oncotarget.15306]
 - 30 **Feng F**, Tian Y, Liu S, Zheng G, Liu Z, Xu G, Guo M, Lian X, Fan D, Zhang H. Combination of PLR, MLR, MWR, and Tumor Size Could Significantly Increase the Prognostic Value for Gastrointestinal Stromal Tumors. *Medicine (Baltimore)* 2016; **95**: e3248 [PMID: 27057867 DOI: 10.1097/MD.0000000000003248]

P- Reviewer: Aurello P, Milone M, Tomažič A, Ueda H
S- Editor: Yan JP **L- Editor:** Wang TQ **E- Editor:** Yin SY



Retrospective Study

Utility of linked color imaging for endoscopic diagnosis of early gastric cancer

Toshihisa Fujiyoshi, Ryoji Miyahara, Kohei Funasaka, Kazuhiro Furukawa, Tsunaki Sawada, Keiko Maeda, Takeshi Yamamura, Takuya Ishikawa, Eizaburo Ohno, Masanao Nakamura, Hiroki Kawashima, Masato Nakaguro, Masahiro Nakatochi, Yoshiki Hirooka

ORCID number: Toshihisa Fujiyoshi (0000-0001-9147-871X); Ryoji Miyahara (0000-0001-7172-4602); Kohei Funasaka (0000-0002-3869-1420); Kazuhiro Furukawa (0000-0003-0980-9095); Tsunaki Sawada (0000-0002-4779-9708); Keiko Maeda (0000-0001-7615-0476); Takeshi Yamamura (0000-0003-4994-016X); Takuya Ishikawa (0000-0001-5814-3555); Eizaburo Ohno (0000-0002-7730-4630); Masanao Nakamura (0000-0002-5444-143X); Hiroki Kawashima (0000-0002-3720-781X); Masato Nakaguro (0000-0001-6987-3043); Masahiro Nakatochi (0000-0002-1838-4837); Yoshiki Hirooka (0000-0001-9639-7425).

Author contributions: Fujiyoshi T and Miyahara R designed and performed the research; Fujiyoshi T, Nakaguro M and Nakatochi M analyzed the data. Fujiyoshi T and Miyahara R wrote the paper. Miyahara R, Funasaka K, Furukawa K, Sawada T, Maeda K, Yamamura T, Ishikawa T, Ohno E, Nakamura M and Kawashima H provided the critical review of the manuscript. Hirooka Y provided administrative support and supervised the study.

Institutional review board statement: The study was reviewed and approved by the Ethics Committee of Nagoya University Hospital.

Informed consent statement: All

Toshihisa Fujiyoshi, Ryoji Miyahara, Kohei Funasaka, Kazuhiro Furukawa, Takuya Ishikawa, Eizaburo Ohno, Masanao Nakamura, Hiroki Kawashima, Department of Gastroenterology and Hepatology, Nagoya University Graduate School of Medicine, Nagoya 4668550, Japan

Tsunaki Sawada, Keiko Maeda, Takeshi Yamamura, Yoshiki Hirooka, Department of Endoscopy, Nagoya University Hospital, Nagoya 4668560, Japan

Masato Nakaguro, Department of Pathology and Laboratory Medicine, Nagoya University Hospital, Nagoya 4668560, Japan

Masahiro Nakatochi, Division of Data Science, Data Coordinating Center, Department of Advanced Medicine, Nagoya University Hospital, Nagoya 4668560, Japan

Corresponding author: Ryoji Miyahara, MD, PhD, Associate Professor, Chief Doctor, Department of Gastroenterology and Hepatology, Nagoya University Graduate School of Medicine, 65 Tsurumai-cho, Showa-ku, Nagoya 4668550, Japan. myhr@med.nagoya-u.ac.jp

Telephone: +81-52-7442172

Fax: +81-52-7442180

Abstract

BACKGROUND

Linked color imaging (LCI) is a method of endoscopic imaging that emphasizes slight differences in red mucosal color.

AIM

To evaluate LCI in diagnostic endoscopy of early gastric cancer and to compare LCI and pathological findings.

METHODS

Endoscopic images were obtained for 39 patients (43 lesions) with early gastric cancer. Three endoscopists evaluated lesion recognition with white light imaging (WLI) and LCI. Color values in Commission Internationale de l'Eclairage (CIE) 1976 L*a*b* color space were used to calculate the color difference (ΔE) between cancer lesions and non-cancer areas. After endoscopic submucosal dissection, blood vessel density in the surface layer of the gastric epithelium was evaluated pathologically. The identical region of interest was selected for analyses of endoscopic images (WLI and LCI) and pathological analyses.

RESULTS

study participants provided informed written consent prior to study enrollment.

Conflict-of-interest statement: All authors declare no conflicts-of-interest related to this article.

Data sharing statement: No additional data are available.

Open-Access: This article is an open-access article which was selected by an in-house editor and fully peer-reviewed by external reviewers. It is distributed in accordance with the Creative Commons Attribution Non Commercial (CC BY-NC 4.0) license, which permits others to distribute, remix, adapt, build upon this work non-commercially, and license their derivative works on different terms, provided the original work is properly cited and the use is non-commercial. See: <http://creativecommons.org/licenses/by-nc/4.0/>

Manuscript source: Unsolicited manuscript

Received: December 31, 2018

Peer-review started: January 2, 2019

First decision: January 18, 2019

Revised: February 14, 2019

Accepted: February 15, 2019

Article in press: February 16, 2019

Published online: March 14, 2019

LCI was superior for lesion recognition ($P < 0.0001$), and ΔE between cancer and non-cancer areas was significantly greater with LCI than WLI (29.4 *vs* 18.6, $P < 0.0001$). Blood vessel density was significantly higher in cancer lesions (5.96% *vs* 4.15%, $P = 0.0004$). An a^* cut-off of ≥ 24 in CIE 1976 $L^*a^*b^*$ color space identified a cancer lesion using LCI with sensitivity of 76.7%, specificity of 93.0%, and accuracy of 84.9%.

CONCLUSION

LCI is more effective for recognition of early gastric cancer compared to WLI as a result of improved visualization of changes in redness. Surface blood vessel density was significantly higher in cancer lesions, and this result is consistent with LCI image analysis.

Key words: Linked color imaging; Early gastric cancer; Endoscopic submucosal dissection; Vessel density; Color difference

©The Author(s) 2019. Published by Baishideng Publishing Group Inc. All rights reserved.

Core tip: This study showed the utility of linked color imaging (LCI) for screening endoscopy of early gastric cancer and the concordant change in blood vessel density with redness in LCI image. The key results of the study were as follows: LCI gave better contrast than white light imaging for the color difference between cancer lesions and surrounding non-cancer tissue; an a^* cutoff ≥ 24 for the value in Commission Internationale de l'Eclairage 1976 $L^*a^*b^*$ color space had good sensitivity and specificity for diagnosis of early gastric cancer; and surface blood vessel density in cancer lesions was significantly higher than that in non-cancer areas.

Citation: Fujiyoshi T, Miyahara R, Funasaka K, Furukawa K, Sawada T, Maeda K, Yamamura T, Ishikawa T, Ohno E, Nakamura M, Kawashima H, Nakaguro M, Nakatochi M, Hirooka Y. Utility of linked color imaging for endoscopic diagnosis of early gastric cancer. *World J Gastroenterol* 2019; 25(10): 1248-1258
URL: <https://www.wjgnet.com/1007-9327/full/v25/i10/1248.htm>
DOI: <https://dx.doi.org/10.3748/wjg.v25.i10.1248>

INTRODUCTION

The mortality of gastric cancer has been decreasing worldwide, but there are still more than 800000 deaths due to this disease. Gastric cancer is the third leading cause of death, followed by lung and colorectal cancer, in overall mortality worldwide^[1]. In Japan, the morbidity of gastric cancer ranks first in males and third after breast and colorectal cancer in females^[2]. Since advanced gastric cancer has a poorer prognosis, early detection and treatment is required to overcome the disease.

Endoscopy is an essential modality for detection of early gastric cancer. Recent advances and innovations in endoscopic devices have provided scopes with a high pixel count, a smaller diameter, and various optical technology. In particular, image-enhanced endoscopy (IEE) that uses imaging and analysis of wavelengths of visible light with illumination has a key role in detection of early gastrointestinal cancer. Among IEE methods, narrow-band imaging (NBI) and blue light imaging (BLI) are commonly used. NBI is effective for observation of capillaries on mucosal surfaces through emission of narrow band light^[3-5] and can be used for qualitative diagnosis (differentiation of cancer from non-cancer tissues, and the extent of cancer)^[6-8] in the oropharynx and hypopharynx^[9], esophagus^[10,11] and stomach. BLI allows observation of surface capillaries^[12], in magnified observation, there is little difference in the diagnostic performances of BLI and NBI^[13].

A new IEE method, referred to as linked color imaging (LCI), with an endoscopic light source was recently introduced by Fujifilm Corp. (Tokyo, Japan). LCI observation is interchangeable with white light imaging (WLI)/BLI with just one push of a button. LCI images are created by emission of white light and narrow-band short-wave light, and processing images to make a well-separated red area. The most important wavelengths for diagnosis of normal mucosa and atrophic mucosa are concentrated around the red color. LCI emphasizes slight differences in the "red"

color of the mucosa by image processing, including enhancement of differences in chroma and hue of the red mucosal color. As a result, red mucosa is visualized as redder and white mucosa as whiter. LCI has a color shade that is closer to WLI than NBI and BLI and processes images to separate the mucosal color more effectively; therefore, LCI is a suitable imaging method to identify early gastric cancer.

The utility of LCI for diagnosis of *Helicobacter pylori* gastritis has been well described^[14], but there are few studies of LCI for diagnosis of gastrointestinal cancer and, to our knowledge, parallel analyses of LCI, WLI, and pathology samples have not been reported. Therefore, the objectives of this study are to evaluate the utility of LCI for endoscopic diagnosis of early gastric cancer and to examine if pathological findings can explain the changes in red shade in LCI.

MATERIALS AND METHODS

Materials

The subjects were 39 patients (43 lesions) with early gastric cancer who underwent endoscopic submucosal dissection (ESD) of the stomach. WLI and LCI at the same time point were used for comparison of endoscopic images. All procedures were performed in the Department of Gastroenterology and Hepatology, Nagoya University Graduate School of Medicine from September 2016 to January 2018. This study was conducted after approval by the ethics committee of Nagoya University, and was performed in accord with the Helsinki Declaration. All subjects gave informed consent to participation after receiving a written explanation of the study.

Methods

Equipment and setting: An ELUXEO™ system (video processor VP-7000, light source BL-7000) and a Video Endoscope EG-760Z (Fujifilm) were used in the study. In WLI, the structure emphasis was set at H+1+3 (SE = Hi, DH = +1, DL = +3). In LCI, the structure emphasis was set at A6 and the color emphasis was set at C1. Endoscopic images were stored as uncompressed TIFF files. Images were 1280 × 1024 pixels and RGB 24-bit color.

Image assessment by endoscopists: WLI and LCI images were taken before endoscopic therapy and not magnified in the study. Lesions were imaged with WLI and LCI at the same timepoint, and the images were placed in a file in random order. These images were then evaluated by three endoscopists who routinely perform endoscopic therapy and are board-certified fellows of the Japan Gastroenterological Endoscopy Society. The evaluators were blinded to clinical data and pathological results. Each evaluator viewed one WLI and one LCI image simultaneously and assessed which image was superior for lesion recognition using a 5-point Likert scale: +2, very much; +1, somewhat; 0, undecided; -1, not really; -2, not at all. The same display was used for assessment. The evaluators assessed images alone without discussion with other evaluators.

Color assessment of endoscopic images: Two regions of interest (ROI, diameter 24 pixels) were picked from each lesion. One was from the cancer lesion and the other from surrounding non-cancer mucosa. Non-cancer mucosa was normal mucosa without ulceration or other specific changes. After ESD, the identical ROI was marked in the ESD resected sample and evaluated pathologically. ROI color in the endoscopic image was assessed using Commission Internationale de l'Eclairage (CIE) 1976 L*a*b* color space. This is a three-dimensional space for presenting a color with axes of L* (from black to white; white is highest), a* (from green to red; red is highest), and b* (from blue to yellow; yellow is highest). The difference between two colors (color difference) was approximated by the distance in the CIE 1976 L*a*b* color space^[15]. L*a*b* values of the ROI in cancer and non-cancer tissues were measured using Adobe Photoshop CS4 (Adobe Systems Inc., San Jose, CA, United States) to estimate the color difference (Figure 1).

Histopathological assessment: Resected gastric tissue was fixed in 10% neutral buffered formalin and embedded in paraffin. Routine hematoxylin and eosin staining (Figure 2A) and immunohistochemical staining were performed using 3- μ m sections. CD31 immunohistochemistry (Figure 2B) was used to highlight the blood vessel wall, using a commercial primary antibody (clone JC/70A, 1:1200; Dako, Glostrup, Denmark). The blood vessel area and its proportion of the total area were analyzed based on photomicrographs for each ROI at $\times 100$ magnification. An area of 350 μ m depth from the surface of the mucosa was trimmed on the photomicrograph (Figure 2C) and the blood vessel area was defined as the sum of the CD31-positive area and

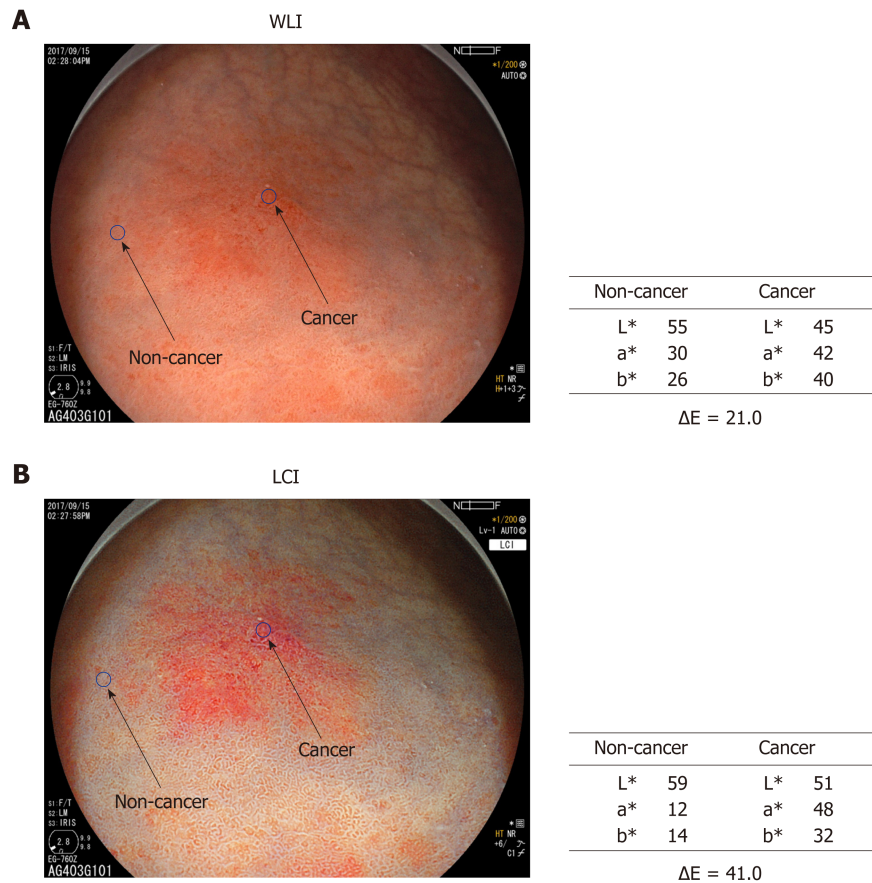


Figure 1 Color values and color differences between cancer and non-cancer areas. A region of interest (diameter: 24 pixels) was established in each lesion. Color values (L*, a*, b*) were measured using Adobe Photoshop CS4 to estimate color differences (ΔE) between cancer and non-cancer areas. The results are shown in **Table 2**. WLI: White light imaging; LCI: Linked color imaging.

the area encircled by CD31-positive endothelial cells (**Figure 2D** and **E**). Recognition and calculation of the positive area was performed automatically using image analysis software (WinRoof v.3.9.0, Mitani Co., Tokyo, Japan).

Statistical analysis: Statistical analysis were performed using SPSS v.22.0 for Windows (IBM Japan, Tokyo, Japan) and SAS 9.4 (SAS Institute, Inc.). Variables are expressed as medians (range). Differences in paired continuous variables were compared by Wilcoxon signed-rank test, and differences in independent continuous variables were compared by Wilcoxon rank sum test. ROC curves were created with values in CIE 1976 L*a*b* color space to differentiate between cancer and non-cancer lesions. Diagnostic performance was estimated based on the area under the curve (AUC), cut-off values, sensitivity and specificity. The significance level was set at a two-tailed P value < 0.05 .

RESULTS

The background and clinicopathological characteristics of the patients and lesions are shown in **Table 1**. Most lesions were differentiated tissue type (well or mod) and intramucosal carcinoma. All cases were completely resected with a free margin. Evaluation by three endoscopists indicated that LCI was superior to WLI for recognition of lesions of early gastric cancer ($P < 0.0001$). This finding being particularly strong for flat/depressed lesions compared to elevated lesions (**Figure 3**). The color difference (ΔE) between cancer and non-cancer areas was significantly higher in LCI than in WLI [29.4 (9.4-63.9) vs 18.6 (5.1-38.4), $P < 0.0001$] (**Table 2**) and thus LCI could differentiate a cancer lesion from a non-cancer area better than WLI. In LCI, using a cut-off from ROC curves of ≥ 24 for detection of a cancer lesion, the diagnostic performance had sensitivity of 76.7%, specificity of 93.0%, positive predictive value (PPV) of 91.7%, negative predictive value (NPV) of 80.0%, and accuracy of 84.9%. In pathological assessment, the blood vessel density in the surface

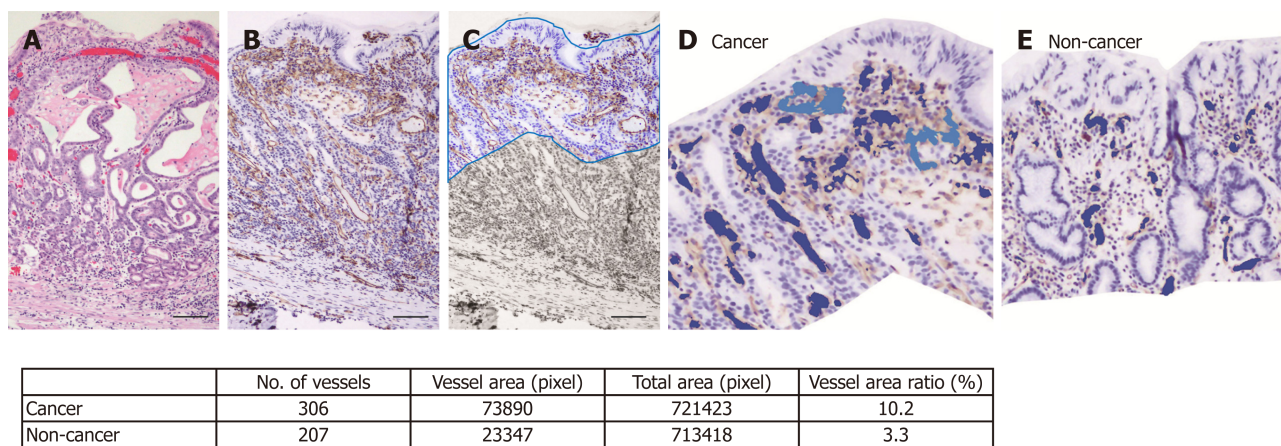


Figure 2 An example of blood vessel density calculation by imaging analysis software. A: Hematoxylin and eosin staining of a cancer lesion (case 43, original magnification $\times 100$, scale bar 100 μm). B: CD31 immunohistochemistry highlights blood vessels. C: A depth of 350 μm was trimmed manually. Automatically recognized blood vessels are colored in the cancer lesion (D) and non-cancer area (E). The calculated blood vessel area and ratio in this case are shown in the table.

layer was significantly higher in cancer lesions than in non-cancer areas [5.96% (2.17-17.08) *vs* 4.15% (1.71-8.22), $P = 0.0004$] (Figure 4). Surface blood vessel density exceeding 9% was only found in cancer lesions. The relationship between the value in CIE 1976 L*a*b* color space and blood vessel density in WLI and LCI is shown in Figure 5.

DISCUSSION

The results of this study show the utility of LCI for screening endoscopy of early gastric cancer and the concordant change in blood vessel density with redness in the LCI image. To our knowledge, this is the first study to compare objective color evaluation of early gastric cancer using the CIE 1976 L*a*b* color space in LCI with a pathological analysis of blood vessel density. This study showed that the large color difference in LCI may be due to the surface blood vessel density. The key results of the study were as follows: LCI recognized early gastric cancer lesions more effectively than WLI; LCI gave better contrast than WLI for the color difference between cancer lesions and the surrounding non-cancer area; an a^* cutoff ≥ 24 for the value in CIE 1976 L*a*b* color space had good sensitivity and specificity for diagnosis of early gastric cancer; and surface blood vessel density in cancer lesions was significantly higher than that in non-cancer areas.

Based on an assessment by three endoscopists, LCI recognized early gastric cancer lesions more easily than WLI. A previous study also indicated that LCI gave images that were easier to review than WLI for both experts and non-experts in $> 70\%$ of patients with early gastric cancer^[16]. Endoscopists attempt to find a lesion using the ruggedness of the mucosa and changes in color shade when observing inside the stomach, but this requires appropriate technology to show slight differences in color shade. Most lesions with slight differences in color shade can be detected by WLI using innovations such as adjusted air volume and progression in lesions. However, it is difficult to recognize a flat lesion without mucosal ruggedness or a slightly recessed lesion. To recognize such lesions, a change in color shade between a cancer lesion and a non-cancer area is important.

Subjective descriptions of color are commonly used in conventional endoscopic findings, and consequently, it is difficult to make an objective evaluation. In this study, CIE 1976 L*a*b* color space was used to assess the color objectively. The results showed that LCI gave better contrast than WLI for the color difference between cancer and non-cancer areas. These results are consistent with the assessment that LCI is a better imaging method than WLI for recognition of early gastric cancer, especially for flat and recessed lesions, which are likely to be assessed based on color difference, rather than on mucosal ruggedness.

The relationship of cancer and the microvascular architecture has been widely examined^[17-20], with reports of an irregular pattern and heterogeneity of the vasculature, and microvascular dilatation. In our study, we used non-magnified endoscopy to analyze the gross vascular effect, rather than the single vessel architecture. Since irregular running and vessel dilatation can increase the blood vessel

Table 1 Characteristics of the patients and tumors

Item	Number	Range or Percentage	
Cases/lesions	39/43		
Age (yr): median (range)	74	(57-88)	
Sex: male/female	27/12		
Tumor major axis (mm): median (range)	15	(6-40)	
Location (%)	U (Fundus)	5 (11.6)	
	M (Corpus)	7 (16.3)	
	L (Antrum and Pylorus)	30 (69.8)	
	Remnant Stomach	1 (2.3)	
Macroscopic type (%)	Elevated	Type 0-I	2 (4.6)
		Type 0-IIa	9 (20.9)
		Type 0-IIa+IIc	2 (4.7)
	Flat	Type 0-IIb	7 (16.3)
		Depressed	Type 0-IIc
Color of tumor in WLI	Red	20 (46.5)	
	White	2 (4.7)	
	Isochromatic	21 (48.8)	
Infection with <i>Helicobacter pylori</i>	Positive	14 (32.6)	
Depth of invasion (%)	M	36 (83.7)	
	SM1	4 (9.3)	
	SM2	3 (7.0)	
Histological type (%)	Differentiated (well or mod)	40 (93.0)	
	Undifferentiated (poor or sig)	3 (7.0)	

M: Mucosa; SM: Submucosa.

density, our results are closely related to previous studies using magnified endoscopy. The endoscopic color of early gastric cancer is widely distributed from strong reddening to fading. Some previous studies have mentioned the role of the number of capillaries in defining the color of the mucosa^[21-23]. An increase in number, as might be assumed, can increase the blood vessel density. Furukawa *et al*^[24] also mentioned the significance of the blood vessel density. Given the depth that endoscopic light can reach, we examined blood vessel density from the surface to a depth of 350 μm ^[25]. For as objective an evaluation as possible, the blood vessel density was assessed using pathological imaging analysis software (WinRoof v.3.9.0). This analysis showed that the blood vessel density was significantly higher in cancer lesions than in non-cancer areas, and exceeded 9% in all cancer lesions in the study. These results are consistent with findings showing that the blood vessel density in cancer lesions is higher than that in non-cancer areas in differentiated gastric cancer^[24].

Changes in redness between cancer and non-cancer areas in pathological images were assessed objectively by estimating a value in CIE 1976 L*a*b* color space. In LCI, ROC curves drawn using this value estimated an AUC of 0.86 at an a* cut-off value of 24. Values of ≥ 24 and < 24 indicated cancer and non-cancer areas, respectively, with a diagnostic sensitivity of 76.7%, specificity of 93.0%, PPV of 91.7%, NPV of 80.0%, and accuracy of 84.9%. We believe that our finding can lead to improved diagnosis of cancer lesions, based on objective evaluation using CIE 1976 L*a*b* color space. If these color values are evaluable in real time, artificial intelligence may permit automatic recognition and diagnosis of lesions.

This study has several limitations. First, it was a single-center and small-scale study. Second, the subjects were patients with early gastric cancer who underwent ESD, and consequently, most had differentiated intramucosal carcinoma. To include patients with undifferentiated cancer and early gastric cancer invading the submucosa, patients who underwent surgical resection would need to be added. Third, in this study, we focused only on cancer, and we did not evaluate inflammation or adenoma. Fourth, because recognition of WLI or LCI is obvious for expert endoscopist, bias is inevitable in the evaluation. To overcome this bias, we used objective color evaluation based on CIE 1976 L*a*b* color space.

In conclusion, LCI was useful for recognition of early gastric cancer lesions because this method provides good contrast in color differences between lesions and

Table 2 Color differences between cancer and non-cancer areas in white light imaging and linked color imaging

	WLI	LCI	P value
Color differences ΔE^1 [median (min-max)]	18.6 (5.1-38.4)	29.4 (9.4-63.9)	< 0.0001
Elevated	15.0 (5.8-34.4)	28.5 (11.0-40.2)	0.0327
Flat and depressed	20.6 (5.1-38.4)	30.9 (9.4-63.9)	< 0.0001

¹Wilcoxon signed-rank test. WLI: White light imaging; LCI: Linked color imaging.

surrounding tissue. Blood vessel density from the surface to a depth of 350 μm was higher in cancer lesions than in non-cancer areas, and LCI clearly shows this feature as a change in redness.

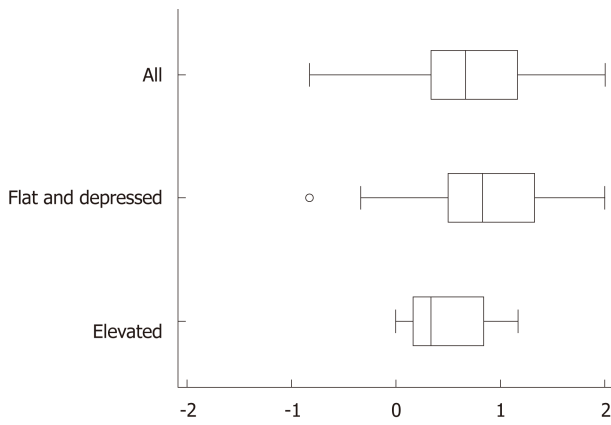


Figure 3 Recognition of early gastric cancer lesions using a Likert scale. Linked color imaging was superior to white light imaging for recognition of early gastric cancer lesions based on evaluations by three endoscopists ($P < 0.0001$). This effect was stronger for flat/depressed lesions than for protruding lesions.

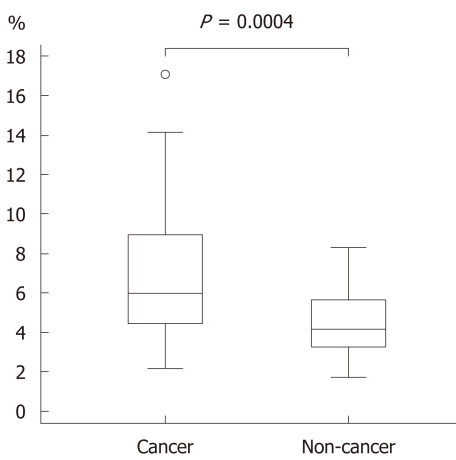


Figure 4 Blood vessel densities from the surface layer to a depth of 350 μm in cancer and non-cancer areas. The blood vessel density was significantly higher in cancer than in non-cancer areas [median (range): 5.96% (2.17-17.08) vs 4.15% (1.71-8.22), $P = 0.0004$].

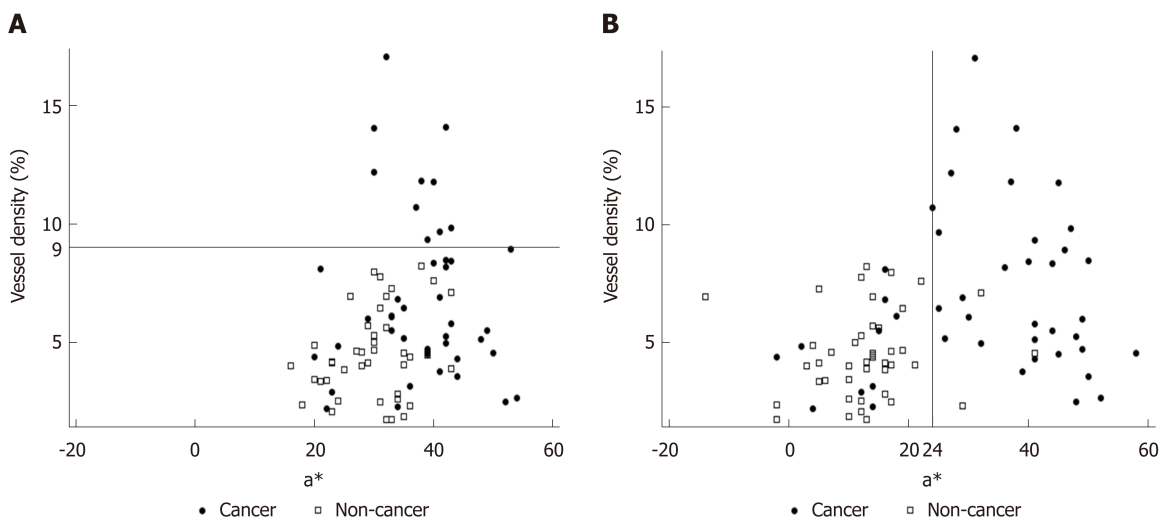


Figure 5 Relationship of a^* in Commission Internationale de l'Eclairage 1976 $L^*a^*b^*$ color space (X axis) with blood vessel density from the surface layer to 350 μm (Y axis) using (A) white light imaging (WLI) and (B) linked color imaging (LCI). Cancer and non-cancer areas were better differentiated with LCI compared to WLI. The blood vessel density was $\geq 9\%$ in all cancer lesions. Using a cut-off value of ≥ 24 for cancer lesions, the diagnostic performance with LCI had sensitivity of 76.7%, specificity of 93.0%, positive predictive value of 91.7%, negative predictive value of 80.0%, and accuracy of 84.9%. WLI: White light imaging; LCI: Linked color imaging.

ARTICLE HIGHLIGHTS

Research background

Linked color imaging (LCI) emphasizes slight differences in the “red” color of the mucosa by image processing, including enhancement of differences in chroma and hue of the red mucosal color.

Research motivation

The utility of LCI for diagnosis of *Helicobacter pylori* gastritis has been well described, but there are few studies of LCI for diagnosis of gastrointestinal cancer and, to our knowledge, parallel analyses of LCI, white light imaging (WLI), and pathology samples have not been reported.

Research objectives

The objectives of this study are to evaluate the utility of LCI for endoscopic diagnosis of early gastric cancer and to examine if pathological findings can explain the changes in red shade in LCI.

Research methods

Three endoscopists evaluated lesion recognition with WLI and LCI. Color values in Commission Internationale de l'Eclairage (CIE) 1976 L*a*b* color space were used to calculate the color difference (ΔE) between cancer lesions and non-cancer areas. After endoscopic submucosal dissection, blood vessel density in the surface layer of the gastric epithelium was evaluated pathologically. The identical region of interest was selected for analyses of endoscopic images (WLI and LCI) and pathological analyses.

Research results

LCI gave better contrast than WLI for the color difference between cancer lesions and surrounding non-cancer tissue; an a^* cutoff ≥ 24 for the value in CIE 1976 L*a*b* color space had good sensitivity and specificity for diagnosis of early gastric cancer; and surface blood vessel density in cancer lesions was significantly higher than that in non-cancer areas.

Research conclusions

LCI was useful for recognition of early gastric cancer lesions because this method provides good contrast in color differences between lesions and surrounding tissue. Blood vessel density from the surface to a depth of 350 μm was higher in cancer lesions than in non-cancer areas, and LCI clearly shows this feature as a change in redness.

Research perspectives

If these color values are evaluable in real time, artificial intelligence may permit automatic recognition and diagnosis of lesions.

REFERENCES

- 1 **Global Burden of Disease Cancer Collaboration**; Fitzmaurice C, Allen C, Barber RM, Barregard L, Bhutta ZA, Brenner H, Dicker DJ, Chimed-Orchir O, Dandona R, Dandona L, Fleming T, Forouzanfar MH, Hancock J, Hay RJ, Hunter-Merrill R, Huynh C, Hosgood HD, Johnson CO, Jonas JB, Khubchandani J, Kumar GA, Kutz M, Lan Q, Larson HJ, Liang X, Lim SS, Lopez AD, MacIntyre MF, Marczak L, Marquez N, Mokdad AH, Pinho C, Pourmalek F, Salomon JA, Sanabria JR, Sandar L, Sartorius B, Schwartz SM, Shackelford KA, Shibuya K, Stanaway J, Steiner C, Sun J, Takahashi K, Vollset SE, Vos T, Wagner JA, Wang H, Westerman R, Zeeb H, Zoeckler L, Abd-Allah F, Ahmed MB, Alabed S, Alam NK, Aldhahri SF, Alem G, Alemayohu MA, Ali R, Al-Raddadi R, Amare A, Amoako Y, Artaman A, Asayesh H, Atnafu N, Awasthi A, Saleem HB, Barac A, Bedi N, Bensenor I, Berhane A, Bernabé E, Betsu B, Binagwaho A, Boneya D, Campos-Nonato I, Castañeda-Orjuela C, Catalá-López F, Chiang P, Chibueze C, Chittheer A, Choi JY, Cowie B, Damtew S, das Neves J, Dey S, Dharmaratne S, Dhillon P, Ding E, Driscoll T, Ekwueme D, Endries AY, Farvid M, Farzadfar F, Fernandes J, Fischer F, G/Hiwot TT, Gebru A, Gopalani S, Hailu A, Horino M, Horita N, Hussein A, Huybrechts I, Inoue M, Islami F, Jakovljevic M, James S, Javanbakht M, Jee SH, Kasaieian A, Kadir MS, Khader YS, Khang YH, Kim D, Leigh J, Linn S, Lunevicius R, El Razek HMA, Malekzadeh R, Malta DC, Marcenes W, Markos D, Melaku YA, Meles KG, Mendoza W, Mengiste DT, Meretoja TJ, Miller TR, Mohammad KA, Mohammadi A, Mohammed S, Moradi-Lakeh M, Nagel G, Nand D, Le Nguyen Q, Nolte S, Ogbo FA, Oladimeji KE, Oren E, Pa M, Park EK, Pereira DM, Plass D, Qorbani M, Radfar A, Rafay A, Rahman M, Rana SM, Søreide K, Satpathy M, Sawhney M, Sepanlou SG, Shaikh MA, She J, Shiue I, Shore HR, Shrimo MG, So S, Soneji S, Stathopoulou V, Stroumpoulis K, Suffyan MB, Sykes BL, Tabarés-Seisdedos R, Tadese F, Tedla BA, Tessema GA, Thakur JS, Tran BX, Ukwaja KN, Uzochukwu BSC, Vlassov VV, Weiderpass E, Wubshet Terefe M, Yeboyo HG, Yimam HH, Yonemoto N, Younis MZ, Yu C, Zaidi Z, Zaki MES, Zenebe ZM, Murray CJL, Naghavi M. Global, Regional, and National Cancer Incidence, Mortality, Years of Life Lost, Years Lived With Disability, and Disability-Adjusted Life-years for 32 Cancer Groups, 1990 to 2015: A Systematic Analysis for the Global Burden of Disease Study. *JAMA Oncol* 2017; **3**: 524-548 [PMID: 27918777 DOI: 10.1001/jamaoncol.2016.5688]
- 2 **Hori M**, Matsuda T, Shibata A, Katanoda K, Sobue T, Nishimoto H; Japan Cancer Surveillance Research Group. Cancer incidence and incidence rates in Japan in 2009: a study of 32 population-based cancer registries for the Monitoring of Cancer Incidence in Japan (MCIJ) project. *Jpn J Clin Oncol* 2015; **45**: 884-891 [PMID: 26142437 DOI: 10.1093/jjco/hyv088]
- 3 **Yao K**, Yao T, Iwashita A. Determining the horizontal extent of early gastric carcinoma: two modern techniques based of differences in the mucosal microvascular architecture and density between

- carcinomatous and non-carcinomatous mucosa. *Dig Endosc* 2002; **14**: 83-87 [DOI: [10.1046/j.1443-1661.14.s1.16.x](https://doi.org/10.1046/j.1443-1661.14.s1.16.x)]
- 4 **Yao K**, Oishi T, Matsui T, Yao T, Iwashita A. Novel magnified endoscopic findings of microvascular architecture in intramucosal gastric cancer. *Gastrointest Endosc* 2002; **56**: 279-284 [PMID: [12145613](https://pubmed.ncbi.nlm.nih.gov/12145613/)]
 - 5 **Gono K**, Obi T, Yamaguchi M, Ohyama N, Machida H, Sano Y, Yoshida S, Hamamoto Y, Endo T. Appearance of enhanced tissue features in narrow-band endoscopic imaging. *J Biomed Opt* 2004; **9**: 568-577 [PMID: [15189095](https://pubmed.ncbi.nlm.nih.gov/15189095/) DOI: [10.1117/1.1695563](https://doi.org/10.1117/1.1695563)]
 - 6 **Yao K**, Anagnostopoulos GK, Ragunath K. Magnifying endoscopy for diagnosing and delineating early gastric cancer. *Endoscopy* 2009; **41**: 462-467 [PMID: [19418401](https://pubmed.ncbi.nlm.nih.gov/19418401/) DOI: [10.1055/s-0029-1214594](https://doi.org/10.1055/s-0029-1214594)]
 - 7 **Nagahama T**, Yao K, Maki S, Yasaka M, Takaki Y, Matsui T, Tanabe H, Iwashita A, Ota A. Usefulness of magnifying endoscopy with narrow-band imaging for determining the horizontal extent of early gastric cancer when there is an unclear margin by chromoendoscopy (with video). *Gastrointest Endosc* 2011; **74**: 1259-1267 [PMID: [22136775](https://pubmed.ncbi.nlm.nih.gov/22136775/) DOI: [10.1016/j.gie.2011.09.005](https://doi.org/10.1016/j.gie.2011.09.005)]
 - 8 **Yao K**, Nagahama T, Hirai F, Sou S, Matsui T, Tanabe H, Iwashita A, Ragunath K. *Clinical application of magnification endoscopy with NBI in the stomach and the duodenum*. Cohen J, editor. *Comprehensive atlas of high-resolution endoscopy*. Oxford: Blackwell Publishing 2007; 83-103 [DOI: [10.1002/9781118705940](https://doi.org/10.1002/9781118705940)]
 - 9 **Muto M**, Nakane M, Katada C, Sano Y, Ohtsu A, Esumi H, Ebihara S, Yoshida S. Squamous cell carcinoma in situ at oropharyngeal and hypopharyngeal mucosal sites. *Cancer* 2004; **101**: 1375-1381 [PMID: [15368325](https://pubmed.ncbi.nlm.nih.gov/15368325/) DOI: [10.1002/cncr.20482](https://doi.org/10.1002/cncr.20482)]
 - 10 **Muto M**, Minashi K, Yano T, Saito Y, Oda I, Nonaka S, Omori T, Sugiura H, Goda K, Kaise M, Inoue H, Ishikawa H, Ochiai A, Shimoda T, Watanabe H, Tajiri H, Saito D. Early detection of superficial squamous cell carcinoma in the head and neck region and esophagus by narrow band imaging: a multicenter randomized controlled trial. *J Clin Oncol* 2010; **28**: 1566-1572 [PMID: [20177025](https://pubmed.ncbi.nlm.nih.gov/20177025/) DOI: [10.1200/JCO.2009.25.4680](https://doi.org/10.1200/JCO.2009.25.4680)]
 - 11 **Goda K**, Tajiri H, Ikegami M, Urashima M, Nakayoshi T, Kaise M. Usefulness of magnifying endoscopy with narrow band imaging for the detection of specialized intestinal metaplasia in columnar-lined esophagus and Barrett's adenocarcinoma. *Gastrointest Endosc* 2007; **65**: 36-46 [PMID: [17185078](https://pubmed.ncbi.nlm.nih.gov/17185078/) DOI: [10.1016/j.gie.2006.03.938](https://doi.org/10.1016/j.gie.2006.03.938)]
 - 12 **Osawa H**, Yamamoto H. Present and future status of flexible spectral imaging color enhancement and blue laser imaging technology. *Dig Endosc* 2014; **26** Suppl 1: 105-115 [PMID: [24373002](https://pubmed.ncbi.nlm.nih.gov/24373002/) DOI: [10.1111/den.12205](https://doi.org/10.1111/den.12205)]
 - 13 **Yoshida N**, Hisabe T, Inada Y, Kugai M, Yagi N, Hirai F, Yao K, Matsui T, Iwashita A, Kato M, Yanagisawa A, Naito Y. The ability of a novel blue laser imaging system for the diagnosis of invasion depth of colorectal neoplasms. *J Gastroenterol* 2014; **49**: 73-80 [PMID: [23494646](https://pubmed.ncbi.nlm.nih.gov/23494646/) DOI: [10.1007/s00535-013-0772-7](https://doi.org/10.1007/s00535-013-0772-7)]
 - 14 **Dohi O**, Yagi N, Onozawa Y, Kimura-Tsuchiya R, Majima A, Kitaichi T, Horii Y, Suzuki K, Tomie A, Okayama T, Yoshida N, Kamada K, Katada K, Uchiyama K, Ishikawa T, Takagi T, Handa O, Konishi H, Naito Y, Itoh Y. Linked color imaging improves endoscopic diagnosis of active Helicobacter pylori infection. *Endosc Int Open* 2016; **4**: E800-E805 [PMID: [27556101](https://pubmed.ncbi.nlm.nih.gov/27556101/) DOI: [10.1055/s-0042-109049](https://doi.org/10.1055/s-0042-109049)]
 - 15 **Commission Internationale de l'Eclairage**. Colorimetry, 3rd Edition Publication CIE 15: 2004. Available from: <http://www.cie.co.at/publications/colorimetry-3rd-edition>
 - 16 **Yoshifuku Y**, Sanomura Y, Oka S, Kurihara M, Mizumoto T, Miwata T, Urabe Y, Hiyama T, Tanaka S, Chayama K. Evaluation of the visibility of early gastric cancer using linked color imaging and blue laser imaging. *BMC Gastroenterol* 2017; **17**: 150 [PMID: [29216843](https://pubmed.ncbi.nlm.nih.gov/29216843/) DOI: [10.1186/s12876-017-0707-5](https://doi.org/10.1186/s12876-017-0707-5)]
 - 17 **Kanesaka T**, Uedo N, Yao K, Ezoe Y, Doyama H, Oda I, Kaneko K, Kawahara Y, Yokoi C, Sugiura Y, Ishikawa H, Kato M, Takeuchi Y, Muto M, Saito Y. A significant feature of microvessels in magnifying narrow-band imaging for diagnosis of early gastric cancer. *Endosc Int Open* 2015; **3**: E590-E596 [PMID: [26716118](https://pubmed.ncbi.nlm.nih.gov/26716118/) DOI: [10.1055/s-0034-1392608](https://doi.org/10.1055/s-0034-1392608)]
 - 18 **Ohashi A**, Niwa Y, Ohmiya N, Miyahara R, Itoh A, Hirooka Y, Goto H. Quantitative analysis of the microvascular architecture observed on magnification endoscopy in cancerous and benign gastric lesions. *Endoscopy* 2005; **37**: 1215-1219 [PMID: [16329020](https://pubmed.ncbi.nlm.nih.gov/16329020/) DOI: [10.1055/s-2005-870339](https://doi.org/10.1055/s-2005-870339)]
 - 19 **Kaise M**, Kato M, Urashima M, Arai Y, Kaneyama H, Kanzazawa Y, Yonezawa J, Yoshida Y, Yoshimura N, Yamasaki T, Goda K, Imazu H, Arakawa H, Mochizuki K, Tajiri H. Magnifying endoscopy combined with narrow-band imaging for differential diagnosis of superficial depressed gastric lesions. *Endoscopy* 2009; **41**: 310-315 [PMID: [19340733](https://pubmed.ncbi.nlm.nih.gov/19340733/) DOI: [10.1055/s-0028-1119639](https://doi.org/10.1055/s-0028-1119639)]
 - 20 **Araki Y**, Sasaki Y, Hanabata N, Yoshimura T, Sawaya M, Hada R, Fukuda S. Morphometry for microvessels in early gastric cancer by narrow band imaging-equipped magnifying endoscopy. *Dig Endosc* 2011; **23**: 233-239 [PMID: [21699567](https://pubmed.ncbi.nlm.nih.gov/21699567/) DOI: [10.1111/j.1443-1661.2010.01093.x](https://doi.org/10.1111/j.1443-1661.2010.01093.x)]
 - 21 **Adachi Y**, Mori M, Enjoji M, Sugimachi K. Microvascular architecture of early gastric carcinoma. Microvascular-histopathologic correlates. *Cancer* 1993; **72**: 32-36 [PMID: [8508426](https://pubmed.ncbi.nlm.nih.gov/8508426/)]
 - 22 **Takemura S**, Iwashita A, Yao K, Yao T. The correlation between the quantified microvascular density and the endoscopic color in elevated type of gastric neoplastic lesions. *Gastroenterol Endosc* 2002; **44**: 745-754 [DOI: [10.11280/gee1973b.44.745](https://doi.org/10.11280/gee1973b.44.745)]
 - 23 **Honmyo U**, Misumi A, Murakami A, Mizumoto S, Yoshinaka I, Maeda M, Yamamoto S, Shimada S. Mechanisms producing color change in flat early gastric cancers. *Endoscopy* 1997; **29**: 366-371 [PMID: [9270917](https://pubmed.ncbi.nlm.nih.gov/9270917/) DOI: [10.1055/s-2007-1004217](https://doi.org/10.1055/s-2007-1004217)]
 - 24 **Furukawa K**, Yao K, Iwashita A, Matsui T, Yao T. Microvascular architecture of depressed type early gastric cancer -quantified vascular density using computer analysis with special reference to the color of endoscopic findings. *Gastroenterol Endosc* 1997; **39**: 1358-1369 [DOI: [10.11280/gee1973b.39.1358](https://doi.org/10.11280/gee1973b.39.1358)]
 - 25 **Yamaguchi H**, Saito T, Shiraiishi Y, Arai F, Morimoto Y, Yuasa A. Quantitative study on appearance of microvessels in spectral endoscopic imaging. *J Biomed Opt* 2015; **20**: 036005 [PMID: [25751029](https://pubmed.ncbi.nlm.nih.gov/25751029/) DOI: [10.1117/1.JBO.20.3.036005](https://doi.org/10.1117/1.JBO.20.3.036005)]

P- Reviewer: Kim YJ, Petrucciani N

S- Editor: Ma RY **L- Editor:** A **E- Editor:** Yin SY



Retrospective Study

Endoloop ligation after endoscopic mucosal resection using a transparent cap: A novel method to treat small rectal carcinoid tumors

Ding-Guo Zhang, Su Luo, Feng Xiong, Zheng-Lei Xu, Ying-Xue Li, Jun Yao, Li-Sheng Wang

ORCID number: Ding-Guo Zhang (0000-0001-7728-9672); Su Luo (0000-0001-7459-4743); Feng Xiong (0000-0002-4021-0817); Zheng-Lei Xu (0000-0002-3093-0626); Ying-Xue Li (0000-0001-6350-612X); Jun Yao (0000-0002-3472-1602); Li-Sheng Wang (0000-0002-7418-6114).

Author contributions: Luo S, Xu ZL, and Li YX contributed to study conception and design; Zhang DG and Xiong F contributed to data acquisition, analysis, and interpretation, and writing of the article; Yao J and Wang LS contributed to editing, reviewing, and final approval of the article.

Institutional review board

statement: This study was approved by the institutional review board of Shenzhen People's Hospital.

Informed consent statement:

Informed consent was obtained from each patient.

Conflict-of-interest statement: The authors declare no conflicts of interest.

Data sharing statement: No additional data are available.

Open-Access: This article is an open-access article which was selected by an in-house editor and fully peer-reviewed by external reviewers. It is distributed in accordance with the Creative Commons Attribution Non Commercial (CC BY-NC 4.0) license, which permits others to

Ding-Guo Zhang, Su Luo, Feng Xiong, Zheng-Lei Xu, Ying-Xue Li, Jun Yao, Li-Sheng Wang, Department of Gastroenterology, Shenzhen People's Hospital, First Affiliated Hospital of Southern University of Science and Technology, Second Clinical Medical College of Jinan University, Shenzhen 518020, Guangdong Province, China

Corresponding author: Jun Yao, MD, Associate Professor, Doctor, Department of Gastroenterology, Shenzhen People's Hospital, First Affiliated Hospital of Southern University of Science and Technology, Second Clinical Medical College of Jinan University, 1017 East Gate Road, Shenzhen 518020, Guangdong Province, China. yao.jun@szhospital.com

Telephone: +86-755-22943300

Fax: +86-755-25533497

Abstract**BACKGROUND**

Local endoscopic resection is an effective method for the treatment of small rectal carcinoid tumors, but remnant tumor at the margin after resection remains to be an issue.

AIM

To evaluate the efficacy and safety of resection of small rectal carcinoid tumors by endoloop ligation after cap-endoscopic mucosal resection (LC-EMR) using a transparent cap.

METHODS

Thirty-four patients with rectal carcinoid tumors of less than 10 mm in diameter were treated by LC-EMR ($n = 22$) or endoscopic submucosal dissection (ESD) ($n = 12$) between January 2016 and December 2017. Demographic data, complete resection rates, pathologically complete resection rates, operation duration, and postoperative complications were collected. All cases were followed for 6 to 30 mo.

RESULTS

A total of 22 LC-EMR cases and 12 ESD cases were enrolled. The average age was 48.18 ± 12.31 and 46.17 ± 12.57 years old, and the tumor size was 7.23 ± 1.63 mm and 7.50 ± 1.38 mm, respectively, for the LC-EMR and ESD groups. Resection time in the ESD group was longer than that in the LC-EMR group (15.67 ± 2.15 min vs 5.91 ± 0.87 min; $P < 0.001$). All lesions were completely resected at one time. No perforation or delayed bleeding was observed in either group.

distribute, remix, adapt, build upon this work non-commercially, and license their derivative works on different terms, provided the original work is properly cited and the use is non-commercial. See: <http://creativecommons.org/licenses/by-nc/4.0/>

Manuscript source: Unsolicited manuscript

Received: January 13, 2019

Peer-review started: January 14, 2019

First decision: January 23, 2019

Revised: January 29, 2019

Accepted: January 30, 2019

Article in press: January 30, 2019

Published online: March 14, 2019

Pathologically complete resection (P-CR) rate was 86.36% (19/22) and 91.67% (11/12) in the LC-EMR and ESD groups ($P = 0.646$), respectively. Two of the three cases with a positive margin in the LC-EMR group received transanal endoscopic microsurgery (TEM) and tumor cells were not identified in the postoperative specimens. The other case with a positive margin chose follow-up without further operation. One case with remnant tumor after ESD received further local ligation treatment. Neither local recurrence nor lymph node metastasis was found during the follow-up period.

CONCLUSION

LC-EMR appears to be an efficient and simple method for the treatment of small rectal carcinoid tumors, which can effectively avoid margin remnant tumors.

Key words: Rectal carcinoid; Endoscopic submucosal dissection; Endoscopic mucosal resection; Ligation

©The Author(s) 2019. Published by Baishideng Publishing Group Inc. All rights reserved.

Core tip: Rectal carcinoid is a common clinical submucosal tumor of the digestive tract. Small rectal carcinoids rarely have lymph node metastasis or distant metastasis, and local endoscopic resection is an effective method for the treatment of small rectal carcinoid tumors, but remnant tumor at the margin after resection remains to be an issue. Endoloop ligation after cap-endoscopic mucosal resection using a transparent cap appears to be an efficient and simple method for the treatment of small rectal carcinoid tumors, which can effectively avoid margin remnant tumors.

Citation: Zhang DG, Luo S, Xiong F, Xu ZL, Li YX, Yao J, Wang LS. Endoloop ligation after endoscopic mucosal resection using a transparent cap: A novel method to treat small rectal carcinoid tumors. *World J Gastroenterol* 2019; 25(10): 1259-1265

URL: <https://www.wjgnet.com/1007-9327/full/v25/i10/1259.htm>

DOI: <https://dx.doi.org/10.3748/wjg.v25.i10.1259>

INTRODUCTION

Rectal carcinoid tumor is one of the most common neuroendocrine tumors in the digestive tract. Most of them have no clinical symptoms and are unintentionally discovered by colonoscopy^[1]. The risk of lymph node metastasis and distant metastasis for rectal carcinoid with a diameter less than 10 mm is small. Thus, microscopic local excision is currently the commonly used method for the treatment of rectal carcinoid tumors^[2]. However, because most of these tumors are located in the submucosal layer of the rectal wall in the lower rectum^[3], traditional endoscopic resection methods do not ensure complete removal of the tumor, leading to a positive margin of resection, which often requires further surgical intervention. Recently, endoscopic submucosal dissection (ESD) is considered to be an effective method for the treatment of rectal carcinoid tumors, but its technical requirements and the associated complications are relatively high^[4]. Nylon endoloop ligation method has been proved to be an effective treatment for submucosal lesions of the upper digestive tract. For subepithelial tumors derived from the muscularis propria, the nylon endoloop used after resection can automatically fall off to achieve "let it go" effect^[5,6]. Few studies have evaluated the use of nylon ligation in the treatment of rectal carcinoma after endoscopic resection of rectal carcinoid tumor. Therefore, this study compared the efficacy of ESD and ligation after cap-endoscopic mucosal resection (LC-EMR) in the treatment of rectal carcinoid tumors by retrospective analysis. We also evaluated the advantages of LC-EMR in the treatment of rectal carcinoid tumors.

MATERIALS AND METHODS

We retrospectively analyzed the cases diagnosed as rectal carcinoid tumors and treated by LC-EMR or ESD in the gastroenterology unit of Shenzhen People's Hospital between January 2016 and December 2017. The studied cohort was selected

based on the following criteria: (1) rectal carcinoid tumors confirmed by histological diagnosis; (2) lesions ≤ 10 mm by EUS; (3) carcinoid syndrome without symptoms; and (4) no pararectal lymph node or distant metastasis as determined by pelvic and abdominal computed tomography (CT) before the procedure. The study protocol was approved by the ethics committee of the hospital and all patients gave their informed consent before the procedures. "Complete resection" refers to the absence of any visible residual tumor under endoscopy after tumor resection. A pathologically complete resection (P-CR) was defined as an *en bloc* resection with no lateral or deep margins of the tumor.

Endoscopic devices and procedures

LC-EMR procedure: A wide (14.9 mm-diameter), soft, straight, transparent cap with an inside rim (D-201-11802, Olympus) was fitted onto the tip of a standard single-channel endoscope (GIF-260, Olympus). A ligating device with a 20mm maximum detachable nylon loop (MAJ-339, Olympus) was inserted into the accessory channel of the endoscope. Other devices include Dual knife, injection needles, snares, and hot biopsy forceps from Olympus, as well as a high-frequency generator (ICC-200, ERBE).

There were four steps in LC-EMR. The first step was to loop the crescent-shaped snare around the rim of the transparent cap. The second step was aspiration and ligation of the lesion with a high-frequency electrocautery snare. The third step was the resection of the lesion *via* electrocautery. The fourth step was the aspiration of the lesion into the ligator device, followed by deployment of the endoloop (Figure 1A-F).

ESD procedure: ESD was performed using a single-channel endoscope with a short transparent cap that was attached to the tip of endoscope. First, the submucosal solution was injected and the circumferential mucosa of the lesion was incised using a dual knife. Then, according to the method reported in the literature^[5], circumferential incision, submucosal dissection, and treatment of wounds were performed. All procedures were conducted by two skilled endoscopists (Zhang DG and Wang LS). Pathological examination included identification of histopathologic type, invasion depth, lateral and vertical resection margins, lymphovascular involvement, as well as immunohistochemical testing, and grades were determined by mitotic count and Ki-67 labeling index. All patients were routinely fasted for 1 d after surgery and discharged if there were no any significant complications.

Statistical analysis

All statistical analyses were performed using SPSS 16.0 statistical software (SPSS Inc, United States). Continuous variables are represented as the mean \pm standard deviation (SD) and categorical data are showed as number (*n*) and percentage (%).

RESULTS

A total of 34 patients including 24 males and 10 females with an average of 19-79 (47.47 ± 12.25) years participated in the study. The LC-EMR group had 22 cases and the ESD group had 12 cases. The mean ages of the ESD and LC-EMR groups were 48.18 ± 12.31 and 46.17 ± 12.57 , respectively. Tumor size of the ESD and LC-EMR groups was 7.23 ± 1.63 mm and 7.50 ± 1.38 mm, respectively. The resection time (including resection and closure time) of the ESD group was longer than that of the LC-EMR group (15.67 ± 2.15 min *vs* 5.91 ± 0.87 min, $P < 0.001$). All lesions had one-time complete resection. No perforation or delayed bleeding was observed in either group. P-CR was 86.36% (19/22) and 91.67% (11/12) in the LC-EMR group and ESD group ($P = 0.646$), respectively. Pathology diagnosis was confirmed as G1. Two of the three cases with a positive margin in the LC-EMR group received transanal rectal tumor resection and tumor cells were not identified in the postoperative specimens (Figure 1G-L). The other case with a positive margin chose follow-up without further operation. One case with remnant tumor after ESD received further local ligation treatment. Generally, colonoscopy was performed and postoperative scar and recurrence were observed 6 months after resection, and then at an interval of 1 to 2 years. For the two patients with remnant tumor after LC-EMR or ESD who did not choose further surgery, colonoscopy was performed and postoperative scar and recurrence were observed 3 mo after resection, and then repeat colonoscopy and abdominal CT scan were performed at an interval of 1 year. Neither local recurrence nor lymph node metastasis was found during the follow-up period (Tables 1-3).

DISCUSSION

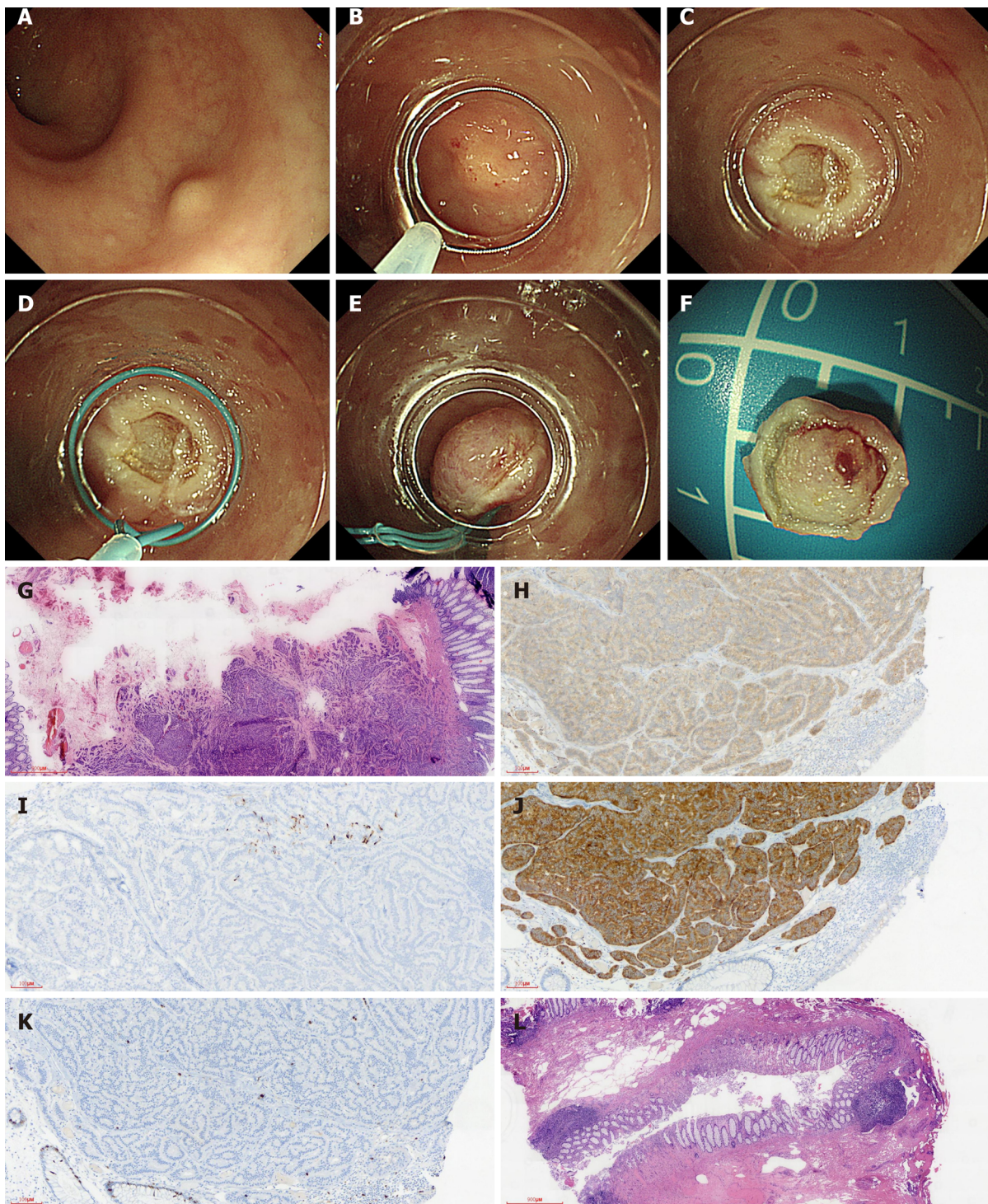


Figure 1 Utilizing endoloop ligation after cap-endoscopic mucosal resection using a transparent cap to remove rectal carcinoid tumor. Pathology suggested positive margins and further transanal endoscopic microsurgery pathology was negative. A: Endoscopy showing a rectal carcinoid about 10 mm in diameter; B: An electric snare mounted on the transparent cap on the inner lens end; C: Wound after resection; D: Nylon endoloop device installed on the inner lens end; E: Wound after nylon endoloop ligation resection; F: Endoscopic resection of the intact tumor; G: Pathological specimen suggesting a carcinoid, vertical margin positive ($\times 10$); H: Positive immunohistochemical staining for CD56 ($\times 100$); I: Positive immunohistochemical staining for chromogrin ($\times 100$); J: Positive immunohistochemical staining for Syn ($\times 100$); K: Immunohistochemical staining for Ki-67 ($< 2\%$; $\times 100$); L: Transanal endoscopic microsurgery surgery did not identify tumor cells ($\times 10$).

Rectal carcinoid tumors were restricted to the submucosa and had a lower risk of metastasis when the tumor was less than 10 mm in diameter without lymphoid or vascular infiltration^[2,4]. Local or endoscopic excision is considered curative for these tumors^[7]. However, it is difficult to completely resect carcinoid tumors of the rectum by conventional EMR, because about 75% of the tumors have extended into the submucosa^[8]. Compared with EMR, ESD is considered a better method for the treatment of rectal carcinoid tumors, but it requires higher technical means and is

Table 1 General information of patients in the two groups

	LC-EMR (n = 22)	ESD (n = 12)	P-value
Age (yr)	48.18 ± 12.31	46.17 ± 12.57	0.907
Sex (M/F)	17/5	7/5	0.016
Tumor size (mm)	7.23 ± 1.63	7.50 ± 1.38	0.531
Distance from anal verge (cm)	6.27 ± 0.98	6.75 ± 1.48	0.281

LC-EMR: Ligation after cap-endoscopic submucosal resection; ESD: Endoscopic submucosal dissection.

relatively time consuming and has more complications^[7]. Other improved EMR methods, such as endoscopic double snare polypectomy (EDSP)^[9], EMR with a ligation device (ESMR-L)^[10], EMR with double ligation (ESMR-DL)^[11], or EMR after circumferential pre-cutting (EMR-P)^[12], can remove deeper layers of the tumor without significant complications for small rectal carcinoids. However, the edge remnant is always the problem that needs to be solved for local endoscopic resection. Recent studies have shown that the treatment method is the only independent factor affecting the P-CR rate of rectal carcinoid tumors. Wang *et al.*^[13] compared the therapeutic effects of EMR-C (30 cases) and ESD (25 cases) for rectal carcinoids < 16 mm in diameter, and the results showed that nine cases in the EMR-C group had positive basal margins. During the 18 mo of follow-up, five cases in the EMR-C group had local recurrence, while no recurrence was found in the ESD group. Chen *et al.*^[14] conducted a retrospective study of 66 patients with rectal carcinoids less than 15 mm in diameter, and the results showed that P-CR was 96.43% and 93.94% for ESD and circumferential incision before EMR (CI-EMR) groups, respectively. For smaller rectal carcinoid tumors, if residual lesions appear after endoscopic resection, more of them were vertical resection margin positive. Theoretically, ligation after endoscopic resection can reduce the incidence of residual tumor, so this study selected LC-EMR and ESD for comparison and further evaluated the effect of LC-EMR in the treatment of small rectal carcinoid.

Our study showed that although there were three positive margins in the LC-EMR group and two of them underwent further surgical local resection, no tumor invasion was found in the surgical specimens. We speculated that this is because local endoloop ligation after EMR-C led to ischemic necrosis, which further achieved the effect of clearing local lesions, similar to the effect of “let it go” in the treatment of SET by endoloop as reported in the previous literature^[6]. This might also be the reason that the other LC-EMR patient who chose follow-up did not have recurrence. Compared to ESD, LC-EMR is easier and less time consuming. Furthermore, endoloop ligation after EMR-C helps prevent wound bleeding and seal wounds.

Compared with band ligation, endoloop ligation can achieve more robust ligation even if there is local scarring^[15]. Another ESD patient with a positive margin refused further surgery. In spite of wound fibrosis, we chose to perform local endoloop ligation 1 wk after resection. In the follow-up period, no tumor recurrence or metastasis was found, and no tumor cells were found in the local biopsy at 3 mo after resection.

The study had some limitations. First, this study is a single-center retrospective study with limited sample size. In addition, considering that rectal carcinoid is a slow-growing tumor, long-term follow-up is necessary to determine the efficacy of LC-EMR. However, LC-EMR appears to be an efficient and simple method for the treatment for small rectal carcinoid tumors less than 10 mm, which can effectively prevent remnant tumors at the resection margin, especially in case of absence of ESD availability.

Table 2 Summary of the therapeutic efficacy in the two groups *n* (%)

	LC-EMR (<i>n</i> = 22)	ESD (<i>n</i> = 12)	<i>P</i> -value
Endoscopic complete resection	22 (100)	12 (100)	1.000
Pathologically complete resection	19 (86.36)	11 (91.67)	0.646
Histological margin involvement			
Lateral	0 (0)	0 (0)	1.000
Vertical	3 (13.64)	1 (8.33)	0.646
Resection time (min, ± SD)	5.91 ± 0.87	15.67 ± 2.15	0.001
Recurrence follow-up	0 (0)	0 (0)	1.000

LC-EMR: Ligation after cap-endoscopic mucosal resection; ESD: Endoscopic submucosal dissection.

Table 3 Further treatment of patients with a positive resection margin in the two groups

	LC-EMR (<i>n</i> = 3)	ESD (<i>n</i> = 1)
TEM (<i>n</i>)	2	0
Religation (<i>n</i>)	0	1
Histological after surgery or endoscopy	Negative	Negative
Recurrence follow-up (<i>n</i>)	0	0

LC-EMR: Ligation after cap-endoscopic mucosal resection; ESD: Endoscopic submucosal dissection; TEM: Transanal endoscopic microsurgery.

ARTICLE HIGHLIGHTS

Research background

Rectal carcinoid tumor is a clinically common submucosal tumor of the digestive tract. Lymph node metastasis risk of rectal carcinoid tumors less than 1 cm is low. Endoscopic local resection is currently the main treatment method, of which endoscopic submucosal dissection (ESD) is the first choice. Endoscopic mucosal resection (EMR) is also a commonly used treatment method for digestive tract mucosal lesions, with low technical requirements and relatively easy to grasp. Previous studies have shown that EMR also has a good effect on rectal carcinoids, but there is a residual risk of basal tumors, even with improved EMR (such as EMR-cap, EMR-P, C-EMR and so on). Therefore, it is of certain clinical value to explore a simple and effective method to treat small rectal carcinoids on the basis of EMR.

Research motivation

This study aimed to explore a simple and effective endoscopic resection method for the treatment of small rectal carcinoids, especially when ESD is not available.

Research objectives

The clinical application of ligation assisted endoscopic resection is extensive, especially for gastrointestinal submucosal tumors, and even the tumors less than 2 cm derived from the muscularis propria also can achieve satisfactory results. For some submucosal tumors that may have residual tumor in the basal part after endoscopic resection, the ligation method after endoscopic resection can lead to the final ischemic necrosis of the residual tumor and achieve the purpose of complete resection. The purpose of this study was to explore the efficacy of transparent cap assisted endoscopic mucosal resection combined with postoperative endoloop ligation in the treatment of rectal carcinoids.

Research methods

This study retrospectively analyzed the cases diagnosed as rectal carcinoid tumors and treated by ligation after cap (LC)-EMR or ESD in the gastroenterology unit of Shenzhen People's Hospital between January 2016 and December 2017. Patients' demographic data, the complete resection rates, operation duration, and postoperative complications were collected.

Research results

A total of 34 patients including 24 males and 10 females with an average of 19-79 (47.47 ± 12.25) years participated in the study. The mean ages, tumor size, resection time, and pathologically complete resection (P-CR) rates of the ESD (*n* = 12) and LC-EMR (*n* = 22) groups were 48.18 ± 12.31 years *vs* 46.17 ± 12.57 years, 7.23 ± 1.63 mm *vs* 7.50 ± 1.38 mm, 15.67 ± 2.15 min *vs* 5.91 ± 0.87 min, and 91.67% (11/12) *vs* 86.36% (19/22), respectively. No perforation or delayed bleeding was observed in either group. Pathology diagnosis was confirmed as G1. Two of the three cases with a positive margin in the LC-EMR group received transanal rectal tumor resection and tumor cells

were not identified in the postoperative specimens. The other case with a positive margin chose follow-up without further operation. One case with remnant tumor after ESD received further local ligation treatment. Neither local recurrence nor lymph node metastasis was found during the follow-up period. Both LC-EMR and ESD were effective methods to treat small rectal carcinoid tumors.

Research conclusions

LC-EMR appears to be an efficient and simple method for the treatment for small rectal carcinoid tumors less than 10 mm, especially when ESD is not available. LC-EMR can effectively prevent remnant tumors at the resection margin. Considering rectal carcinoid is a slow-growing tumor, long-term follow-up is necessary to determine the long-term efficacy of LC-EMR.

Research perspectives

To avoid local tumor residue after endoscopic resection, it is necessary to perform postoperative prophylactic endoloop ligation, even after ESD.

REFERENCES

- 1 **Koura AN**, Giacco GG, Curley SA, Skibber JM, Feig BW, Ellis LM. Carcinoid tumors of the rectum: effect of size, histopathology, and surgical treatment on metastasis free survival. *Cancer* 1997; **79**: 1294-1298 [PMID: 9083149 DOI: 10.1002/(SICI)1097-0142(19970401)79:7<1294::AID-CNCR4>3.0.CO;2-H]
- 2 **Shields CJ**, Tirt E, Winter DC; International Rectal Carcinoid Study Group. Carcinoid tumors of the rectum: a multi-institutional international collaboration. *Ann Surg* 2010; **252**: 750-755 [PMID: 21037430 DOI: 10.1097/SLA.0b013e3181fb8df6]
- 3 **Yoshikane H**, Goto H, Niwa Y, Matsui M, Ohashi S, Suzuki T, Hamajima E, Hayakawa T. Endoscopic resection of small duodenal carcinoid tumors with strip biopsy technique. *Gastrointest Endosc* 1998; **47**: 466-470 [PMID: 9647370 DOI: 10.1016/S0016-5107(98)70246-9]
- 4 **Lee DS**, Jeon SW, Park SY, Jung MK, Cho CM, Tak WY, Kweon YO, Kim SK. The feasibility of endoscopic submucosal dissection for rectal carcinoid tumors: comparison with endoscopic mucosal resection. *Endoscopy* 2010; **42**: 647-651 [PMID: 20669076 DOI: 10.1055/s-0030-1255591]
- 5 **Zhang D**, Lin Q, Shi R, Wang L, Yao J, Tian Y. Ligation-assisted endoscopic submucosal resection with apical mucosal incision to treat gastric subepithelial tumors originating from the muscularis propria. *Endoscopy* 2018; **50**: 1180-1185 [PMID: 29913532 DOI: 10.1055/a-0625-6326]
- 6 **Yague AS**, Shah JN, Nguyentang T, Soetikno R, Binmoeller KF. Simplified treatment of gastric GISTs by endolooping without resection: "loop-and-let-go". *Gastrointest Endosc* 2009; **69**: AB174-AB175 [DOI: 10.1016/j.gie.2009.03.337]
- 7 **Zhou PH**, Yao LQ, Qin XY, Xu MD, Zhong YS, Chen WF, Ma LL, Zhang YQ, Qin WZ, Cai MY, Ji Y. Advantages of endoscopic submucosal dissection with needle-knife over endoscopic mucosal resection for small rectal carcinoid tumors: a retrospective study. *Surg Endosc* 2010; **24**: 2607-2612 [PMID: 20361212 DOI: 10.1007/s00464-010-1016-z]
- 8 **Matsumoto T**, Iida M, Suekane H, Tominaga M, Yao T, Fujishima M. Endoscopic ultrasonography in rectal carcinoid tumors: contribution to selection of therapy. *Gastrointest Endosc* 1991; **37**: 539-542 [PMID: 1936832 DOI: 10.1016/S0016-5107(91)70824-9]
- 9 **Koyama N**, Yoshida H, Nihei M, Sakonji M, Wachi E. Endoscopic Resection of Rectal Carcinoids Using Double Snare Polypectomy Technique. *Dig Endosc* 1998; **10**: 42-45 [DOI: 10.1111/j.1443-1661.1998.tb00538.x]
- 10 **Ono A**, Fujii T, Saito Y, Matsuda T, Lee DT, Gotoda T, Saito D. Endoscopic submucosal resection of rectal carcinoid tumors with a ligation device. *Gastrointest Endosc* 2003; **57**: 583-587 [PMID: 12665777 DOI: 10.1067/mge.2003.142]
- 11 **Moon JH**, Kim JH, Park CH, Jung JO, Shin WG, Kim JP, Kim KO, Hahn T, Yoo KS, Park SH, Park CK. Endoscopic submucosal resection with double ligation technique for treatment of small rectal carcinoid tumors. *Endoscopy* 2006; **38**: 511-514 [PMID: 16767589 DOI: 10.1055/s-2006-925074]
- 12 **Lee HJ**, Kim SB, Shin CM, Seo AY, Lee DH, Kim N, Park YS, Yoon H. A comparison of endoscopic treatments in rectal carcinoid tumors. *Surg Endosc* 2016; **30**: 3491-3498 [PMID: 26514133 DOI: 10.1007/s00464-015-4637-4]
- 13 **Wang X**, Xiang L, Li A, Han Z, Li Y, Wang Y, Guo Y, Zuang K, Yan Q, Zhong J, Xiong J, Yang H, Liu S. Endoscopic submucosal dissection for the treatment of rectal carcinoid tumors 7-16 mm in diameter. *Int J Colorectal Dis* 2015; **30**: 375-380 [PMID: 25596026 DOI: 10.1007/s00384-014-2117-2]
- 14 **Chen R**, Liu X, Sun S, Wang S, Ge N, Wang G, Guo J. Comparison of Endoscopic Mucosal Resection With Circumferential Incision and Endoscopic Submucosal Dissection for Rectal Carcinoid Tumor. *Surg Laparosc Endosc Percutan Tech* 2016; **26**: e56-e61 [PMID: 27213787 DOI: 10.1097/SLE.0000000000000266]
- 15 **Zhang D**, Shi R, Yao J, Zhang R, Xu Z, Wang L. Treatment of massive esophageal variceal bleeding by Sengstaken-Blackmore tube compression and intensive endoscopic detachable mini-loop ligation: a retrospective study in 83 patients. *Hepatogastroenterology* 2015; **62**: 77-81 [PMID: 25911872]

P- Reviewer: Chiba H, Eleftheriadis NP, Sato Y

S- Editor: Ma RY **L- Editor:** Wang TQ **E- Editor:** Yin SY



Observational Study

Consecutive fecal calprotectin measurements for predicting relapse in pediatric Crohn's disease patients

Alice Jane Foster, Matthew Smyth, Alam Lakhani, Benjamin Jung, Rollin F Brant, Kevan Jacobson

ORCID number: Alice Jane Foster (0000-0002-3133-7541); Matthew Smyth (0000-0002-2058-319X); Alam Lakhani (0000-0002-4360-6817); Benjamin Jung (0000-0001-8994-0506); Brand F Rollin (0000-0002-8026-2451); Kevan Jacobson (0000-0001-7269-8557).

Author contributions: Foster AJ and Jacobson K designed the study; Foster AJ, Smyth M, Lakani A, and Jacobson K performed the research; Foster AJ, Jung B, Brant RF and Jacobson K analyzed and interpreted the data; Foster AJ and Jacobson K wrote the manuscript with critical input from Jung B, Brant RF, Smyth M, and Lakani A.

Supported by an unrestricted grant from the Lutsky Foundation; Abbvie pharmaceuticals provided initial funding to purchase the Buhlmann ELISA kits.

Institutional review board

statement: The study was reviewed and approved by the University of British Columbia Clinical Research Ethics Board and the British Columbia Children's and Women's Research Review Committee (H12-03533).

Informed consent statement: All study participants or their legal guardian provided informed written consent prior to study enrolment.

Conflict-of-interest statement: All the Authors have no conflict of interest related to the manuscript.

Data sharing statement: No additional data are available.

Alice Jane Foster, Matthew Smyth, Alam Lakhani, Benjamin Jung, Rollin F Brant, Kevan Jacobson, Division of Gastroenterology, Hepatology and Nutrition, British Columbia Children's Hospital, Vancouver, BC V6H 3V4, Canada

Alice Jane Foster, Matthew Smyth, Alam Lakhani, Benjamin Jung, Kevan Jacobson, Pediatrics, B.C. Children's Hospital Research Institute, Vancouver, BC V6H 3V4, Canada

Alice Jane Foster, Matthew Smyth, Alam Lakhani, Rollin F Brant, Kevan Jacobson, Pediatrics, British Columbia children's Hospital, University of British Columbia, Vancouver, BC V6T 1Z4, Canada

Rollin F Brant, Department of Statistics, University of British Columbia, Vancouver, BC V6T 1Z4, Canada

Kevan Jacobson, Department of Cellular and Physiological Sciences, Faculty of Medicine, Vancouver, BC V6T 1Z3, Canada

Corresponding author: Kevan Jacobson, FRCP (C), MD, Doctor, Professor, Senior Scientist, Division of Gastroenterology, Hepatology and Nutrition, British Columbia children's Hospital, 4480 Oak Street, Room K4-181, Vancouver, BC V6H 3V4, Canada. kjacobson@cw.bc.ca
Telephone: +1-6048752332
Fax: +1-6048753244

Abstract**BACKGROUND**

Asymptomatic children with Crohn's disease (CD) require ongoing monitoring to ensure early recognition of a disease exacerbation.

AIM

In a cohort of pediatric CD patients, we aimed to assess the utility of serial fecal calprotectin measurements to detect intestinal inflammatory activity and predict disease relapse.

METHODS

In this prospective longitudinal cohort study, children with CD on infliximab therapy in clinical remission were included. Fecal calprotectin levels were assessed at baseline and at subsequent 2-5 visits. Clinical and biochemical disease activity were assessed using the Pediatric Crohn's Disease Activity Index, C-reactive protein and erythrocyte sedimentation rate at baseline and at visits over the following 18 mo.

RESULTS

STROBE statement: The authors have read the STROBE Statement-checklist of items, and the manuscript was prepared and revised according to the STROBE Statement-checklist of items.

Open-Access: This article is an open-access article which was selected by an in-house editor and fully peer-reviewed by external reviewers. It is distributed in accordance with the Creative Commons Attribution Non Commercial (CC BY-NC 4.0) license, which permits others to distribute, remix, adapt, build upon this work non-commercially, and license their derivative works on different terms, provided the original work is properly cited and the use is non-commercial. See: <http://creativecommons.org/licenses/by-nc/4.0/>

Manuscript source: Unsolicited manuscript

Received: December 5, 2018

Peer-review started: December 6, 2018

First decision: January 6, 2019

Revised: January 16, 2019

Accepted: January 18, 2019

Article in press: January 18, 2019

Published online: March 14, 2019

53 children were included and eighteen patients (34%) had a clinical disease relapse during the study. Baseline fecal calprotectin levels were higher in patients that developed symptomatic relapse [median (interquartile range), relapse 723 $\mu\text{g/g}$ (283-1758) *vs* 244 $\mu\text{g/g}$ (61-627), $P = 0.02$]. Fecal calprotectin levels $> 250 \mu\text{g/g}$ demonstrated good predictive accuracy of a clinical flare within 3 mo (area under the receiver operator curve was 0.86, 95% confidence limits 0.781 to 0.937).

CONCLUSION

Routine fecal calprotectin testing in children with CD in clinical remission is useful to predict relapse. Levels $> 250 \mu\text{g/g}$ are a good predictor of relapse in the following 3 mo. This information is important to guide monitoring standards used in this population.

Key words: Fecal calprotectin; Disease relapse; Biomarker; Crohn's disease; Children

©The Author(s) 2019. Published by Baishideng Publishing Group Inc. All rights reserved.

Core tip: It has becoming increasingly evident that many children with Crohn's disease (CD) who are in clinical remission continue to have ongoing active intestinal inflammation. This prospective paediatric study demonstrates the utility of fecal calprotectin monitoring in asymptomatic children with CD. In this study, a significant number of children were found to have elevated levels despite clinical remission, and levels of $> 250 \mu\text{g/g}$ were found to be a good predictor of clinical relapse in the subsequent 3 mo.

Citation: Foster AJ, Smyth M, Lakhani A, Jung B, Brant RF, Jacobson K. Consecutive fecal calprotectin measurements for predicting relapse in pediatric Crohn's disease patients. *World J Gastroenterol* 2019; 25(10): 1266-1277

URL: <https://www.wjgnet.com/1007-9327/full/v25/i10/1266.htm>

DOI: <https://dx.doi.org/10.3748/wjg.v25.i10.1266>

INTRODUCTION

Crohn's disease (CD) is a type of inflammatory bowel disease (IBD) with clinical course characterized by periods of disease remission and exacerbation. In children, worsening disease activity can be complicated by poor growth and development, hospitalizations, surgeries, and school absences. In addition, quality of life is correlated with disease activity, further supporting the importance of maintaining disease remission^[1]. IBD patients have regular follow-up appointments with their gastroenterologist to closely monitor the inflammatory state of the disease with the aim of implementing timely adjustments to medical therapy to prevent worsening of disease activity and development of complicated disease. Unfortunately, clinical symptoms typically lag behind the early intestinal inflammatory changes. Consequently treatment changes are often initiated only after deterioration in clinical status has occurred reinforcing the need for closer monitoring and better evaluation of intestinal inflammatory activity.

Clinicians utilize different tests to monitor inflammatory burden and predict relapse in children with IBD. The most accurate methods include endoscopic evaluation, capsule endoscopy and magnetic resonance enterography; though, these options are invasive, costly, time consuming and can have associated complications^[2-4]. Alternatively, less expensive and less invasive serum biomarkers such as C-reactive protein (CRP) and erythrocyte sedimentation rate (ESR) are also used to monitor inflammatory activity^[5]. However, up to one third of children with IBD were found to have normal ESR and CRP levels at diagnosis despite endoscopic evidence of active inflammation, thus demonstrating the lack of sensitivity of these markers to reliably detect active intestinal inflammation^[5].

More recently research efforts have been directed towards the use of fecal calprotectin (FC), a stool test that is non-invasive, sensitive and less expensive than imaging or endoscopic procedures^[6,7]. Calprotectin is a calcium and zinc binding cytosolic protein found in neutrophilic granulocytes released upon their activation^[8]. This protein is stable in feces, and can be measured as a marker of intestinal

inflammation^[9]. Indeed, FC levels have been reported to correlate with endoscopic evidence of mucosal healing a clinical measure that has been associated with a lower two-year probability for a clinical disease flare^[9,10]. In particular, FC levels < 250 µg/g have been found to be a reliable marker of endoscopic mucosal healing in IBD patients^[11].

While FC has been studied extensively in disease diagnosis, responses to therapy and post-operative monitoring^[12-16], there is a paucity of robust data evaluating the predictive role of FC for disease relapse in pediatric IBD patients in clinical disease remission. Studies in adults have shown that FC is an accurate marker of intestinal inflammation and provides a useful tool for predicting disease relapse in IBD patients in clinical remission^[7,17,18]. Most recently, a prospective study in adults evaluated the accuracy of routine FC measurements to predict flares in IBD patients on maintenance infliximab therapy, showing that FC was a good predictor of relapse and remission over the subsequent 4 mo^[19]. However, knowledge in pediatric patients is limited, as prior studies lack long-term, prospective data using validated instruments to define remission^[20-23]. The aim of this study was to evaluate the accuracy of serial FC measurements to predict clinical flares in pediatric CD patients on maintenance anti-tumor necrosis factor (anti-TNF) therapy and in clinical remission.

MATERIALS AND METHODS

Study design and methodology

In this blinded prospective longitudinal cohort study, pediatric patients with CD receiving infliximab, and in clinical remission were consecutively recruited from BC Children's Hospital Division of Gastroenterology, Hepatology and Nutrition in Vancouver, British Columbia, Canada between June 2013 and May 2015. Ethical approval was obtained from the University of British Columbia Clinical Research Ethics Board and the British Columbia Children's and Women's Research Review Committee. Written informed consent was obtained prior to inclusion in the study.

Study population

Children ages 6-18 years old with an established diagnosis of moderate to severe CD based on the revised Porto criteria were included^[24]. Disease was characterized using the Paris classification based on age at diagnosis, disease location and behaviour^[25]. All participants were on maintenance infliximab infusions (*i.e.*, > 14 wk from initiation of therapy) at dosing intervals between 4 and 8 wk, and in clinical remission at commencement of the study as defined by a Pediatric CD Activity Index (PCDAI) score of < 10^[26]. Potential subjects were excluded if they had at any time during the study known infectious enteritis or colitis, regular use of non-steroidal anti-inflammatory drugs (> 2 tablets/wk), or a diagnosis of celiac disease. All subjects were required to have a minimum of 3 stool samples and on infliximab throughout the study period.

Sample size was determined pragmatically based on the number of patients available at our center and fulfilling inclusion criteria. Review of our clinical IBD database showed 73 patients with CD receiving infliximab infusions. Based on our departmental data over the preceding 4 years, we estimated an additional 10-12 new patients per year eligible for the study. With 70%-80% enrolment, we estimated a potential sample size of 58 to 66 patients. All consecutive cases during the study period fulfilling inclusion criteria were invited to participate.

Fecal calprotectin

At enrolment patients provided a baseline stool sample, for baseline FC level, followed by collections at subsequent 2-5 infliximab infusion visits (**Figure 1**). Treating physicians, patients and families were blinded to FC results and no management decisions during the study were based on FC results. Stool samples were stored at 4 °C and processed within 7 d of collection to ensure stability of FC; 100 mg of stool was extracted using the Buhlmann Smart Prep kit following vendor's instructions, and frozen at - 80°C until the day of the assay. Manual ELISA was performed within 4 mo of sample extraction using the Buhlmann fCAL® ELISA kit (Buhlmann EK-CAL, rev 2012-11-20) following vendor's instructions for the lower range procedure (working 10-600 µg/g). Samples with levels > 600 µg/g were diluted according to vendor protocol and re-assayed. A FC level < 50 µg/g stool was considered to be within the normal range. Imprecision studies and comparability of patient results with other laboratories using the same assay were performed as part of the method validation (See Supplementary data, Supplemental Figures 1 and 2).

In addition, stool samples from 25 healthy children between ages 6 to 18 years with

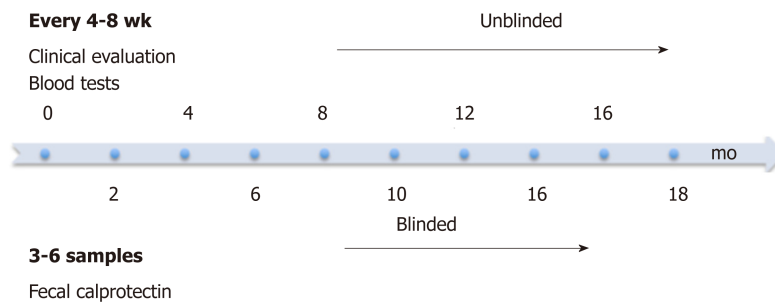


Figure 1 Study design. Patients were clinically evaluated at study entry and then every 4-8 wk at infusion visits. Blood tests for CRP, ESR and albumin were performed at each infusion visit. FC levels were measured every 4-8 wk for the first 3-6 visits. FC: Fecal calprotectin; ESR: Erythrocyte sedimentation rate; CRP: C-reactive protein.

no inflammatory conditions were tested. These subjects were recruited from the general population and were screened for gastrointestinal symptoms and diseases, associated inflammatory conditions, and nonsteroidal anti-inflammatory drugs use.

Clinical activity indices and additional data collection

The treating physician evaluated clinical disease activity at study enrolment and each subsequent visit (4-8 weekly) using a PCDAI score (Figure 1). Standard laboratory investigations including a complete blood count, CRP, ESR and albumin were measured at each infusion visit and available to the physician. Appropriate results were used to calculate the PCDAI including hematocrit, ESR, albumin, height, weight and disease symptoms. Patients were followed for 18 mo to provide long-term data on routine clinical evaluation and to monitor for clinical disease relapse. The primary endpoint was symptomatic disease relapse defined as a PCDAI score of ≥ 10 with a change of at least 10 points from the prior visit.

Patient characteristics included age, sex, age of diagnosis, disease location and behaviour, other medications (both IBD and non-IBD related), IBD-related surgeries, time from diagnosis to infliximab start, and infliximab infusion dosing and interval were collected. Any medication changes including the addition of new medications or changes in the infliximab infusions (dosing or time interval) were recorded.

Statistical analysis

Continuous variables following a skewed distribution are presented using median values and interquartile range (IQR) and Wilcoxon signed-rank test was used to compare differences between patients that relapsed and those that remained in clinical remission. Categorical data are presented as percentages. Time-to-event data are presented using Kaplan-Meier survival curves for FC, ESR, CRP and albumin levels. One predictor logistic regression and receiver operating characteristic (ROC) curve analyses for FC, ESR, CRP and albumin were used to evaluate the cumulative incidence of flares in a 2-wk time window around (before or after) 3 and 6 mo after the FC and a 4-wk window around 12 mo after the FC. Specificity, sensitivity and optimal threshold values of FC were determined from ROC curve analysis. The area under the curve (AUC) of the ROC was used to determine accuracy of FC, which was defined as poor (0.6-0.7), fair (0.7-0.8), good (0.8-0.9) and excellent (0.9-1.0)^[27].

Variance components analysis and Bland-Altman plots were used to evaluate the correlation between FC levels completed at our laboratory, the comparison laboratory, and the Buhlmann Diagnostics comparison samples. A significance level of $P < 0.05$ was used in our analysis. Statistical analysis was performed using R (version 3.3.3)^[28] and cp-R Clinical Chemistry Software V 0^[29].

RESULTS

Of the 25 healthy children evaluated, 17 had FC levels $< 25 \mu\text{g/g}$, 7 had levels between $50 \mu\text{g/g}$ and $200 \mu\text{g/g}$, and 1 had a level $> 200 \mu\text{g/g}$. Additional stool samples were evaluated from 3 subjects with FC levels $> 50 \mu\text{g/g}$. The subject with the highest level ($247.9 \mu\text{g/g}$) had a normal repeat FC ($12.4 \mu\text{g/g}$) and the other 2 subjects had levels of $47.6 \mu\text{g/g}$ (original $114.1 \mu\text{g/g}$) and $88.5 \mu\text{g/g}$ ($90.1 \mu\text{g/g}$). The median (IQR) of the group of health controls (following normalization of FC levels in the two individuals) was $35 \mu\text{g/g}$ (IQR $20\text{-}50 \mu\text{g/g}$).

Subject characteristics

Sixty-two patients were prospectively enrolled. Three subjects withdrew because of difficulty completing stool samples, 3 were transferred to adult care, 1 had a change in diagnosis to ulcerative colitis, and 2 patients stopped infliximab treatment during the study. Consequently, 53 children were analyzed. Thirty-six patients (68%) were male and the median follow-up time was 1.5 years. A total of 205 stool samples were collected during the study with a mean of 4 stool samples per patient. In addition to infliximab, 46 (87%) of patients received co-immunosuppressive therapy, with azathioprine prescribed most commonly (51% of patients). Patients' clinical characteristics are shown in [Table 1](#).

Inflammatory markers at enrolment and subsequent relapse

At enrolment when all patients were in clinical remission (PCDAI < 10), serum inflammatory markers and FC were initially evaluated (baseline data). The cumulative number of patients with symptomatic relapse was 18 (34%), and the mean time from enrolment to clinical flare was 7.1 mo (range, 1.5-15 mo). Baseline FC level in the group with symptomatic relapse was higher than those remaining in clinical remission [median 723 µg/g (IQR 283-1758) *vs* 244 µg/g (IQR 61-627), *P* = 0.02] ([Figure 2](#)). The median FC level at the visit prior to relapse was 765 µg/g (IQR 504-1800). Four outliers in the non-relapsing group had elevated FC at enrolment; 1 was 6 mo post diagnosis and FC levels gradually decreased to the normal range with no intervention, 2 had a decrease in FC levels after antibiotic administration for concurrent infections (urinary tract infection, pharyngitis) but FC levels remained elevated (> 400 µg/g) and the final outlier had a persistent FC levels > 1800 µg/g at study completion but remained in clinical remission. Both ESR and CRP levels were elevated in this individual triggering infliximab dose escalation; however this did not impact the FC level.

To further assess risk of clinical disease relapse in relationship to baseline FC levels, time to clinical relapse curves were calculated for the first year of the study using baselines FC levels < or ≥ 250 µg/g. Significant differences in relapse rates were noted in patients with FC < 250 µg/g compared to those with levels ≥ 250 µg/g ([Figure 3A](#), *P* = 0.004). Significant differences were also noted for baseline CRP levels ≤ 5 and > 5 mg/L ([Figure 3C](#), *P* = 0.015) and albumin < 35 and ≥ 35 g/L ([Figure 3D](#), *P* = 0.008). However, baseline ESR levels < 20 and ≥ 20 mm/h were not significantly different in predicting clinical relapse over time ([Figure 3B](#), *P* = 0.141).

Serial fecal calprotectin to predict relapse (longitudinal analysis)

Repeated measures analysis was used to determine if FC, ESR, CRP and albumin at an individual visit were predictive of a clinical disease relapse at subsequent visits. Visits with clinical relapse carried over from a previous visit were excluded. FC had good accuracy in predicting clinical disease relapse within 3 mo of collection with a ROC value of 0.86 [95% confidence interval (CI) 0.781 to 0.937], ([Figure 4A](#)). In contrast, the ROC values for ESR, CRP and albumin were lower at 0.651 (95% CI 0.481-0.821), 0.697 (95% CI 0.527-0.866) and 0.773 (95% CI 0.662-0.883) respectively. The ability of FC to predict clinical disease relapse decreased significantly at 6 and 12-mo time intervals from stool collection with ROC values of 0.746 (95% CI 0.626-0.866) and 0.687 (95% CI 0.554-0.82) respectively ([Figure 4B](#) and [C](#)). ESR, CRP and albumin were also unreliable predictors at 6 and 12-mo time points (Supplemental Table 1). Repeated measures analysis showed that a FC value of approximately 500 µg/g provided a sensitivity of 85% and specificity of 73% for predicting clinical relapse at the next visit ([Figure 5A](#) and [B](#)).

Disease management

Management decisions were based on PCDAI score, clinical assessment and serum laboratory values. We expected that high FC would be associated with a high PCDAI and vice versa, however this relationship was only seen in 24 children (45%) (Supplemental Figures 3 and 4). In the remaining 29 children the PCDAI and FC level did not correlate. Despite normal FC levels (< 250 µg/g) throughout the study in 14 patients, 4 (29%) had a medication escalation (Supplemental Figure 3). FC levels > 250 µg/g were reported in 39 (74%) patients at one or more time points, however 25 (64%) did not have a clinical flare, and in 4 of these patients (16%) therapy was actually de-escalated (Supplemental Figure 4). In the 14 patients with a clinical flare and raised FC, six (43%) had escalation of therapy, while eight (57%) had no medication change (Supplemental Figure 4).

DISCUSSION

Several studies in adult IBD patients have reported a strong association between

Table 1 Clinical characteristics of the pediatric Crohn's disease patients included in the study (n = 53) n (%)

Clinical characteristics of the pediatric Crohn's disease	
Males	36 (68)
Age years (median, IQR)	14.9 (11.9-16.0)
Age at diagnosis years (median, IQR)	10.9 (8.3-13.1)
Duration of disease years (median, IQR)	3.0 (1.3-5.1)
Concomitant immunosuppressant	
Azathioprine	27 (51)
Methotrexate	19 (36)
None	7 (13)
Previous IBD related surgery	
Perianal surgery	1 (2)
Resectional surgery	6 (11)
Crohn's disease: Age at diagnosis (Paris classification)	
A1a: 0-< 10 yr	20 (38)
A1b: 10-< 17 yr	33 (62)
Crohn's disease: Location (Paris classification)	
L1	5 (9)
L2	22 (42)
L3	26 (49)
L4	35 (66)
Crohn's disease: Behaviour (Paris classification)	
B1: non-stricturing, non-penetrating	31 (59)
B2: stricturing	12 (23)
B3: penetrating	7 (13)
B2B3: penetrating and structuring	3 (5)
P: Perianal disease	17 (32)
Crohn's disease: Growth impairment (Paris classification)	
Evidence of growth delay	0 (0)
Infliximab dosing	
Interval between infliximab doses (wk), mean (range)	7 (4-8)
Mean dose (mg/kg)	6.8

IQR: Interquartile range; IBD: inflammatory bowel disease.

elevated FC levels and clinically active inflammatory disease as well as the utility of FC to predict disease relapse^[17-19,30]. However, in children the data is more limited and mostly confined to retrospective data collection or prospective studies with single FC measurements and short study follow-up times^[20-23]. This prospective study is the first to evaluate serial blinded FC measurements to assess their value in predicting clinical disease relapse in children with IBD. Our study showed that serial FC levels could predict clinical disease relapse in patients with quiescent CD on infliximab during an 18-mo follow up period. Moreover, FC demonstrated good predictive accuracy of clinical disease relapse within 3 mo and was superior, but not significantly so, to other currently available serum biomarkers at predicting clinical relapse.

Consistent with the adult and pediatric studies that reported higher baseline FC levels in patients who developed symptomatic relapse, our patients who developed symptomatic relapse had significantly higher baseline median FC levels than those patients who maintained clinical remission (723 µg/g vs 244 µg/g). Reported cut-off of FC to predict risk of relapse in adults and children with IBD vary widely ranging from 120-340 µg/g in adults^[18,19,31] and 108-500 µg/g in paediatrics^[20,21,23]. Dierderen *et al*^[20] in their recent retrospective study in pediatric IBD patients noted that a baseline FC of 250 µg/g was predictive of symptomatic relapse within 6-mo, with a hazard ratio of 1.46 (95%CI: 1.21-1.77) with a good predictive accuracy (AUC: 0.82). Similarly, in our study, Kaplan-Meier time-to-relapse plots using FC level ≥ 250 µg/g determined that patients followed prospectively over 18-mo had a significant 7.9-fold (95%CI 1.1-56.1) increased risk of developing a clinical relapse than patients with

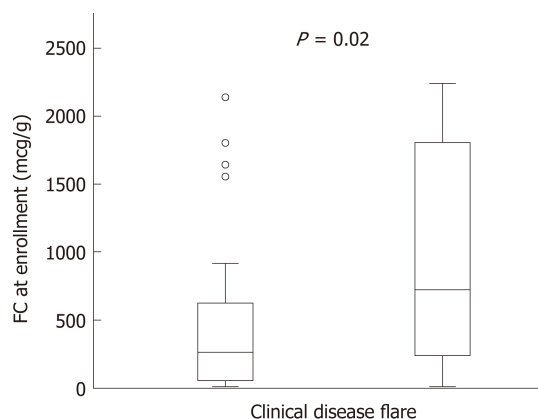


Figure 2 Increased baseline fecal calprotectin values in pediatric patients with inflammatory bowel disease are associated with elevated risk for clinical relapse. $P = 0.02$. Bar graphs represent median values with interquartile range. FC: Fecal calprotectin.

lower values ($P = 0.004$). Moreover, FC had good accuracy in predicting clinical disease relapse within 3 mo of collection with an ROC value of 0.86 (95% CI 0.781-0.937).

Dierderen *et al*^[20] reported an optimal FC cut off in pediatric IBD patients ($n = 114$) of 350 $\mu\text{g/g}$ with a sensitivity and specificity of 82% and 79% and a positive and negative predictive value of 41% and 96% respectively. Conversely, in a short term cross-sectional, observational, prospective cohort study in adult patients with IBD in clinical remission on maintenance Infliximab a FC concentration $> 160 \mu\text{g/g}$ was reported to have a sensitivity and specificity for predicting relapse of 91.7% and 82.9% respectively^[32]. In contrast, we determined that FC values $> 500 \mu\text{g/g}$ provided the best sensitivity and specificity to predict a clinical disease relapse at the next visit.

A comparable study to ours but in adult IBD patients in clinical remission on anti-TNF therapy followed prospectively until relapse or for 16-mo reported that FC levels $\geq 300 \mu\text{g/g}$ predicted relapse over the following 4 mo with a probability of 78.3%^[19]. Moreover, two consecutive FC values $\geq 300 \mu\text{g/g}$ increased the probability of predicting clinical relapse to 85.7%. However, the study population included both CD ($n = 71$) and ulcerative colitis ($n = 24$) patients. In the CD cohort a FC value $> 290 \mu\text{g/g}$ predicted relapse at any time over the following 4 mo with a probability of 96%. The variability in FC cut offs is multifactorial and likely related to differences in study design, populations, duration of follow-up, use of clinical indicators of symptomatic relapse, differences in methodology for FC quantification and fewer FC measurements. Notably, our study prospectively assessed serial FC only in CD patients on infliximab in clinical remission and the methodology for FC quantification was validated in our laboratory prior to measuring levels. Indeed, FC levels $< 500 \mu\text{g/g}$ correlated more closely than those in the upper range and given that our study found optimal cut-offs for predicting relapse to be $< 600 \mu\text{g/g}$, using the lower range procedure is valid.

Notably, in keeping with adult IBD practice, our study shows that children should also have FC levels checked every 3 mo to ensure adequate monitoring. Indeed, earlier detection of intestinal inflammation, with more timely management changes could result in fewer disease flares, improvement in patient quality of life and ultimately a decreased burden on the health care system.

A major strength of our study was the blinded and prospective longitudinal design with repeated measurements of FC, ESR, CRP and PCDAI scores. The blinding of FC results ensured that therapeutic changes were based upon our current disease monitoring practices and were not made based upon the FC result. The repeated measures allowed us to evaluate the temporal relationship between test results and clinical relapse providing new information that prior studies are lacking^[20]. Furthermore, evaluation of management decisions following study completion exposed the deficiencies in routine assessment methods when compared to FC. Of the 39 patients with elevated FC levels, FC remained elevated in 49% of patients during the study. While only one patient in our study had a disease complication, longer-term follow-up may uncover complications that occur in the group with persistent elevations of FC levels. Notably, in the CALM multicentre, randomized controlled study in adult patients with CD, escalation to adalimumab based on the tight control (FC $\geq 250 \mu\text{g/g}$, CRP $\geq 5 \text{ mg/L}$, CDAI ≥ 150 , or prednisone use in the previous week) compared to standard clinical management (symptom-driven decisions alone)

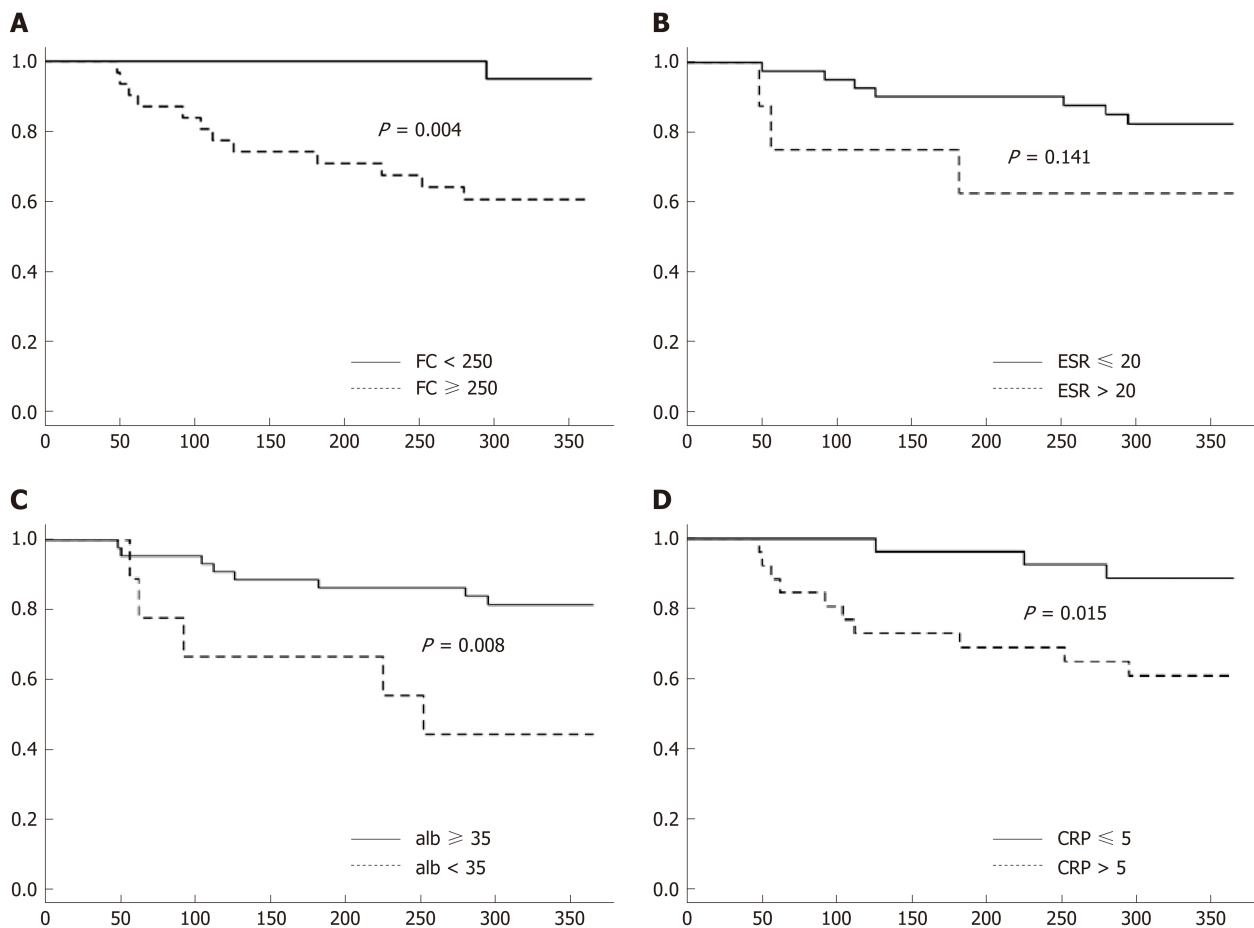


Figure 3 Kaplan-Meier curves at baseline through the first year of follow-up showing differences in predicting clinical relapse. A: Kaplan-Meier curves for FC; B: Kaplan-Meier curves for ESR; C: Kaplan-Meier curves for CRP; D: Kaplan-Meier curves for albumin. FC: Fecal calprotectin; ESR: Erythrocyte sedimentation rate; CRP: C-reactive protein.

resulted in better clinical and endoscopic outcomes at week 48^[33].

While this study was limited by sample size and by the limited sensitivity of the PCDAI clinical score this was offset by the inclusion of repeated measurements of biomarkers and PCDAI scores collected prospectively at multiple visits over an 18 mo follow up period. Notable, the PCDAI remains a tool frequently used in clinical care and research studies in children; however, the gold standard assessment tool for disease activity is endoscopic evaluation. Indeed endoscopic guided management of IBD is becoming increasingly recommended, although its true value and frequency of use and the role of FC in guiding endoscopic intervention remain to be evaluated prospectively. Although symptom based monitoring remains an important outcome variable, it has become increasingly evident that it correlates poorly with more objective measures of disease activity, necessitating evaluating the predictive value of biochemical markers of inflammation. The inclusion of endoscopy to guide management of IBD is increasingly recommended, although its true value remains to be prospectively evaluated.

In conclusion, this prospective longitudinal pediatric study is the first to demonstrate that routine serial FC measurements are an independent valuable predictor of symptomatic relapse. Moreover, FC elevation was noted up to 3 mo prior to the appearance of symptomatic relapse. Consequently, implementing a 3-monthly test to treat FC monitoring strategy would allow clinicians to make timely therapeutic adjustments in advance of disease relapse. However, future prospective studies are also necessary to evaluate the impact of routine FC monitoring on long-term patient outcomes and healthcare system burdens. Furthermore, research evaluating the relationship between FC levels and infliximab drug trough levels will be necessary to better understand the relationship and to further guide management decisions.

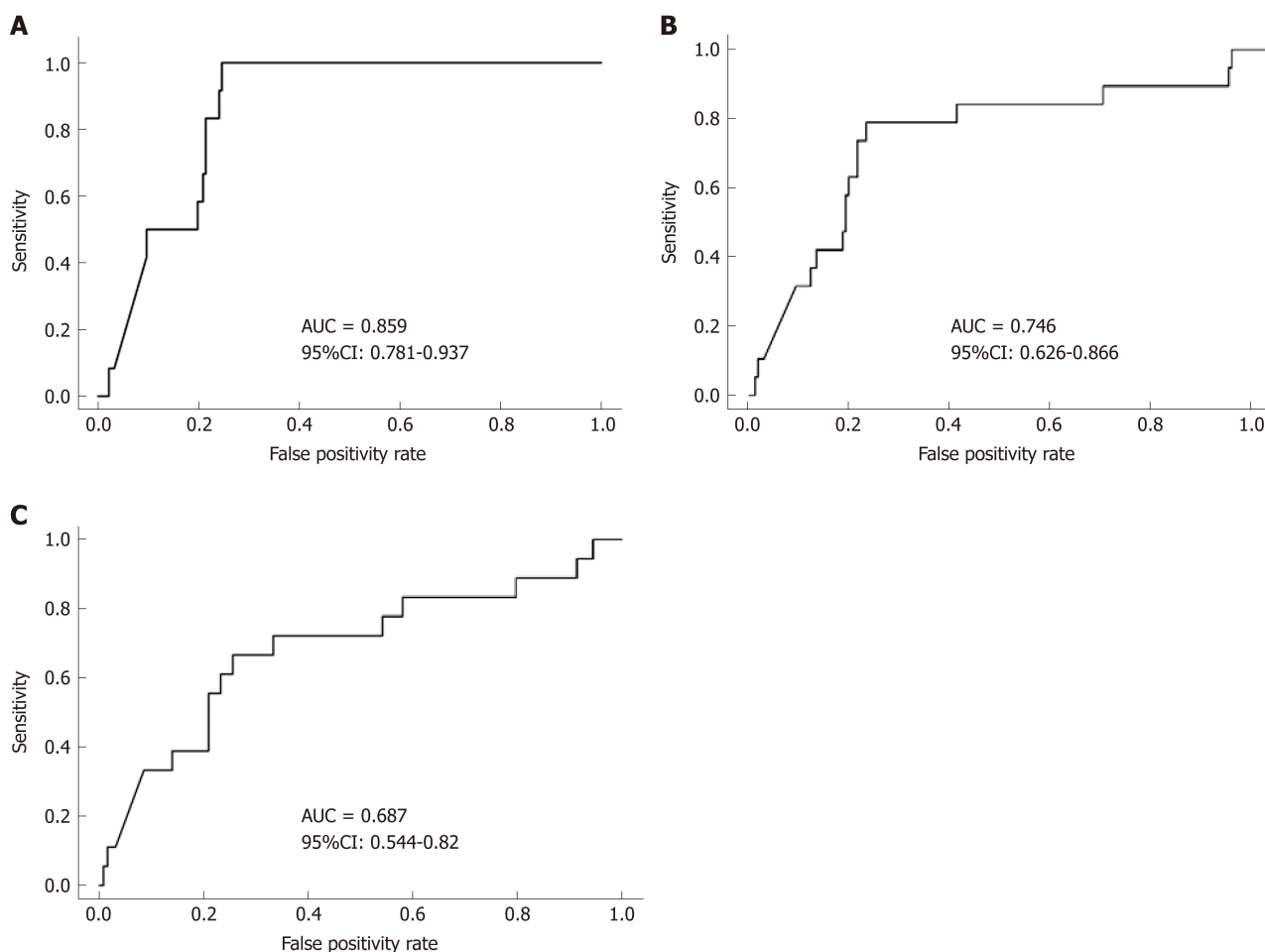


Figure 4 Receiver operator characteristic curve analysis for predicting clinical disease relapse. A: 3-mo; B: 6-mo; C: 12-mo. FC levels at the 3-mo visit more accurately predict clinical disease relapse than at 6-mo and 12-mo post baseline (univariate analysis). FC: Fecal calprotectin; AUC: Area under the curve; CI: Confidence interval.

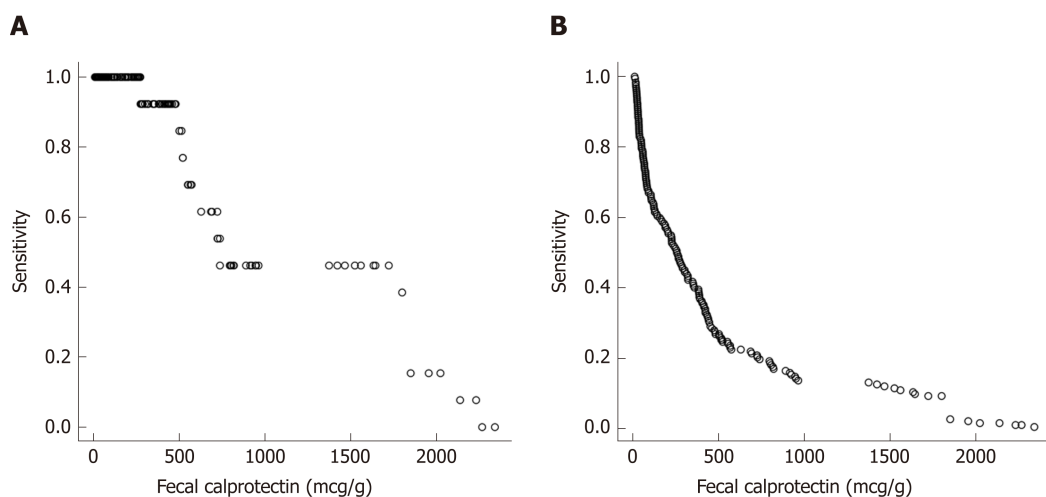


Figure 5 Sensitivity at various fecal calprotectin cut off values to predict a clinical disease flare. A: Sensitivity at various fecal calprotectin cut off values to predict a clinical disease flare at the next visit; B: False positive rates to predict a disease flare at the next visit for various FC levels (repeated measures). FC: Fecal calprotectin.

ARTICLE HIGHLIGHTS

Research background

Inflammatory bowel disease (IBD) is a chronic relapsing intestinal inflammatory disorder

requiring ongoing monitoring to optimize care. It has become increasing evidence that sustained remission reduces the likelihood of complicated disease. Consequently the incorporation of effective monitoring tools is required to assess disease activity allowing for the escalation of therapy in a timely manner. Fecal calprotectin (FC) has been studied in disease diagnosis and response to therapy but there is limited data evaluating its role in disease relapse in pediatric IBD patients in clinical remission. In the present prospective pediatric IBD study, we show that routine serial FC measurements are a valuable predictor of symptomatic relapse.

Research motivation

The motivation of the study was to evaluate the utility of FC as a predictive marker of disease relapse and in doing so reinforce the use of this strategy in clinical practice. Moreover adopting the strategy outlined in the paper will hopefully lead to better monitoring of disease activity with early optimization of therapy reducing the likelihood of fully blown clinical flare ups. Further research will need to look at the utility of this monitoring strategy and the role and relationship to endoscopic monitoring of disease activity and mucosal healing.

Research objectives

The main objective was to evaluate the accuracy of serial FC measurements to predict clinical flares in pediatric Crohn's disease (CD) patients on maintenance anti-tumor necrosis factor therapy and in clinical remission. The realization of this objective infers that serial FC done 3-monthly should be incorporated into clinical practice. Future research should also evaluate whether this strategy improves the quality of care, patient outcomes and costs to health care systems.

Research methods

This was a prospective observational study where serial FC levels were measure in pediatric patients with IBD in clinical remission on Remicade. The responsible clinicians were blinded to the FC results. Patient characteristics included age, sex, age of diagnosis, disease location and behaviour, other medications (both IBD and non-IBD related), IBD-related surgeries, time from diagnosis to infliximab start, and infliximab infusion dosing and interval were collected. The PDCAI was recorded at each visit. FC levels were measure by ELISA within 4-mo of sample extraction. Standard statistical methodology was used. Continuous variables are presented using median values and interquartile range (IQR) and Wilcoxon signed-rank test was used to compare differences between patients who relapsed and remaining in clinical remission. Categorical data are presented as percentages. Kaplan-Meier survival curves (time-to-event data) are used for biomarkers [FC, erythrocyte sedimentation rate (ESR), C-reactive protein (CRP), albumin]. One predictor logistic regression and receiver operating characteristic (ROC) curve analyses for biomarkers were used to evaluate the cumulative incidence of flares in a 2-wk time window around (before or after) 3 and 6 mo after the FC and a 4-wk window around 12 mo after the FC. Specificity, sensitivity and optimal threshold values of FC were determined from ROC curve analysis.

Research results

Of the 62 patients prospectively enrolled, 53 were analyzed; 68% were male and median follow-up time 1.5 years. A total of 205 stool samples were collected and analyzed (mean of 4 stool samples per patient). Symptomatic relapse was recorded in 18 (34%) patients (mean time from enrolment to clinical flare 7.1 mo, range, 1.5-15 mo). Baseline FC level in the symptomatic relapse group was higher than those remaining in clinical remission [median 723 µg/g (IQR 283-1758) *vs* 244 µg/g (IQR 61-627), $P = 0.02$]. The median FC level at the visit prior to relapse was 765 µg/g (IQR 504-1800). Time to clinical relapse curves calculated for the first year of the study using baselines FC levels $<$ or ≥ 250 µg/g showed a significant differences in relapse rates in patients with FC < 250 µg/g compared to those with levels ≥ 250 µg/g ($P = 0.004$). In addition, FC had good accuracy in predicting clinical disease relapse within 3 mo of collection with a ROC value of 0.86 [95% confidence interval (CI) 0.781-0.937]. Treatment decisions were based on clinical symptoms and standard biomarkers of inflammation (ESR and CRP) and thus did not reflect the potential benefit of the FC result. Consequently prospective evaluation of sequential FC testing is required to evaluate the short and long-term benefits on disease remission and outcome.

Research conclusions

FC had good accuracy in predicting clinical disease relapse within 3 mo of collection with a ROC value of 0.86 (95%CI: 0.781-0.937). Prospective monitoring with proactive intervention with either endoscopy assessment of disease activity and extent and, or optimization of medical therapy will reduce the likelihood of clinical flares, reduce the risk of complication and improve patient outcomes. FC is a useful biological tool to evaluate disease activity in patients in clinical remission on a biological agent. The Pediatric CD Activity Index (PCDAI) is not sensitive enough to monitor disease activity in children with CD. The addition of FC monitoring improves the quality of care for children with IBD. Regular 3-monthly FC monitoring should be incorporated into clinical practice. However it is important to follow the trend in level and not rely on a single level. That 3-monthly FC monitoring is a good addition to currently available biomarkers of inflammation. That FC is a good predictor of clinical relapse. That 3-monthly FC monitoring detects patients who will experience a symptomatic flare of disease. The inclusion of regular 3-monthly FC monitoring into clinical practice. The addition of FC monitoring will improve the quality of care and outcomes for children with IBD.

Research perspectives

Such studies are important to do. Colonoscopy should be included as an endpoint. A treatment decision can be made based on the FC result with subsequent determination whether the change had positive benefit (*i.e.*, normalization of FC level and evidence of mucosal healing at colonoscopy). To prospectively evaluate sequential FC testing and to determine the short and long-term benefits on disease remission, quality of life, patient outcome and related health care-costs. To define the relationship between FC monitoring and endoscopic monitoring of disease activity and mucosal healing. To determine the best cut off for FC for patients in remission. Prospective interventional studies with clearly defined FC levels, endoscopic score and treatment strategies with clearly defined primary and secondary outcomes (*i.e.*, disease in steroid free remission, disease biochemical remission, and mucosal healing).

ACKNOWLEDGEMENTS

The authors would like to thank Dr. Mat Provencal and his laboratory staff at the Hôpital Maisonneuve-Rosemont, Quebec for their help with validation of our Elisa method, and to Buhlmann for supplying the ELISA kits. Laboratory support at BC Children's Hospital was kindly provided by Diana Ralston. In addition, many thanks to our research team including Alam Lakhani and Carlie Penner for assisting with data collection. Dr Foster is supported by a research award provided by the Clinical Investigator program (CIP), University of British Columbia and Dr Jacobson is a Senior Clinician Scientist supported by the Children with Intestinal and Liver Disorders (CHILD) Foundation and the BC Children's Hospital Research Institute Clinician Scientists Award Program, University of British Columbia. The authors would also like to thank the children and their families who courageously live with IBD on a daily basis and the members of the Division of Gastroenterology, Hepatology and Nutrition at British Columbia Children's Hospital.

REFERENCES

- 1 **Chouliaras G**, Margoni D, Dimakou K, Fessatou S, Panayiotou I, Roma-Giannikou E. Disease impact on the quality of life of children with inflammatory bowel disease. *World J Gastroenterol* 2017; **23**: 1067-1075 [PMID: 28246481 DOI: 10.3748/wjg.v23.i6.1067]
- 2 **Makkar R**, Bo S. Colonoscopic perforation in inflammatory bowel disease. *Gastroenterol Hepatol (NY)* 2013; **9**: 573-583 [PMID: 24729766]
- 3 **Nemeth A**, Wurm Johansson G, Nielsen J, Thorlacius H, Toth E. Capsule retention related to small bowel capsule endoscopy: A large European single-center 10-year clinical experience. *United European Gastroenterol J* 2017; **5**: 677-686 [PMID: 28815031 DOI: 10.1177/2050640616675219]
- 4 **Stoddard PB**, Ghazi LJ, Wong-You-Cheong J, Cross RK, Vandermeer FQ. Magnetic resonance enterography: State of the art. *Inflamm Bowel Dis* 2015; **21**: 229-239 [PMID: 25222657 DOI: 10.1097/MIB.000000000000186]
- 5 **Alper A**, Zhang L, Pashankar DS. Correlation of Erythrocyte Sedimentation Rate and C-Reactive Protein With Pediatric Inflammatory Bowel Disease Activity. *J Pediatr Gastroenterol Nutr* 2017; **65**: e25-e27 [PMID: 27741061 DOI: 10.1097/MPG.0000000000001444]
- 6 **Mosli MH**, Zou G, Garg SK, Feagan SG, MacDonald JK, Chande N, Sandborn WJ, Feagan BG. C-Reactive Protein, Fecal Calprotectin, and Stool Lactoferrin for Detection of Endoscopic Activity in Symptomatic Inflammatory Bowel Disease Patients: A Systematic Review and Meta-Analysis. *Am J Gastroenterol* 2015; **110**: 802-19; quiz 820 [PMID: 25964225 DOI: 10.1038/ajg.2015.120]
- 7 **Sands BE**. Biomarkers of Inflammation in Inflammatory Bowel Disease. *Gastroenterology* 2015; **149**: 1275-1285.e2 [PMID: 26166315 DOI: 10.1053/j.gastro.2015.07.003]
- 8 **Fagerhol MK**. Calprotectin, a faecal marker of organic gastrointestinal abnormality. *Lancet* 2000; **356**: 1783-1784 [PMID: 11117904 DOI: 10.1016/S0140-6736(00)03224-4]
- 9 **Kostas A**, Siakavellas SI, Kosmidis C, Takou A, Nikou J, Maropoulos G, Vlachogiannakos J, Papatheodoridis GV, Papaconstantinou I, Bamias G. Fecal calprotectin measurement is a marker of short-term clinical outcome and presence of mucosal healing in patients with inflammatory bowel disease. *World J Gastroenterol* 2017; **23**: 7387-7396 [PMID: 29151692 DOI: 10.3748/wjg.v23.i41.7387]
- 10 **Baert F**, Moortgat L, Van Assche G, Caenepeel P, Vergauwe P, De Vos M, Stokkers P, Hommes D, Rutgeerts P, Vermeire S, D'Haens G; Belgian Inflammatory Bowel Disease Research Group; North-Holland Gut Club. Mucosal healing predicts sustained clinical remission in patients with early-stage Crohn's disease. *Gastroenterology* 2010; **138**: 463-8; quiz e10-1 [PMID: 19818785 DOI: 10.1053/j.gastro.2009.09.056]
- 11 **Kristensen V**, Røseth A, Ahmad T, Skar V, Moum B. Fecal Calprotectin: A Reliable Predictor of Mucosal Healing after Treatment for Active Ulcerative Colitis. *Gastroenterol Res Pract* 2017; **2017**: 2098293 [PMID: 29225617 DOI: 10.1155/2017/2098293]
- 12 **Carroccio A**, Iacono G, Cottone M, Di Prima L, Cartabellotta F, Cavataio F, Scalici C, Montalto G, Di Fede G, Rini G, Notarbartolo A, Aversa MR. Diagnostic accuracy of fecal calprotectin assay in distinguishing organic causes of chronic diarrhea from irritable bowel syndrome: A prospective study in adults and children. *Clin Chem* 2003; **49**: 861-867 [PMID: 12765980 DOI: 10.1373/49.6.861]
- 13 **Kostakis ID**, Cholidou KG, Vaiopoulos AG, Vlachos IS, Perrea D, Vaos G. Fecal calprotectin in pediatric inflammatory bowel disease: A systematic review. *Dig Dis Sci* 2013; **58**: 309-319 [PMID: 22899243 DOI: 10.1007/s10620-012-2347-5]
- 14 **Fagerberg UL**, Löf L, Myrdal U, Hansson LO, Finkel Y. Colorectal inflammation is well predicted by fecal calprotectin in children with gastrointestinal symptoms. *J Pediatr Gastroenterol Nutr* 2005; **40**: 450-455 [PMID: 15795593 DOI: 10.1097/01.MPG.0000154657.08994.94]

- 15 **Pavlidis P**, Gulati S, Dubois P, Chung-Faye G, Sherwood R, Bjarnason I, Hayee B. Early change in faecal calprotectin predicts primary non-response to anti-TNF α therapy in Crohn's disease. *Scand J Gastroenterol* 2016; **51**: 1447-1452 [PMID: 27400728 DOI: 10.1080/00365521.2016.1205128]
- 16 **Hukkinen M**, Pakarinen MP, Merras-Salmio L, Koivusalo A, Rintala R, Kolho KL. Fecal calprotectin in the prediction of postoperative recurrence of Crohn's disease in children and adolescents. *J Pediatr Surg* 2016; **51**: 1467-1472 [PMID: 26891835 DOI: 10.1016/j.jpedsurg.2016.01.017]
- 17 **Mao R**, Xiao YL, Gao X, Chen BL, He Y, Yang L, Hu PJ, Chen MH. Fecal calprotectin in predicting relapse of inflammatory bowel diseases: A meta-analysis of prospective studies. *Inflamm Bowel Dis* 2012; **18**: 1894-1899 [PMID: 22238138 DOI: 10.1002/ibd.22861]
- 18 **Chew TS**, Mansfield JC. Can faecal calprotectin predict relapse in inflammatory bowel disease: A mini review. *Frontline Gastroenterol* 2018; **9**: 23-28 [PMID: 29484157 DOI: 10.1136/flgastro-2016-100686]
- 19 **Ferreiro-Iglesias R**, Barreiro-de Acosta M, Lorenzo-Gonzalez A, Dominguez-Muñoz JE. Accuracy of Consecutive Fecal Calprotectin Measurements to Predict Relapse in Inflammatory Bowel Disease Patients Under Maintenance With Anti-TNF Therapy: A Prospective Longitudinal Cohort Study. *J Clin Gastroenterol* 2018; **52**: 229-234 [PMID: 27984399 DOI: 10.1097/MCG.0000000000000774]
- 20 **Diederer K**, Hoekman DR, Leek A, Wolters VM, Hummel TZ, de Meij TG, Koot BG, Tabbers MM, Benninga MA, Kindermann A. Raised faecal calprotectin is associated with subsequent symptomatic relapse, in children and adolescents with inflammatory bowel disease in clinical remission. *Aliment Pharmacol Ther* 2017; **45**: 951-960 [PMID: 28138990 DOI: 10.1111/apt.13950]
- 21 **van Rheeën PF**. Role of fecal calprotectin testing to predict relapse in teenagers with inflammatory bowel disease who report full disease control. *Inflamm Bowel Dis* 2012; **18**: 2018-2025 [PMID: 22275341 DOI: 10.1002/ibd.22896]
- 22 **Walkiewicz D**, Werlin SL, Fish D, Scanlon M, Hanaway P, Kugathasan S. Fecal calprotectin is useful in predicting disease relapse in pediatric inflammatory bowel disease. *Inflamm Bowel Dis* 2008; **14**: 669-673 [PMID: 18240279 DOI: 10.1002/ibd.20376]
- 23 **Sipponen T**, Kolho KL. Faecal calprotectin in children with clinically quiescent inflammatory bowel disease. *Scand J Gastroenterol* 2010; **45**: 872-877 [PMID: 20377469 DOI: 10.3109/00365521003782389]
- 24 **Levine A**, Koletzko S, Turner D, Escher JC, Cucchiara S, de Ridder L, Kolho KL, Veres G, Russell RK, Paerregaard A, Buderus S, Greer ML, Dias JA, Veereman-Wauters G, Lionetti P, Sladek M, Martin de Carpi J, Staiano A, Ruemmele FM, Wilson DC; European Society of Pediatric Gastroenterology, Hepatology, and Nutrition. ESPGHAN revised porto criteria for the diagnosis of inflammatory bowel disease in children and adolescents. *J Pediatr Gastroenterol Nutr* 2014; **58**: 795-806 [PMID: 24231644 DOI: 10.1097/MPG.0000000000000239]
- 25 **Levine A**, Griffiths A, Markowitz J, Wilson DC, Turner D, Russell RK, Fell J, Ruemmele FM, Walters T, Sherlock M, Dubinsky M, Hyams JS. Pediatric modification of the Montreal classification for inflammatory bowel disease: The Paris classification. *Inflamm Bowel Dis* 2011; **17**: 1314-1321 [PMID: 21560194 DOI: 10.1002/ibd.21493]
- 26 **Hyams JS**, Ferry GD, Mandel FS, Gryboski JD, Kibort PM, Kirschner BS, Griffiths AM, Katz AJ, Grand RJ, Boyle JT. Development and validation of a pediatric Crohn's disease activity index. *J Pediatr Gastroenterol Nutr* 1991; **12**: 439-447 [PMID: 1678008 DOI: 10.1097/00005176-199105000-00005]
- 27 **Swets JA**. Measuring the accuracy of diagnostic systems. *Science* 1988; **240**: 1285-1293 [PMID: 3287615 DOI: 10.1126/science.3287615]
- 28 **R Core Team (2017)**. A language and environment for statistical computing. R Foundation for Statistical Computing, Vienna, Austria. Available from: URL <http://www.R-project.org/>.
- 29 **Holmes DT**. cp-R, an interface the R programming language for clinical laboratory method comparisons. *Clin Biochem* 2015; **48**: 192-195 [PMID: 25448032 DOI: 10.1016/j.clinbiochem.2014.10.015]
- 30 **Heida A**, Park KT, van Rheeën PF. Clinical Utility of Fecal Calprotectin Monitoring in Asymptomatic Patients with Inflammatory Bowel Disease: A Systematic Review and Practical Guide. *Inflamm Bowel Dis* 2017; **23**: 894-902 [PMID: 28511198 DOI: 10.1097/MIB.0000000000001082]
- 31 **Kallel L**, Ayadi I, Matri S, Fekih M, Mahmoud NB, Feki M, Karoui S, Zouari B, Boubaker J, Kaabachi N, Filali A. Fecal calprotectin is a predictive marker of relapse in Crohn's disease involving the colon: A prospective study. *Eur J Gastroenterol Hepatol* 2010; **22**: 340-345 [PMID: 19581809 DOI: 10.1097/MEG.0b013e32832bab49]
- 32 **Ferreiro-Iglesias R**, Barreiro-de Acosta M, Otero Santiago M, Lorenzo Gonzalez A, Alonso de la Peña C, Benitez Estevez AJ, Dominguez-Muñoz JE. Fecal Calprotectin as Predictor of Relapse in Patients With Inflammatory Bowel Disease Under Maintenance Inliximab Therapy. *J Clin Gastroenterol* 2016; **50**: 147-151 [PMID: 25811118 DOI: 10.1097/MCG.0000000000000312]
- 33 **Colombel JF**, Panaccione R, Bossuyt P, Lukas M, Baert F, Vaňásek T, Danalioğlu A, Novacek G, Armuzzi A, Hébuterne X, Travis S, Danese S, Reinisch W, Sandborn WJ, Rutgeerts P, Hommes D, Schreiber S, Neimark E, Huang B, Zhou Q, Mendez P, Petersson J, Wallace K, Robinson AM, Thakkar RB, D'Haens G. Effect of tight control management on Crohn's disease (CALM): A multicentre, randomised, controlled phase 3 trial. *Lancet* 2018; **390**: 2779-2789 [PMID: 29096949 DOI: 10.1016/S0140-6736(17)32641-7]

P- Reviewer: Kapel N, Matowicka-Karna J, Mesquita J, Talebi Bezmin Abadi A,

S- Editor: Yan JP **L- Editor:** A **E- Editor:** Yin SY



Prospective Study

Non-guided self-learning program for high-proficiency optical diagnosis of diminutive and small colorectal lesions: A single-endoscopist pilot study

Marco Bustamante-Balén, Carla Satorres, Lorena Puchades, Belén Navarro, Natalia García-Morales, Noelia Alonso, Marta Ponce, Lidia Argüello, Vicente Pons-Beltrán

ORCID number: Marco Bustamante-Balén (0000-0003-2019-0158); Carla Satorres (0000-0002-1442-634X); Lorena Puchades (0000-0001-8213-5440); Belén Navarro (0000-0002-5700-3160); Natalia García-Morales (0000-0003-0130-3778); Noelia Alonso (0000-0003-4979-9522); Marta Ponce (0000-0002-8897-0284); Lidia Argüello Viudez (0000-0002-3041-033X); Vicente Pons-Beltrán (0000-0001-8909-8929).

Author contributions: Navarro B, Satorres C and Garcia-Morales N performed the literature research and reviewed the manuscript draft; Puchades L acquired data for analysis and reviewed the manuscript draft; Alonso N, Ponce M, Argüello L and Pons-Beltrán V revised the article for important intellectual content; Bustamante-Balén M conceived of and designed the project, contributed to data analysis, drafted the initial manuscript, and reviewed the different versions of the manuscript.

Institutional review board

statement: The study protocol was approved by the Hospital La Fe Institutional Review Board, No. 2014/0074.

Informed consent statement:

Informed consent was obtained from each patient.

Conflict-of-interest statement: The authors have no conflicts of interest to declare.

Marco Bustamante-Balén, Carla Satorres, Noelia Alonso, Marta Ponce, Lidia Argüello, Vicente Pons-Beltrán, Gastrointestinal Endoscopy Research Group, Gastrointestinal Endoscopy Unit, Digestive Diseases Department, La Fe Polytechnic University Hospital, Valencia 46026, Spain

Lorena Puchades, Digestive Diseases Department, La Fe Polytechnic University Hospital, Valencia 46026, Spain

Belén Navarro, Natalia García-Morales, Gastrointestinal Endoscopy Unit, Digestive Diseases Department, La Fe Polytechnic University Hospital, Valencia 46026, Spain

Corresponding author: Marco Bustamante-Balén, MD, PhD, Doctor, Gastrointestinal Endoscopy Research Group, Gastrointestinal Endoscopy Unit, Digestive Diseases Department, La Fe Polytechnic University Hospital, Avda. Fernando Abril Martorell, 106, Valencia 46026, Spain. bustamante_mar@gva.es

Telephone: +34-96-12440225

Fax: +34-96-1246278

Abstract**BACKGROUND**

The implementation of optical diagnosis (OD) of diminutive colorectal lesions in clinical practice has been hampered by differences in performance between community and academic settings. One possible cause is the lack of a standardized learning tool. Since the factors related to better learning are not well described, strong evidence upon which a consistent learning tool could be designed is lacking. We hypothesized that a self-designed learning program may be enough to achieve competency in OD of diminutive lesions of the colon.

AIM

To assess the accuracy of OD of diminutive lesions in real colonoscopies after application of a self-administered learning program.

METHODS

This was a single-endoscopist prospective pilot study, in which an experienced endoscopist followed a self-designed, self-administered learning program in OD of colorectal lesions. An assessment phase divided in two halves with a 6-mo period in between without performance of OD was developed in a population-based colorectal cancer screening program. The accomplishment of the

Data sharing statement: No additional data are available.

CONSORT 2010 statement: The authors have read the CONSORT 2010 Statement, and the manuscript was prepared and revised according to the CONSORT 2010 Statement.

Open-Access: This article is an open-access article which was selected by an in-house editor and fully peer-reviewed by external reviewers. It is distributed in accordance with the Creative Commons Attribution Non Commercial (CC BY-NC 4.0) license, which permits others to distribute, remix, adapt, build upon this work non-commercially, and license their derivative works on different terms, provided the original work is properly cited and the use is non-commercial. See: <http://creativecommons.org/licenses/by-nc/4.0/>

Manuscript source: Invited manuscript

Received: December 31, 2018

Peer-review started: January 2, 2019

First decision: January 30, 2019

Revised: February 20, 2019

Accepted: February 22, 2019

Article in press: February 23, 2019

Published online: March 14, 2019

Preservation and Incorporation of Valuable Endoscopic Innovations criteria and performance measures were calculated overall and in the two halves of the assessment phase, assessing their response to the 6-mo stopping period. The evolution of performance through blocks of 50 lesions was also assessed.

RESULTS

Overall, 152 patients and 522 lesions (≤ 5 mm: 399, and 6-9 mm: 123) were included. The negative predictive value for the OD of adenoma in rectosigmoid lesions diagnosed with high confidence was 91.7% [95% confidence interval (CI): 87.3-96.6]. The proportion of agreement on surveillance interval between OD and pathological diagnosis was higher than 95%. Overall accuracy for diminutive lesions diagnosed with high confidence was 89.5% (95%CI: 86.3-92.7). The overall accuracy of OD was similar in the two halves of the assessment phase [90.1 (95%CI: 85.6-94.7) *vs* 88.2 (95%CI: 87.9-95.9)]. All the other performance parameters were also equivalent, except for specificity. Specificity, negative predictive value and accuracy were the parameters most affected by the stopping period between the two halves. Upon analyzing trends on blocks of 50 lesions, an improvement on sensitivity ($P = 0.02$) was detected only in the first half and an improvement on accuracy ($P = 0.01$) was detected only in the second half.

CONCLUSION

A self-administered learning program is sufficient to achieve expert-level OD. To maintain performance, continuous practice is needed, with a refresher course following any long non-practice period.

Key words: Optical diagnosis; Accuracy; Learning; Polyp; Colonoscopy; Education

©The Author(s) 2019. Published by Baishideng Publishing Group Inc. All rights reserved.

Core tip: The learning process for optical diagnosis (OD) of diminutive colorectal polyps is not standardized, and this may influence the described differences in OD performance between community and academic settings. Our study shows that an individual following a self-designed and self-administered learning program is able to reach the expert level of OD performance completely fulfilling the criteria of Preservation and Incorporation of Valuable Endoscopic Innovations. However, continuous practice is needed to maintain performance and, if a non-practice period is expected, a refresher course is needed to avoid a significant drop in performance parameters.

Citation: Bustamante-Balén M, Satorres C, Puchades L, Navarro B, García-Morales N, Alonso N, Ponce M, Argüello L, Pons-Beltrán V. Non-guided self-learning program for high-proficiency optical diagnosis of diminutive and small colorectal lesions: A single-endoscopist pilot study. *World J Gastroenterol* 2019; 25(10): 1278-1288

URL: <https://www.wjgnet.com/1007-9327/full/v25/i10/1278.htm>

DOI: <https://dx.doi.org/10.3748/wjg.v25.i10.1278>

INTRODUCTION

Optical diagnosis (OD) of gastrointestinal epithelial lesions has become a reality due to the development of new image enhancing technologies. The ability to perform *in situ* differentiation of adenomatous and hyperplastic colorectal lesions has led to the proposal of a resect-and-discard strategy for the management of diminutive (≤ 5 mm) polyps^[1]. Following this strategy, diminutive lesions would be resected and discarded after an adenoma high-confidence OD has been made, while rectal diminutive lesions with an OD of hyperplastic would be left in place. This strategy has been shown to be cost-efficient^[2].

An excellent accuracy of OD is a requirement for applying such a strategy, and it has been shown to be so in many studies, most of them performed in academic centers^[3]. However, this good accuracy has not been well replicated in community settings^[4,5]. Learning of OD is key for its implementation in clinical practice, and the lack of standardized learning tools may explain part of the problem. A wide variety of

learning tools has been described, including classroom type^[6], self-directed computer-based^[3] or web-based teaching programs^[7]. Still pictures, videos or both have been used to explain the optical features of each type of polyp^[8,9]. However, there are no head-to-head comparisons between learning tools and most of them have not been validated.

Moreover, people learn at different rates, as has been shown by some studies monitoring the learning curve of OD. Some learners never get competency in OD, while others need long-term monitoring^[4,6]. Unfortunately, since the factors related to better learning are not well described, the strong evidence upon which a consistent learning tool could be designed is lacking. Despite these challenges, we hypothesized that a self-designed learning program may be enough to achieve competency in OD of diminutive lesions of the colon.

Our study was designed according to the following aims: (1) to assess the accuracy of OD of diminutive lesions in real colonoscopies from a colorectal carcinoma (CRC) screening program using narrow band imaging (NBI) and the NBI International Colorectal Endoscopic (NICE) classification after following a non-guided self-administered learning program; and (2) to describe the OD learning curve by analyzing which parameters may be more suitable for monitoring competency.

MATERIALS AND METHODS

Study design and population

This was a single-endoscopist prospective pilot study, in which an experienced endoscopist (> 500 colonoscopies per year and adenoma detection rate of 68%) followed a self-designed, self-administered learning program for OD of colorectal lesions. In this learning program, the NICE classification was reviewed and a published set of still pictures^[8] was used to identify the main optical characteristics of hyperplastic and adenomatous polyps under NBI. Then, the NICE classification was put into practice on 50 consecutive colorectal lesions identified in CRC screening colonoscopies. The endoscopist reviewed the pathological records, when available, comparing this diagnosis with the provided OD. A detailed evaluation of inconsistencies was performed and diagnostic disagreements were reviewed with the pathologist.

After completing the learning program, an assessment phase was begun in which individuals scheduled for colonoscopy in the setting of the Valencian Government Colorectal Screening Program were consecutively included. This screening program is based on results from the immunological fecal occult blood test administered every 2 years and colonoscopy administered in cases of positivity. Exclusion criteria were poor quality preparation (Boston < 2 in any colon segment), incomplete colonoscopy, inflammatory bowel disease, coagulopathy that precluded taking samples, or unwillingness to participate in the study. This assessment phase was divided in two halves, with a predefined stopping period of 6 mo in between, in which no OD was performed. No OD refresher course was given before the beginning of the second phase.

Colonoscopy procedure

For bowel preparation, a split-dose scheme using sodium picosulphate plus magnesium citrate (Citraflet®; Casen Recordati, S.L., Zaragoza, Spain) or 2-L polyethylene glycol (PEG) plus ascorbate (Moviprep®; Salix Pharmaceuticals, Bridgewater, NJ, United States) was administered. All colonoscopies were performed using high-resolution CF-HQ190AL or CF-H190L endoscopes (Olympus, Optical Co., Ltd., Tokyo, Japan) and a video endoscope system (EVIS EXERA III; Olympus).

Variables

Data on age, sex, and personal and familiar histories of colon polyps or CRC were recorded. For every lesion, data on size, morphology (following the Paris classification^[10]), location, NICE classification^[11] group, and final OD were also recorded. All data were prospectively included in a database built in Access 2003 (Microsoft Corp., Redmon, WA, United States). Pathological diagnosis was introduced in the database by a researcher involved neither in the colonoscopies nor in the OD process. Therefore, during this phase of the study, the endoscopist was blind to the pathological report and no feedback was provided. Only diminutive lesions (1-5 mm) or small lesions (6-9 mm) were considered for the analysis.

The optical and pathologic diagnostics were compared for the diagnosis of adenoma *vs* non-adenomatous lesions, considering pathology as the gold standard. For analysis purposes, hyperplastic polyps, sessile serrated polyps, inflammatory

polyps, and biopsies informed as normal were considered as non-adenomatous lesions.

Study end-points

The primary end-point was the Preservation and Incorporation of Valuable Endoscopic Innovations (PIVI) criteria^[1] accomplishment at the end of the study. The final surveillance recommendation when using OD was the combination of OD of diminutive lesions and the pathology report of larger lesions. The concordance between the recommended follow-up from OD and from pathology was calculated for the three main currently available guidelines (European Union^[12], European Society of Gastrointestinal Endoscopy^[13], and American Society for Gastrointestinal Endoscopy^[14]). Patients in whom an *in-situ* surveillance recommendation could not be given (*i.e.*, those with no diminutive lesions, with at least one polyp diagnosed with low confidence, or diagnosed with a CRC or a large polyp scheduled for endoscopic mucosal resection) were not included in this analysis. Secondary end-points were the evaluation of overall accuracy, sensitivity, specificity, positive and negative predictive values (PPV and NPV, respectively), and positive likelihood ratio for the diagnosis of adenoma. All performance values were calculated at the end of the first half, at the end of the study and during the assessment phase in groups of 50 lesions.

Sample size estimate on and statistical methods

To obtain a precision of 3% in the estimation of the accuracy of OD for diminutive lesions, using a bilateral 95% confidence interval (CI) and expecting an accuracy of 90%, at least 385 diminutive lesions had to be included.

Each patient's and lesion's characteristics were summarized by median (standard deviation) for continuous variables and by number (percentage) for categorical variables. Sensitivity, specificity, PPV and NPV, and positive likelihood ratio were calculated as measures of accuracy together with their 95% CIs. True positive and negative values were defined as an agreement between OD and histology. The Cochran-Armitage test for trend was used to determine if performance improved through blocks of 50 lesions in both halves of the study. *P*-values were two-sided, and differences were considered significant at $P < 0.05$. Analysis was performed by using the Stata statistical package, version 14.2 (Stata Corp, College Station, TX, United States). The results of this study are reported in accordance with Standards for Reporting of Diagnostic Accuracy guidelines^[15].

RESULTS

From January 2015 to January 2017, 152 individuals who underwent a CRC screening colonoscopy were selected for study inclusion. Their main characteristics are summarized in [Table 1](#). These patients harbored 522 lesions [1-5 mm in 399 (76.4%) and 6-9 mm in 123 (23.6%)], the main characteristics of which are summarized in [Table 2](#).

PIVI criteria

Overall, 55 (59.8%) diminutive rectosigmoid lesions were diagnosed as hyperplastic and 34 (36.9%) as adenoma. One lesion was lost for analysis and two were categorized as normal mucosa. The NPV for the OD of adenoma in rectal lesions diagnosed with high confidence was 91.7% (95%CI: 87.3-96.6). In 59 patients (38.8%), an *in-situ* surveillance recommendation could not be given; these patients included 40 with at least one lesion diagnosed with low confidence, 7 with no diminutive lesion, 9 with a CRC or a malignant polyp diagnosed in the same colonoscopy, and 3 with large polyps suitable for endoscopic mucosal resection. The proportion of agreement on surveillance interval between OD and pathological diagnosis following the different guidelines for the remaining 92 patients is summarized in [Table 3](#).

Accuracy of OD

Regarding the OD with NBI, 520 lesions were classified as adenomas or hyperplastic polyps, with 347 (87.0%) diminutive lesions and 116 (94.3%) small lesions diagnosed with high confidence ([Table 2](#)).

The performance values for the OD of small and diminutive lesions are summarized in [Table 4](#). Overall accuracy for diminutive and small lesions diagnosed with high confidence was 89.5% (95%CI: 86.3-92.7) and 99.1% (95%CI: 97.4-100.0) respectively. Values were, as expected, much lower for lesions diagnosed with low confidence ([Table 4](#)). These values did not differ significantly when comparing location (distal *vs* proximal) and morphology (sessile *vs* flat) (data not shown).

Table 1 Patient characteristics, n = 152

Characteristic	Value
Age, yr	61.1 ± 6.2
Female sex n (%)	56 (36.8)
Familiar history of CRC n (%)	33 (21.7)
Number of polyps	3.8 ± 3.0
Number of adenomas	2.7 ± 2.6
Number of advanced adenomas	0.6 ± 1.0

CRC: Colorectal cancer.

Learning curve assessment

The overall accuracy of OD was similar in the two halves of the study [90.1% (95% CI: 85.6-94.7) vs 88.2 (95% CI: 87.9-95.9)]. All the other performance parameters were also equivalent, except for specificity (Table 5). The NPV for adenoma in rectosigmoid lesions and agreement on surveillance intervals were also similar between both halves of the study (Table 5).

Figure 1 depicts the evolution during time of OD performance of diminutive lesions. Specificity, NPV and accuracy were the parameters most affected by the stopping period between the two halves. However, sensitivity and the percentage of lesions diagnosed with high confidence are more robust parameters. Analyzing trends on blocks of 50 lesions showed an improvement in specificity ($P = 0.0001$) and NPV ($P = 0.00001$) in both halves. However, an improvement in sensitivity ($P = 0.02$) was detected only in the first half and an improvement in accuracy ($P = 0.01$) was detected only in the second half. There was no significant improvement in the percentage of lesions diagnosed with high confidence in either of the two halves as the trainee progressed through lesion batches.

DISCUSSION

Our study shows that a good accuracy, reaching an expert level, and complete fulfillment of the PIVI criteria can be accomplished by self-learning. At the end of the study, the NPV for the OD of adenoma in rectal lesions was 91.7% and the proportion of agreement in the surveillance intervals between OD and pathology was higher than 95%.

Previous studies on OD learning have shown conflicting results. When it comes to performing OD in real colonoscopies, several studies and a meta-analysis have shown lower levels of performance (*i.e.*, not fulfilling the PIVI criteria) in community hospitals than in academic centers, despite a structured learning program having been followed^[4,5,16]. On the contrary, other authors have shown that trainees without previous experience in NBI can meet PIVI thresholds after following a standardized learning program^[17]. One of the possible explanations for this discrepancy may be the different design of the learning tool.

We used a validated set of still pictures followed by a practice on real colonoscopies with auto-administered feedback, hypothesizing that the latter would ease the transition from still pictures to real practice and shorten the learning curve. For the initial learning steps, several training modules have been used in the literature, including classroom-type^[8,18], computer training^[19] and web-based^[20] modules. All systems may have similar efficacy as it has been suggested in a recent report showing that self-learning using a computer-based program with pictures and videos is as efficient as a classroom-type teaching session for learning OD^[21]. Therefore, the key to efficacy of the learning program may be more in other add-ons or modifications.

Other authors have also shown a good efficacy of learning when introducing an *in vivo* phase during the learning program, with a pre-defined number of colonoscopies^[22] or lesions^[6]. In our study, 50 lesions were sufficient to meet the PIVI criteria at the end of the assessment phase.

Other modifications that have been tested in the literature are refresher teaching sessions and periodic feedback. We did not introduce any refresher session, not even before the beginning of the second period of the assessment phase after the 6-mo stopping period, and it did not affect the final results on efficacy. Any feedback was allowed during the assessment phase and the endoscopist was blinded to the pathology results. Regarding these two modifications, there is some controversy in

Table 2 Lesion characteristics n (%)

Characteristic	1-5 mm	6-9 mm
Number of lesions by size	399 (76.4)	123 (23.6)
Paris classification		
0-Ip	3 (0.7)	22 (17.9)
0-Is	273 (68.4)	88 (71.5)
0-IIa	117 (29.3)	11 (8.9)
0-IIc	2 (0.5)	0
0-IIa + IIc	3 (0.7)	0
0-IIb	1 (0.2)	2 (1.6)
Pathology		
Adenoma	255 (63.9)	97 (78.9)
Hyperplastic	106 (26.6)	17 (13.6)
SSP	8 (2.0)	7 (5.6)
Other	26 (6.5)	1 (0.8)
Lost/not enough sample	4 (1.0)	1 (0.8)
Location		
Proximal	248 (62.2)	56 (45.5)
Distal	151 (37.8)	67 (54.5)
Optical diagnosis ¹		
NICE 1	288 (72.2)	102 (82.9)
NICE 2	110 (27.6)	20 (16.3)
High-confidence diagnosis	347 (87.0)	116 (94.3)

¹Only available for 520 lesions (1 lesion excluded because a poor approach to application of narrow band imaging, and 1 subepithelial lesion). NBI: Narrow band imaging; NICE: NBI International Colorectal Endoscopic classification system; SSP: Sessile serrated polyp.

the literature. Paggi *et al*^[23] introduced refresher teaching sessions every 2 mo and monthly feedback on individual performance, achieving an overall NPV for adenoma in rectosigmoid lesions of 91.3% and more than 90% of agreement on surveillance intervals. Patel *et al*^[17] delivered periodic feedback to all the participants in a prospective study and were able to show an overall NPV for high-confidence diagnosis of rectosigmoid lesions of 94.7% and a surveillance interval agreement of 91.2%. However, a randomized trial was not able to show any influence of feedback on final performance^[6].

We planned a stopping period at the middle of the study to investigate if a non-practice period could influence performance and to detect which parameters were affected the most. Following the stopping period (which was not followed by a refresher course), almost all performance parameters dropped significantly. Specificity was the most affected parameter, and it took 200 lesions to reach previous levels. On the other hand, sensitivity was very resistant to inactivity. Accuracy dropped from 0.89 to 0.77, and it took 150 lesions to reach 0.90. NPV for adenoma in rectal lesions also dropped significantly, from 0.90 to 0.67.

Regarding trends for improvement through blocks of 50 lesions, a significant improvement was detected in both halves for specificity and NPV, suggesting that the number of false positives and false negatives are only significantly reduced after ongoing practice. The significant trend for improvement of accuracy only in the second period suggests that if a long non-practice period has occurred, a refresher course in OD is needed. A previous study^[24] of 12 endoscopists evaluating 80 videos at 12 wk apart found a significant improvement in accuracy in both periods; however, that study did not include real colonoscopies.

The strength of the current study described herein is its design as a single-endoscopist study, which allowed for detailed analysis of the learning process. Another strength is that the PIVI criteria on surveillance agreement has been calculated for the most widely applied international guidelines, showing that learning is consistently strong under different circumstances. However, some issues may limit generalizability. First, the single-endoscopist study design carries the risk of the results being dependent on the trainee's characteristics. Studies including several endoscopists have shown that despite an overall good performance, many individuals

Table 3 Concordance between proposed surveillance interval between optical diagnosis and pathology, *n* = 93

Guideline	Concordance		Too long		Too short	
	<i>n</i>	% (95%CI)	<i>n</i>	% (95%CI)	<i>n</i>	% (95%CI)
EU	89	95.7 (91.9-100)	2	2.1 (0-21.4)	2	2.1 (0-21.4)
ESGE	90	96.8 (93.5-100)	2	2.1 (0-21.4)	1	1.1 (0-20.5)
ASGE	89	95.7 (91.9-100)	3	3.2 (0-22.3)	1	1.1 (0-20.5)

ASGE: American Society of Gastrointestinal Endoscopy; CI: Confidence interval; ESGE: European Society of Gastrointestinal Endoscopy; EU: European Union.

do not reach the PIVI thresholds^[4,22] and that in many cases a continuous monitoring is needed. Nonetheless, the statement that an efficient self-learning program is possible when the trainee is highly motivated seems conclusive.

Another limitation is that all patients belong to a FIT-positive population. In this situation, the probability of finding polyps is higher and this may enhance the learning process. The diagnosis of sessile serrated polyp was not considered, and these polyps were included in the non-adenomatous group. However, this only comprised 2% of samples and none of the hyperplastic lesions were more than 10 mm, having little relevance to the final results.

In conclusion, a self-administered learning program including real colonoscopies is sufficient to learn OD at an expert level. However, continuous practice is needed to maintain performance and a refresher course is needed if a long non-practice period occurs. Performance values behave differently after a stopping period, and this should be taken into account when planning a monitoring program.

Table 4 Overall diagnostic performance of narrow band imaging and the Narrow Band Imagig International Colorectal Endoscopic classification system

Parameter	High-confidence		Low-confidence	
	1-5 mm, n = 347	6-9 mm, n = 115	1-5 mm, n = 51	6-9 mm ¹ , n = 7
Sensitivity	97.0 (95.2-98.8)	100.0	76.0 (64.3-87.7)	N/A
Specificity	74.3 (69.4-78.6)	94.4 (90.2-98.6)	46.1 (32.4-59.8)	57.1 (20.4-57.1)
PPV	88.5 (84.6-91.4)	99.0 (97.2-100.0)	57.6 (44.0-71.2)	0
NPV	92.3(89.1-94.8)	100.0	66.7 (53.8-79.6)	100.0
LR+	3.8 (1.2-4.8)	18.0 (10.1-23.9)	1.4 (-1.8-4.6)	N/A
Accuracy	89.5 (85.7-92.3)	99.1 (97.4-100.0)	60.7 (47.3-74.1)	57.1 (20.4-57.1)

Data are given as % (95%CI).

¹No adenoma was diagnosed with low-confidence.

CI: Confidence interval; LR: Likelihood ratio; N/A: Non-applicable; NPV: Negative predictive value; PPV: Positive predictive value.

Table 5 Comparison of the diagnostic performance measures and Preservation and Incorporation of Valuable Endoscopic Innovations criteria fulfillment between the two halves of the study

Parameter	1 st half, n = 165 ¹	2 nd half, n = 182 ¹
Sensitivity	96.1 (93.1-99.0)	97.6 (95.4-99.8)
Specificity	82.0 (76.1-87.9)	65.4 (58.5-72.3)
PPV	90.1 (85.5-94.7)	87.2 (82.3-92.0)
NPV	92.6 (88.6-96.6)	91.9 (87.9-95.9)
Accuracy	90.1 (85.6-94.7)	88.2 (87.9-95.9)
NPV rectosigmoid lesions	92.3 (87.3-96.6)	90.5 (86.2-94.8)
Surveillance interval agreement		
UE	100.0	93.3 (89.7-96.9)
ESGE	100.0	95.1 (92.0-98.2)
ASGE	100.0	93.3 (91.6-98.2)

Data are given as % (95%CI).

¹Only for diminutive lesions diagnosed with high-confidence.

ASGE: American Society of Gastrointestinal Endoscopy; ESGE: European Society of Gastrointestinal Endoscopy; EU: European Union; NPV: Negative predictive value; PIVI: Preservation and Incorporation of Valuable Endoscopic Innovations; PPV: Positive predictive value.

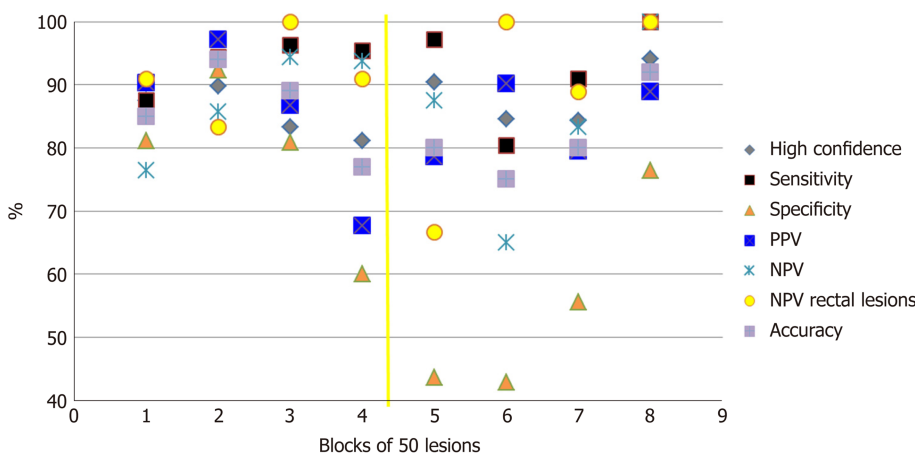


Figure 1 Performance parameters by blocks of 50 lesions during the two halves of the study. The yellow line represents the 6-mo stopping period. NPV: Negative predictive value; PPV: Positive predictive value.

ARTICLE HIGHLIGHTS

Research background

The resect-and-discard strategy for the management of diminutive colon polyps is a paradigm shift based on an accurate optical diagnosis (OD). Such a high accuracy has only been achieved by experts, while the performance in community hospitals does not reach thresholds that would allow its universal implementation. The lack of a standardized learning tool for OD of colon lesions may contribute to this problem.

Research motivation

Although several learning tools have been described, most of them are not validated and there is a great variability in their components and designs. We hypothesized that self-learning of OD is feasible and that accuracy thresholds can be achieved with a self-administered program. A detailed description of the learning process can provide valuable information for the design of an OD learning system.

Research objectives

We aimed to assess the accuracy of OD of diminutive lesions in real colonoscopies using the International Colorectal Endoscopic classification system for narrow band imaging after following a non-guided self-administered learning program. We also aimed to describe in detail the learning process by analyzing which parameters may be more suitable for monitoring competency.

Research methods

An experienced endoscopist followed a self-designed, self-administered learning program in OD of colorectal lesions. Then, OD was applied to lesions detected in colorectal cancer screening colonoscopies. The study period was divided in two halves, with a 6-mo period in between with no performance of OD. Sensitivity, specificity, predictive values and accuracy of the OD compared to the pathological report were calculated for overall results and for the two halves of the study. The accomplishment of the Preservation and Incorporation of Valuable Endoscopic Innovations (PIVI) criteria and the evolution of performance parameters through blocks of 50 lesions were also assessed.

Research results

Overall, 152 patients and 522 lesions were included in the analysis. Regarding the accomplishment of the PIVI criteria, the negative predictive value for the OD of adenoma in rectal lesions diagnosed with high confidence was 92.6% (95% confidence interval: 86.4-97.6) and the proportion of agreement on surveillance interval between OD and pathological diagnosis following the different guidelines was over 95%. Overall accuracy for diminutive lesions diagnosed with high confidence was 89.5% (95% confidence interval: 85.7-92.3). Specificity, negative predictive value and accuracy were the parameters most affected by the stopping period between the two halves. Analyzing trends on blocks of 50 lesions showed an improvement in sensitivity ($P = 0.02$) only in the first half of the study and an improvement on accuracy ($P = 0.01$) only in the second half.

Research conclusions

This study shows that a self-administered learning program based on still pictures plus an *in vivo* phase with auto-feedback is feasible to reach quality standards on OD of colorectal lesions. It also shows that a non-practice period deteriorates performance, and in that case a refresher course seems advisable. These results have practical implications in the design of OD learning tools and in the development of a quality monitoring system.

Research perspectives

These data have become the base for the design and validation of a self-administered learning tool that are currently in process. The efficacy of this kind of tool should be tested with endoscopists having different levels of experience and being from different backgrounds.

REFERENCES

- 1 **Rex DK**, Kahi C, O'Brien M, Levin TR, Pohl H, Rastogi A, Burgart L, Imperiale T, Ladabaum U, Cohen J, Lieberman DA. The American Society for Gastrointestinal Endoscopy PIVI (Preservation and Incorporation of Valuable Endoscopic Innovations) on real-time endoscopic assessment of the histology of diminutive colorectal polyps. *Gastrointest Endosc* 2011; **73**: 419-422 [PMID: [21353837](#) DOI: [10.1016/j.gie.2011.01.023](#)]
- 2 **Vleugels JLA**, Greuter MJE, Hazewinkel Y, Coupé VMH, Dekker E. Implementation of an optical diagnosis strategy saves costs and does not impair clinical outcomes of a fecal immunochemical test-based colorectal cancer screening program. *Endosc Int Open* 2017; **5**: E1197-E1207 [PMID: [29202003](#) DOI: [10.1055/s-0043-113565](#)]
- 3 **Ignjatovic A**, Thomas-Gibson S, East JE, Haycock A, Bassett P, Bhandari P, Man R, Suzuki N, Saunders BP. Development and validation of a training module on the use of narrow-band imaging in differentiation of small adenomas from hyperplastic colorectal polyps. *Gastrointest Endosc* 2011; **73**: 128-133 [PMID: [21184878](#) DOI: [10.1016/j.gie.2010.09.021](#)]
- 4 **Ladabaum U**, Fioritto A, Mitani A, Desai M, Kim JP, Rex DK, Imperiale T, Gunaratnam N. Real-time optical biopsy of colon polyps with narrow band imaging in community practice does not yet meet key thresholds for clinical decisions. *Gastroenterology* 2013; **144**: 81-91 [PMID: [23041328](#) DOI: [10.1053/j.gastro.2012.09.054](#)]

- 5 **ASGE Technology Committee**; Abu Dayyeh BK, Thosani N, Konda V, Wallace MB, Rex DK, Chauhan SS, Hwang JH, Komanduri S, Manfredi M, Maple JT, Murad FM, Siddiqui UD, Banerjee S. ASGE Technology Committee systematic review and meta-analysis assessing the ASGE PIVI thresholds for adopting real-time endoscopic assessment of the histology of diminutive colorectal polyps. *Gastrointest Endosc* 2015; **81**: 502.e1-502.e16 [PMID: 25597420 DOI: 10.1016/j.gie.2014.12.022]
- 6 **Vleugels JLA**, Dijkgraaf MGW, Hazewinkel Y, Wanders LK, Fockens P, Dekker E; DISCOUNT study group. Effects of Training and Feedback on Accuracy of Predicting Rectosigmoid Neoplastic Lesions and Selection of Surveillance Intervals by Endoscopists Performing Optical Diagnosis of Diminutive Polyps. *Gastroenterology* 2018; **154**: 1682-1693.e1 [PMID: 29425923 DOI: 10.1053/j.gastro.2018.01.063]
- 7 **Dias-Silva D**, Pimentel-Nunes P, Magalhães J, Magalhães R, Veloso N, Ferreira C, Figueiredo P, Moutinho P, Dinis-Ribeiro M. The learning curve for narrow-band imaging in the diagnosis of precancerous gastric lesions by using Web-based video. *Gastrointest Endosc* 2014; **79**: 910-20; quiz 983-e1, 983.e4 [PMID: 24287281 DOI: 10.1016/j.gie.2013.10.020]
- 8 **Raghavendra M**, Hewett DG, Rex DK. Differentiating adenomas from hyperplastic colorectal polyps: narrow-band imaging can be learned in 20 minutes. *Gastrointest Endosc* 2010; **72**: 572-576 [PMID: 20561618 DOI: 10.1016/j.gie.2010.03.1124]
- 9 **Singh R**, Bhat YM, Thurairajah PH, Shetti MP, Jayanna M, Nind G, Tam W, Walmsey R, Bourke M, Moss A, Chen R, Bampton P, Roberts-Thomson I, Schoeman M, Tucker G. Is narrow band imaging superior to high-definition white light endoscopy in the assessment of diminutive colorectal polyps? *J Gastroenterol Hepatol* 2013; **28**: 472-478 [PMID: 23278252 DOI: 10.1111/jgh.12098]
- 10 The Paris endoscopic classification of superficial neoplastic lesions: esophagus, stomach, and colon: November 30 to December 1, 2002. *Gastrointest Endosc* 2003; **58**: S3-43 [PMID: 14652541]
- 11 **Hewett DG**, Kaltenbach T, Sano Y, Tanaka S, Saunders BP, Ponchon T, Soetikno R, Rex DK. Validation of a simple classification system for endoscopic diagnosis of small colorectal polyps using narrow-band imaging. *Gastroenterology* 2012; **143**: 599-607.e1 [PMID: 22609383 DOI: 10.1053/j.gastro.2012.05.006]
- 12 **Atkin WS**, Valori R, Kuipers EJ, Hoff G, Senore C, Segnan N, Jover R, Schmiegel W, Lambert R, Pox C; International Agency for Research on Cancer. European guidelines for quality assurance in colorectal cancer screening and diagnosis. First Edition--Colonoscopic surveillance following adenoma removal. *Endoscopy* 2012; **44** Suppl 3: SE151-SE163 [PMID: 23012119 DOI: 10.1055/s-0032-1309821]
- 13 **Hassan C**, Quintero E, Dumonceau JM, Regula J, Brandão C, Chaussade S, Dekker E, Dinis-Ribeiro M, Ferlitsch M, Gimeno-García A, Hazewinkel Y, Jover R, Kalager M, Loberg M, Pox C, Rembacken B, Lieberman D; European Society of Gastrointestinal Endoscopy. Post-polypectomy colonoscopy surveillance: European Society of Gastrointestinal Endoscopy (ESGE) Guideline. *Endoscopy* 2013; **45**: 842-851 [PMID: 24030244 DOI: 10.1055/s-0033-1344548]
- 14 **Lieberman DA**, Rex DK, Winawer SJ, Giardiello FM, Johnson DA, Levin TR. Guidelines for colonoscopy surveillance after screening and polypectomy: a consensus update by the US Multi-Society Task Force on Colorectal Cancer. *Gastroenterology* 2012; **143**: 844-857 [PMID: 22763141 DOI: 10.1053/j.gastro.2012.06.001]
- 15 **Bossuyt PM**, Reitsma JB, Bruns DE, Gatsonis CA, Glasziou PP, Irwig LM, Lijmer JG, Moher D, Rennie D, de Vet HC; Standards for Reporting of Diagnostic Accuracy. Towards complete and accurate reporting of studies of diagnostic accuracy: the STARD initiative. *BMJ* 2003; **326**: 41-44 [PMID: 12511463]
- 16 **Vu HT**, Sayuk GS, Hollander TG, Clebanoff J, Edmundowicz SA, Gyawali CP, Thyssen EP, Weinstein LB, Early DS. Resect and discard approach to colon polyps: real-world applicability among academic and community gastroenterologists. *Dig Dis Sci* 2015; **60**: 502-508 [PMID: 25287002 DOI: 10.1007/s10620-014-3376-z]
- 17 **Patel SG**, Schoenfeld P, Kim HM, Ward EK, Bansal A, Kim Y, Hosford L, Myers A, Foster S, Craft J, Shopinski S, Wilson RH, Ahnen DJ, Rastogi A, Wani S. Real-Time Characterization of Diminutive Colorectal Polyp Histology Using Narrow-Band Imaging: Implications for the Resect and Discard Strategy. *Gastroenterology* 2016; **150**: 406-418 [PMID: 26522260 DOI: 10.1053/j.gastro.2015.10.042]
- 18 **Dai J**, Shen YF, Sano Y, Li XB, Xue HB, Zhao YJ, Gao YJ, Song YJ, Ge ZZ. Evaluation of narrow-band imaging in the diagnosis of colorectal lesions: is a learning curve involved? *Dig Endosc* 2013; **25**: 180-188 [PMID: 23368810 DOI: 10.1111/j.1443-1661.2012.01367.x]
- 19 **Rastogi A**, Rao DS, Gupta N, Grisolano SW, Buckles DC, Sidorenko E, Bonino J, Matsuda T, Dekker E, Kaltenbach T, Singh R, Wani S, Sharma P, Olyae MS, Bansal A, East JE. Impact of a computer-based teaching module on characterization of diminutive colon polyps by using narrow-band imaging by non-experts in academic and community practice: a video-based study. *Gastrointest Endosc* 2014; **79**: 390-398 [PMID: 24021492 DOI: 10.1016/j.gie.2013.07.032]
- 20 **Dinis-Ribeiro M**, Correia R, Santos C, Fernandes S, Palhares E, Silva RA, Amaro P, Areia M, Costa-Pereira A, Moreira-Dias L. Web-based system for training and dissemination of a magnification chromoendoscopy classification. *World J Gastroenterol* 2008; **14**: 7086-7092 [PMID: 19084915 DOI: 10.3748/wjg.14.7086]
- 21 **Khan T**, Cinnor B, Gupta N, Hosford L, Bansal A, Olyae MS, Wani S, Rastogi A. Didactic training vs. computer-based self-learning in the prediction of diminutive colon polyp histology by trainees: a randomized controlled study. *Endoscopy* 2017; **49**: 1243-1250 [PMID: 28806820 DOI: 10.1055/s-0043-116015]
- 22 **McGill SK**, Soetikno R, Rastogi A, Rouse RV, Sato T, Bansal A, McQuaid K, Kaltenbach T. Endoscopists can sustain high performance for the optical diagnosis of colorectal polyps following standardized and continued training. *Endoscopy* 2015; **47**: 200-206 [PMID: 25264764 DOI: 10.1055/s-0034-1378096]
- 23 **Paggi S**, Rondonotti E, Amato A, Fuccio L, Andrealli A, Spinzi G, Radaelli F. Narrow-band imaging in the prediction of surveillance intervals after polypectomy in community practice. *Endoscopy* 2015; **47**: 808-814 [PMID: 26070008 DOI: 10.1055/s-0034-1392042]
- 24 **Patel SG**, Rastogi A, Austin G, Hall M, Siller BA, Berman K, Yen R, Bansal A, Ahnen DJ, Wani S. Gastroenterology trainees can easily learn histologic characterization of diminutive colorectal polyps with narrow band imaging. *Clin Gastroenterol Hepatol* 2013; **11**: 997-1003.e1 [PMID: 23466714 DOI: 10.1016/j.cgh.2013.02.020]

P- Reviewer: Saligram S

S- Editor: Ma RY L- Editor: A E- Editor: Yin SY





Published By Baishideng Publishing Group Inc
7041 Koll Center Parkway, Suite 160, Pleasanton, CA 94566, USA
Telephone: +1-925-2238242
Fax: +1-925-2238243
E-mail: bpgoffice@wjgnet.com
Help Desk: <http://www.f6publishing.com/helpdesk>
<http://www.wjgnet.com>

